THE BEHAVIOUR OF MATERIALS UNDER DYNAMIC SHEAR LOADING

by

A. M. Dowling

Worcester College

Thesis submitted for the degree of Doctor of Philosophy.

October 1968

The University of Oxford

Department of Engineering Science

Parks Road

OXFORD



A B S T R A C T.

Part I

This section is concerned with the propagation of stress waves in metals such that the material is at some stage in the plastic state. An account is given of previous work on the subject of plastic wave propagation whence two distinct theories emerge, the so-called strain-rate dependent and inde-pendent theories. The greatest difference between the two theories is in their prediction of the propagation speed of an incremental stress superimposed on an already plastic stress field. From criticisms of earlier attempts to decide which is the more applicable theory it is deduced that the most convincing way of answering that question is to apply torsional increments to thin-walled tubes already plastically strained in torsion.

A brief outline of the two theories as they apply to the torsion of thin-walled tubes is provided in Chapter 3, during which the values of the predicted incremental wave speed are derived.

Some of the problems encountered in designing apparatus to carry out the required experiments are discussed in Chapter 4, which includes a full description of the final design. This consists of a standard torsion machine in which is placed the specimen, fixed between two long bars. The relative strengths and sizes of the specimens and bars are such that the latter remain elastic even at large plastic strains in the specimen.

A friction clamp fits round the input bar and is

pressed on to it by tensioning a length of high tensile steel wire. By rotating the end of the input bar, the specimen can be prestrained whilst slip at the clamp builds up a small friction torque. The friction torque is rapidly released by breaking the tensioning wire and the resulting stress waves in the system are detected by means of strain gauges on the input and output bars. The time of travel of an incremental stress through the specimen can then be calculated. The rise time of the stress wave is approximately 30 μsec.

Following the description of the apparatus, details of the specimens are given. These were made from mild steel and commercially pure aluminium and copper, all in the annealed state. Four different sizes were made, three for use in the wave propagation tests, the fourth was used in the cams machine but to provide an indication of the strain rate sensitivity of copper and aluminium.

The results of the tests on all the above types of specimen are laid out in Chapter 6. Prestrains of up to 25% were used in the wave propagation work and in all cases it was found that the propagation speed was equal to the torsional elastic wave speed as predicted by the strain-rate dependent theory. Also shown in this chapter are the variations in transmitted pulse shape between the various materials and prestrains.

Part II

The second part of the thesis is concerned with the process of punching or blanking and opens with an account of previous work on the subject.

The following chapter describes the apparatus which

enables the punch speed to be varied from 10^{-5} to 10^{3} in/sec. and allows the punch load to be measured at each instant of the deformation process. Three different machines are described, a standard Instron testing machine which provides the low punch speeds, a special hydraulic machine giving higher punch speeds and a drop-weight impact testing machine from which the highest speeds are obtained.

Load-displacement curves were obtained over this range of punch speeds for six materials, mild steel, copper, aluminium (all annealed), soft and hard brass, and a high tensile steel. The load-displacement curves of the first three materials, which had very similar compositions to those materials used in Part I, were converted into shear stress - shear strain curves by assuming the deformation to be of a simple shear form, and using a gauge length estimated from microhardness traverses of the sectioned specimens.

In Chapter 11 the strain rate sensitivities obtained from the punch test are used to discuss the observed pulse magnitudes of the wave propagation tests, in conjunction with the predictions of the strain-rate dependent theory. It is shown that the predictions agree qualitatively with the observed trends.

The second part of this chapter examines the effects of increasing the punch velocity in the blanking process on the quality of product and the energy absorbed by the process. It is shown that the high speed punching process is most advantageous when using brittle materials.

A C K N O W L E D G M E N T S.

I would like to thank everyone who has helped in any way during the course of this research. In particular I would like to thank :-

The University Grants Committee and the Science Research Council for their financial support of the research and of me.

Dr. J. D. Campbell, who supervised the work, and Dr. J. Harding, who filled the role temporarily, for their continual, extremely useful, advice and guidance.

Dr. R. H. Cooper, for many helpful suggestions and especially for his encouragement during the first year of this programme.

Members of the technical staff of the laboratory, especially Messrs. R. C. Stone, J. Moore and M. A. Miles.

Mr. R. E. Croker for help with the photography.

My mother, Mrs. E. L. Dowling, for typing this thesis.

C O N T E N T S.

ABSTRACT

ACKNOWLEDGEMENTS

LIST OF FIGURES

1. GENERAL INTRODUCTION 1

P A R T I

2. AN OUTLINE OF EARLIER WORK ON PLASTIC WAVE PROPAGATION 4

3. STRESS WAVES IN SOLIDS 22
Characteristic Curves and Equations 22
Torsional Stress Waves 26
Strain-Rate Independent Theory 27
Strain-Rate Dependent Theory 33

4. WAVE PROPAGATION - APPARATUS 38
General 38
The Transmitter Bars 41
The Friction Clamp and Release Mechanism 41
Instrumentation 45
Incremental Torque Measurement 46
'Static' Torque Measurement 49
Incremental Torque Recording 51
Wire Load Indication 51
Supports 51

5. WAVE PROPAGATION - SPECIMENS 53
Shape and Size of Specimens 53
Steel Specimens 54
Copper Specimens 54
Aluminium Specimens 56
Attachment to Loading Bars 57
Densities 60

6. WAVE PROPAGATION - RESULTS 61
The Apparatus 61
Aluminium Incremental Loading Results 62
The Shape of the Transmitted Wave for Aluminium 64
Copper Incremental Loading Results 65
The Shape of the Transmitted Wave for Copper 66
Incremental Loading Tests on Mild Steel 67
The Transmitted Pulse Shapes for Mild Steel 68
Short Specimen Results. General 68
Aluminium Short Specimens 70
Copper Short Specimens 71

P A R T II

7. AN OUTLINE OF EARLIER WORK ON THE BLANKING OF METALS 72

8. BLANKING APPARATUS 80
The Hydraulic Machine and Punch-Die Assembly 80
The Instron Loading Machine 83
The Modified Low and Medium Speed Punch-Die Assembly 83
The Impact Loading Machine and its Punch-Die Assembly 84

9. BLANKING SPECIMENS AND THEIR TREATMENT 89
Dimensions 89
Materials 89
Mild Steel 90
Copper 90
Aluminium 91
Soft Brass 91
Hard Brass 92
SAE 4130 Alloy Steel 93
Post-test Treatment 93
Etchants 95
Microhardness Measurement 97

10. BLANKING RESULTS 98
Apparatus 98
Mild Steel Results 99
Copper Results 105
Aluminium Blanking Results 107
Soft Brass Results 109
Hard Brass Results 111
High Tensile Steel Results 113

---

11. DISCUSSION 115
PART I
The Incremental Torque Propagation Speed 115
The Strain-Rate Sensitivity of the Specimen Materials 120
Copper 120
Aluminium 124
Mild Steel 125
The Magnitude of the Initial Peak of the Transmitted Increment 127
PART II
The Blanking Process 132

12. CONCLUSIONS 141

REFERENCES 144

APPENDIX 1 149

APPENDIX 2 152

LIST OF FIGURES

2.1(a) Residual strain distribution as predicted by the Taylor - von Karman theory.

(b) Stress-strain curve for annealed aluminium (Dead weight static compression test.)

3.1 Strain-rate-independent theory: Characteristics and strain distribution.

3.2 Strain-rate-dependent theory : Characteristics and strain distribution.

4.1 Strain gauge positions and idealised torque distribution.

4.2 The clamp.
Inset: Force diagram.

4.3 'Close-up' of the clamp.

4.4 Strain gauge connections.

4.5 Circuit diagram.

4.6 The triggering system.

4.7 The complete apparatus.

5.1 Typical specimens.

5.2 Jig for specimen attachment.

6.1 Elastic test record.

6.2 Shear stress - shear strain curves for aluminium.

6.3 Graph of dimensionless incremental wave speed v. shear prestrain for aluminium.

6.4 Oscilloscope traces for aluminium (i).

6.5 Oscilloscope traces for aluminium (ii).

6.6 Oscilloscope traces for the 'half-length' aluminium specimen.

6.7 Graph of dimensionless incremental wave speed v. shear prestrain for copper.

6.8 Shear stress - shear strain curve for copper.

6.9 Oscilloscope traces for copper (i).

6.10 Oscilloscope traces for copper (ii).

6.11 Oscilloscope traces for the 'half-length' copper specimen.

6.12 Shear stress - shear strain curves for mild steel.

6.13 Graph of dimensionless incremental wave speed v. shear prestrain for mild steel.

6.14 Oscilloscope traces for mild steel (i).

6.15 Oscilloscope traces for mild steel (ii).

6.16 Oscilloscope traces for very short specimens.

6.17 Shear stress - shear strain curves for the short specimens of aluminium.

6.18 Shear stress - shear strain curves for the short specimens of copper.

8.1 Low and medium speed punch-die assemblies.

8.2 Arrangement for low speed punch testing.

8.3 Apparatus for impact punch testing.

10.1 Typical test records for mild steel (i).

10.2 Typical test records for mild steel (ii).

10.3 Load-displacement curves for 1/8 in. mild steel.

10.4 Load-displacement curves for 1/16 in. mild steel.

10.5 Load-displacement curves for 1/32 in. mild steel.

10.6 The deformed region in mild steel.

10.7 Microhardness traverses for 1/8 in. mild steel.

10.8 Microhardness traverses for 1/32 in. mild steel.

10.9 Cracks in part-punched specimens.

10.10 Mild steel slugs.

10.11 Typical test records for copper.

10.12 Load-displacement curves for copper.

10.13 Microhardness traverses for copper.

10.14 (a) Copper specimens.

(b) Aluminium specimens.

10.15 Typical test records for aluminium.

10.16 Load-displacement curves for aluminium.

10.17 Microhardness traverses for aluminium.

10.18 Typical test records for soft brass.

10.19 Load-displacement curves for annealed brass.

10.20 The deformed region in soft brass.

10.21 Microhardness traverses for annealed brass.

10.22 (a) Mounted soft brass sections.

(b) Soft brass specimens.

10.23 Typical test records for hard brass.

10.24 Load-displacement curves for hard brass.

10.25 Comparison of the hard and soft brass load-displacement curves.

10.26 Micrographs for hard brass.

10.27 (a) Hard brass specimens.

(b) SAE 4130 steel specimens.

10.28 Typical test records for SAE 4130 steel.

10.29 Load-displacement curves for SAE 4130 steel.

10.30 Micrographs for SAE 4130 steel.

11.1 Shear stress - shear strain curves for copper from punch tests.

11.2 Concerning the lower strain-rate stress-strain curve of the strain-rate change tests.

11.3 Strain-rate sensitivity of copper.

11.4 Shear stress - shear strain curves for aluminium from punch tests.

11.5 The results of a strain-rate change test on aluminium.

11.6 Strain-rate sensitivity of aluminium.

11.7 Shear stress - shear strain curves for mild steel from punch tests.

11.8 Strain-rate sensitivity of mild steel.

11.9 Graph of reciprocal 'g' function against overstress for copper.

11.10 Graph of reciprocal 'g' function against overstress for aluminium.

11.11 Graph of reciprocal 'g' function against overstress for mild steel.

11.12 Variation of punch penetration with strain rate.

11.13 Strain-rate sensitivities of hard and soft brass and high tensile steel.

Ap. 1 Elastic incremental torque values.

C H A P T E R 1.

GENERAL INTRODUCTION.

For many years it has been observed that the mechanical behaviour of engineering materials depends to some extent on the rate of loading. Under conditions of impact or high rates of strain many materials are apparently stronger than if loaded slowly. As early as 1909 Ludwik (1) proposed a theory taking into account the effect of strain-rate in stress-strain relations.

One material parameter upon which the loading rate has apparently no effect is the elastic modulus so that the behaviour of an elastic solid is independent of the loading rate. One process which involves a high rate of loading is the propagation of stress waves through a material, and the shorter the wavelength the higher the strain-rate. It follows that the subject of wave propagation in elastic solids is a relatively simple one, and a well developed mathematical theory describing the behaviour of materials under elastic deformation is available (2). When one extends this theory to include the propagation of stresses large enough to cause yielding difficulties are immediately encountered. Firstly, various representations of inelastic behaviour have to be assumed which often only very approximately describe the behaviour of real materials and secondly, as has already been stated, the strain-rate has some effect on the yield and post-yield behaviour.

It may be wondered why there is a necessity for studying the propagation of plastic waves but investigating the

effects of strain-rate and stress wave propagation in engineering materials serves several practical needs. Data is needed in the fields of vehicle safety, armament research and, more recently, space research where materials have to exist under similar conditions, i.e. large forces being applied for short times. Also large strain-rates exist in the many new high-speed mechanical working processes and information is needed for advising on the best methods for deforming particular materials.

This thesis is divided into two parts, the first of which is concerned with the propagation of incremental shear pulses through plastically deformed material; and the second part consists of a study of the blanking or punching process, in which a circular piece is sheared from a plate or strip.

As work on plastic wave propagation continued, two distinct theories were proposed. The first, due to Taylor (3), von Karman (4) and Bakhmatulin (5), is known as the strain-rate-independent theory and the second, proposed by Malvern (6), is called the strain-rate-dependent theory. The purpose of Part I of this thesis is to examine one particular aspect of the two theories in which they differ a great deal, and to determine whether either of them describes the observed practical behaviour. This aspect is the propagation of small plastic stress pulses through prestressed material. There have been many criticisms of earlier work performed on this subject and it was necessary to avoid these and not to leave the way open for more.

In order to achieve this, a new apparatus was designed

• This theory was more general than the earlier strain-rate-dependent proposal of Sokolovsky (100) who gave a numerical treatment using the special static stress-strain relation, $\sigma_s = \text{const.}$

and developed to apply a sudden torsional stress pulse to a specimen already being strained plastically in torsion. It was also required that several different materials could be used in the investigation, and the resulting apparatus is described in Chapter 4.

Mild steel, copper and aluminium were used in this study, and the same machine was used to obtain some indication of the effect of strain-rate on their material properties.

It was not expected that the machine described here would produce the wide range of strain-rate necessary for obtaining an accurate measure of the strain-rate sensitivity of the three materials used. Thus the blanking process discussed in Part II was used to try to fulfil this need. A simply performed test involving primarily shear deformation was required and blanking is such a test.

Although blanking is a very simple process to perform, there has only been one previous attempt to measure the load supported by the specimen throughout the deformation at a number of punch speeds. This was by Davies and Thawan (7) and was unsuccessful in that very oscillatory results were obtained. In the present work, load-displacement curves were obtained over a wide range of punch velocities for six materials, namely mild steel, copper, aluminium, hard and soft brass and a high-tensile steel. The effects of increasing the punch velocity by eight orders of magnitude are discussed.

The complex stress system present in blanking is simplified to one of pure shear, using suitable corrections, in order to obtain the strain-rate-sensitivity information necessary for a proper discussion of the wave propagation work of Part I.

PART I

CHAPTER 2.

AN OUTLINE OF EARLIER WORK ON PLASTIC WAVE PROPAGATION.

The first serious attempt to understand the problem of plastic wave propagation was made by Donnell (8) in 1930. He analysed stress waves in a long bar by a superposition technique in which the stress wave was treated as being made up of two steps in stress. Each step was assumed to travel at a velocity determined by the slope of the material stress-strain curve which was simplified to a bilinear form, in the region of the particular stress level.

The coming of World War II and the developments in armour-piercing shells and armour plating led to a much greater interest in the subject. The same problem was treated independently in three countries, Great Britain, United States and Russia by Taylor (3) von Karman (4) and Rakhmatulin (5) respectively. Their solutions were more rigorous than that of Donnell and applied to materials with more general stress-strain relations. Both von Karman and Rakhmatulin used Lagrangian co-ordinate in solving the problem whilst Taylor used the Eulerian system. By a suitable transformation of the notation both treatments can be shown to give the same result. The von Karman - Taylor theory is based on the assumption that the stress-strain curve is concave towards the strain axis, linear up to a critical value of strain above which it is univalued for increasing stresses. Thus $\sigma = \sigma(\varepsilon)$ where $\sigma(\varepsilon)$ is a known function of strain ε. It is also assumed that the stress-strain relation is independent of the rate of loading and that the cross-section of the material is sufficiently small for the effects of

kinetic energy due to radial motion to be ignored. It will be noticed that the treatment is one dimensional.

The theory predicted that if a stress σ, greater than the yield stress of the material, were applied to the end of a bar, a wave of stress, of magnitude equal to the yield stress of the material, would propagate with a velocity equal to the elastic velocity,

$$C_0 = \sqrt{\frac{E}{\rho}} \qquad (2.1)$$

whilst stresses greater than the yield stress would propagate with velocities given by,

$$C = \sqrt{\frac{1}{\rho} \cdot \frac{d\sigma}{d\epsilon}} \qquad (2.2)$$

where $\frac{d\sigma}{d\epsilon}$ is the local slope of the engineering stress-strain curve. From the original assumption that the stress-strain curve is concave towards the strain axis it can be seen that the higher the stress above yield, the slower the speed with which that stress is propagated. One can, therefore, calculate the strain distribution in a bar at a time t after impact at constant velocity (see Chapter 3) and this is shown in Fig. 2.1 (a)

This figure shows a region of uniform strain (strain plateau) at the impact end with a region of gradually decreasing strain along the bar. The length of the strain plateau depends on the time t and its magnitude depends on the impact velocity.

Experiments were carried out by Duwez and Clark (9) to try to verify certain consequences of the rate-independent theory. They used tensile impact on annealed copper wires, together with other experiments, and found general qualitative agreement with the theory. It was found that the theoretical relationship between strain at the impact end and impact velocity was substantially correct as was the length of the strain plateau. However,

measurements recorded during the actual wave propagation, for example, the stress-time curve at the end of an 8in. gauge length, showed a definite tendency towards more rapid propagation velocities than those which could be deduced from the stress-strain curve. The discrepancies could be explained by strain-rate effects and von Karman and Duwez (10) suggested that this was the case.

This suggestion was taken up further in 1950 by Malvern (6, 11) who thought that materials might be thought to behave in a general viscoplastic sense in which the application of a stress produced a plastic strain rate in addition to the normal elastic strain rate. The plastic strain rate ($\dot{\epsilon}_p$) was assumed to depend also on the instantaneous state of the material which is determined by ϵ_p so that,

$$\dot{\epsilon}_p = g(\sigma, \epsilon) \tag{2.3}$$

or

$$\dot{\epsilon} = \dot{\epsilon}_p + \dot{\epsilon}_e$$

$$= g(\sigma, \epsilon) + \dot{\sigma}/E \tag{2.4}$$

There are several differences between the consequences of this formulation and the rate independent theory. First, the velocity of stress propagation for all stresses in a strain-rate sensitive material can be shown to be equal to $\sqrt{\frac{E}{\rho}}$, the elastic wave velocity (see Chapter 3). In addition, the stress at the wave front decreases as the wave passes through the material, due to the dissipation of elastic strain energy as plastic work.

If one considers the theory of plastic flow in crystalline materials, the strain rate assumptions seem to fit in quite well. Campbell et al. (12) considered the effect of shock loading on a

Frank-Read source and suggested that, because of the inertia of dislocations, the shock produced no plastic strain. Thus the instantaneous total strain was completely elastic and hence the stress wave must propagate with the elastic velocity regardless of its magnitude. When the dislocations have reached their limiting velocity they begin to interact and also exert back stresses on the sources. Thus the strain rate decreases and, if the dislocation arrangement can be considered to be a function of the plastic strain, equation (2.4) can be expected to approximate the physical facts. In the intermediate time whilst the dislocations are accelerating such an equation would not apply but it was shown that this time was only 5×10^{-10} sec. so that for all practical purposes equation (2.4) could be expected to describe the behaviour.

The most marked difference between the strain-rate dependent and independent theories is that the wave propagation velocities are so dissimilar. Consequently, experimental work to try to decide between the two has centred on this difference. Bell (13) working in 1949-1950 introduced incremental tension waves into 6 ft. long rods while they were already stressed into the plastic region. The theoretical propagation velocity according to the Taylor - von Karman theory is proportional to the square root of the local slope of the governing stress-strain curve but according to Malvern the elastic wave speed. Thus the experiment was expected to show whether the governing curve was the quasi-static stress-strain curve of the material or not.

The experimental results showed that the velocity of an incremental wave was equal to the velocity of an elastic wave. As this was contrary to what he expected, Bell altered the specimen shape in order to remove any possibility that the loading

wave had been transmitted through the loading machine or the strain measurement apparatus. The experiments were extended by Steruglass and Stuart (14) this time on copper instead of steel. Copper strips were preloaded statically into the plastic region but when impact experiments were carried out, they too found that, even in the plastic region, the stress fronts propagated with the elastic velocity and all levels of stress travelled with much higher speeds than predicted by the von Karman - Taylor theory. Similar results have been shown on copper by Riparbelli (15) and in lead by Alter and Curtis (16)

This latter work is interesting in that the authors devised a method of applying a dynamic preload to the material. They used a Hopkinson Pressure Bar to do the impact experiments but with the modification that the bar was stepped in diameter. Thus, due to reflections within the bar, the lead was given a plastic preloading, followed shortly afterwards by a second increase of stress. This second disturbance was found to travel with the elastic bar velocity. This dynamic preloading removed one of the doubts about previous work, that due to quasi-static preloading in long bars there might have been inhomogeneous behaviour.

In 1956 Lee (17) re-examined the original data of Clark and Duwez and found that the plastic strain at the impact end was not in fact uniform but had a slightly higher value near the point of impact. This result could be explained by a strain-rate law but was impossible according to the strain-rate-independent theory. Thus it seemed more and more conclusive that the strain-rate dependent theory was more consistent with experiments than the rate independent theory. So much was this so, that many

people turned away from the wave propagation problem to a different one, namely, could the mechanical behaviour of materials be approximated by a relationship of the form of equation (2.4) or were other relationships more appropriate?

Even here, however, the results obtained by different investigators differed a great deal. As as example, in tests on short pure aluminium cylinders in compression, Hauser et al. (18) and Karman (19) found that the material was definitely strain-rate sensitive while Bell (20) maintained that aluminium was not strain-rate sensitive at all. On the other hand Kolsky and Douch (21) found that the dynamic stress-strain relation for aluminium could be represented by a single curve for which the stresses were always higher than those obtained in quasi-static tests.

In contrast to the above results, there was little doubt of a pronounced strain-rate effect on the yield and post-yield behaviour of mild steel. Work by Clark and Wood (22) Campbell and Duby (23) and others showed that with a time to yield of between 10 sec. and 10 μsec. the yield stresses, both upper and lower, were raised to up to 2.5 times the 'static' values. In short it can be said that the strain-rate effect is very noticeable in materials with a sharp yield point but that results are not so conclusive (quantitatively if not qualitatively) in materials without such a sharp yield point.

Returning to the question of wave propagation, there were still several people who stuck to the idea of a strain-rate-independent theory. In 1947 Hoppmann (24) had investigated a different aspect of the theory, that of a critical velocity. This came about from considering the tensile quasi-static stress-strain curve. If the slope of this determined the wave speed

then there would be a limiting particle velocity corresponding to the ultimate stress where the gradient is zero. Hoppmann studied energy and elongation as functions of the impact velocity in short tensile specimens of copper. By integration using the slopes of the quasi-static curve up to the strain at the horizontal tangent in the equation

$$v = \int \sqrt{\frac{1}{\rho} \cdot \frac{d\sigma}{d\epsilon}} \, d\epsilon$$

he found excellent agreement with a critical velocity determined from the strain-rate-independent theory. This agreement was considered to show that strain rate played at most only a small part in wave propagation.

Perhaps the most devoted supporter of the strain-rate-independent theory, however, has been Bell. After his incremental wave experiments he developed a technique for measuring strain directly at any instant by means of diffraction gratings engraved on the specimen itself (25, 26, 27). It was this technique which brought about a revival of the controversy between the two wave propagation theories. The rate-independent theory stated that the wave speed at each level of strain should be constant and that in terms of these constant wave speeds an integral relation between particle velocity and strain should hold for all strains and velocities including the maxima. Thus Bell thought that if he were able to make direct measurement of dynamic plastic strain $\epsilon(x,t)$ and of particle velocity $\dot{u}(x,t)$ along the specimen itself during wave propagation, he would be able to determine the applicability of the theory to a particular material without recourse to an assumption about the constitutive equation. If it could be shown experimentally that both the above conditions held then the stress-strain law governing the deformation could

be determined. Bell used an optical displacement method for measuring the particle velocity during the wave propagation.

Using this technique on aluminium, Bell (28) showed that the strain-rate-independent theory gave good agreement with the experimental behaviour. Similar results were obtained by Bell and Werner (29) in copper and by Speranza (30) in lead but in each case it was found that the quasi-static curve was not the one which was deduced from the measured values. This had previously been shown by W. R. Campbell (31) and predicted by White and Griffis (32).

In 1962 Bell and Stein (33) using a dynamic pre-stress on aluminium, similar to the experiments of Alter and Curtis (16) again found the incremental wave speed to be equal to the elastic bar velocity. They attributed this result to the form of the stress-strain curve for the dead annealed material. The compression test at a very low strain rate produced a step-like stress-strain curve for the material, as shown by Dillon (34) and Hanson and Wheeler (35); see Fig. (2.1b). It was found that the slope of the rising portion of each step was approximately equal to that of the first elastic region. Thus, it was explained, due to the dynamic pre-stress, the strain must terminate at the foot of one of these rises (the only stable position) and the addition of the increment would then cause an initial path, in the stress-strain plane, up the 'elastic' slope. As it was found in the experiments that only the initial very low strain part of the increment travelled with the elastic velocity, this seemed a plausible explanation.

After more work by Bell (36) studying the wave behaviour in the vicinity of the impact face, it was conceded by Malvern(37)

that some of the wave propagation phenomena originally motivating the rate-dependence study could have been due to three-dimensional effects at or near the impact end. Bell showed that, through reflections at the side-walls of the cylinder, an initially very high stressed, short-lived front collapses to an unstable weak shock front having a maximum stress equal in magnitude to the previously measured dynamic overstress. After approximately one diameter from the impact face the dispersive plastic wave is developed from the unstable shock front. This explanation involves no strain-rate-dependence assumptions at all but, as has already been stated, this behaviour was not the only discrepancy between the two plastic wave propagation theories, so that the above realisation was by no means a complete solution to the controversy.

A further suggestion was made in 1964 by de Vault (38) casting even more doubt on the experiments which assumed a strain-rate effect as a reason for their findings. This suggestion was that lateral inertia had to be taken into account in analysing the wave propagation in the type of investigations undertaken.

Corrections for radial inertia and radial shear (caused by rapid cross-section changes) had already been calculated for elastic longitudinal waves by Mindlin and Herrmann (39). The results had been experimentally checked by Miklowitz (40). It was also well known that a uniaxial stress approximation could be used as long as rates of change of stress and strain were small. This is the case if the Fourier transforms of the stress and strain contain no large contributions for periods and wavelengths small compared with the characteristic time and space dimensions of the bar. It is reasonable to assume that the same

conditions would hold with plastic wave propagation yet in all the plastic wave propagation work done up to this time, the end loading approximated to a step function of either stress or velocity. There would, therefore, be a considerable contribution from waves of small wavelength and consequently an appreciable lateral inertia effect.

The predictions of de Vault's work with constant stress input were that the strain would overshoot the Taylor - von Karman result and oscillate about a value higher than the Taylor-von Karman final value. Both the amplitude of the oscillations and the final value of strain would decay with distance and the elastic plateau would also be higher than the Taylor-von Karman prediction. There would be no sharp elastic and plastic fronts and the variation in strain between these regions would differ considerably from simple theory, indicating that in general constant velocities were not associated with given levels of strain. With a constant velocity input the results were closer to those of the rate-independent theory in that the final strains were the same, but the other differences described above were still present. The work also showed that an additional disturbance of stress propagated faster than predicted by simple theory, thus showing that the results of Alter and Curtis (16) Steraglass and Stuart (14) and Riparbelli (15) could not be taken as proof of a strain rate effect.

Experimental work on lead by Grimm (41) indicated that the lateral inertia model was at least qualitatively reasonable in the transition region between elastic and large plastic strains. Attempts were made by Plass and Ripperger (42) to measure the radial particle velocities in copper. Although no

quantitative values could be obtained with any certainty, the experiments showed qualitatively that there were appreciable velocities as the material was plastically strained.

Although the theoretical treatment of the lateral inertia problem was not available until 1964, awareness of the problem certainly existed many years earlier. Attempts were made to separate the effects of radial motion from those of the strain rate. Hauser, Simmons and Dorn (18) suggested varying the tube width in their experiments and investigating the effect on the strain rate function. In compression tests on high purity aluminium they had shown that the strain rate function, $g(\sigma, \epsilon)$, was independent of the stress and strain history but that it was not a simple function of the overstress above the static stress-strain curve.

Yet another criticism of experiments concerned with the problem of plastic wave propagation was brought forward after work by Kipperger and Karnes (43). A strain-rate-dependent theory would predict that higher increments of strain in a pulse would propagate at velocities slower than would be obtained from a rate independent theory. Kipperger and Karnes observed such a slowing but it was said by some researchers that this apparent decrease in the wave propagation speed was due to the failure of the measuring devices faithfully to follow the deformation. Although gauges of both foil and wire resistance types had been used successfully to follow 'static' stresses into the plastic range, it was uncertain whether they could be relied upon to respond accurately to large strains at high strain rates.

The next phase in the development of plastic wave propagation research was an attempt to bring together the

theories rather than to emphasize their differences. In 1963, Manchi (44) did some work on the propagation of longitudinal plastic waves in long prestressed specimens of annealed copper. The waves and prestress in this case were tensile in nature and comparison of results with numerical calculations showed that the strain rate dependent theory in a linear form, and possibly even more so in a non-linear form, gave a good description of the whole phenomenon for all values of time, static preloading and distance from the impact end. If, however, the impact velocity rose regularly to a steady state value, the asymptotic behaviour was given by the solution of the strain-rate-independent theory. Hence the latter was an approximation to the solution at any section for large enough values of time and very useful if all that was needed was the distribution of the final strain. In addition Manchi stated that if there were no prestress, then the approximation became good for all values of time at sections away from the impact face. In this case the strain-rate effects were much less noticeable since a portion of the wave was below the limit of proportionality and for the most part the wave above that limit was already travelling with velocities as predicted by the rate independent theory.

Also in 1963, Jacob Lubliner (45) brought out what he called a generalized theory for strain-rate-dependent plastic wave propagation in bars, and he set out to show that the strain-rate-dependent and strain-rate-independent theories were both special cases of the same theory. As in the other theories, Lubliner started with an equation of motion and an equation of continuity. Then using a constitutive equation in a very general form, first used by Cristescu (46), he built up his general theory.

Working under Malvern, Efron (47) did more work on the compression of commercially pure aluminium under dynamic impact tests. By means of electro-magnetic transducers he was able to measure the particle velocity at several stations along the bar. Test results showed that given levels of velocity and strain propagated with constant velocity. Within the small range of strain rates obtained, this did not change with strain rate. However, it was observed that the velocities differed noticeably from those predicted by the rate-independent theory based on the 'static' stress-strain curve. For calculations based on a single dynamic curve there was excellent agreement between theory and experiments. Etched foil gauges were used to obtain transient strain records and it was found that the wave propagation speed versus strain level plots derived from these showed consistently lower speeds than those obtained from the velocity records. Bell (46) had already observed that the gauge response lagged behind the strain in the material but he found that the lag was proportional to strain rate whereas Efron found closest agreement at the highest rate.

It was due to Efron (47) that the strain-rate-independent and dependent theories were brought even closer together. In the calculations undertaken by Malvern (11), a constant applied velocity and condition had been used. Efron used a constant stress boundary condition and found after all that the Malvern theory predicted a strain plateau near the impact end, and of the same value as that predicted by the strain-rate-independent theory. This plateau was only formed if the pulse was applied long enough for the material near the impact face to reach equilibrium, as had been pointed out by Mercado (49).

Lood and Phillips (50) undertook a study of this strain plateau and showed on theoretical grounds that it should always appear in a semi-infinite bar subjected to an axially applied impact stress. It was also shown that for a given static stress-strain curve, the time needed for the appearance of a given length of plateau depended on a characteristic time of the material and that the Taylor - von Karman theory was a special case for which this characteristic time was zero. They also considered the influence of strain hardening and found that the time needed for a given length of plateau to appear increased as the strain-hardening decreased. They concluded that the early work of Malvern (11) did not obtain a strain plateau because the analysis was not carried out for as long as required by the amount of strain hardening at the load level used. In the later work of Efron (47) and Malvern (37), on the other hand, the load level was much smaller and hence the amount of strain-hardening higher, resulting in a quicker formation of the plateau.

A variation in experimental procedure was conceived by Bodner and Clifton (51) who decided to take into account the effect of temperature variation in elastic - plastic pulse propagation. They only considered observations at fairly large distances from the impact end and found, as would be expected from Bianchi's work (44), that the one-dimensional rate independent theory could properly describe the results of the experiment. There was a Bauschinger effect but the experiment could serve to determine the dynamic proportional limit stress. This is the name given to the maximum stress which propagates with the elastic wave velocity. Since Bodner and Clifton used commercially pure aluminium whose proportional limit even in quasi-

-static tests is sensitive to small changes in impurities, no absolute measurement of the dynamic proportional limit stress was possible. Qualitatively the dependence on temperature was found to be much less than in 'static' tests. The conclusion that the strain-rate independent theory could be used to describe the pulse shape and characteristics meant that a single stress-strain relation could be used for the theoretical comparison of the results. At room temperature it was found that this relation was very nearly the same as the quasi-static one but that at higher temperatures ($750^{\circ}F$ was the highest temperature used) there was an appreciable difference. The general conclusion was, therefore, that the material was at least strain-rate dependent in that its static and dynamic stress-strain curves were different but since the plastic strains considered were small this conclusion could only be applied for small strains beyond the proportional limit.

Kipperger and Watson (52) in 1967 showed theoretically that the shape of a wavefront was not a unique function of a particular constitutive equation. They also calculated that given levels of strain propagated at nearly constant speeds for several types of constitutive relation and thus concluded that measurement of $v(\epsilon)$ did not determine the relation. They also showed that of several different analytical forms of strain-rate sensitivity assumed only one did not produce a strain plateau at the impact end.

It is convenient at this point to summarise some of the problems facing investigators of the propagation of plastic stress waves when trying to decide which of their observations are relevant. First of all there is the lateral motion of the material caused by the passage of a stress wave and, because

of the inertia of the material, the associated complication of the wave motion. De Vault (37) showed mathematically that the effects of this were very similar to those attributed to the strain rate.

Secondly there is the building up of a wave at the impact end due to sidewall reflections. Bell (36) showed that effects previously thought to be due to strain-rate dependence could be explained by this. This was most unfortunate since it was known that both the strain-rate dependent and independent theories gave practically the same results away from the impact face.

Looking to the largest difference between the theories, the speed of propagation of incremental loads, there were still uncertainties in the experimental investigations. There was the possibility that by the use of a straining machine to apply a prestrain, a certain amount of relaxation, no matter how small, might have occurred by the time the increment was actually applied so that the material was in fact no longer in a plastic state. Even if it were certain that the material was in a plastic state then there was the problem of unstable materials exhibiting a step-like stress-strain curve. Then any amount of preload would put the stress-strain point at the foot of a rise in the curve so that the increment would produce a path up the elastic slope of the next step.

It was because of these defects that Craggs (53, 54) suggested that there was only one sort of experimental programme to undertake in order to decide whether a strain-rate dependent or independent type of theory was the more applicable. This programme was to follow the propagation of pure torsional waves in thin-walled tubes which were initially stressed beyond the

elastic limit in pure torsion. After a statement like that of Craggs it is somewhat surprising that little work was in fact done on these lines especially in view of the fact that a complete elastic - plastic analysis is available for the torsion of a thin-walled tube.

Convery and Pugh (55) did in fact take up this suggestion and, using incremental pulses on already yielded thin tubes of mild steel and copper found that the pulse still travelled with the velocity of elastic waves. The pulse was produced by the brittle fracture of a rod of material in the centre of the specimen tube. As the assembly was loaded both the specimen and rod were strained until the rod reached its breaking load. As the rod broke the torque was released and propagated as an unloading wave in the loading bar and a loading wave in the specimen. Unfortunately multiple reflections occurred between the source of the wave and the specimen and also the rise time of the wave was quite large. Thus the experiment was not entirely conclusive but it did give some indication that the incremental experiments of Steraglass and Stuart (14) and others might be perfectly valid after all.

The only other known research into the plastic wave propagation problem in torsion has been by a group working at the University of Texas. Work has been done on the strain distribution by Baker and Yew (56) and on the incremental plastic wave by Yew and Richardson (57) both in copper. Baker and Yew compared experimentally measured strain pulses with those computed by using both the strain-rate dependent and independent theories. The results showed that the former gave significantly better agreement than the latter.

The flow constant was obtained from their own impact torsion tests and one suggestion was that by a better choice of this value (obtained in this case by a split Hopkinson bar type of test) there would have been even better agreement with the strain-rate-dependent theory. One fact which must be mentioned however is that the copper showed considerably less strain-rate sensitivity in these measurements than had been found in previous compression tests by Parmen (19) and Malib (58).

The results of Yew and Richardson (57) showed that the wave speeds measured for large amplitude strains agreed well with the strain-rate-independent theory. However for statically pre-stressed specimens it was found that low level strains travelled at much higher speeds than those predicted by the Taylor - von Karman theory but that large level strains propagated at the predicted speeds. The conclusion was that when the material was impacted it deviated from the quasi-static curve to another curve compatible with the high strain rate and the higher speeds were derived from the increased slope in the transition region. The fact that high level strains propagated at velocities nearly equal to those predicted by the rate independent theory implied that the slopes of the quasi-static and particular dynamic curves were nearly equal away from the transition region.

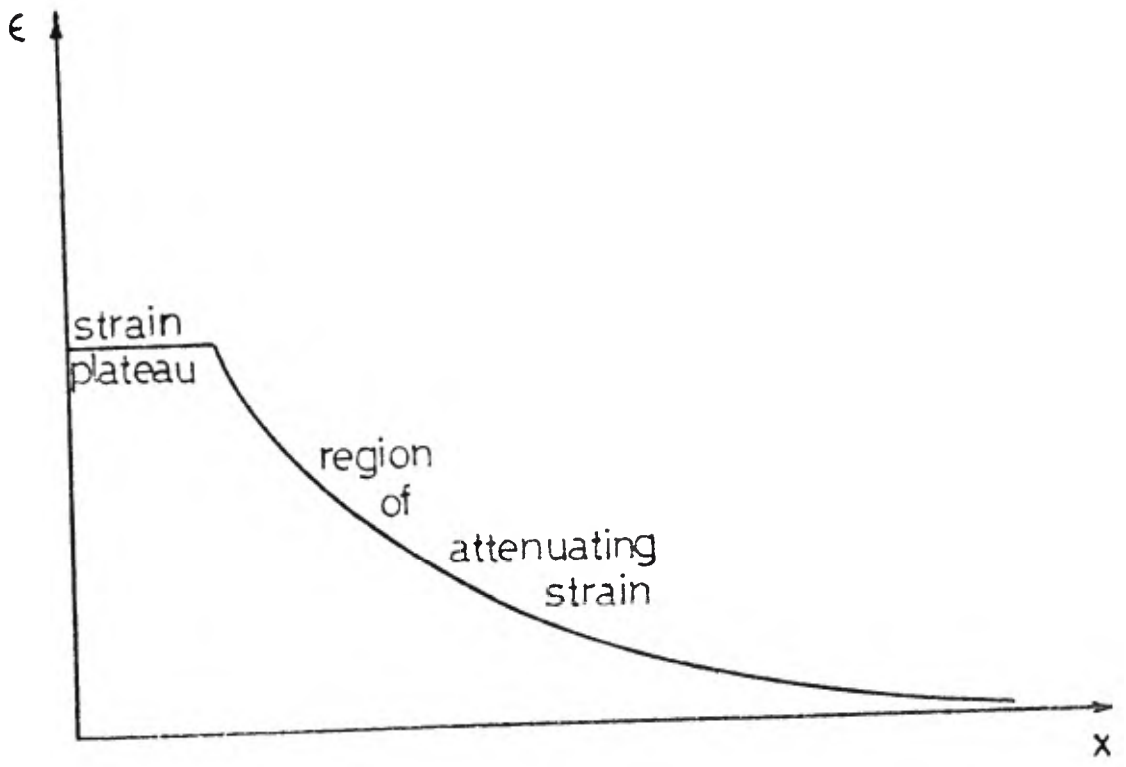


FIG. 2.1(a) Residual strain distribution as predicted by the Taylor-von Karman theory.

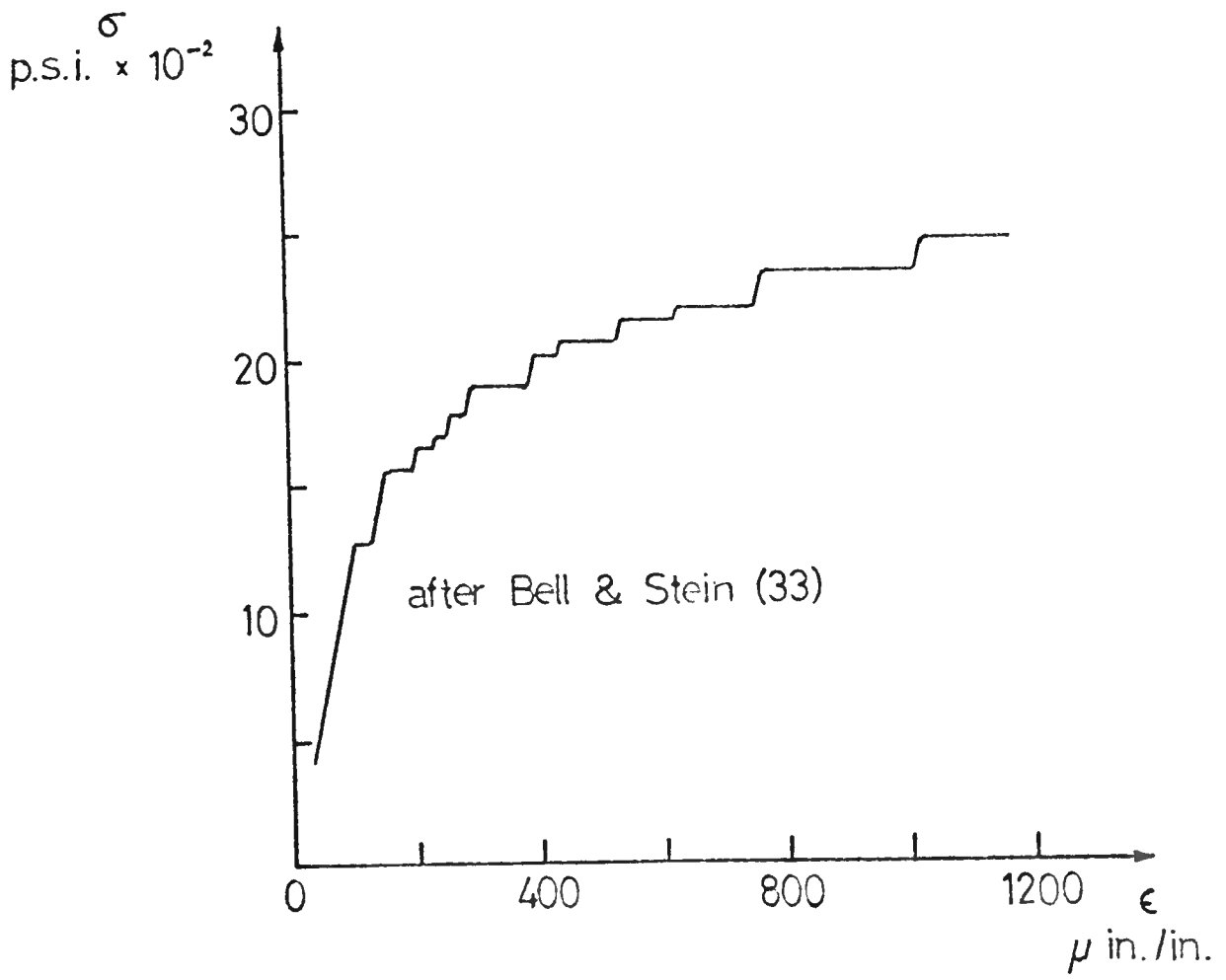


FIG. 2.1(b) Stress-strain curve for annealed aluminium. (Dead weight static compression test.)

C H A P T E R 3.

STRESS WAVES IN SOLIDS.

The one-dimensional theory of longitudinal wave propagation in rods is based on several simplifying assumptions, notably that inertial effects due to radial motion are negligible, so that the only non-zero component of stress is the axial one. As stated by Hopkins (59) in his account of this theory, its precise status is difficult to assess but clearly it becomes inadequate when applied to the propagation of pulses containing components of wavelength comparable with the transverse dimensions of the rod. Several attempts have been made (Hunter and Johnson (60), de Vault (38)) to determine the errors involved in the neglect of radial inertia, and it appears that these errors may be such as to make it seem that a rate independent material is rate-sensitive. Experiments involving longitudinal pulse-propagation have been criticized on these grounds by Craggs (53, 54).

The difficulties discussed above are eliminated by the use of torsional waves in thin-walled tubes and an exact one-dimensional theory can then be derived. This theory is summarized in the present section, which is based on Hopkins's (59) treatment of the approximate theory of longitudinal wave propagation in rods.

Characteristic Curves and Equations.

It is advantageous at this point to give a brief

general outline of characteristic curves and equations because the behaviour of stress waves is most easily described in terms of them.

Consider the equations :

$$L_i \equiv \sum_{j=1}^{n} \left(a_{ij} \frac{\partial u^j}{\partial x} + b_{ij} \frac{\partial u^j}{\partial t} \right) + c_i = 0 \qquad (3.1)$$

$$(i,j = 1,2 \ldots n)$$

These can be more easily represented by :

$$L_i \equiv a_{ij} u^j_x + b_{ij} u^j_t + c_i = 0 \qquad (3.2)$$

$$(i,j = 1,2 \ldots n)$$

(Here it is understood that the free suffix i can have any value from 1 to n ; the repeated suffix and index j implies summation over the complete range of values $1 \ldots n$; the suffices x and t denote partial differentiation with respect to these variables).

The problem to be solved is as follows :-

For a specific solution $S = * u(x,t)$, with n components $* u^i(x,t)$, can there exist real curves, C, in the (x,t) - plane with equations $x = x(s)$, $t = t(s)$, (3.3) where s is a suitable parametric co-ordinate, such that linear combinations of (3.2), say $L = \lambda_i L_i$, can be found in which differentiations occur only with respect to s, i.e. tangential not transverse to the curves C ?

In other words can there be λ_i's such that :

$$L = \lambda_i L_i \equiv \alpha_i \, {}^*u^i_s + \beta = 0 \qquad (3.4)$$

where $u^i_s = x_s u^i_x + t_s u^i_t$ (3.5)

The comparison of the L in (3.2) and (3.4) shows that :

$$\begin{aligned} \lambda_i a_{ij} &= \alpha_j x_s \\ \lambda_i b_{ij} &= \alpha_j t_s \\ \lambda_i c_i &= \beta \end{aligned} \qquad (3.6)$$

From (3.6) we can eliminate α_j giving :

$$\lambda_i (t_s a_{ij} - x_s b_{ij}) = 0 \qquad (3.7)$$

Also substituting in (3.4) from (3.6) gives us :

$$Lx_s \equiv \lambda_i (a_{ij} u^j_s + c_i x_s) = 0 \qquad (3.8)$$

and $Lt_s = \lambda_i (b_{ij} u^j_s + c_i t_s) = 0$

These last two equations are not independent because of (3.7) and hence the condition for the existence of curves Σ is the compatibility of the (n + 2) equations of (3.7) and (3.8) for the λ_i's.

This means that all nth order determinants of the matrix of the coefficients in (3.7) and (3.8) must vanish.

Firstly from (3.7)

$$| a_{ij} t_s - b_{ij} x_s | = 0 \qquad (3.9)$$

This determinantal equation is equivalent to an nth degree algebraic equation for the slope ϕ of the curve Σ in the (x,t) plane, i.e.

$$\phi = \frac{dx}{dt} = \frac{\lambda_i}{t_s} \qquad (3.10)$$

If the n roots of (3.9) are real and distinct then the system (3.2) is called totally hyperbolic and there exist n real families of characteristics C_ν satisfying the ordinary differential equations :

$$\frac{dx}{dt} = \phi_\nu \quad (\nu = 1,2 \ldots n) \qquad (3.11)$$

and just one member of each family will pass through any general point of the (x,t) - plane.

These values of ϕ_ν depend upon the coefficients a_{ij} (x, t, $^*u$) and b_{ij} (x, t, $^*u$) and so depend upon the specific solution $^*u$ that has been chosen. Hence the characteristics are not fixed curves in the (x,t)-plane. However, the above result applies for any solution U and so it can be said that $\phi_\nu = \phi_\nu$ (x, t, u).

Secondly, taking any (n - 1) equations of (3.7) and either of (3.8), an nth order determinantal equation is obtained after elimination of the λ_i's which expresses the linear combination of the system (3.2) in the form :

$$A_{\nu i}\, u^i_s + B_\nu\, x_s = 0 \quad \text{on} \quad C_\nu \quad (\nu = 1, 2 \ldots n) \qquad (3.12)$$

$A_{\nu i}$ and B_ν are known functions of x, t and U, and det. $(A_{\nu i}) \neq 0$.

This can also be written $A_{\nu i}\, u^i_s + B_\nu\, \phi_\nu\, t_s = 0$, and equations (3.10) and (3.12) are the characteristic equations for the original differential equations (3.2).

Equations (3.12) are equivalent to differential relations along the characteristics :

$$A_{vi}\, du^i + B_v\, dx = 0 \quad \text{on} \quad C_v \tag{3.13}$$

If the values of U are given on some non-characteristic curve R, then from any point $P(x,t)$, n characteristics may be traced back to intersect R in n points, $P_v(x_v, t_v)$. To a first approximation, if P is sufficiently close to all P_v from (3.13) :

$$A_{vi}\, \Delta u^i + B_v\, \Delta x = 0 \quad \text{on} \quad C_v \tag{3.14}$$

$$\Delta u^i = u^i(P) - u^i(P_v)$$

$$\Delta x = x(P) - x(P_v)$$

A_{vi}, B_v are given values at P_v.

The increments Δu^i are calculable from (3.14) as:

$\Delta u^i = \gamma_{iv}\, \Delta x^v$ (summation over v) on C_v, where the value of γ_{iv} is known.

Having given this brief outline of the theory of characteristics, the propagation of torsional stress waves in solids will now be studied and in particular the two theories which could be applied, i.e. strain-rate-dependent and strain-rate-independent.

Torsional stress waves.

It is convenient to use Lagrangian co-ordinates for defining the system.

Let $\theta(x,t)$ be the rotation of the cross-section at the distance x, at the time t.

Then $\theta(x + \delta x, t)$ is rotation at distance $x + \delta x$ and the same time.

The shear strain is given by

$$\text{Lt}_{\delta x \to 0} \left\{ \frac{r\,\theta(x + \delta x, t) - r\,\theta(x,t)}{\delta x} \right\} \quad \text{which becomes}$$

$$r \frac{\partial \theta}{\partial x} (x,t) \tag{3.15}$$

The velocity of a particle at a distance x, at time t, is given by

$$v = r \frac{\partial \theta}{\partial t} (x,t) \tag{3.16}$$

By differentiating (3.15) with respect to t and (3.16) with respect to x we obtain the continuity equation :

$$\frac{\partial \gamma}{\partial t} = \frac{\partial v}{\partial x} \tag{3.17}$$

The equation of motion for a section of the bar reduces to :

$$\frac{\partial \tau}{\partial x} = \rho \frac{\partial v}{\partial t} \tag{3.18}$$

These two equations (3.17) and (3.18) together with a constitutive equation :

$$F(\tau, \dot{\tau}, \ddot{\tau}, \ldots; \gamma, \dot{\gamma}, \ddot{\gamma}, \ldots) \tag{3.19}$$

form the basis of formulation of the theories of stress wave propagation.

In the following, unloading is not envisaged, the material undergoing elastic - plastic loading only.

<u>Strain - Rate Independent Theory.</u>

The constitutive equation which applies in this case is of the form :

$$\tau = f(\gamma) \tag{3.20}$$

hence for a given particle,

$$\frac{\partial \tau}{\partial \gamma} = f'(\gamma) = T \text{ , the tangent shear modulus} \tag{3.21}$$

Eliminating τ between (3.20) and (3.16) we obtain :

$$\frac{\partial \tau}{\partial \gamma} \cdot \frac{\partial \gamma}{\partial x} = \rho \frac{\partial v}{\partial t}$$

or

$$T \frac{\partial \gamma}{\partial x} = \rho \frac{\partial v}{\partial t} \tag{3.22}$$

Writing $c = (T/\rho)^{1/2}$ assuming $T > 0$ (3.22) can be rewritten

$$\frac{\partial \gamma}{\partial x} - \frac{1}{c^2} \cdot \frac{\partial v}{\partial t} = 0 \tag{3.23}$$

we now have as a basic set of equations, (3.23) and (3.17) :

$$L_1 = \frac{\partial \gamma}{\partial t} - \frac{\partial v}{\partial x} = 0$$

$$L_2 = \frac{\partial \gamma}{\partial x} - \frac{1}{c^2} \frac{\partial v}{\partial t} = 0 \tag{3.24}$$

If the stresses are in the elastic range then $T = G$, the elastic shear modulus and hence $c = (G/\rho)^{1/2} = c_e$ the wave velocity for the propagation of torsional elastic disturbances in a bar. In addition all variables satisfy the one-dimensional linear wave equation :

$$\left(\frac{\partial^2}{\partial x^2} - \frac{1}{c^2} \frac{\partial^2}{\partial t^2}\right)(\theta, \gamma, v, \tau) = 0$$

If the stress is beyond the elastic range then c is no longer constant but depends on the stress amplitude. The general discussion of the system (3.24) requires the use of the method of characteristics but the special situation involving the small perturbation of an existing disturbance can be separately treated. The perturbation considered is a small dynamic plastic loading of a region already in a plastic stress field.

Initial disturbance static and uniform:

$$\gamma = \gamma_1 = \text{const.}$$
$$\tau = \tau_1 = f(\gamma_1)$$
$$r\theta = r\theta_1 = \gamma_1 z \qquad (3.25)$$

Let small perturbation be denoted by $r\,\Delta\theta\,(z,t)$

so that
$$r\theta = r\theta_1 + r\Delta\theta$$
$$\gamma = \gamma_1 + \Delta\gamma \qquad (3.26)$$

From equation (3.23) $\left(\frac{\partial^2}{\partial z^2} - \frac{1}{c^2(\gamma)} \cdot \frac{\partial^2}{\partial t^2}\right)\theta = 0$ and hence it follows that $\Delta\theta$ satisfies the same equation.

$$c(\gamma) = c(\gamma_1 + \Delta\gamma) = c(\gamma_1) + \left(\frac{dc}{d\gamma}\right)_{\gamma=\gamma_1} \Delta\gamma + \ldots \qquad (3.27)$$
$$= c_1 + \frac{dc_1}{d\gamma_1}\Delta\gamma + \ldots$$

and so
$$\left(\frac{\partial^2}{\partial z^2} - \frac{1}{c^2} \cdot \frac{\partial^2}{\partial t^2}\right)\Delta\theta = 0 \qquad (3.28)$$

can be expressed in the form :

$$\left(\frac{\partial^2}{\partial z^2} - \frac{1}{c_1^2} \cdot \frac{\partial^2}{\partial t^2}\right)\Delta\theta + \frac{2}{c_1^3} \cdot \frac{dc}{d\gamma_1} \cdot \Delta\gamma \cdot \frac{\partial^2 \Delta\theta}{\partial t^2} + \ldots = 0 \qquad (3.29)$$

i.e.
$$\left(\frac{\partial^2}{\partial z^2} - \frac{1}{c_1^2} \cdot \frac{\partial^2}{\partial t^2}\right)\Delta\theta = 0 \qquad (3.30)$$

if second order terms and higher are neglected.

In (3.30) c_1 is independent of $\Delta\theta$ and is a constant depending only on the initial uniform strain γ_1.

Thus $\Delta\theta$ satisfies a linear wave equation and c_1 is called the acoustic plastic wave velocity. Any small perturbation propagates unchanged in size and shape, to a first approximation, with this velocity. This velocity $c_1 = (T/\rho)^{1/2}$

and so for any appreciable value of initial plastic strain e_1 / e_e will be considerably less than unity, say of the order of 0.1.

If the initial disturbance is dynamic and non-uniform a similar analysis can be undertaken at a particular point x_o and time t_o to linearise the equations. The same result is observed but obviously only applies locally.

Returning to the general case and the system of equations (3.24) we form the linear combination :

$$L \equiv L_1 + \lambda L_2$$

$$\equiv \left(\frac{\partial \gamma}{\partial t} - \frac{\partial v}{\partial x}\right) + \lambda \left(\frac{\partial \gamma}{\partial x} - \frac{1}{c^2} \cdot \frac{\partial v}{\partial t}\right) = 0$$

$$\text{or} \quad L \equiv \left(\lambda \frac{\partial}{\partial x} + \frac{\partial}{\partial t}\right)\gamma + \left(- \frac{\partial}{\partial x} - \frac{\lambda}{c^2} \frac{\partial}{\partial t}\right) v = 0 \qquad (3.31)$$

In this expression if the two dependent variables γ and v are both differentiated in the same direction given by the ratio $\frac{dx}{ds} : \frac{dt}{ds}$ then :-

$$\lambda : 1 = -1 : -\lambda/c^2 = \frac{dx}{ds} : \frac{dt}{ds} \qquad (3.32)$$

Hence $\frac{dx}{dt} = \lambda$, $\lambda = \pm c$ and there are two real distinct characteristic directions (which depend on the solution through γ) so that the system (3.24) is totally hyperbolic. The characteristic equations are now obtained from (3.31) and (3.32).

$$L \frac{dt}{ds} = \frac{d\gamma}{ds} - \frac{dt}{dx} \cdot \frac{dv}{ds}$$

$$\frac{d\gamma}{ds} \mp \frac{1}{c} \frac{dv}{ds} = 0 \quad \text{on} \quad \frac{dx}{dt} = \pm c \quad \text{respectively.}$$

For this particular case it is convenient to introduce parameters α and β such that $x = x(\alpha)$ and $t = t(\alpha)$ for a member of the first family of characteristics $\frac{dx}{dt} = +c$ and $x = x(\beta)$, $t = t(\beta)$ for the second family. Then the families are represented by the curves C_+ and C_- Fig. (3.4a) and

$$\frac{d\gamma}{d\alpha} - \frac{1}{c}\frac{dv}{d\alpha} = 0 \quad \text{on} \quad C_+$$

$$\frac{d\gamma}{d\beta} + \frac{1}{c}\frac{dv}{d\beta} = 0 \quad \text{on} \quad C_- \qquad (3.33)$$

These equations may be integrated along the characteristics to give :

$$v - \int_o^\gamma c(\gamma)d\gamma = R_1(\beta) \quad \text{on} \quad C_+ \ (\beta \text{ const.})$$

$$v + \int_o^\gamma c(\gamma)d\gamma = R_2(\alpha) \quad \text{on} \quad C_- \ (\alpha \text{ const.}) \qquad (3.34)$$

In order to compare the predictions of this theory with the strain-rate dependent theory, let us take the problem of a long thin-walled tube, one end of which is suddenly twisted with constant uniform velocity of ω_1.

Let $V_1 = r\omega_1$

It has already been shown that no disturbance can travel faster than the elastic wave velocity c_e so that the +ve (x,t) region of the (x,t) - plane is divided by the leading wave front $x - c_e t = 0$ into an undisturbed region $x - c_e t > 0$ and a disturbed region $x - c_e t < 0$

$x = c_e t$ is the first C_+ characteristic Fig.(3.4b)

Equations (3.34) apply to the complete region and it can be seen that every C_- characteristic must pass through a section of the undisturbed region where the variables $(\theta, v, \gamma, \tau)$

are zero. Consequently $R_2(\alpha) = 0$.

Hence along a C_+ characteristic, which is intersected at every point by some negative characteristic, the following relations apply :

$$v - \int_0^{\gamma} c(\gamma)d\gamma = R_1(\beta)$$

$$v + \int_0^{\gamma} c(\gamma)d\gamma = 0$$

Consequently v and $\int_0^{\gamma} c(\gamma)d\gamma$ are constant on each positive characteristic and $v = -\int_0^{\gamma} c(\gamma)d\gamma$, $= I(\gamma)$, a function of β only.

Since $c(\gamma) > 0$ it follows that $I(\gamma)$ has a unique solution for γ. Therefore γ and hence τ $[= f(\gamma)]$ are constant on each positive characteristic.

Thus v, γ and τ are all constant for a particular characteristic but vary from one characteristic to another.

The slope of the characteristic is $\frac{dx}{dt} = c(\gamma)$ and so each positive characteristic has a constant slope and all negative characteristics cross a given positive characteristic at a constant slope. The positive characteristics are, therefore, a family of straight lines in the (x,t) - plane. The present problem consists of a variable velocity increasing from 0 to V_1 in zero time. Consequently the initial points of the positive characteristics must all be coincident, Fig. (3.1c). The slope of each characteristic is $x/t = c(\gamma)$ and it can be readily seen that for the initial velocity V_1, there must be a maximum strain γ_1. By taking any instant of time one can obtain the strain distribution along the tube and it appears as in Fig. (3.1d). Note that the shape of this curve is independent of time though the axial extent increases linearly with time.

Strain - Rate Dependent Theory.

For time - dependent behaviour the constitutive equation is no longer simply $f(\gamma) = \tau$ but must include the time derivatives of τ and/or γ. This means that τ can no longer be eliminated between equation (3.18) and the constitutive equation and so we have to deal with a system of three equations instead of two.

Various constitutive equations have been put forward for longitudinal waves and the most general one involving stress, strain and their first time derivatives is that proposed by Cristescu (61) and Lubliner (62) :

$$\frac{\partial \epsilon}{\partial t} = \phi(\sigma, \epsilon) \frac{\partial \sigma}{\partial t} + \psi(\sigma, \epsilon)$$

A particular case of this equation is that put forward by Malvern (6,11) in which the function ϕ is taken as a constant. In terms of shear stress and strain, Malvern's equation can be written :

$$G \frac{\partial \gamma}{\partial t} = \frac{\partial \tau}{\partial t} + g(\tau, \gamma)$$

and this relation is assumed for discussion of time-dependent behaviour.

The system of basic equations is :

$$\begin{aligned} L_1 &\equiv \frac{\partial \gamma}{\partial t} - \frac{\partial v}{\partial x} = 0 \\ L_2 &\equiv \rho \frac{\partial v}{\partial t} - \frac{\partial \tau}{\partial x} = 0 \\ L_3 &\equiv G \frac{\partial \gamma}{\partial t} - \frac{\partial \tau}{\partial t} - g(\tau, \gamma) = 0 \end{aligned} \qquad (3.35)$$

$$L = L_1 + \lambda L_2 + \mu L_3$$

$$= \left(\frac{\partial \gamma}{\partial t} - \frac{\partial v}{\partial x}\right) + \lambda\left(\rho \frac{\partial v}{\partial t} - \frac{\partial \tau}{\partial x}\right) + \mu\left(\theta \frac{\partial \gamma}{\partial t} - \frac{\partial \tau}{\partial t} - g(\tau,\gamma)\right)$$

$$\text{i.e. } L = (1 + \mu\theta)\left(\frac{\partial}{\partial t}\right)\gamma + \left(-\frac{\partial}{\partial x} + \lambda\rho\frac{\partial}{\partial t}\right)v + \left(-\lambda\frac{\partial}{\partial x} - \mu\frac{\partial}{\partial t}\right)\tau - \mu g = 0 \qquad (3.36)$$

If the variables γ, v, τ are differentiated in the same direction given by the ratio $\frac{dx}{ds} : \frac{dt}{ds}$ then :

$$0 : 1 + \mu\theta = -1 : \lambda\rho = -\lambda : -\mu = \frac{dx}{ds} : \frac{dt}{ds}$$

There are, therefore, three different solutions for this ratio :

$$\frac{dx}{dt} = 0 \text{ when } 1/\lambda = 0, \quad \lambda/\mu = 0$$

$$\frac{dx}{dt} = \pm c_e \text{ when } \lambda = \mp(\theta\rho)^{-1/2}, \ \mu = -1/\theta \qquad (3.37)$$

c_e = elastic wave speed.

The characteristic equations are now obtained from (3.36) and (3.37) thus :

$$\theta\frac{d\gamma}{ds} - \frac{d\tau}{ds} - g(\tau,\gamma)\frac{dt}{ds} = 0 \text{ on } \frac{dx}{dt} = 0$$

$$\frac{d\tau}{ds} - \rho c_e\frac{dv}{ds} + g(\tau,\gamma)\frac{dt}{ds} = 0 \text{ on } \frac{dx}{dt} = +c_e \qquad (3.38)$$

$$\frac{d\tau}{ds} + \rho c_e\frac{dv}{ds} + g(\tau,\gamma)\frac{dt}{ds} = 0 \text{ on } \frac{dx}{dt} = -c_e$$

The families of characteristics are parallel straight lines with equations $x = \text{const.}$, $x - c_e t = \text{const.}$, $x + c_e t = \text{const.}$

and shown in Fig. (3.2a) being designated C_0 , C_+ and C_- respectively.

The characteristics are fixed in space and do not depend on the particular solution. They correspond to the paths of linear elastic disturbances from which we find the special feature that a small perturbation on an existing disturbance is always propagated at the elastic wave velocity.

If we turn to the general constitutive equation replacing σ, ϵ by τ, γ then the same solution (3.38) holds if we replace θ by τ/ϕ and ε by ψ/ϕ . However the characteristics are now given by $\frac{dx}{dt} = 0, \; + (\rho\phi)^{-1/2} - (\rho\phi)^{-1/2}$ or $+c$, $-c$. In other words the characteristics are similar to those from the rate-independent theory, no longer fixed but depending on the solution through $\phi(\tau, \gamma)$.

Returning to the Malvern type constitutive equation, ε must represent the quasi-static stress-strain relation when $\frac{d\tau}{dt}$, $\frac{d\gamma}{dt}$ are zero so that dynamic stresses in excess of the quasi-static stress for a given strain are possible, though relaxation will occur after a time. Thus the strain-rate dependent behaviour does not show the strain plateau of the rate-independent solution. However, as Hopkins has shown, the two solutions give the same result if either the strain rate sensitivity is small, i.e. ε is very large except in the neighbourhood of the quasi-static stress-strain curve, or the time tends to infinity; the strain plateau must therefore, reappear after sufficient time has elapsed.

Demonstrating the use of the rate dependent set of characteristics, the same problem as before will be used, i.e. constant impact velocity.

Again the leading elastic wave front divides the (x,t) - plane into two regions, and immediately behind the wave front;

$$d\tau = \rho c_e\, dv = -g(\tau,\gamma)dt \quad \text{on} \quad x = c_e t$$

Integrating the third of equations (3.38) across the leading wave front we obtain

$$\tau + \rho c_e v = -\int g(\tau,\gamma)dt = 0 \quad \text{for a steep wave.}$$

Thus the increments of τ and v along the wave front are related by $d\tau + \rho c_e dv = 0$.

Eliminating dv gives :

$$2d\tau = -g(\tau,\gamma)dt = -g(\tau,\tau/\beta)dt \quad \text{on} \quad x = c_e t$$

$$\therefore \quad t = 2\int_{\tau}^{\tau_o} \frac{d\tau'}{g(\tau',\tau'/\beta)} \qquad (3.39)$$

where τ_o = stress at $x = 0$, $t = 0$.

This equation describes the stress relaxation along the leading elastic wave front.

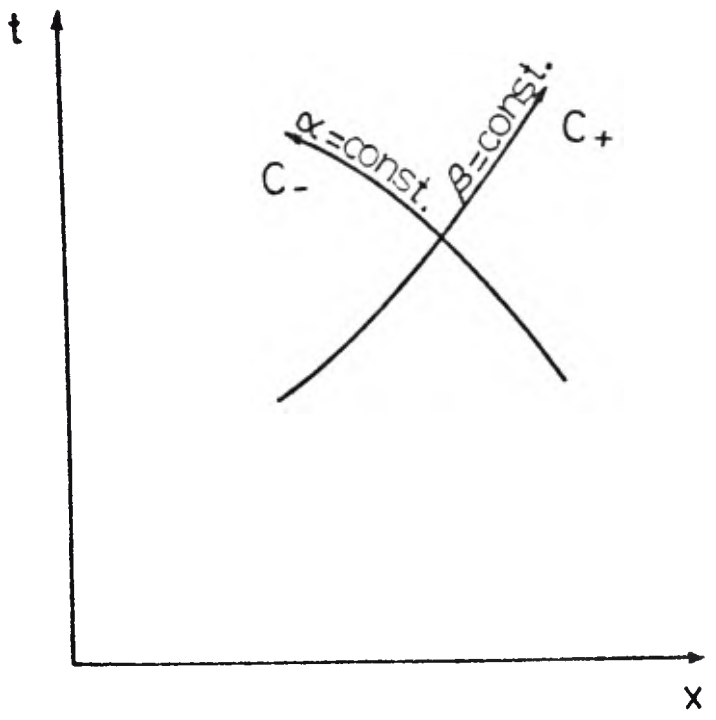
For the given problem $v = V_1$ for $t > 0$ and our boundary conditions are v along $x = 0$, and τ, γ, v along the leading elastic wave front; as we have shown $\tau = -\rho c_e v$ and τ is known from (3.39).

At the origin, O, all variables are known, Fig.(3.2a).

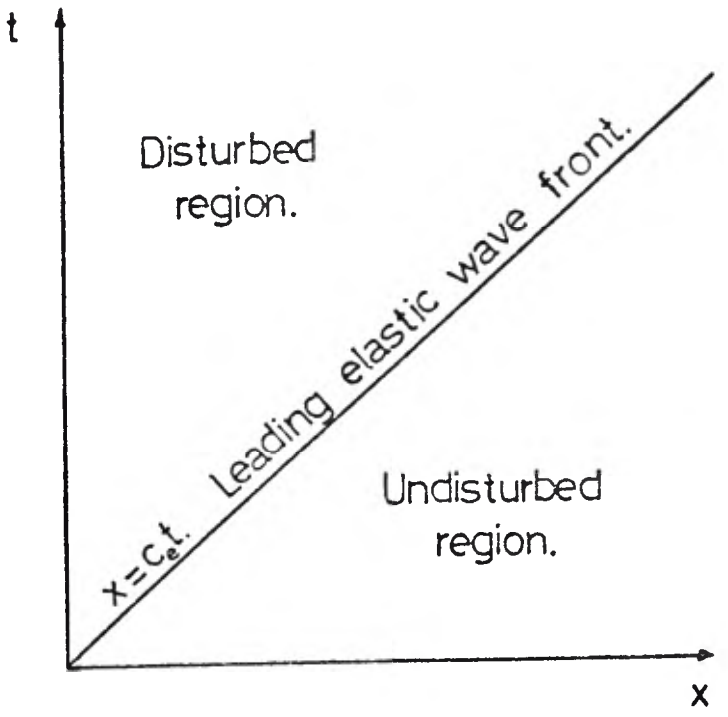
Consider points P_{rr} $(0, r\,\Delta t)$, $(r = 1,2 \ldots)$ on the t axis where Δt is sufficiently small. P_{mn} is the point of intersection on the C_+ characteristic through $(0, m\,\Delta t)$ with the C_- characteristic through $(0, n\,\Delta t)$. The unknown data at P_{11} are found from the differential characteristic relations applied to segments $P_{11}\ P_{00}$ and $P_{11}\ P_{01}$. The unknown data at P_{12} are supplied from the same relations applied to $P_{12}\ P_{11}$, $P_{12}\ P_{01}$, and $P_{12}\ P_{02}$ and so on along C_+. Data at P_{22} determined

from relations on F_{22} F_{11} , F_{22} F_{12} and so on along C_+ . By continuing the process the whole solution can be built up.

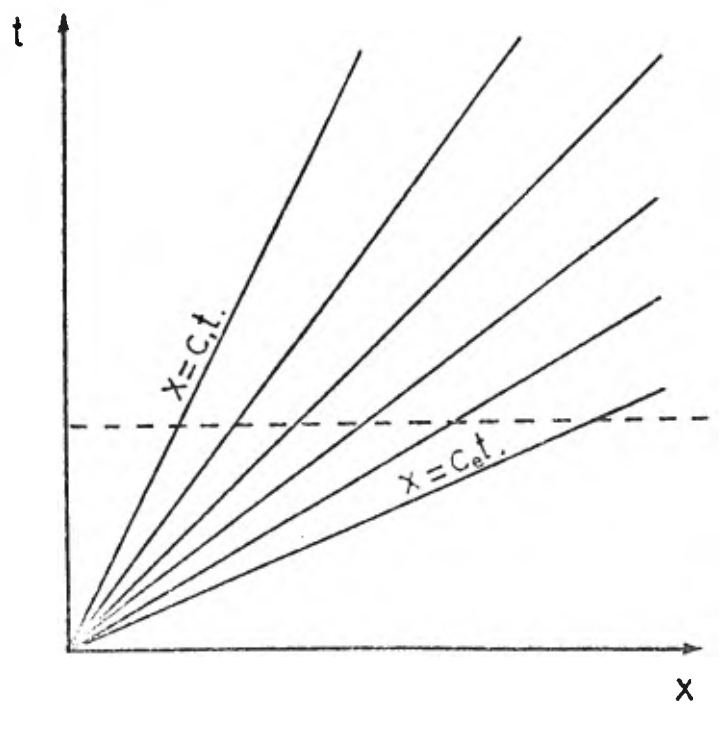
The strain distribution is shown in Fig. (3.2b).



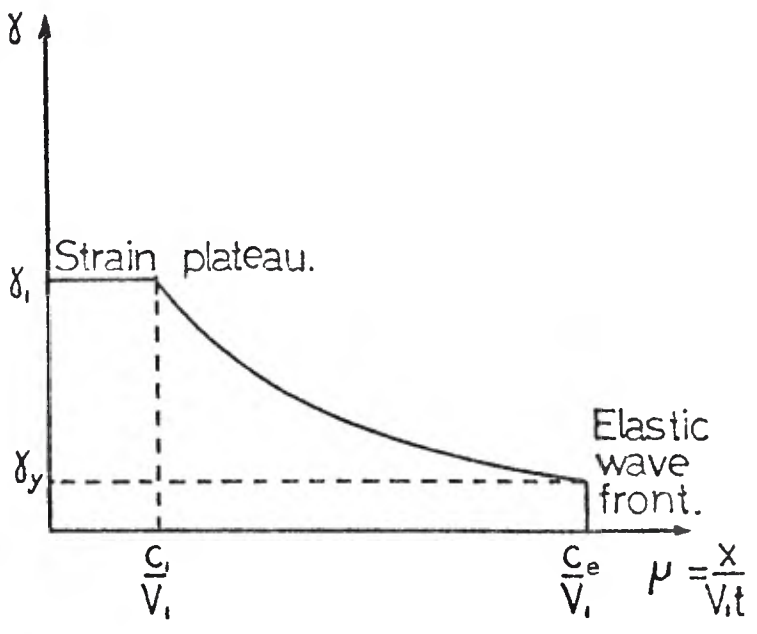
(a) Characteristic Curves.



(b) Leading elastic wave front.

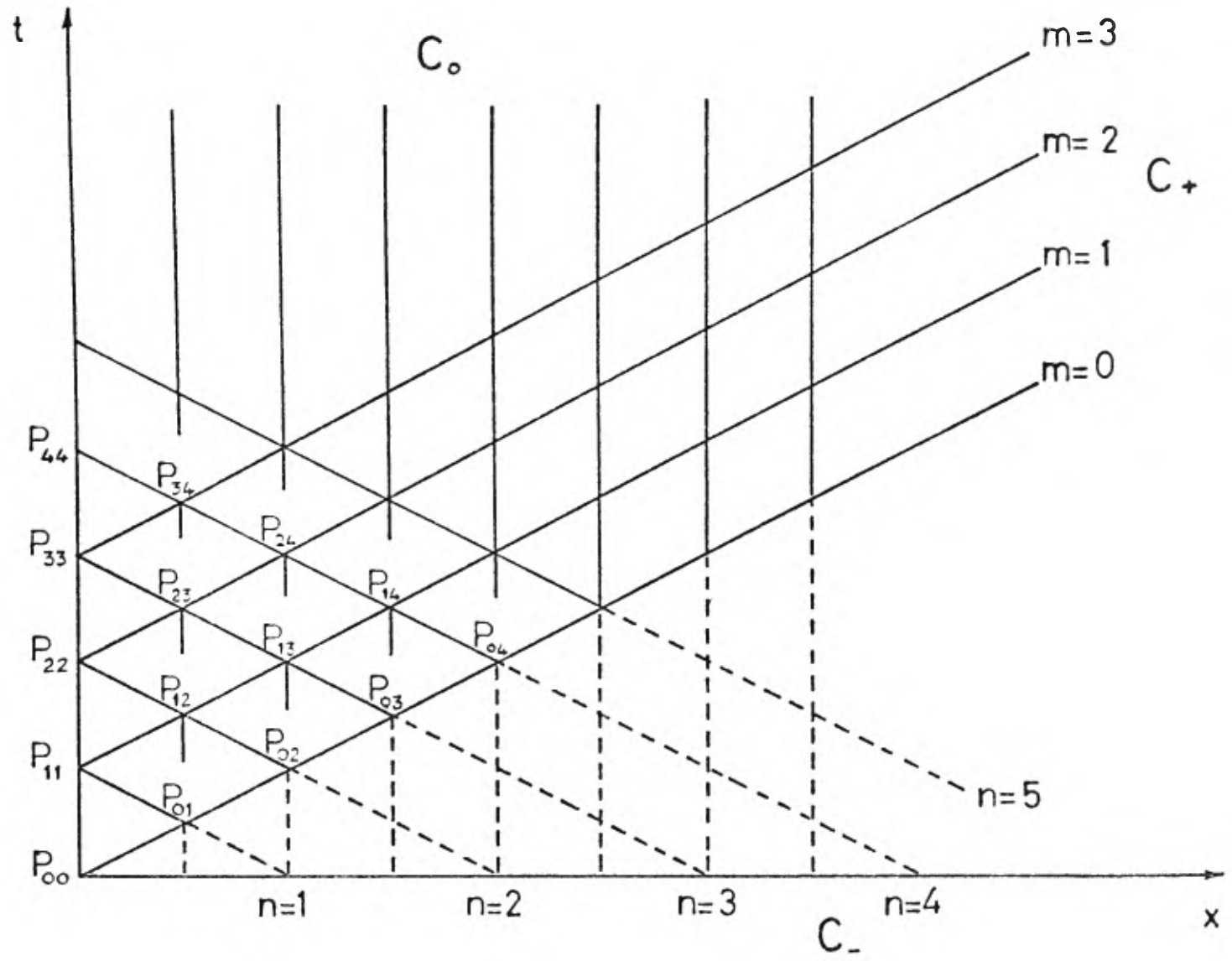


(c) Centered fan of characteristics.

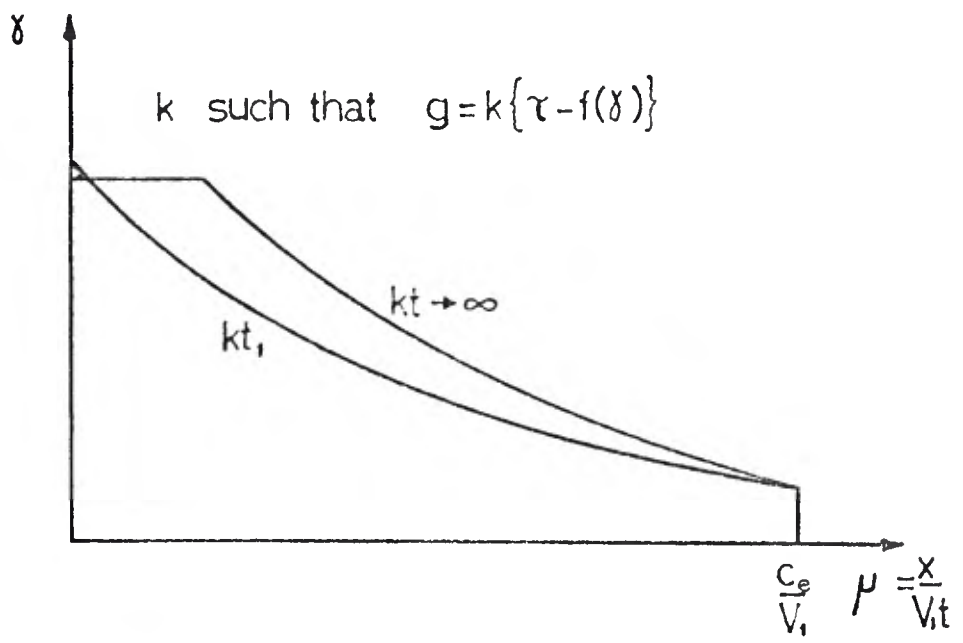


(d) Strain variation along tube.

FIG. 3.1 Strain-rate Independent Theory : Characteristics and strain distribution.



(a) Characteristics.



(b) Strain variation along tube.

FIG. 3.2 Strain-rate Dependent Theory: Characteristics and strain distribution.

C H A . T E R 4.

WAVE PROPAGATION - APPARATUS.

General.

It was shown in Chapter 3 that the greatest single difference between the strain-rate dependent and strain-rate independent theories of plastic wave propagation is in their predictions concerning the propagation of a small increment of stress superimposed upon a plastic stress field. According to the former, the increment will propagate with the elastic wave speed, while the latter predicts a much lower speed, assuming a stress-strain curve concave towards the strain axis. Thus the primary purpose of the experimental set-up was to measure the speed of propagation of such a stress increment. In order to avoid difficulties pointed out in criticisms of previous incremental stress propagation studies, it was decided that the stress system should be torsional, applied to thin-walled tubes, and that the specimens should be continuously strained up to, and during, the application of the increment.

The apparatus was designed round a standard Avery 6609 Torsion Testing Machine, so that this could be used to provide the 'static' or 'slowly increasing' torque to the specimen. This machine had a working length of 45 ins. and this was a major factor in deciding upon the rest of the design.

Dynamic testing of materials in torsion is still in its infancy, due to the fact that the rapid application of a pure torque is extremely difficult. The more obvious ways of applying such a load usually involve a net transverse or axial force acting on the apparatus, and even if such a force is present for

only a short time, the pure torque requirement is not met. The elastic shear wave velocity in materials is less than that of longitudinal waves so, even if the position of the specimen were made remote from the 'torque' application point, any axial stress that happened to be set up would be sure to reach the specimen first and thus upset any calculations based on pure torque. The velocity of flexural waves, too, approaches the torsional wave speed for wavelengths short compared with the bar dimensions. When a machine is designed for the purpose of measuring material properties, such axial or transverse stresses can be made small compared with the shear stresses and the calculated material properties will not then be significantly affected by them. However when dealing with incremental stresses and time measurement it is necessary to be sure that the speeds measured are those of the shear waves and that no initial longitudinal stresses are present to alter the 'static' stress distribution before the increment arrives.

Consequently many of the previous methods of dynamic torque application used for material property investigations were of little value when considering this problem of increment production and propagation. The majority of these used some form of flywheel and clutch. ((Itihara (63), Greene and Stout (64), Work and Lolan (65), Calvert (66), Chang (67) and Hodierne (68))). Here the force applied to the system would be longitudinal as the clutch was brought home. Taylor and Tadros (69) used a weight dropping on to a torque arm so that their unwanted force was transverse.

A different approach to the problem was needed whereby energy was stored with radial symmetry either in the plane at

which the energy had to be transferred to the bar system or in the system itself. Pope, Vreeland, Jr. and Wood (70), Baker and Yew (56) and Bowery and Pugh (35) each devised a way of doing this. Their systems used, respectively, a glass disc whose connection to 'earth' was broken by an electric discharge, a friction clamp held round the bar by hydraulic pressure and released by shooting out a section of the jack with an air gun, and a concentric brittle specimen which broke at a given torque. It was decided that the friction clamp was best suited to the present work, as it permits continuous straining of the specimen up to the instant of application of the dynamic torque increment.

Before the friction clamp idea was finally adopted, trials were carried out on a system employing a brittle ring. This ring was to fit around the loading bar, connected at its outside diameter to a rigid support. Several brittle plastics were moulded and tested in shear for strength and ductility. None proved to have the required properties. Cast iron was the next material used and discs $\frac{1}{2}$ in. thick were machined to reduce the thickness at a diameter of 1 in. to only 1/16 in. This was done by a V-groove on each side of the disc and it was hoped that a crack would propagate round the ring when the material failed. However, in order to transmit a torque from the loading bar to the cast iron the centre of the disc had to be machined with either slots or flats. This introduced stress concentrations and it was found that the discs always fractured here rather than at the groove. Although this produced a drop in torque, and hence an incremental increase in the specimen, the whole of the torque held by the cast iron was not given up nor was the size of the increment repeatable. For this reason no further

attempts were made to design a brittle ring apparatus. Instead the work was concentrated on the design and development of a friction clamp.

Since the elastic torsional wave speed in steel and aluminium is about 120,000 in./sec., it can be seen that specimens several inches long would be needed in order that time measurements and hence wave speeds could be found. With 45 ins. available on the torsion machine it was decided that the specimens should be 10 ins. and the transmitter bars should be identical with a length of 17½ ins. The clamp was positioned at the end of one of the bars, next to the specimen. Fig. (4.1) illustrates the system and its idealized behaviour during a test.

The Transmitter Bars.

The Transmitter Bars, which had to remain elastic even when the specimens were strained well into the plastic region, were made from Hadfields Speon En 25 steel bar, turned down to 0.846" o.d. End fixings were welded on to the ends of the bars so that they would fit the Avery machine. The passing of the stress pulse through the bar was measured by means of strain gauges, positioned as shown in Fig. (4.1).

The Friction Clamp and Release Mechanism.

As has already been indicated, it was decided to use a friction clamp to generate the incremental torque. The design of this clamp and its release mechanism, which posed considerable problems, was crucial to the success of the experiment. One of the chief requirements of the clamp was that the release time had to be very small, since it was necessary that the rise time of the torque increment should be small compared with the time taken for reflected waves to reach the strain gauge

stations. If this were not so analysis of the waves would be so complicated that valid results would be impossible to obtain. These considerations indicated a maximum allowable rise time of 50 μ sec.

A second important requirement was that the clamp should not apply any significant resultant force to the bars. A system such as that used by Baker and Yew (56) in which the bar is pressed against a nominally fixed cradle, involves statically indeterminate forces in addition to the required pure torque. It was therefore decided to design the clamp in such a way that both horizontal and vertical components of force would be statically determinate and as small as possible.

A diagram of the clamp and release system is shown in Fig. (4.2) and a photograph of the stand in position on the test rig is shown in Fig. (4.3). The clamp itself consists of a mild steel bridge piece A and a cradle B, turned to an inside diameter of 0.846", the diameter of the loading bar. Mild steel was used for both A and B, so that they were softer than the loading bar. Consequently when slipping takes place the parts A and B will become slightly worn or scored while the bar remains finely polished. The surfaces of the clamp and bar were mated by fixing the bar in a lathe, clamping the bridge piece and cradle round it and running the bar through the clamp using a grinding paste. The length, i.e. axial spread, of the clamp was $\frac{1}{2}$ in.

The cradle was fitted to the stand C by means of two bolts running in slots such that the horizontal position of the cradle could be adjusted by the two screws E. The stand fitted on to the torsion machine, being located in slots at the side of the machine bed. Thus the stand was fixed

laterally but could move to any axial position on the machine and had a certain amount of vertical adjustment. When setting up for a test the stand was placed in the correct axial position, the screws E were loosened and the height of the cradle B was adjusted by the bolts F . The correct position was when B just came into contact with the loading bar. Then the screws E were adjusted to fix the lateral position of B .

The uprights of the stand were made from steel 1" box section. The top horizontal member was an inverted - U section built up from 1/8" mild steel strip, and the lower horizontal member was 1" x ½" mild steel bar. The sections through which the feet screwed were made from 1" square bar and all joints were welded to ensure that the stand was as rigid as possible.

The clamp was pressed on to the loading bar in the following manner. High-tensile steel wire (piano wire) of diameter [illegible] or 0.040" was fastened to the frame by tightening screws G_1 . This clamp consisted of a flat mild steel plate 1/2" x 1" x 1/8" which was pressed on to the wire by two socket screws. The clamp at the other side of the frame was identical. There were no grooves or knurls machined on to these clamp faces, in order to minimise stress concentrations in the wire.

The free end of the wire was passed over the top of the bridge piece A , through holes in B and C , and then threaded through the pulley frame J round the two pulleys. Leaving the second pulley, the free end was passed back through C and B , round A again and clamped at the other side of the stand by screws G_2 .

In order to impose a force on the clamp, the wire

was tensioned by pulling down on the pulley frame. The vertical force was obtained by means of the nut N which turned on the slotted bolt I . This bolt was slotted so that it fitted keys in the stand's lower horizontal member, and hence resisted the turning moment applied to the nut N . The force was transmitted from the bolt I to the pulley frame by means of the dynamometer L which was used to measure the force in the wire. This will be described in more detail in the Instrumentation section.

The clamp has now been tensioned on to the loading bar and it can be seen that, if the stand adjustment stated previously had been carried out, the only vertical deflection of the bars would be due to the weight of the stand. This follows because, when the wire was tensioned, there was a compressive force in the vertical struts of the stand, which therefore shortened and lifted the stand off its feet. When the clamp was holding a torque there would be an additional horizontal force as can be seen from the force diagram, Fig. (4.2 Insert).

The rapid release of the clamp was obtained by loading up the wire to a load near to its breaking point, which had previously been measured on a Hounsfield Tensometer, and then nicking the wire at the point K with a pair of wire clippers. This caused the wire to break at that point, sending unloading waves along both halves of the wire up to the clamps at C_1 and C_2 . Thus the bridge piece was symmetrically unloaded, the symmetry being necessary to avoid a large lateral force on the loading bar.

By using 0.032" wire a clamp force of 450 lb. could

be obtained, resulting in a maximum 'held' torque of 150 lb-in.; the friction torque from 0.040" wire was 225 lb-in. from a clamp force of 675 lb. It will be noticed that no torque was actually applied to the system by the clamp but that the 'held' torque was obtained by rotation of one end of the loading bar - specimen assembly in the Torsion machine thus creating a friction torque. When the torque in the loading bar was increased above the value of the limiting friction torque, the specimen and second transmitter bar began to rotate and hence become strained. The fact that the wire was actually nicked to initiate the fracture made it possible to choose the moment of application of the incremental torque; thus the starting of the test did not depend on variations in the strength of the wire, which would have introduced some lack of control into the experiment.

The whole process of threading, tensioning and breaking the wire could be completed within a few minutes without unloading the specimen. This was a very useful facility when doing successive tests on single specimens, and would not have been possible had the experimental rig been designed on the lines of those of Convery and Pugh (55) or Pope, Vreeland and Wood (70).

Instrumentation.

The stress increment was detected by strain gauges as it passed down the bars. The gauges had to be small so that their axial spread was not big enough appreciably to smooth out the shape of the incremental wave. For this reason T.M.L. type PC-3 gauges were chosen as they had a gauge length of 3 mm. and, since the gauges, for torsional

measurement, were placed at 45° to the bar axis, the axial spread of the gauges was approximately 2 mm. This corresponds to a wave transit time of about 0.7 μ sec. Each PC-3 gauge consisted of two single strain gauges at 90° to each other placed one above the other. They were polyester backed.

It was necessary to measure both the incremental torque as a function of time and also the 'static' torque at the moment of incremental loading. As this latter torque was to be continuously varying it was necessary to record this as a function of time also. The same type of strain gauge was used for this purpose.

Incremental Torque Measurement.

The measurement of the incremental stresses involved a problem in obtaining a sufficient sensitivity. In order that the loading bars should remain elastic throughout the tests it was necessary that they should be strong. This meant that the stresses produced by the small incremental torque would be very small indeed in the input bar and even smaller in the output bar. In order to maximise the output from the gauges, it was decided to use as many gauges as possible, connected in series round the circumference of the bar. It was found that the highest even number of gauges that would fit round the bar was 10.

The adhesive recommended by the makers, their own P-2 adhesive, was used to attach the gauges to the bar, and because of the large number of gauges a special technique was developed for carrying out the operation. First of all a piece of 1" Sellotape was taken and the correct position

of each gauge was scribed on to it. The gauges were then stuck on to the tape with the side to be fixed to the bar facing upwards. Small pieces of Sellotape were then cut out and placed over the gauge leads to act eventually as insulation from the bars. One end of the strip was trimmed to fit the shape of the gauge which would become adjacent to it when in place on the bar. One drop of A-2 adhesive was then placed on each gauge and the Sellotape + strain gauge strip was wrapped round the bar at the appropriate place. The surface of the bar was treated by rubbing with emery paper, the last used being 600 grade, and then degreasing using acetone or trichlorethylene. When the gauges had been placed round the bar a further strip of Sellotape was wrapped tightly round several turns in order to obtain even pressure on the gauges. Then finally, cotton was tied tightly round the Sellotape to counteract any creep there might have been in the tape. The adhesive was then allowed to cure at room temperature.

With so many leads, 40 in all from the set of gauges, care had to be taken in connecting them up and insulating where necessary. An even number of gauges was required so that the gauges could be connected up in a complete bridge with in this case, five single gauges in each arm of the bridge. Initially the gauges were connected as shown in Fig. (4.4 (a)) the letters corresponding with the points shown on the circuit diagram. Fig. (4.5). Since all four arms of the bridge circuits were made up of gauges there was no necessity for any dummy gauges for temperature compensation, nor for extra resistances in the bridge.

Both bridges were run off the same voltage supply and, since there were also two paths for the gauge current in each, it was found that the lantern batteries, which were used initially, ran down extremely quickly. They were therefore replaced by a Stabilized Voltage Supply, Farnell Type 330 which was much more successful. It was possible to shunt a resistance across one, corresponding, arm of each bridge for calibration purposes.

One complication resulting from bridges made up completely of gauges is that one complete bridge may run at a different temperature from the other. Then with the same applied voltage, otherwise identical bridges would have differing currents due to the variation of resistance with temperature. This occurred here but only during the warm up period and was detectable by using the calibration resistance.

The maximum permissable gauge current was given as 25 mA., which necessitated 30v. across the bridge. This voltage was used at first but it was found that gauges 1, 2, 3 and 4 (see Fig. (4.4)) very quickly short circuited between layers. In other words there was a short circuit between the tension and compression arms of the bridge. The applied voltage was reduced to 24v. in an attempt to cure this fault. What happened was that similar gauges still shorted out but rather more slowly. The times taken to short out the gauges were approximately 15 mins. with 30v. applied and 1 hr. with 24v. applied. When the gauge arrangement was studied it was found that the top gauge of the pair 1 had a voltage level of about 19v. (24v. applied) whereas the

lower gauge had a voltage level of only about 1v. Consequently the voltage difference between gauge layers was 2v. which was apparently sufficient to break down the insulation between them. Gauge pair 2 had a similar potential difference between layers while that of the rest reduced to the value of 3v. for gauge pairs 9 and 10, in 1v. steps.

The gauge distribution was studied to see if the potential difference between layers could be reduced for all the gauges and this was achieved by connecting up the gauges as in Fig. (4.4(b)). It can be seen that the voltage between layers with this arrangement was reduced to zero for all gauge pairs. However since there were so many gauges in series it was decided not to use the maximum gauge current but to limit it to 20 mA. The reason for this decision was that, should any gauge connection break, the currents in the rest of the circuit would have to be changed and one arm of the bridge would have to carry a larger current. The factor of safety was thought to be more desirable than the 25% increase of sensitivity which was sacrificed. No further trouble from short-circuits was encountered during the experimental programme.

The outputs from the two bridge circuits were fed into the two channels of a Tektronix Type 551 oscilloscope. Type 147 High Gain Differential Amplifier plug-in units were used. These have a bandwidth of D.C. to 500 Kilz with deflection factors from 10v./cm. to 10 μv./cm. Their D.C. offset control enabled calibration to be carried out before each test.

'Static' Torque Measurement.

The requirements for measurement of the 'static' torque were far less stringent than those for measurement of the incremental component. Firstly, the strains to be measured were an

order of magnitude greater than the incremental ones so that it was not necessary to have as many as ten gauges in series. Secondly, as is implied by the definition of 'static' torque, there were no rapidly varying strains to be measured so that the overall frequency response of the system did not have to be very high. It has already been stated that T.M.L. PC-3 strain gauges were also used for static strain measurement. In this case only four double gauges were used but they were again connected in the form of a full bridge, with opposite arms giving the tensile strain, the other pair compressive. These four gauges were fixed to the output bar, 4" from the specimen end, with 'Araldite' twin pack adhesive which was cured at 70°C. In order to obtain a record of the specimen torque as a function of time the strain gauge bridge was connected to a Sanborn Model 324 Dual Channel Carrier Amplifier Recorder. This instrument has a frequency range of D.C. to 125 Hz, the outputs being fed to pen recorders. Only one channel was required as it was not necessary to measure the torque in the input bar. The recorder supplied the power to this set of gauges through a high frequency carrier signal. This signal was at first picked up by the 'dynamic' gauges when using a high amplification, but suitable screening eliminated that difficulty.

Incremental Torque Recording.

The method of producing a 'static' torque record has been described; it was also necessary to be able to record the oscilloscope deflection due to the incremental torque. This record was obtained by using the single sweep facility of the oscilloscope and photographing the traces with a Beattie-Coleman Type K-5 oscillotron camera. To do this it was

imperative that the traces should appear on the screen at the correct moment, so a reliable triggering device was required. It was hoped that it would not be necessary to resort to trigger gauges, as the incremental strain pulse would have needed a very large amplification in order to trigger the oscilloscope. Fortunately another method was found which proved to be very reliable. This method employed a trigger circuit which was extremely simple, as can be seen from the diagram, Fig. (4.6 (a)). It consisted of battery, switch and circuit breaker in series, the circuit being completed by the oscilloscope and earth. The breaking of the tensioned piano wire was used to break the circuit. A Tufnol disc was made to fit on the wire. Through one side of the disc was a screw which clamped on to the wire. To the other side of the Tufnol disc was glued a solder tag, and a piece of fine (46 S.W.G.) copper wire was soldered between this and the piano wire, as shown in Fig. (4.6 (b)). When the wire was broken to initiate a test, the two halves would spring apart and break the trigger circuit wire too. The soldered joints and in fact the complete circuit could be tested by operating the series switch.

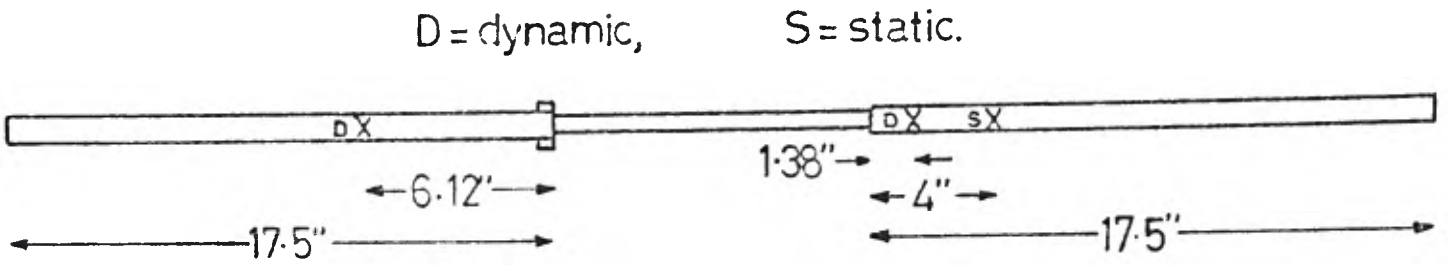
Wire Load Indication.

In order to make it possible to know how near the tensioning wire was to its breaking point, a transducer Ether Type 348/500/350 was fitted in series with the tightening nut. This was connected to an Ether Transducer Indicator Type E.M.I. 6019 which showed the load on the clamp in lb.

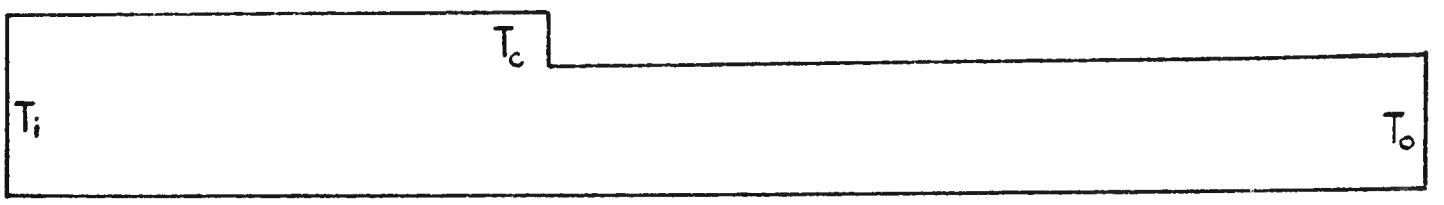
Supports.

The complete apparatus with instruments in position

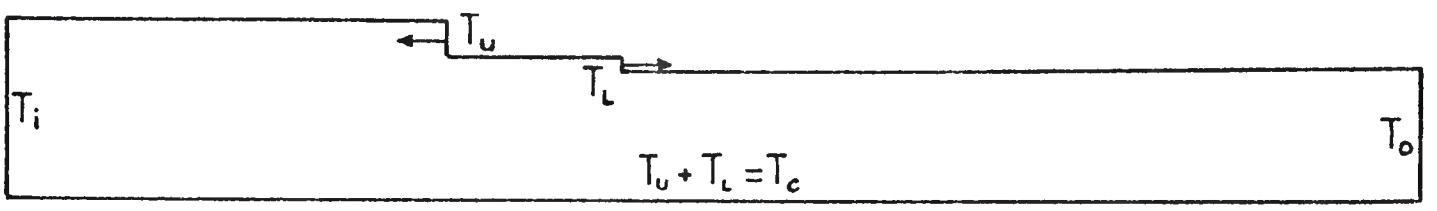
is shown in Fig. (4.7). In this photograph can be seen two stands which have not yet been described. These were to support the bar-specimen system between the grips of the machine and thus to reduce the deflections due to transverse forces. They were of simple design consisting of one piece of 1" mild steel box section with a mild steel plate cap. Through the cap fitted a V-shaped piece of mild steel with a screw at its foot for vertical adjustment. Horizontal adjustment was provided by two bolts which screwed out to fit inside the channel on the bed of the torsion machine. By having a V-shape at the top, two-point contact was possible with the bar. This was desirable since what was required was support without interference with rotation of the bar. An account of the experimental procedure appears in the appendix.



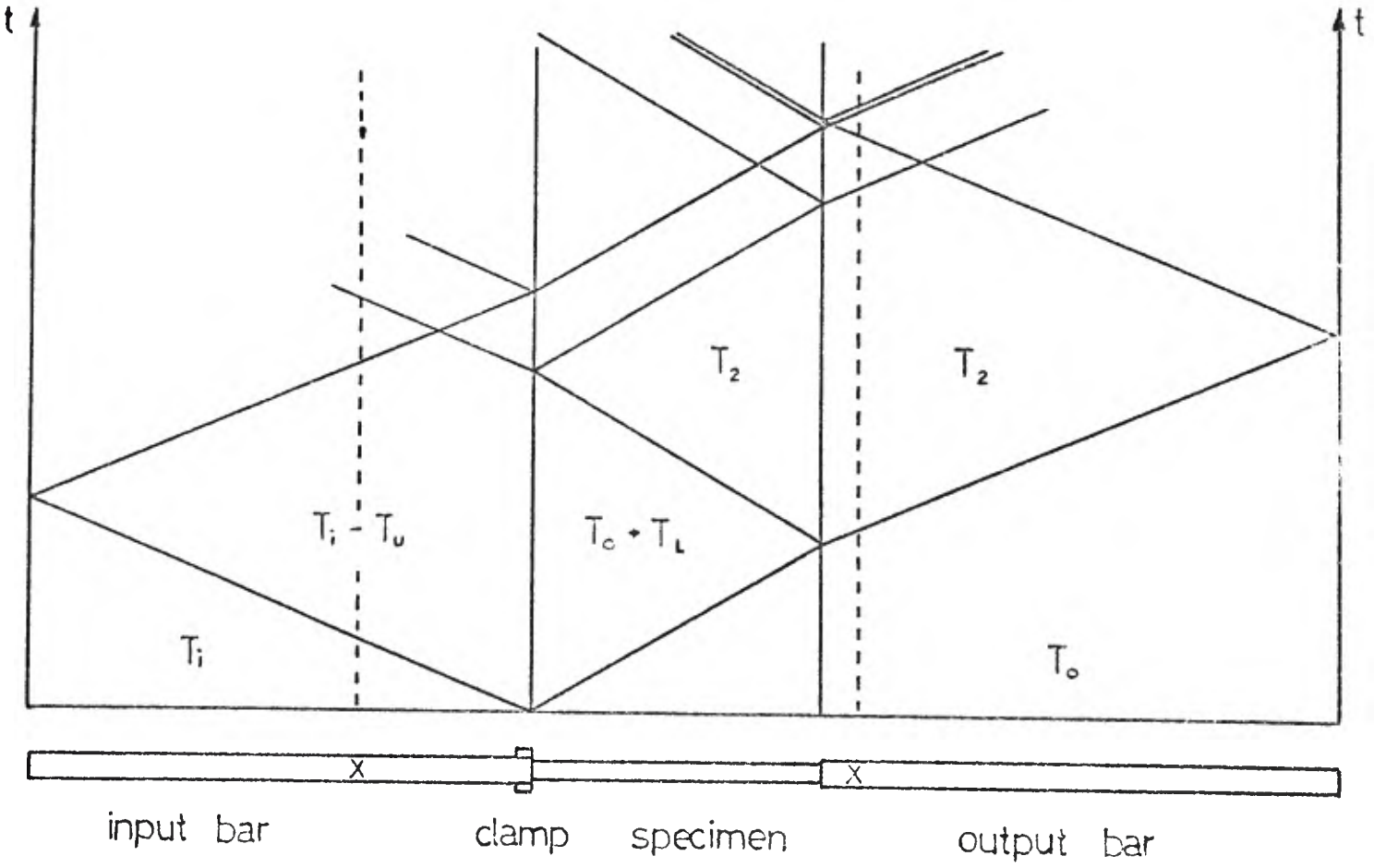
(a) Gauge positions.



(b) Torque distribution immediately before releasing the clamp.

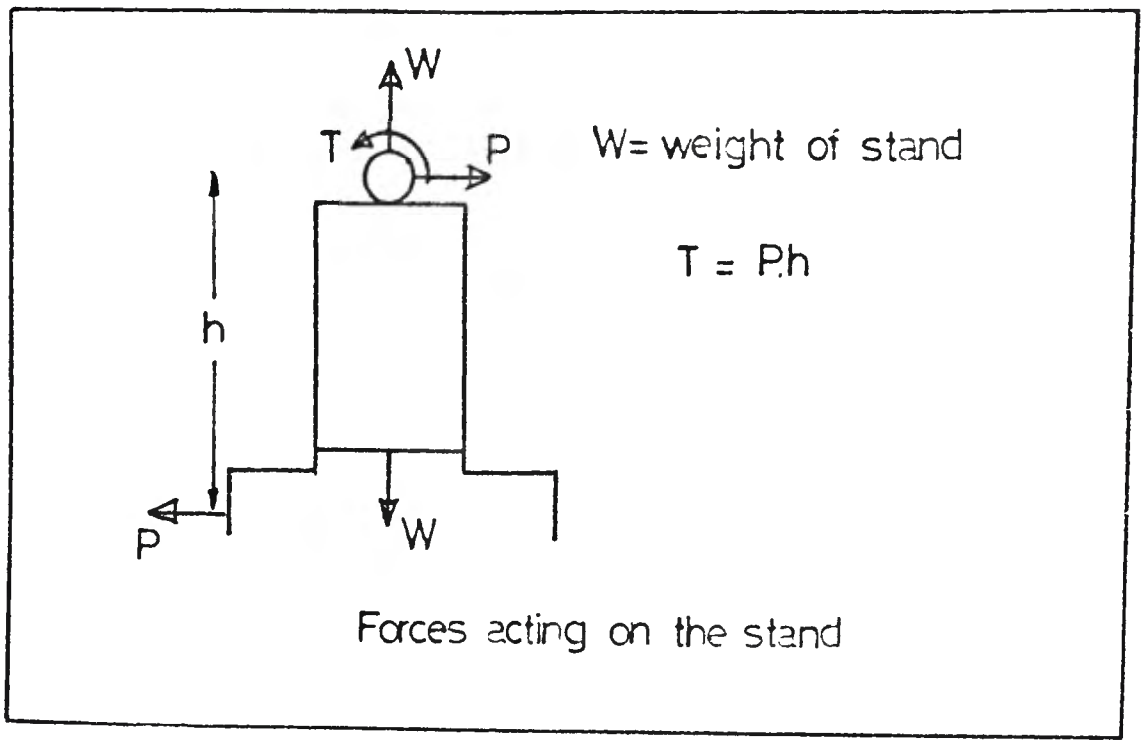


(c) Torque distribution soon after releasing the clamp.



(d) Lagrange diagram. (see Appendix 2 for torque values.)

FIG. 4.1 Strain gauge positions and idealised torque distribution.



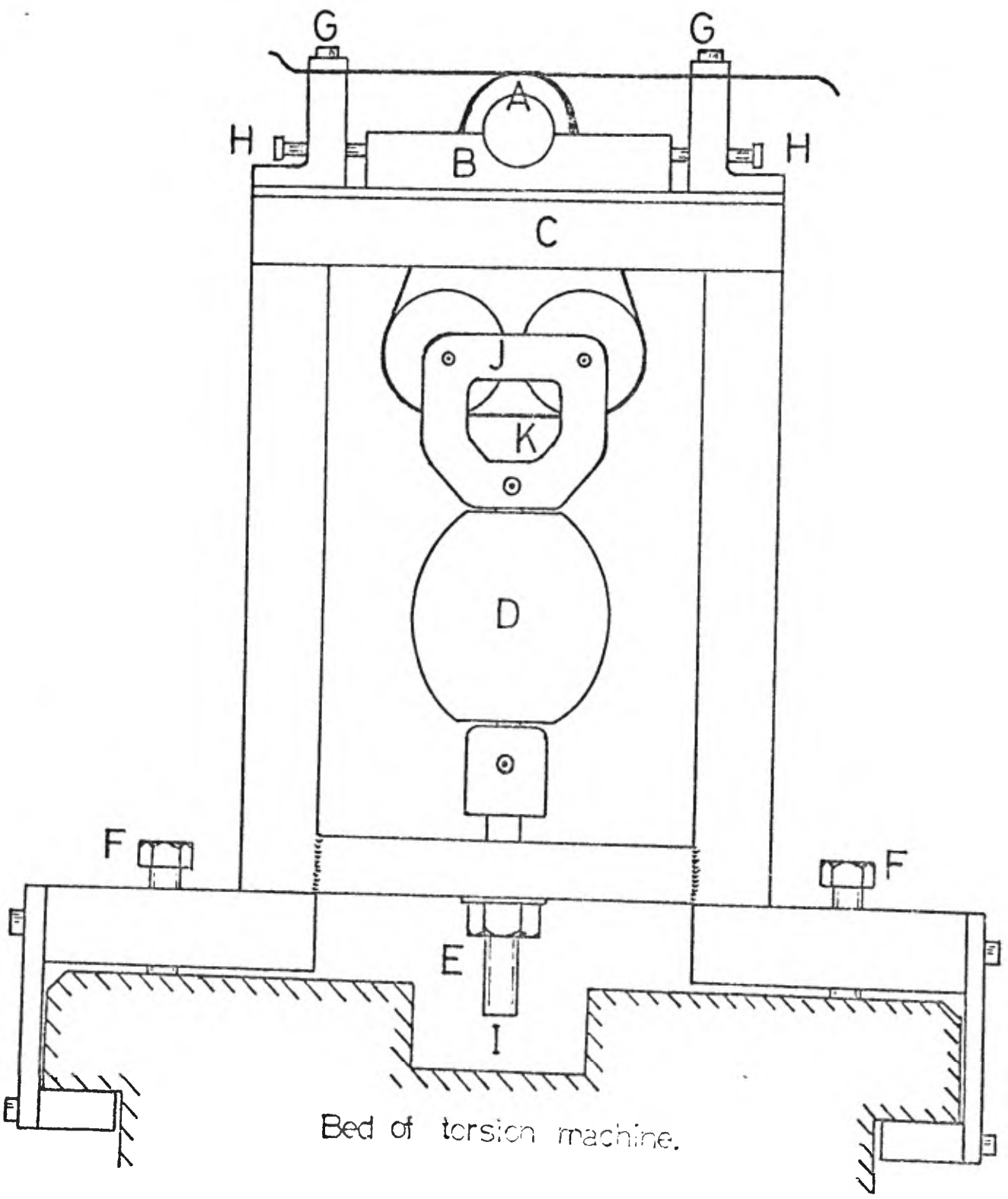


FIG. 4.2 The clamp.
Inset: Force diagram.

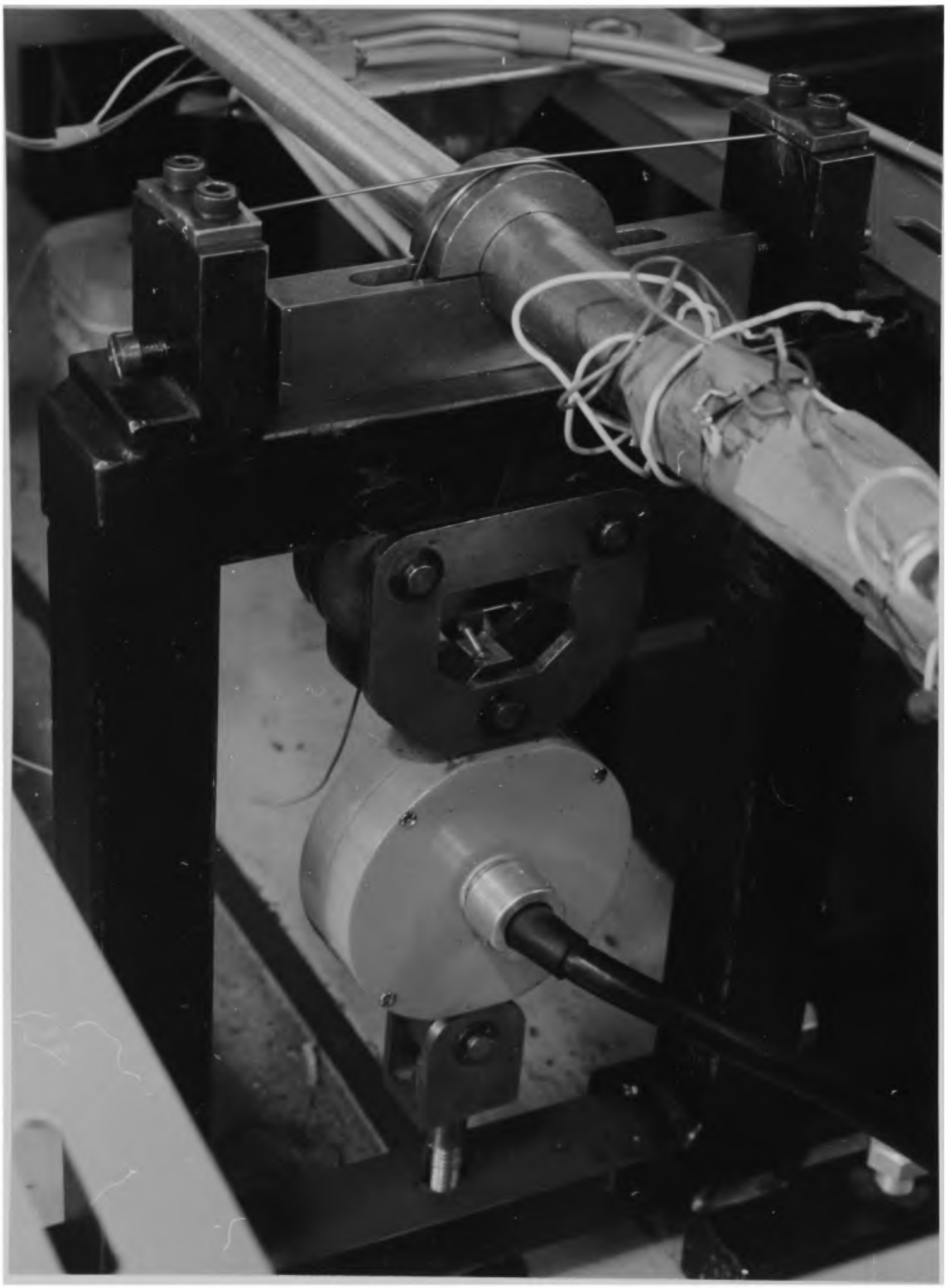
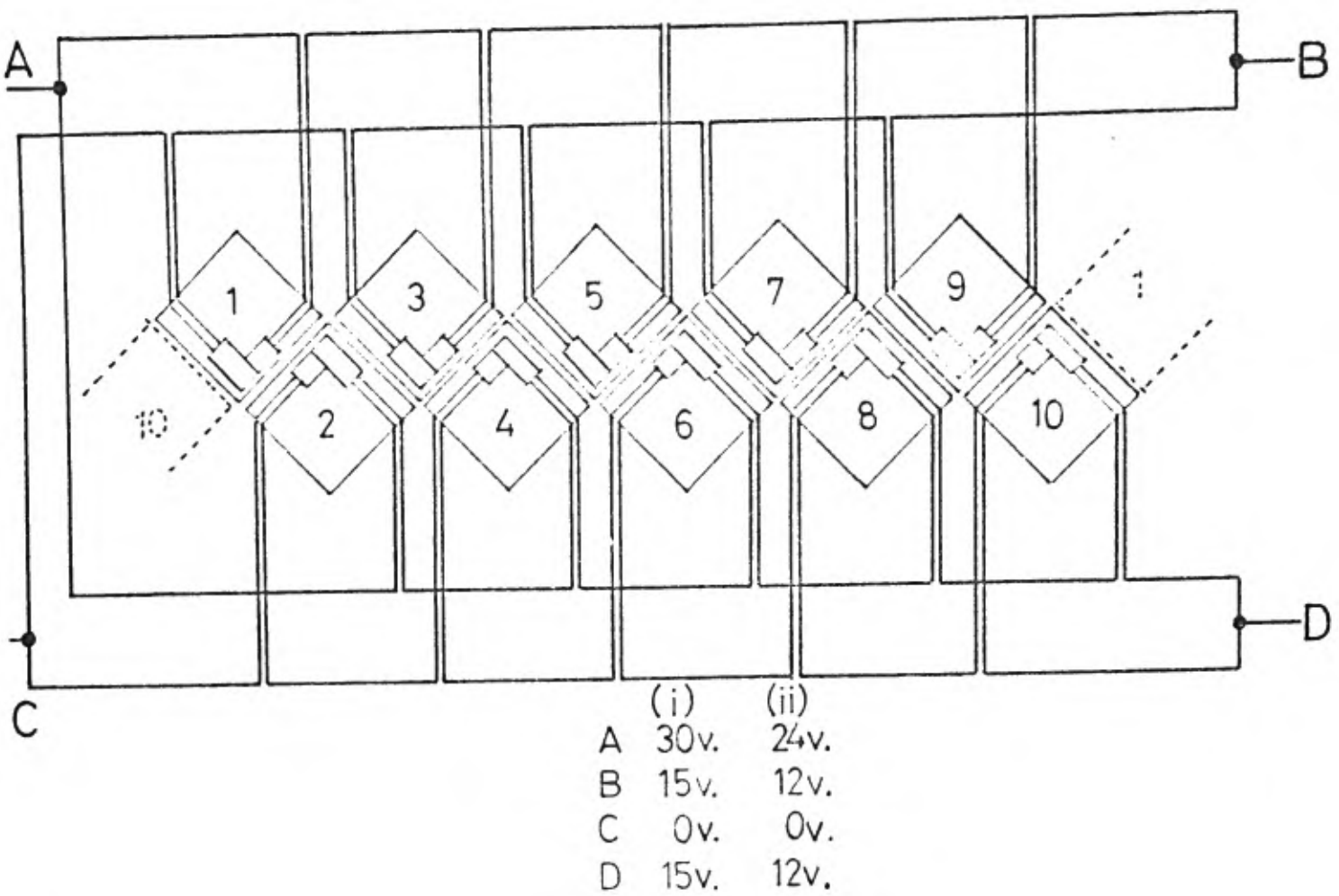
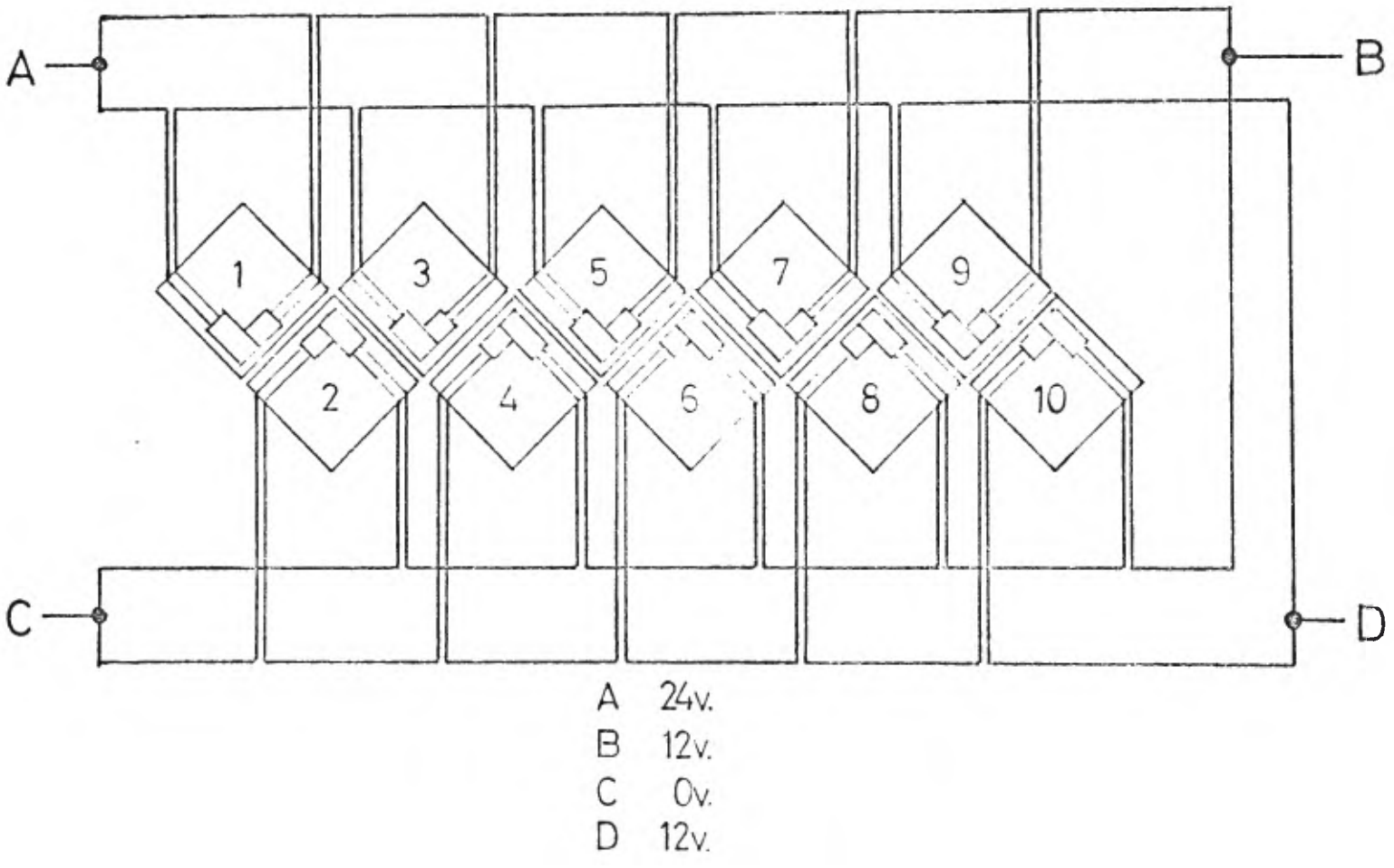


FIG. 4.3 'Close-up' of the clamp.



(a) A development showing the original method of connecting the strain gauges.



(b) A development showing the final method of connecting the strain gauges.

FIG. 4.4 Strain gauge connections.

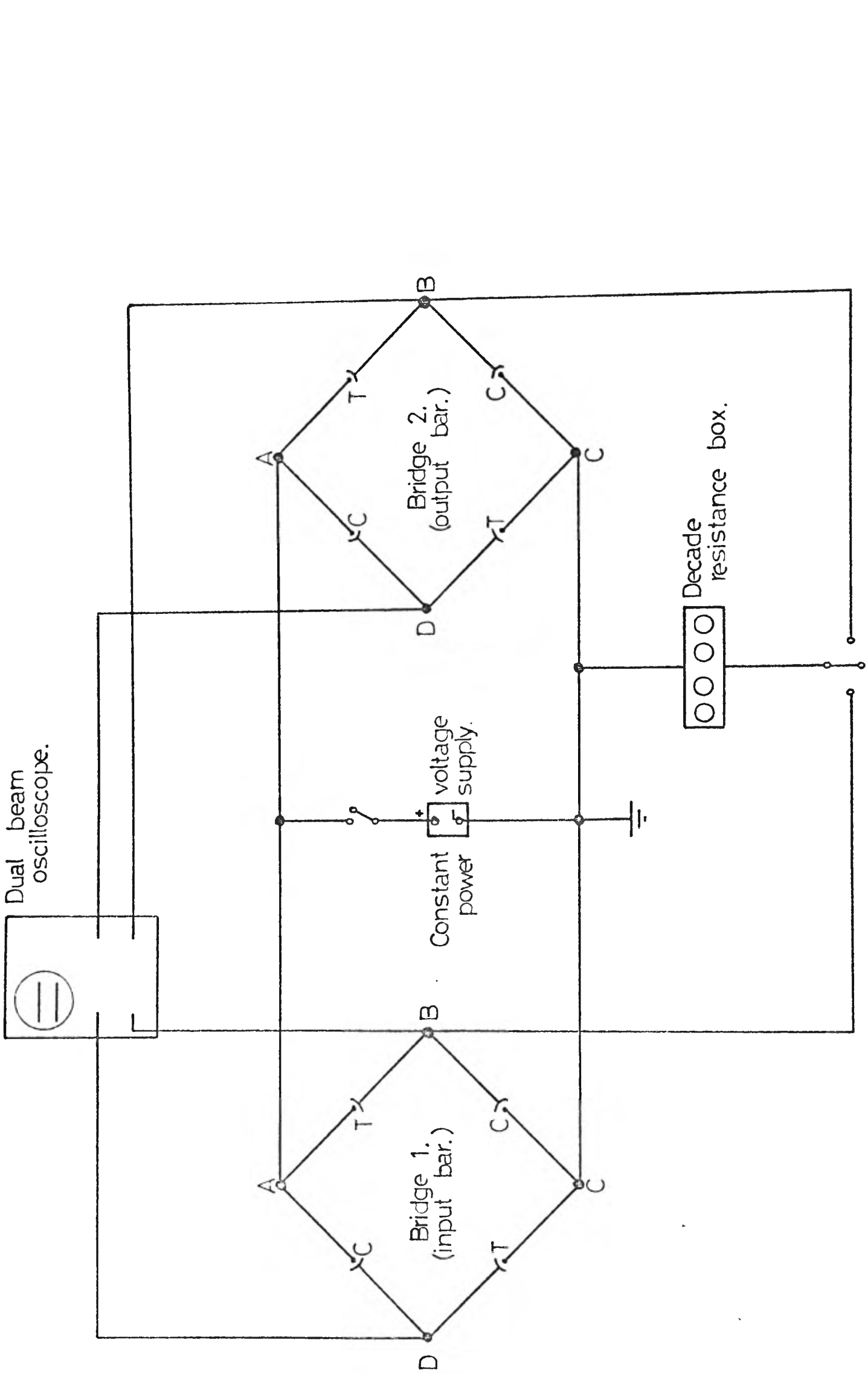
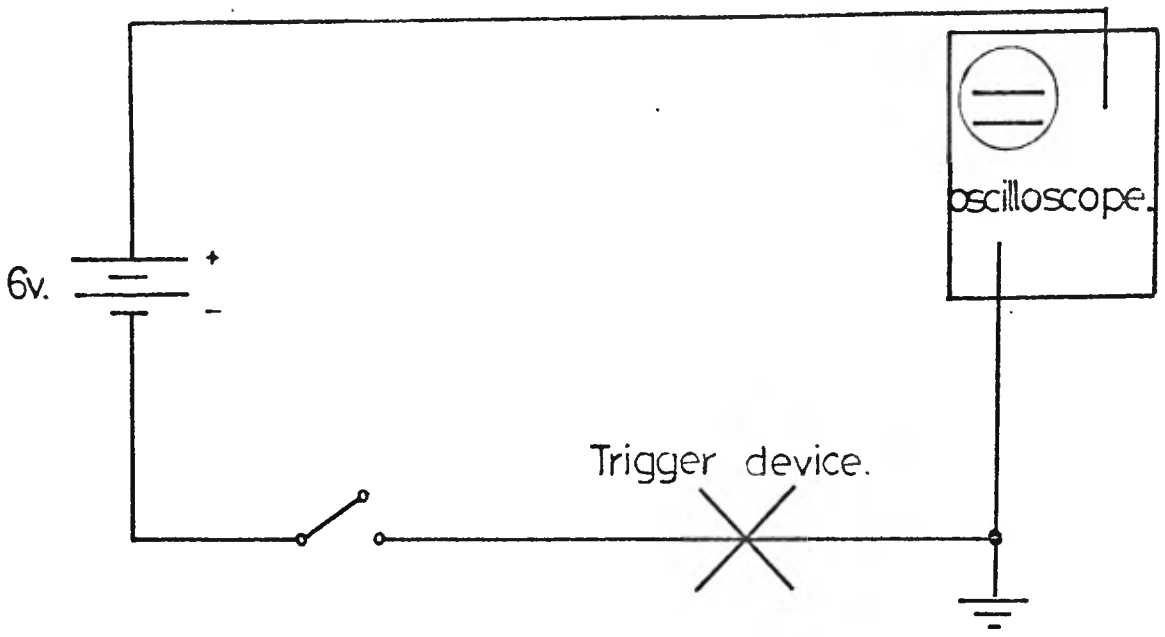
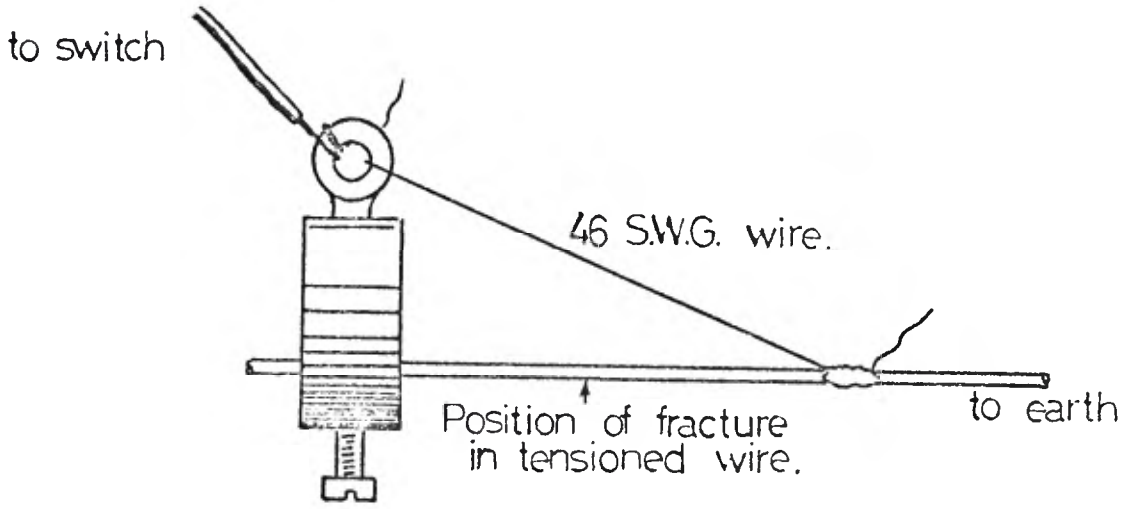


FIG. 4.5 Circuit diagram.



(a) The trigger circuit.



(b) The trigger device.

FIG. 4.6 The triggering system.

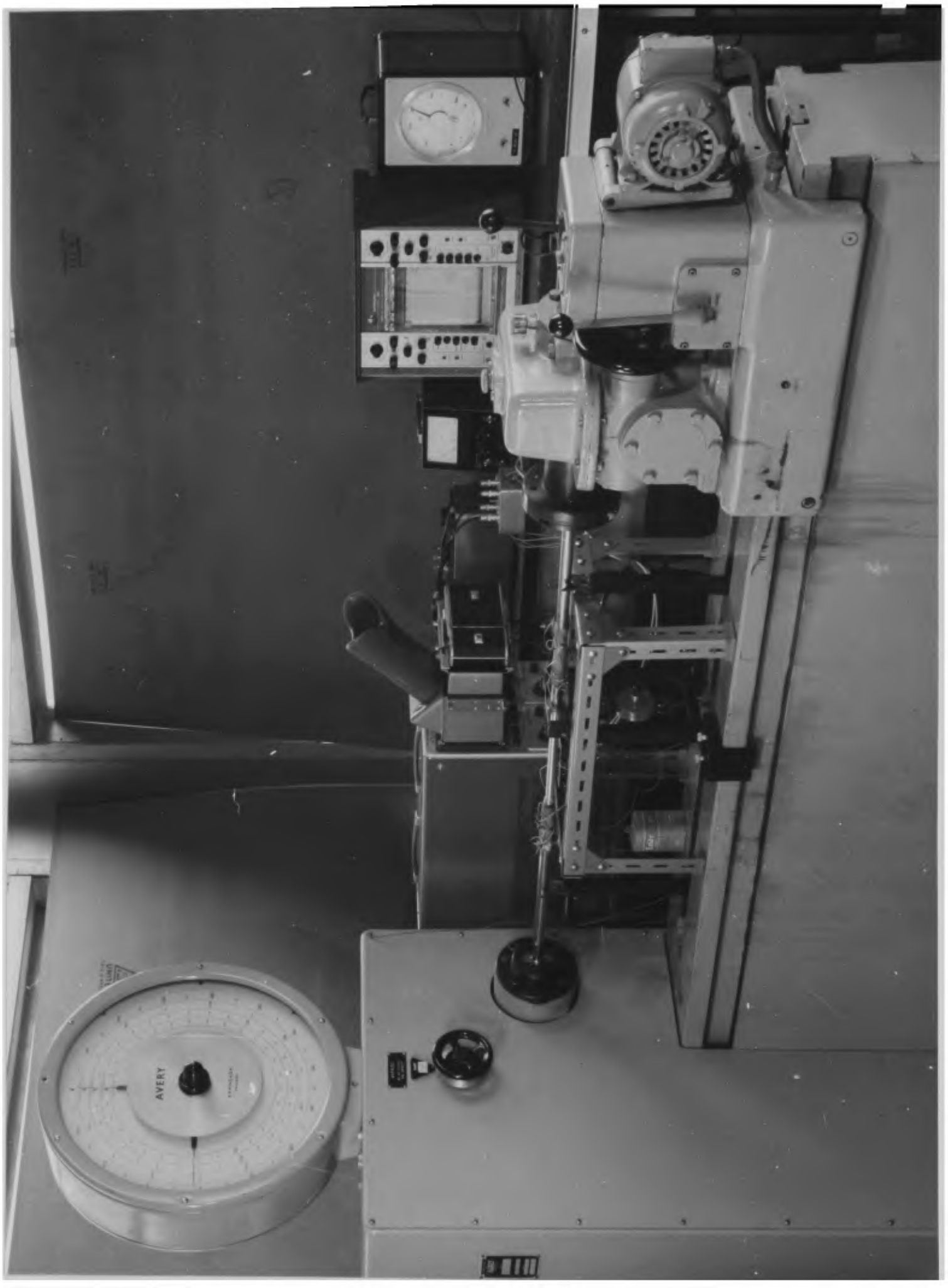


FIG. 4.7 The complete apparatus.

CHAPTER 5

WAVE PROPAGATION - SPECIMENS.

Shape and Size of Specimens.

It has already been stated that a specimen length of about ten inches was decided upon and that thin-walled tubes were to be used for the wave propagation study. A thin-walled tube is of such dimensions that the stresses and strains can be assumed uniform across the cross-section. This condition is satisfied if the t (wall thickness) / d (diameter) ratio is less than 0.1. Since metals, as normally used, are polycrystalline materials, it was essential to have sufficient grains in the thickness of the wall so that the properties could be considered isotropic. With this in mind it was decided that the wall thickness should not be less than 1/16 in.

The smallest possible cross-section compatible with these conditions was a 5/8 in. o.d. tube with 1/16 in. wall thickness. The largest possible size was 0.846 in. o.d., the same as the loading bars, and 0.085 in. wall thickness. The question of which to use was resolved by considering the joins between specimens and transmitter bars. No matter what type of joint was conceived it was necessary for the specimen cross-sectional area to be increased near the interface. If a pinned joint were used the larger area would be necessary to counteract stress concentrations, if adhesives were used it would be required since the strength of the adhesive would probably be lower than the strength of the specimen material, and so on. Being far easier to produce a varying o.d. than i.d. it was

decided to use tubes with o.d. of 5/8 in. and 1/16 in. wall thickness. The change of section at the ends was obtained by welding on rings of a similar material over the last 1/4 in. of specimen, Fig. (5.1).

Steel Specimens.

The steel specimens were made from 5/8 in. o.d. 16 S.W.G. thickness, seamless mild steel tube in the bright as drawn condition obtained from Le Bas Tube Co. Ltd. The composition of this material is given below. (% by wt.).

C	Si	Mn	P	S	Ni
0.09	0.09	0.41	0.012	0.034	0.08

The specimens were annealed by heating to 700°C in a vacuum furnace and holding at that temperature for four hours. They were then furnace cooled.

When using the standard specimens it was found that the joint between loading rods and specimen fractured when the specimen had reached a strain of 6 %. At this strain the material had only just started to work harden and so another specimen was machined to try to obtain a higher strain. This specimen had an o.d. of 0.571 in. but its other dimensions, i.d., length and increased area at the ends were identical to those of the other specimens.

Copper Specimens.

5/8 in. o.d. 16 S.W.G. thickness tubing was again used for the copper specimens. This was supplied by J. Smith & Sons, Ltd., and had the following composition (parts per million except Oxygen which is % by wt.):

O	Ag	Ni	Fe	Sn	Pb	Bi	Cd	Mg	Mn	Si
0.006	80	40	10	5	2	1	<1	<1	<1	<1

The specimens were annealed by heating in vacuo to a temperature of 550°C for 20 hrs. and furnace cooling.

'Static' strains of up to 25% could be obtained with the copper standard specimens before buckling became apparent. One different size of specimen was made, however, in order to investigate the variation of the propagated wave with length of specimen. A specimen was made with a 'gauge length' just over half the length of the standard specimen, the other dimensions being the same.

In order to obtain information about the effects of a higher strain rate on material properties, a different type of specimen was needed. For wave propagation study it was necessary that the initial wave could be observed before it was affected by reflected waves, reflected either from the ends of the loading bars or internally in the specimen between the section changes. For material property studies it was necessary that many internal reflections should take place in a time very short compared with the loading time so that the stress condition of the specimen was effectively uniform along its length. The wall thickness was set at 0.030 in. which, it will be noticed, is less than the 1/16 in. decided upon for the wave propagation specimens to give a reasonable number of grains in the wall. There was good agreement between the results of several specimens however, from which it was concluded that the number of grains was sufficient for uniformity of properties. The gauge length was made 0.050 in., through

which an elastic wave can travel in less than 0.5 μsec.

It was not now practicable to weld the rings on to the ends of these specimens for the specimens could quite easily become distorted and the gauge section damaged. Instead the specimens were made by first of all taking a 0.550 in. length of the original tube and turning down the gauge length to an o.d. of 0.570 in. The inside was turned out to a diameter of 0.510 in. Copper rings, 0.546 in. o.d. were then machined to fit over the specimen tube 1/4 in. in length. These did not have to have the same material properties as the specimen and in fact, for these specimens, as-received copper was used.

The specimen tube with machined gauge length was given the same heat treatment as the other longer specimens. The rings were then attached to the specimen tube by means of 'Araldite' twin-pack epoxy adhesive which was cured at 100°C. PTFE spacers were placed round the bar at the gauge section in order to prevent the adhesive from running into the gauge section groove, and also to keep the rings properly spaced.

Aluminium Specimens.

For the aluminium specimens 5/8 in. o.d. 16 S.W.G. thickness tubing was used, supplied by J. Smith & Sons, Ltd., in Aluminium (TIC). The composition of this material is given below (% by wt.) :

Fe	Mg	Si	Cu	Zn	Mg	Cu	Cr	Ni	Ca
>0.1	0.1	0.05	0.02	0.02	0.01	0.007	0.004	0.003	0.003

The annealing of these specimens was done by heating at 400°C for 16 hrs.

The same sizes of specimens were used as for the copper, i.e. in addition to standard ones, there was one with a 'half-size' gauge length and several small specimens for material property studies, which were made in a similar fashion to the copper ones.

Attachment to loading bars.

The study of stress wave propagation was the prime purpose of this experiment which, therefore, required that the specimens should be attached to the loading bars in such a way that the waves would not be distorted appreciably in passing from the bar material to the specimen material. It was also necessary that the path of the waves would be very simple and not involve many points where reflections would occur. Since a number of specimens were to be used it was also desirable that the method of fastening should be fairly quick, though, as several tests could be performed on each specimen, this requirement was not essential.

Thus a simple pinned joint between the specimen was impracticable since this involved the changing of the nature of the stress wave from torsional shear to transverse shear in the pin and back to torsional shear again, involving wave reflections at five section changes and resulting in an extremely small fraction of the input wave reaching the far transmitter bar and strain gauges. For the least possible number of reflections it was necessary for there to be a plane contact between the specimen and bar. This could be achieved either by welding or the use of an adhesive. Welding, which would have provided the stronger bond, would have been difficult to perform since

the gauges were less than 1.1/2 in. from the end of the output bar. Also there was the very real possibility of distorting the specimens or altering the grain structure. For this reason the use of an adhesive was adopted. Elastic tests showed that the stress waves passed through the adhesive layer unchanged in magnitude or shape, for, with elastic waves, the magnitude of the transmitted wave could be calculated and its expected shape could be found from the unloading wav e when no specimen was attached.

In order to strain the test materials well into their plastic ranges it was necessary to have a very strong adhesive. This had preferably to cure at temperatures no greater than about 100°C, otherwise a gauge cooling system would have been needed. 'Araldite' twin pack epoxy adhesive was found to be the most suitable and this was used for attaching all the specimens.

Each specimen had to be fixed so that its axis was coincident and parallel with those of the two loading bars to ensure uniform shear strain. The first step towards the co-linearity of axes was to make the end faces of both loading bars and specimens accurately perpendicular to the axis of the relevant part. The next step towards centring the specimens was to have a 1/4in. extension on each loading bar with an o.d. of 0.005 in. This was a clearance fit with the specimen ends. Thus, also, the specimen-bar assembly could be considered as having only two section changes from a solid 0.846" round section to the tubular specimen section, although there was the transition section between this point and the adhesive plane where the 'solid' section was made up of two materials.

In order to obtain a high-strength joint, the surfaces of the two materials had to be very carefully prepared. Having been machined square it was necessary to obtain a good contact area between the loading bars and the specimens. Using valve grinding paste the two surfaces were rubbed together until it was clear that maximum contact had been achieved. Since the loading bars were much harder than the specimens, their surfaces were ground only a small amount and the specimen surfaces were ground to suit them. The valve grinding compound was then thoroughly washed off with trichlorethylene and 600 grade emery paper was used to roughen the surface as a key to the cement. The surfaces were rewashed in trichlorethylene several times to ensure grease-free surfaces.

For the final centering and lining up operations a jig was required. The building of a jig to line the three members up over 40 in. and to apply a small axial force would not have been particularly simple and it was fortunate that there was an almost ready-made one available. A drop-weight apparatus, a smaller version of the one described in Part II, was slightly modified to act as the jig. The set-up is shown in Fig. (5.2.). The output bar, with 'Araldite' on its top face, was placed on top of what used to be the dropping weight. The 'Araldited' specimen was placed in position on it, passing through the centre of the furnace. The input bar was then placed in position above and the solenoids lowered on to the top of the assembly to provide the joint pressure required for good bonding. The falling weight guide wires had been accurately lined up and tensioned in the apparatus and so they were used to judge the linearity and centrality of the assembly.

The furnace, suspended from the solenoid, was plugged at both ends to stop convection currents and was switched on. Conduction was relied upon to provide the heat for curing the cement and, to check that the gauges were not overheated, thermocouples were stuck on to the bars.

When the shorter specimens and material property specimens were to be attached to the bars the furnace could not be used since it would have covered one set of gauges. Instead, a hot air blower was directed on to the specimen, the temperature again being checked by thermocouples.

When this method of fixing the specimens to the bars was followed it was found that all except the standard steel specimens buckled before the bonds broke. Flats had to be filed on to the ends of the specimens so that a spanner could be used to break the 'Araldite' joint. Torques of up to 600 lb.-in. were transmitted through the cement which means a shear stress in the adhesive of c 2000 p.s.i.

Densities.

The densities of the specimen materials were found by weighing the materials in air and water. It was found that

ρ for steel = 0.286 lb/in.^{3}

ρ for copper = 0.321 lb/in.^{3}

ρ for aluminium = 0.0985 lb/in.^{3}



FIG. 5.1 Typical specimens.

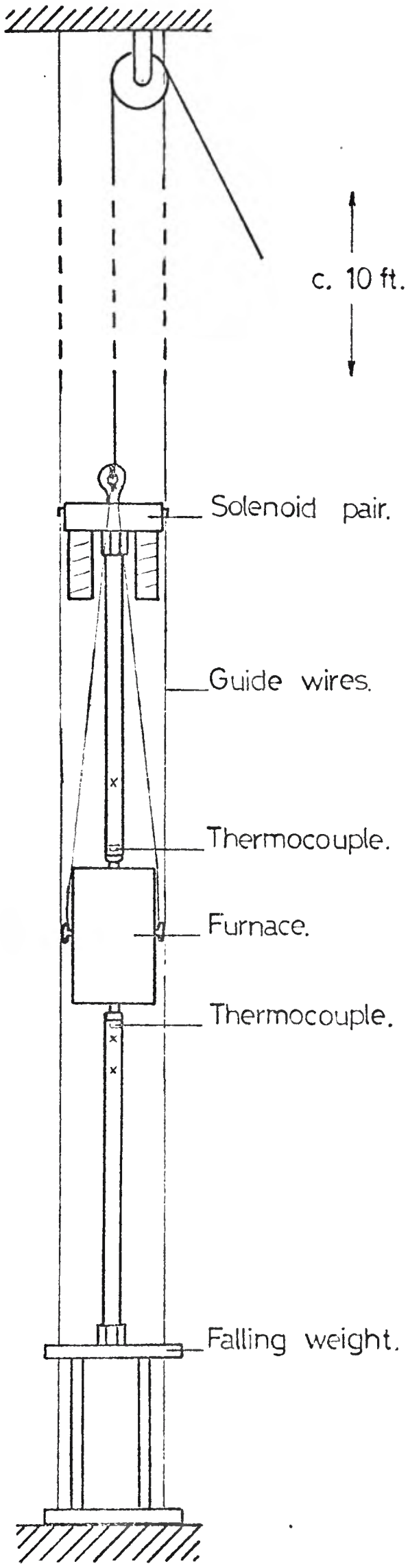


FIG. 5.2 Jig for specimen attachment.

C H A P T E R 6

WAVE PROPAGATION - RESULTS.

The Apparatus.

In order to assess the performance of the clamp, tests were carried out without an output bar or specimen fixed to the loading bar. Thus only one trace for each test appeared on the oscilloscope screen, namely the unloading wave from the clamp. From such traces it was possible to see that the trigger system was working efficiently and that the 'hold' torque varied linearly with clamping force, so that the friction torque in lb.-in. was one third of the clamping force in lb. The rise time of the unloading wave was found to be about 30 μsec., which showed that the release mechanism was well within the limit of 50 μsec. which had been set.

To test the rest of the equipment, and in particular the method of joining the specimens to the steel bars, a 5.1/4 in. length of steel bar was machined to fit the ends of the loading bars with the same o.d. It was made out of the same stock as the loading bars so that it would have the same properties as theirs. It was fixed between the bars using 'Araldite' in the manner described in Chapter 5. Theoretically, therefore, the complete system of loading bars and centre section could be considered as one piece of steel rod and any differences from the theoretical behaviour could be attributed to the effect of the joints. Fig. (6.1) shows the result of a test using this centre section and it can be seen that the two 'Araldite' joints made a negligible difference to the transmitted wave. The

increment can be seen to approximate a step function, with a rise time of 30 μsec. When comparing the observed traces with the expected theoretical ones, it is found that the loading increment and the unloading increment have the same magnitude. In addition the times for particular reflections to reach the gauge stations correlate with the known lengths if an elastic wave speed of 13.1 x 10^4 in./sec. is assumed.

This value for the torsional elastic wave speed in the loading bars was used in calculating the results for all the tests. The oscilloscope time base was calibrated by means of a time-mark generator so that absolute time measurements could be taken from the oscilloscope. The values of G and ρ for the loading bar material were not measured; however, the wave speed using handbook values of G and ρ for steel is 12.7 x 10^4 in./sec.

Having shown that the clamp functioned satisfactorily and that the 'Araldite' did not interfere with the transmission of the waves, it was necessary to test the strength of the joints and at the same time calibrate the 'static' torque measuring equipment. It was found that the joints held up to 600 lb.-in. torque.

Aluminium Incremental loading Results.

For at least the first two tests on each specimen, the stress was kept below the elastic limit. This was done for two reasons. First of all to obtain a measure of the elastic torsional wave speed in each specimen and secondly, to ensure that the wave was transmitted in the expected manner. To achieve this the free end of the output bar was not placed in the torsion machine grip. Thus when the input bar was rotated to provide the 'held' torque the specimen and output bar could rotate freely

and remain unstressed until loaded by the stress wave on release of the clamp. The result of an elastic test on a standard aluminium specimen is shown in Fig. (6.4(a)).

When both ends of the specimen-bar system were fixed in the torsion machine, the 'static' torque-time record indicated when the specimen was flowing plastically. Tests were performed while the specimen was being continuously strained quasi-statically, for various prestrains. The loading was interrupted between tests but the 'static' record showed when relaxation had occurred and when the specimen had been brought back to its loading curve. The difference between successive preloads was always greater than the maximum dynamic load of the previous test, in order to ensure that the specimen tube was being strained plastically when the dynamic load was applied. Fig. (6.2) shows the positions on the stress-strain curves at which the tests were performed.

On the oscilloscope photographs, the times of the initial rises of the two traces were used to calculate the wave speed through the specimen material. On the upper trace this time equals the triggering time (t_t) plus the time for the elastic unloading wave to travel from the clamp to the gauge station 1, $(t_g)^1_{st}$. On the lower trace the time equals the triggering time (t_t), plus the travel time in steel $(t_e)^2_{st}$, plus the travel time in the specimen ends $(t_e)_{al}$, plus the travel time through the gauge length $(t_{pl})_{al}$.

The time difference is obtained by subtraction.

i.e. $$t_d = (t_{pl})_{al} + (t_{el})_{al} + (t_e)^1_{st} - (t_e)^2_{st}$$

$$\text{Wave speed} = \text{gauge length} / (t_{pl})\,al$$

$$= \text{g. length} / t_d + (t_e)\,{}^{2-1}_{st} - (t_e)\,al$$

The values of $(t_e)st$ and $(t_e)al$ were calculated from the known lengths and elastic wave speeds. The incremental wave speed was calculated in this way for each test and this value, divided by the elastic wave speed, is shown plotted against the shear strain in Fig. (6.3). Also shown on this diagram are the values of this ratio as calculated from the strain-rate dependent and independent theories. It can be seen that the strain-rate independent theory's predictions of the speed of propagation of an incremental load are very different from the observed values. The strain-rate dependent theory predicts a propagation speed equal to the elastic wave speed; the largest measured deviation from this speed is 4.5%, the standard deviation for the 36 tests being only 1.6%. However, since it was only possible to measure the wave speed to $\pm$ 2%, it can be stated that within the experimental accuracy the increment always travelled with the speed of an elastic stress wave.

The Shape of the Transmitted Wave for Aluminium.

In Figs. (6.4) to (6.6) are shown a selection of the oscillograms obtained from Aluminium. There was an immediate change in the wave shape* when the specimen was pre-strained past the elastic limit. The height of the initial part of the pulse was approximately halved and instead of remaining at that level as in the elastic case, it now decayed

* For the purposes of this thesis the transmitted wave is that portion of the oscilloscope trace before the first internal reflection in the specimen. For Aluminium standard specimens that is the first 140 μsec. and for the shorter specimen 70 μsec.

with time. It must be remembered that, due to the section and material changes at the specimen ends, the torque shown on the output trace is not the torque actually on the specimen. However, since it has already been established that the wave front propagates with the elastic velocity, elastic conditions can be assumed in calculating the specimen stress, at least for the initial part of the propagated pulse.

Within the plastic region the height of the transmitted pulse increased as the prestrain got larger but the rate of decay with time remained constant. The magnitude of this effect was such that the recorded pulse height increased by approximately 20% for a prestrain change from 2% to 16%. This same effect was shown by the shorter specimen, for which two oscillograms are shown in Fig. (6.6).

Comparing the oscillograms for the standard and 'half-length' specimens it was found that there was no measureable difference in the sizes of the pulses. In comparing the pulses the size was taken as the ratio of transmitted torque to unloading torque. However, one difference between the two types of specimens was that the decay rate was much faster with the shorter specimens.

Copper Incremental Loading Results.

The speed of propagation of the first part of the incremental pulse was calculated for each test in a similar way to that described for the aluminium specimens. The elastic torsional wave speed was calculated separately for each specimen and the incremental wave speed divided by the elastic wave speed is plotted against prestrain in Fig. (6.7). Again the ratios predicted by the two wave propagation theories are indicated in

the figure. Fig. (6.8) shows the quasi-static stress-strain curve for the copper used and also the points in stress-strain space at which the incremental load was added. It can be seen that all three copper specimens had a common stress-strain curve, unlike the aluminium ones. This was to be expected, however, since commercial aluminium varies somewhat from specimen to specimen and the properties of aluminium are particularly sensitive to small changes in impurities, whereas copper is insensitive to small changes in impurity content.

From Fig. (6.7) it can be seen that again the strain-rate dependent theory is much closer to predicting the incremental wave velocity than the strain-rate independent theory. However, in the case of copper there was a significant decrease in the wave velocity with increasing strain and it can no longer be said that the incremental wave speed remains constant at the value of the torsional elastic wave speed. With the copper tests the measured time difference was larger than with the aluminium tests, so that the calculated speeds were more accurate. A line was drawn through the values of c/c_e and it was found that the largest deviation from this line was 3%. The standard deviation from the line was 1.25% for the 55 tests.

<u>The Shape of the Transmitted Wave for Copper.</u>

Figs. (6.9) to (6.11) show a selection of the traces obtained from tests on copper. Fig. (6.9a) shows the result of an elastic test on a standard specimen, in which the transmitted wave shape and size was as expected from theory. Fig. (6.9b) relates to a test on a standard specimen which had a prestrain just less than the yield point. It can be seen that the pulse starts off like the elastic one but that the

slope changes abruptly to give a lower maximum torque and the height of the wave decreases slowly.

On looking at the results for tests in which the prestrain was past the elastic limit it was found that the transmitted wave had a double peak, in contrast to the single peak present in the aluminium results. The presence of the second peak made it more difficult to talk about the decay rate of the wave. There was now a question of whether to consider the first or second peak, or even a smoothed curve.

The decay rates after the first peak showed considerable variation while these after the second peak were approximately constant, as for aluminium.

Regarding the magnitude of the transmitted pulse, again one had to decide whether to take a particular peak or the two together. However whichever course is adopted the same qualitative result holds, that as the prestrain increases the magnitude of the pulse increases. The same result was obtained with both standard specimens and the shorter one. Fig. (6.11) shows the variation of the pulse shape with increasing prestrain. The magnitude of the initial peak increases approximately 100% for a prestrain change of 0.5% to 2% whereas if one considers the pulse as a whole the magnitude is increased approximately four times for the same change of prestrain.

Incremental Loading Tests on Mild Steel.

The quasi-static stress-strain curves for the mild steel tubes used are shown in Fig. (6.12). On these curves, the points at which tests were carried out have been indicated. One of the specimens used suffered two overnight delays between tests so that three yield drops resulted, the initial one and

one after each overnight stand. One specimen did not show a yield drop at all. As has been stated previously, in order to do the test at a prestrain of 9.9% a thinner walled specimen was made up.

For all the tests the incremental wave speed was calculated. This was divided by the elastic wave speed and is plotted against prestrain in Fig. (6.13). The values of this ratio from the rate-dependent and rate-independent theories are shown on this graph.

The calculated incremental wave speeds were all within 2.1/2% of the elastic wave speed for the steel specimens. The accuracy of the measurement was approximately ± 2% so that it can be said that an incremental load in mild steel is always propagated at the elastic wave speed.

The Transmitted Pulse Shapes for Mild Steel.

It was found that for every value of prestrain used in each specimen, the pulse shape was identical to that in an elastic test. This can be seen in Figs. (6.14) and 6.15) where the three photographs refer respectively to tests in the elastic portion, the lower yield region and the work hardening region of the stress-strain curve.

Short Specimen Results.

General.

In order to obtain a constant strain rate from the type of machine used here, it is necessary for the torque in the input bar to be much greater than the torque taken by the specimen. The reasoning behind this statement can best be demonstrated by outlining the method of derivation of the results :

Let the torque held by the clamp be... T_o

the torque transmitted through the specimen to the output bar be ... ... T_s

the torque reflected from the specimen and propagated through the input bar be ... T_R

Then $T_o = T_s + T_R$

Since for elastic conditions $\tau = \rho c w r$

then $T = J\rho c w$

$\therefore$ $T_s = J\rho c w_2$ and, if it is assumed that the clamp is at the bar-specimen join:- $T_R = J\rho c w_1$

where w_1, w_2 are the angular velocities of planes of the input and output bars respectively, J is the bar polar moment of inertia and ρ, c are the density and elastic wave speed of the bar material.

The oscilloscope trace gives us T_s and T_R. Hence the specimen stress can be obtained direct from T_s. The specimen strain rate is given by $(w_{1s} - w_{2s})r/l$; where r,l, are the mean radius and gauge length of the specimen, and the second suffix s denotes the angular velocity at the bar specimen interface.

w_{1s} and w_{2s} can be obtained from w_1, w_2 by suitable time shifts so that :

$$\text{strain rate, } \dot{\gamma} = \left(\frac{T_R}{J\rho c} - \frac{T_s}{J\rho c} \right) \cdot \frac{r}{l}$$

$$= \frac{r}{J\rho c l} \cdot (T_R - T_s)$$ and γ follows by integration.

Thus, since T_s is an increasing function of γ, for a constant strain rate $T_R \gg T_s$.

In the present apparatus there was a limited held torque which meant that it was not practicable to test short specimens of mild steel since T_s and T_R would be of similar magnitude. Tests were performed for short specimens of both aluminium and copper and the strain rate was found to be reasonably constant.

The effective duration of a particular test was governed by the time taken for the first reflected wave to reach the specimen. At the strain rate obtained in the tests, approx. 400 sec.$^{-1}$, this limited the dynamic strain to about 2%. In order to obtain larger strains, the specimens were strained at a low rate, 5×10^{-3} sec.$^{-1}$, and the strain rate suddenly changed at a particular stress to the higher value.

Aluminium Short Specimens.

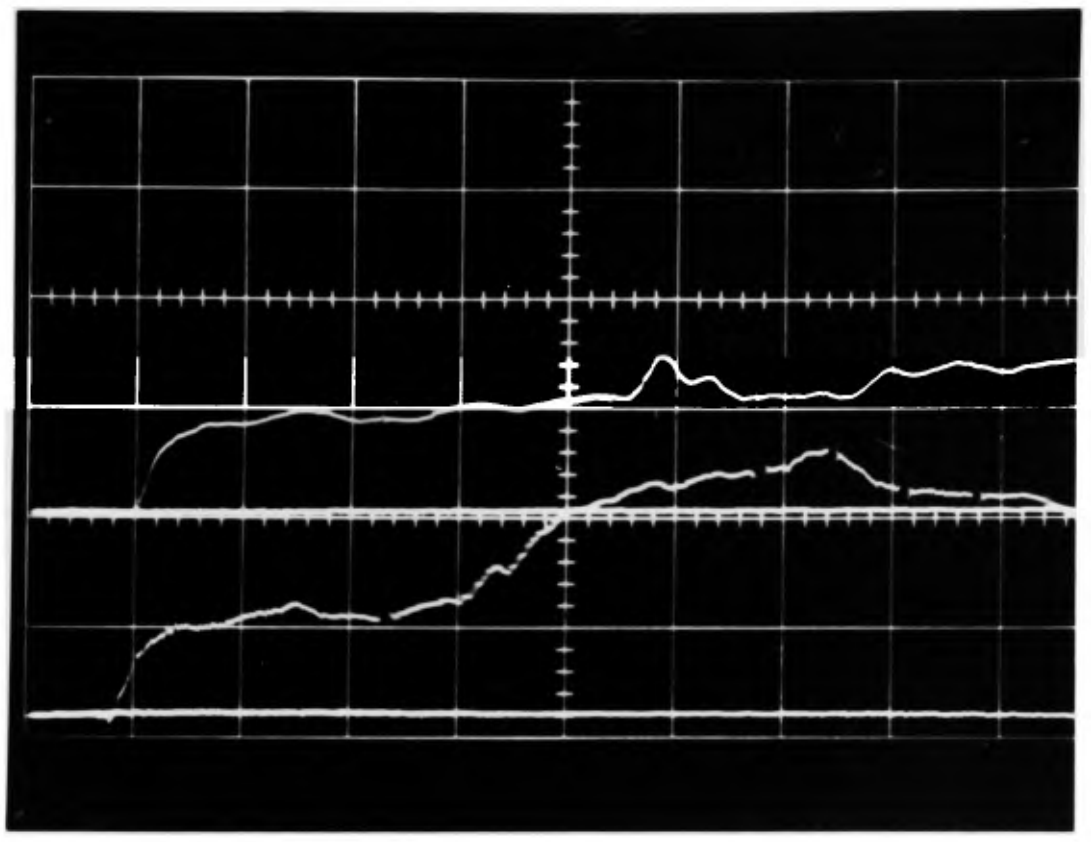
When the standard specimens were used in the wave propagation study, the gauge length deformation was much greater than that of the bars for a particular torque. Thus the specimen strain could be obtained from the known total twist. The effect of using specimens with a gauge length as short as 0.050 in. was to make the angle of twist in the bars comparable with that of the specimens for a particular torque. Thus it was not possible to derive an accurate stress-strain curve for the strain rate of 5×10^{-3} sec.$^{-1}$. For the purpose of fixing the point in stress-strain space at which the strain rate was changed, the stress-strain curve for 5×10^{-3} sec.$^{-1}$ was assumed to be the same as the one for 8.8×10^{-5} sec.$^{-1}$ previously obtained with the standard specimens. Thus knowing

the torque at which the strain rate was changed, and hence the stress, the position could be fixed. This assumption will be discussed later.

A photograph obtained from an aluminium test is shown in Fig. (6.16a) and the derived overstress-overstrain curves for several tests are shown superimposed on a quasi-static aluminium stress-strain curve in Fig. (6.17). It can be seen that the slope of each stress-strain curve at the higher strain rate tends towards that of the quasi-static one. It can also be seen that a continuous curve could be drawn to connect all the incremental ones and that this would diverge slightly from the quasi-static curve.

Copper Short Specimens.

Fig. (6.16b) is an oscilloscope photograph for a short specimen test on copper. The data from several tests are shown as overstress-overstrain curves in Fig. (6.18). If a continuous curve is drawn through these incremental curves it seems to be a constant height above the quasi-static curve. On the scale of these figures it is impossible to obtain a value of the initial slope of the overstress-overstrain curves but it can be said that it is of the same order as the elastic slope.



Hor. scale:- 52·5 μsec./cm. (50 μsec/cm. setting)

Vert. scale:- 70 lb.-in./cm.

The side of one grid square represents 1 cm.

Upper trace:- Transmitted wave at gauge station 2.

Lower trace:- Unloading wave at gauge station 1.

FIG. 6.1 Elastic test record.

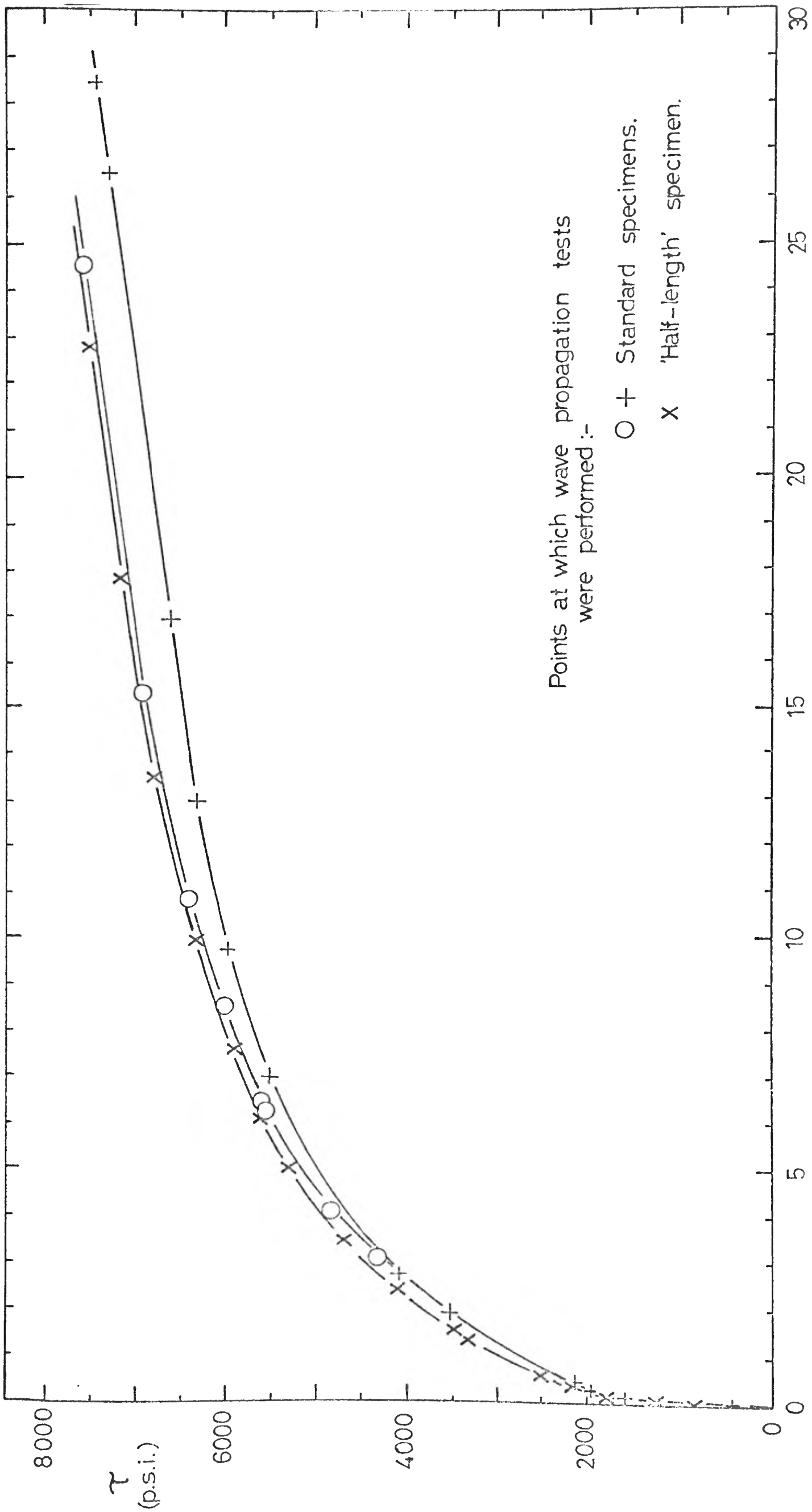


FIG. 6.2 Shear stress-shear strain curves for aluminium.

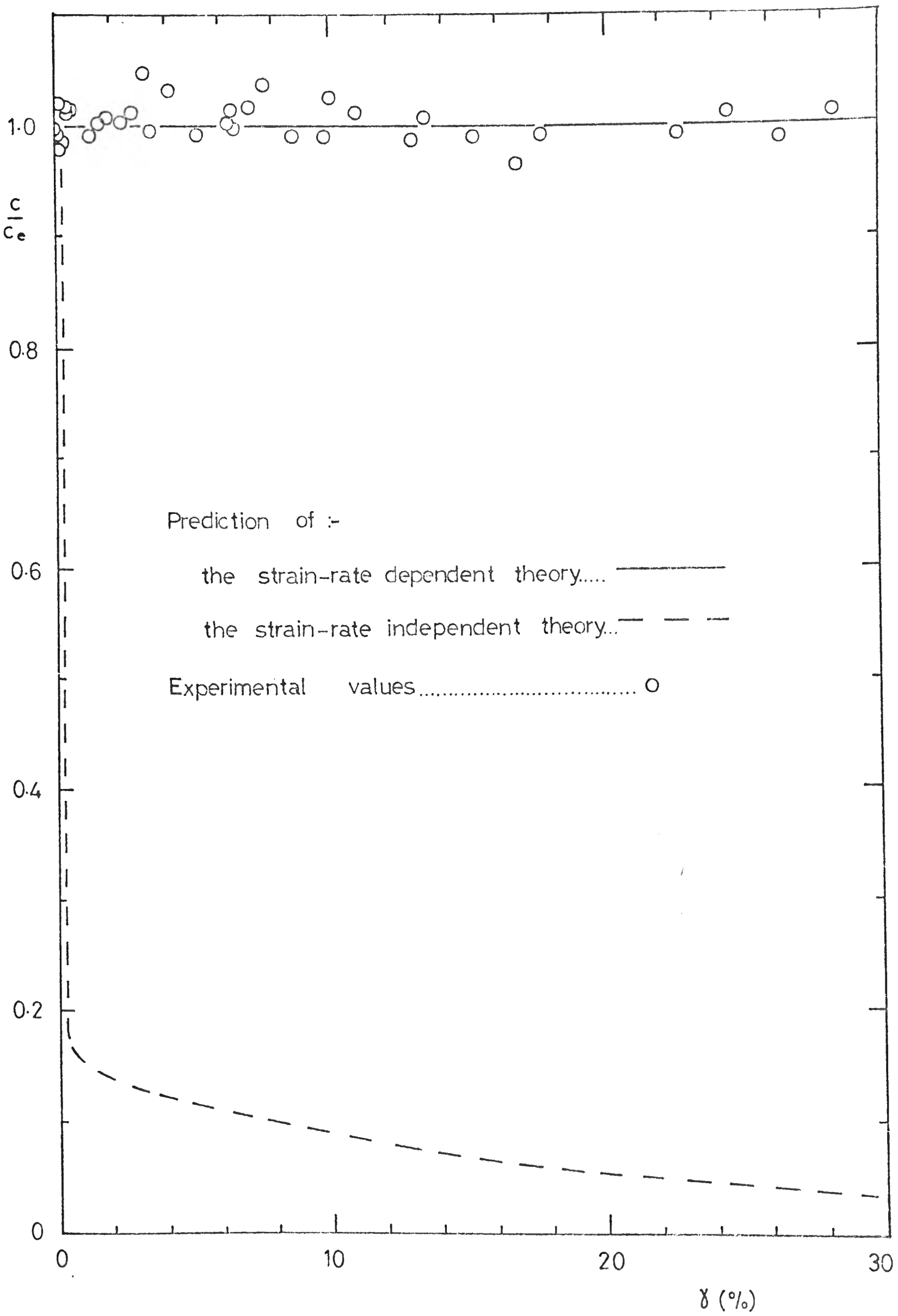
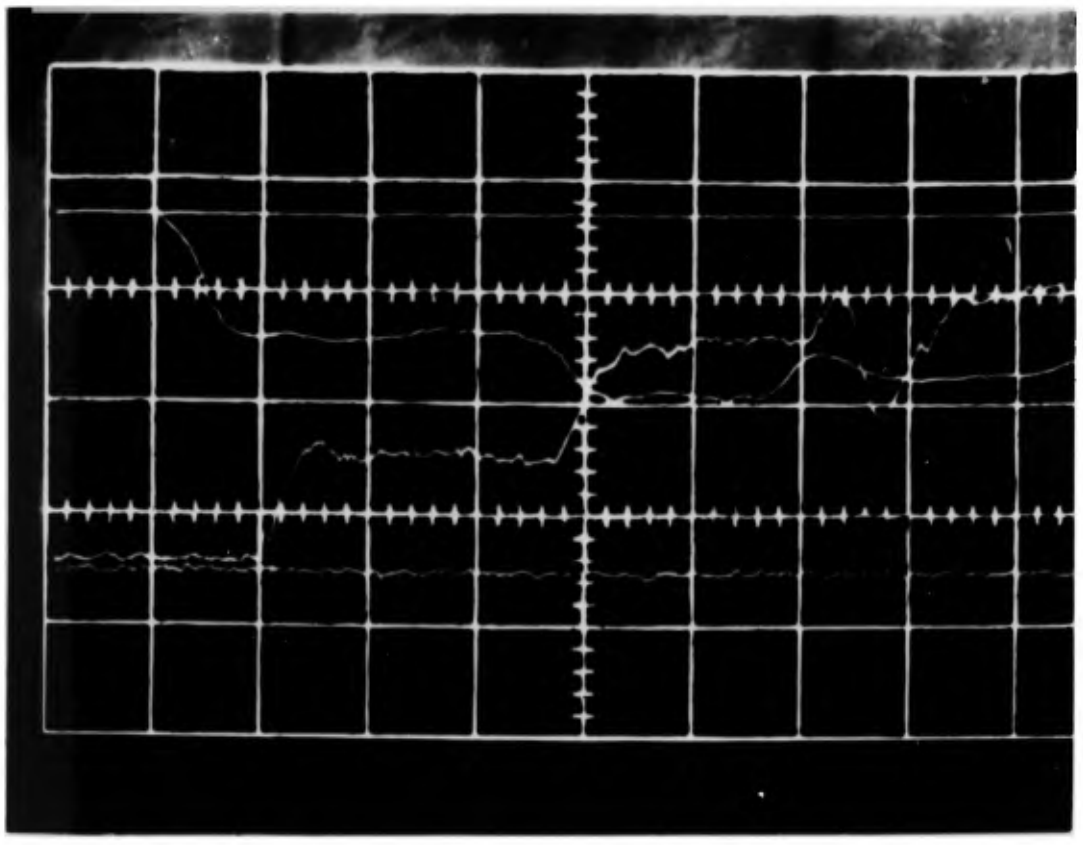
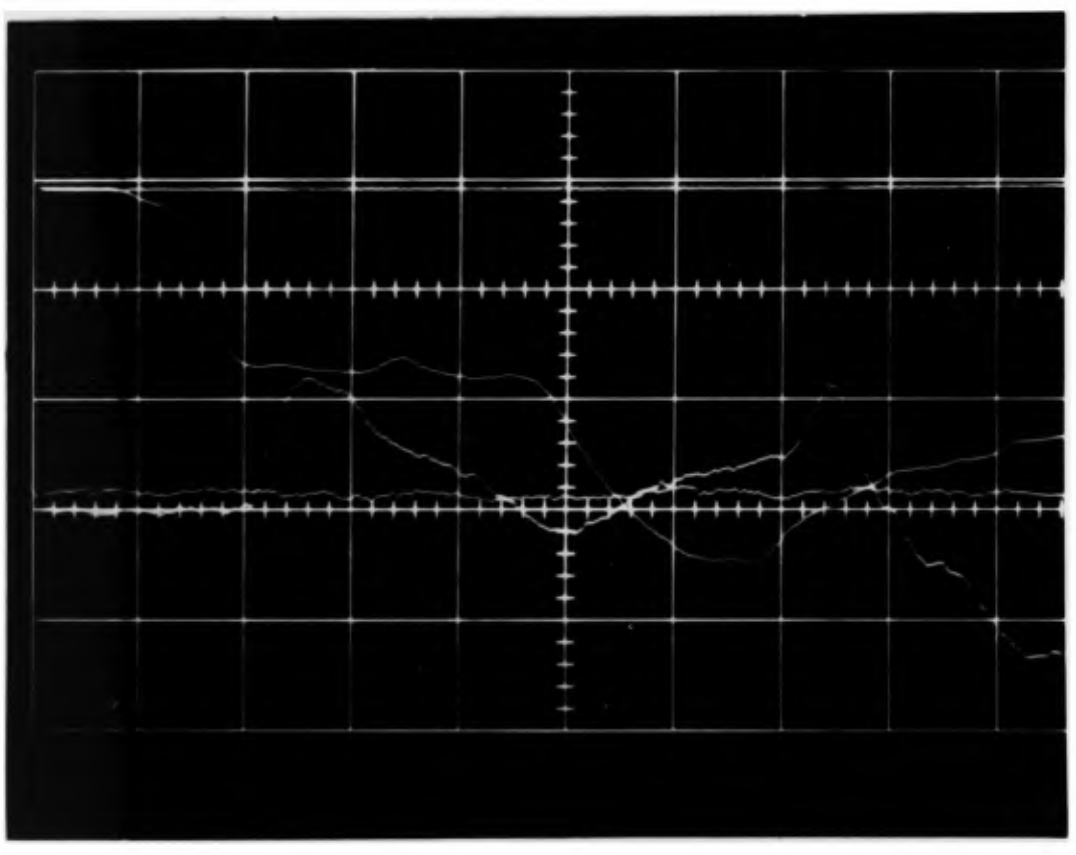


FIG. 6.3 Graph of dimensionless incremental wave speed v. shear prestrain for aluminium.



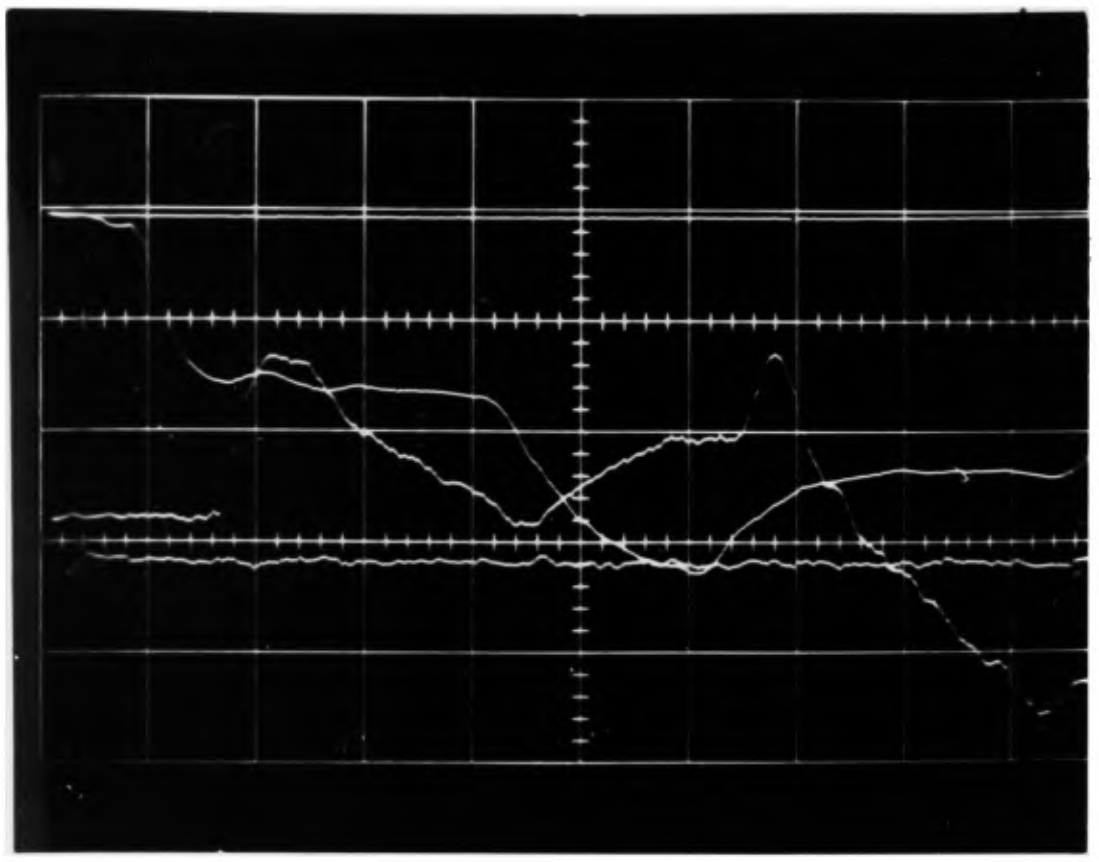
Prestrain 0·005% (elastic)



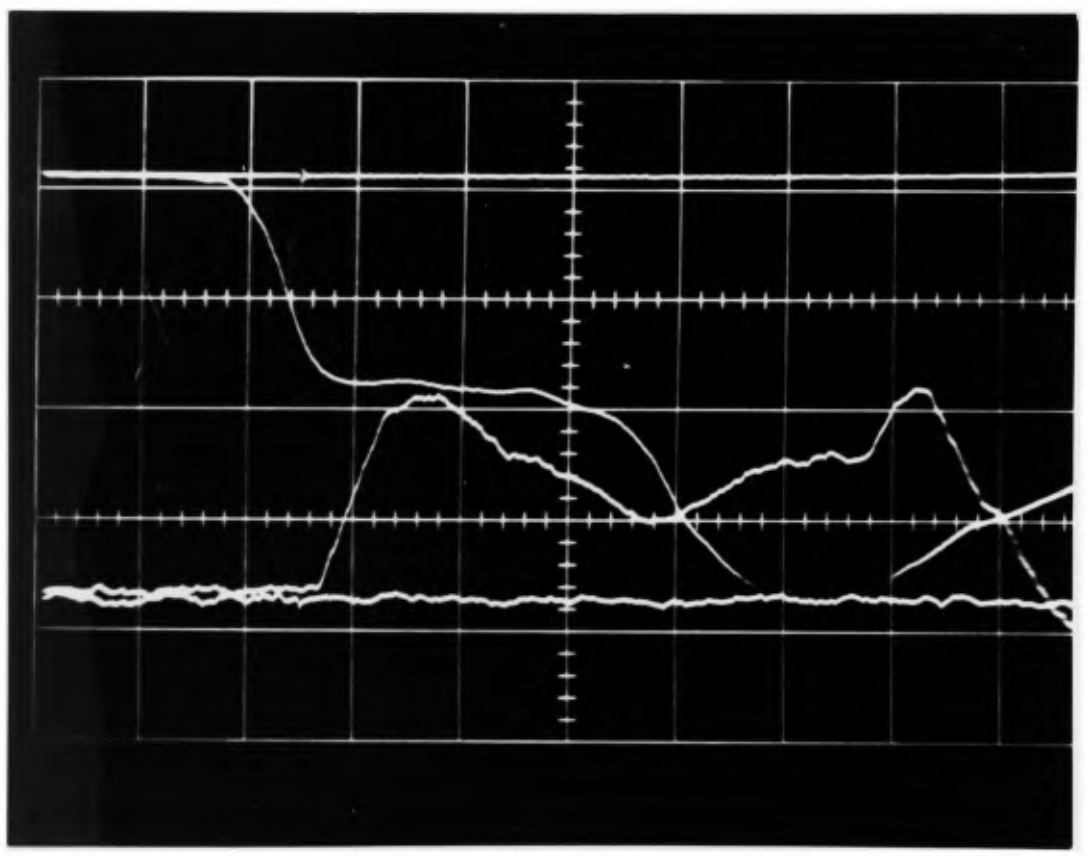
Prestrain 1·9%

N.B. For all the torsion oscilloscope traces except fig. 6.1 the upper trace shows the reflected wave, the lower trace the transmitted increment. In both cases an upward deflection represents loading.

FIG. 6.4 Oscilloscope traces for aluminium (i).

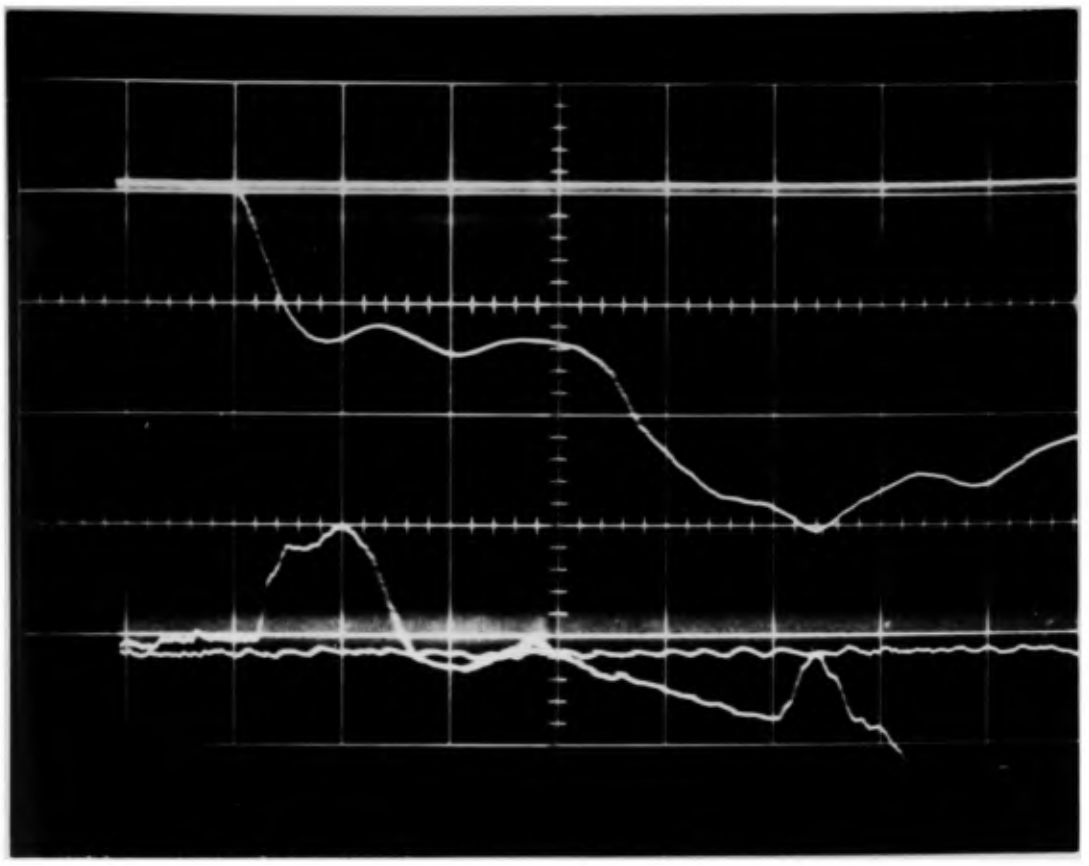


Prestrain 7·0%

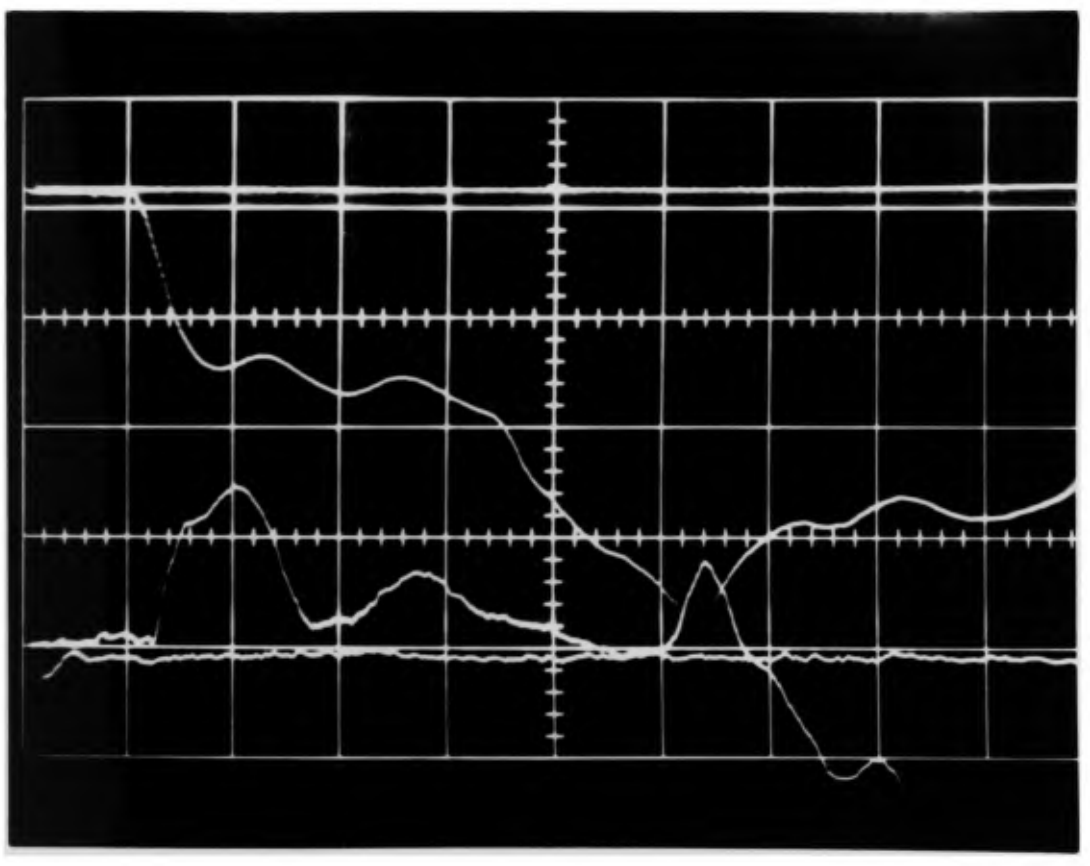


Prestrain 16·8%

FIG. 6.5 Oscilloscope traces for aluminium (ii).



Prestrain 9.96%



Prestrain 22.8%

FIG. 6.6 Oscilloscope traces for the 'half-length' aluminium specimen.

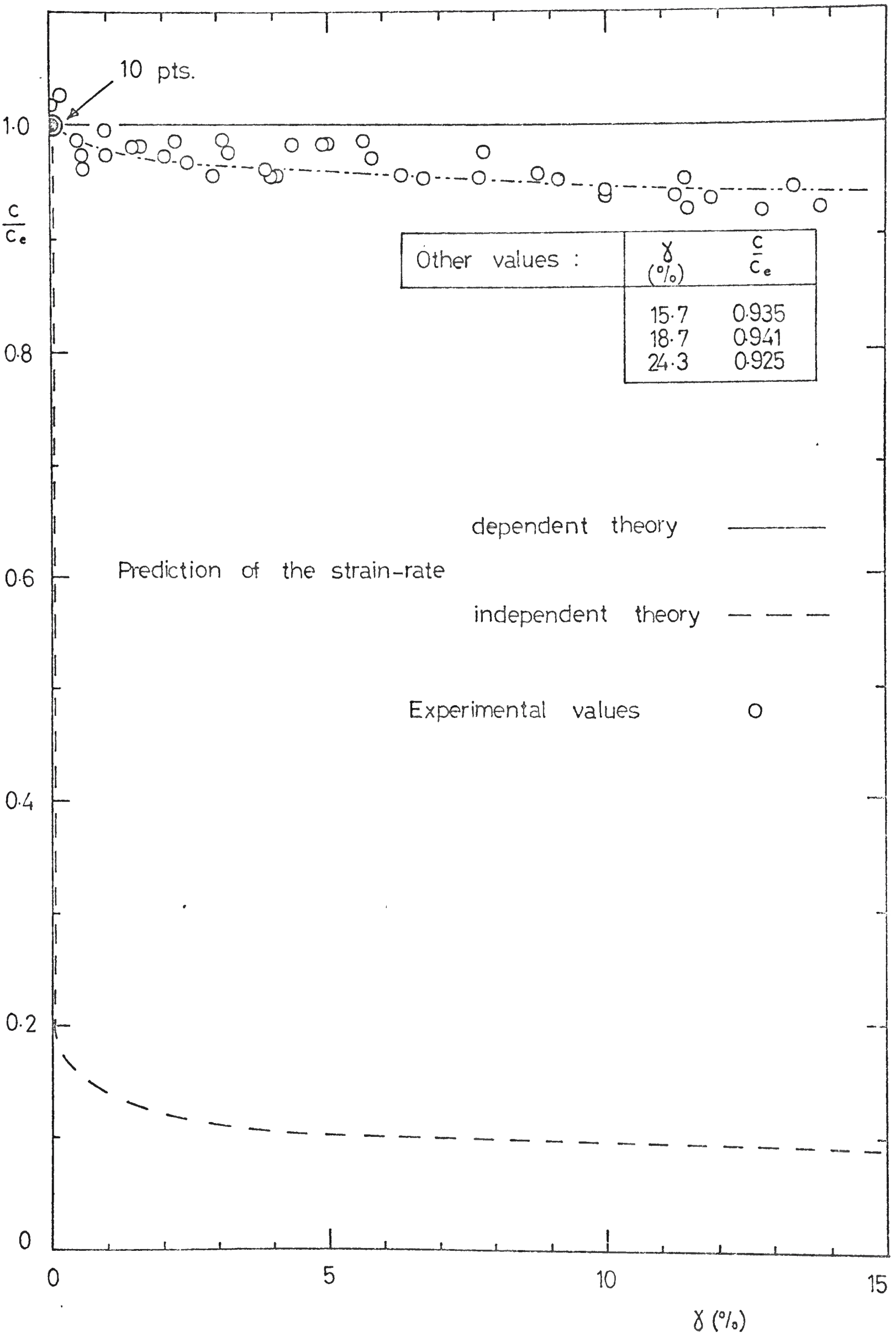
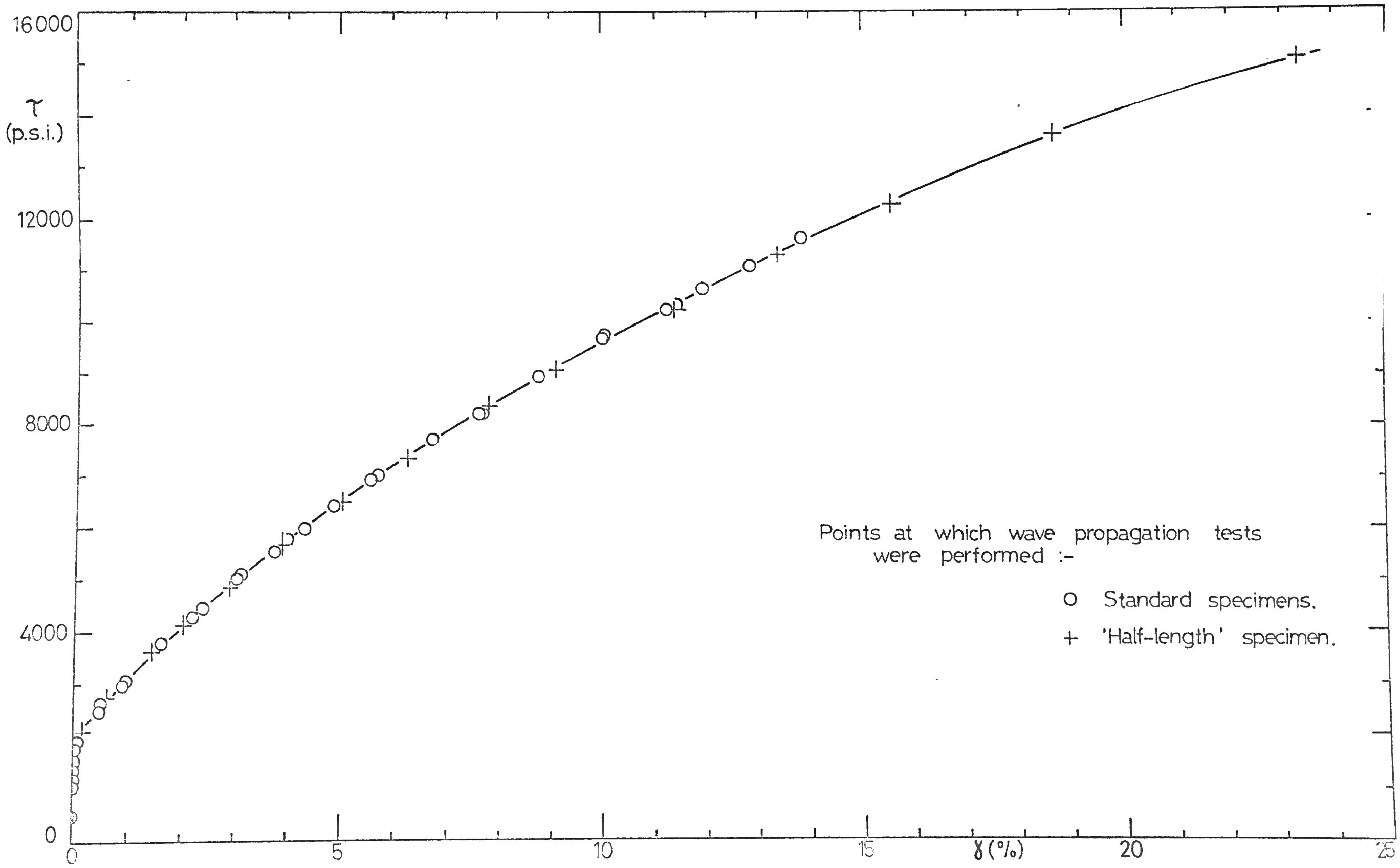
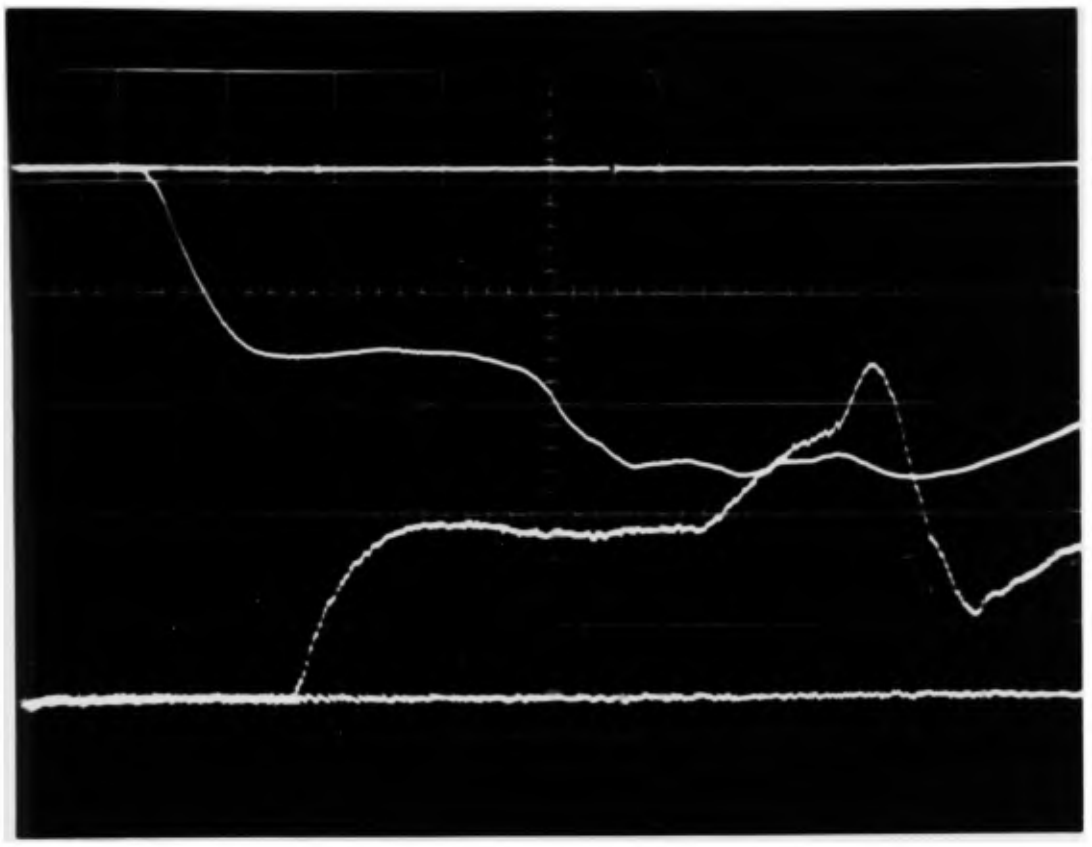


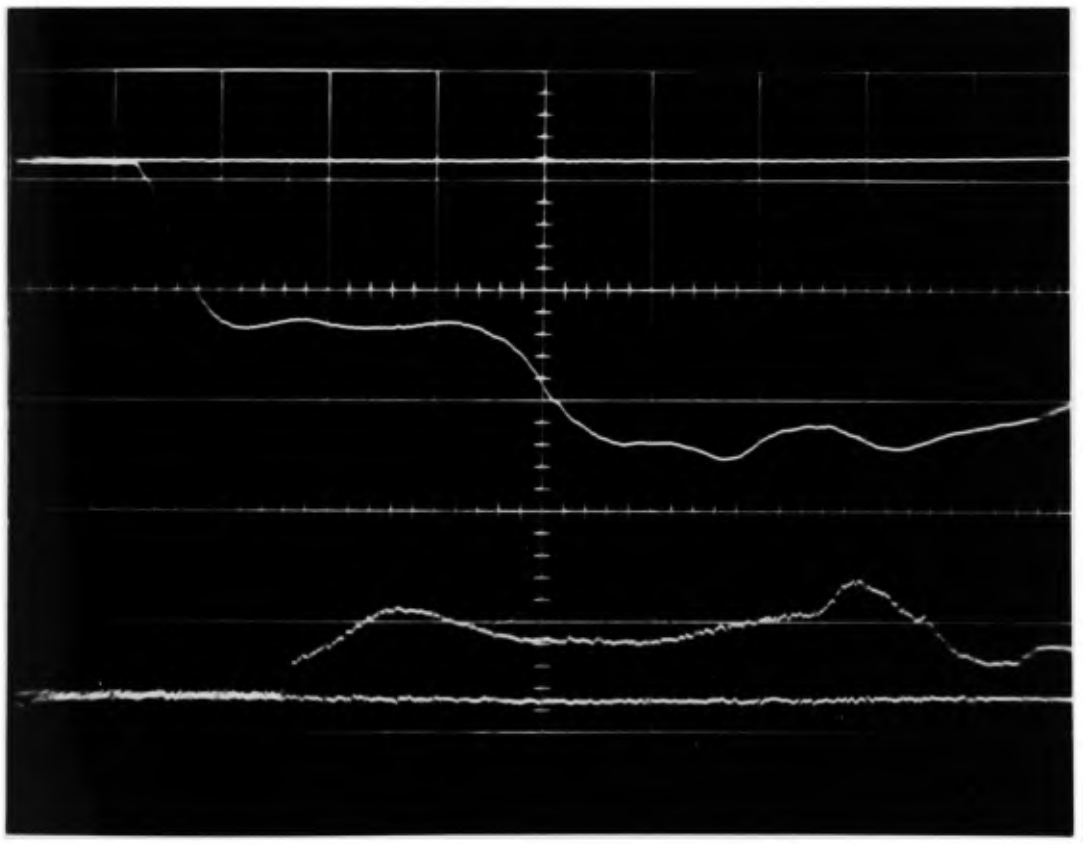
FIG. 6.7 Graph of dimensionless incremental wave speed v. shear prestrain for copper.

FIG. 6.8 Shear stress - shear strain curve for copper.



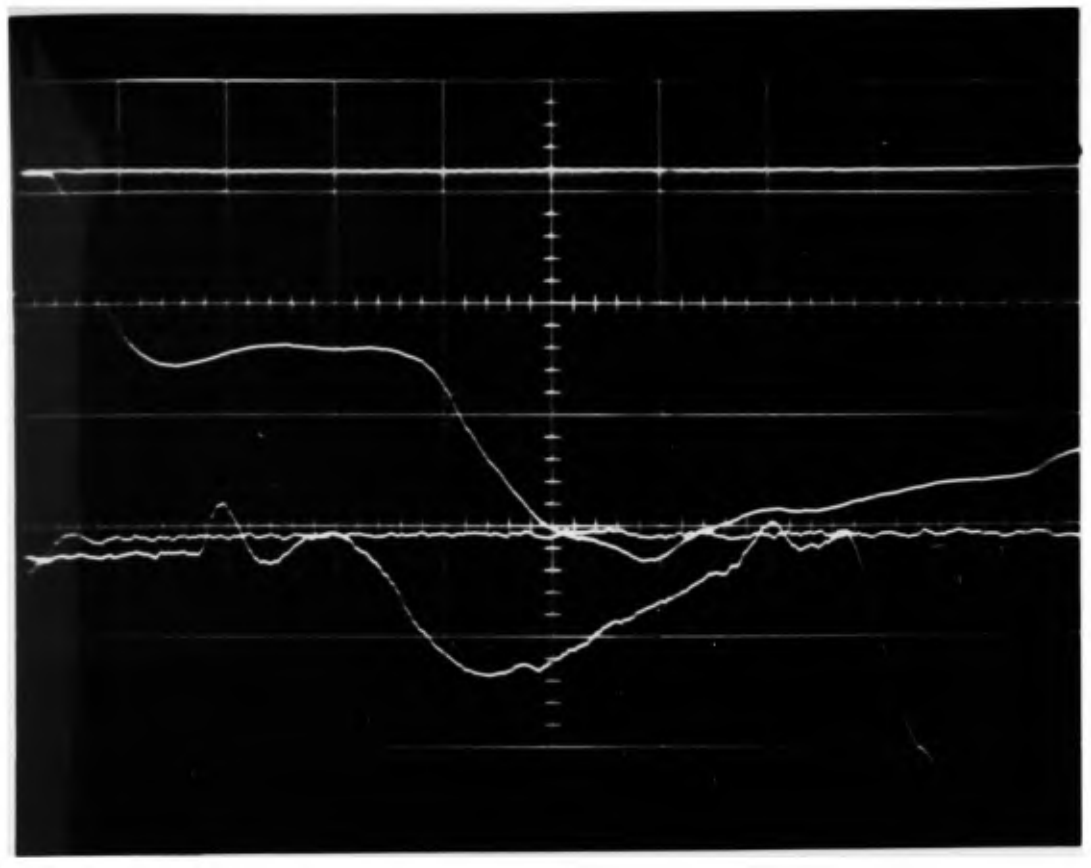


No prestrain (elastic)

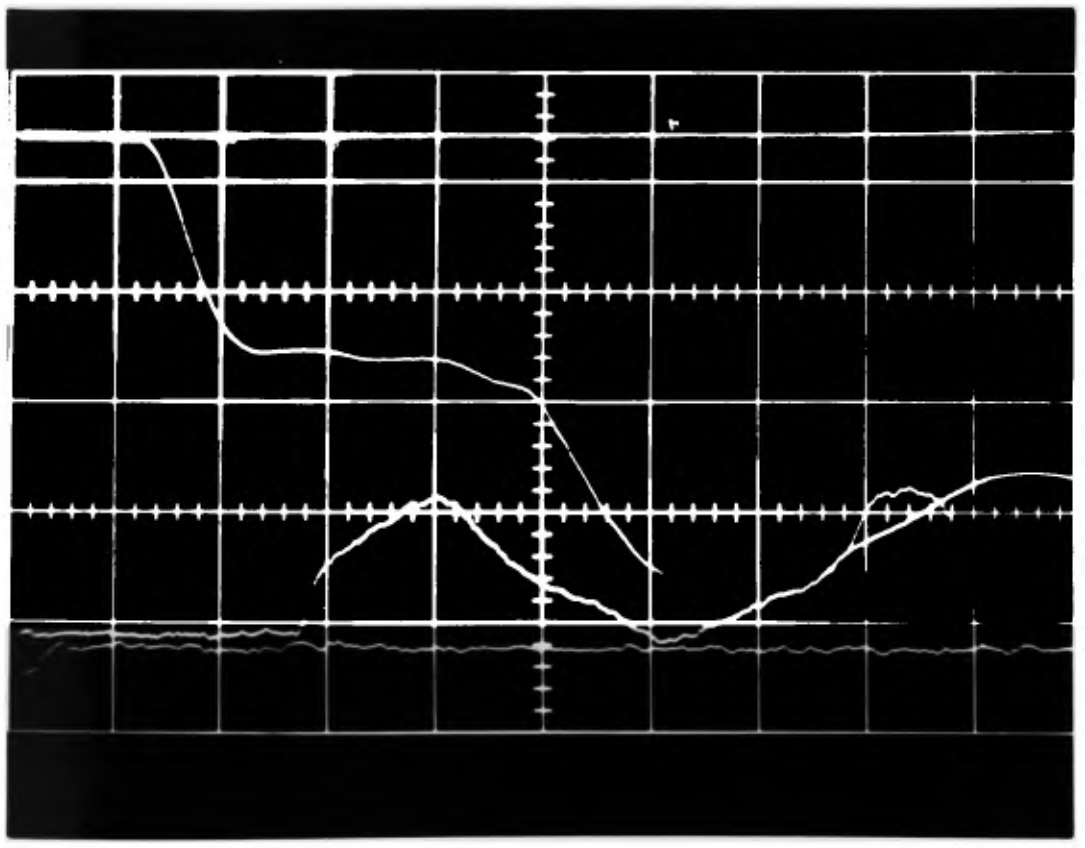


Prestrain 0·03%

FIG. 6.9 Oscilloscope traces for copper (i).

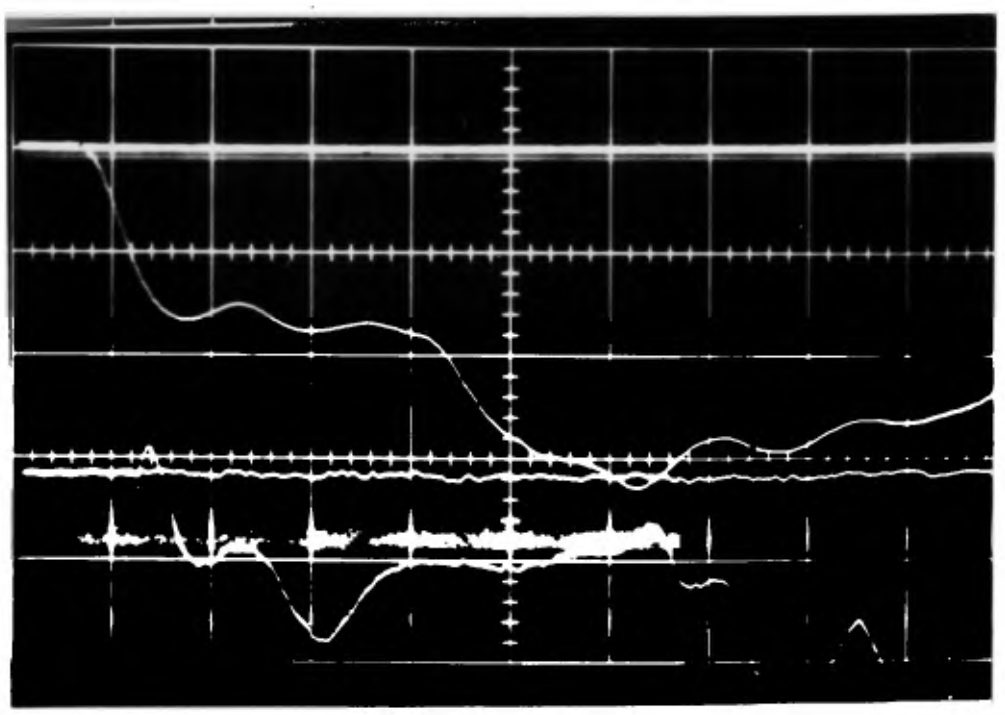


Prestrain 3·19 %



Prestrain 10·0 %

FIG. 6.10 Oscilloscope traces for copper (ii).

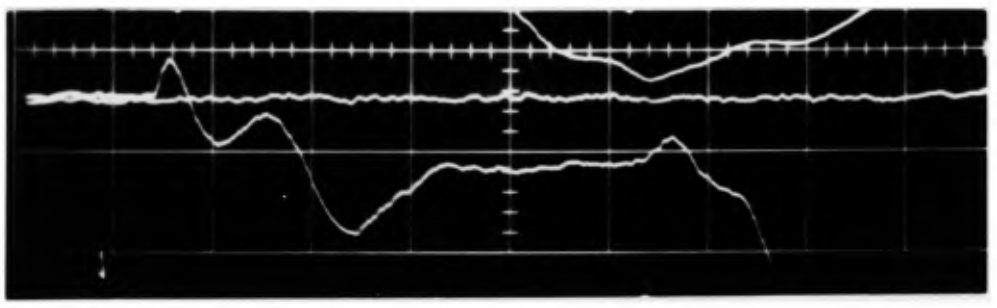


70 lb.-in./cm.

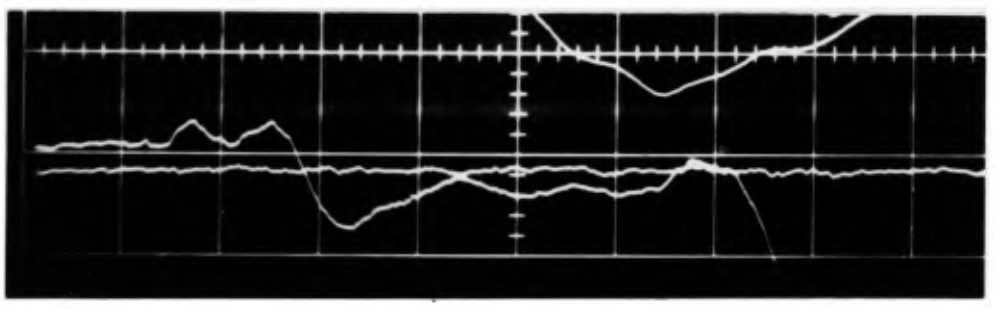
52.5μs./cm.

3.5 lb.-in./cm.

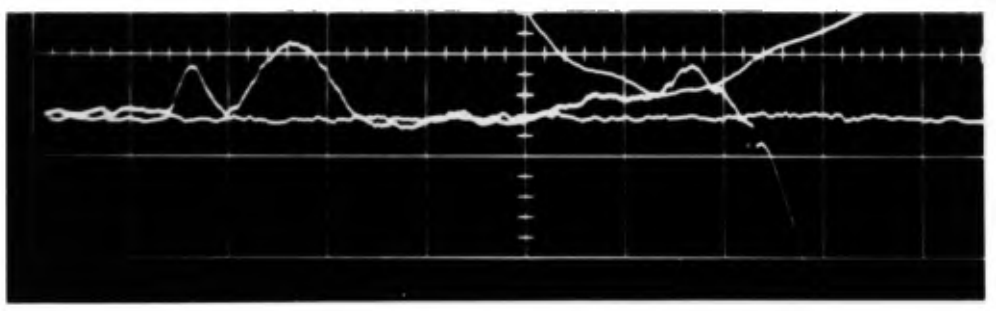
Prestrain 0.565%



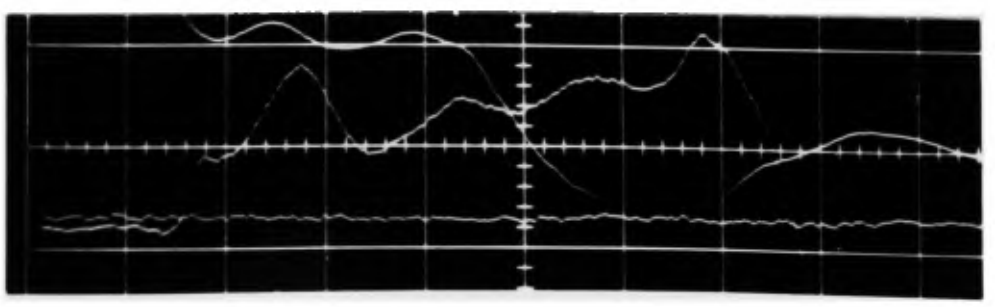
Prestrain 3.9[illegible]%



Prestrain 7.82%



Prestrain 11.4%



Prestrain 24.3%

FIG. 6.11 Oscilloscope traces for the 'half-length' copper specimen.

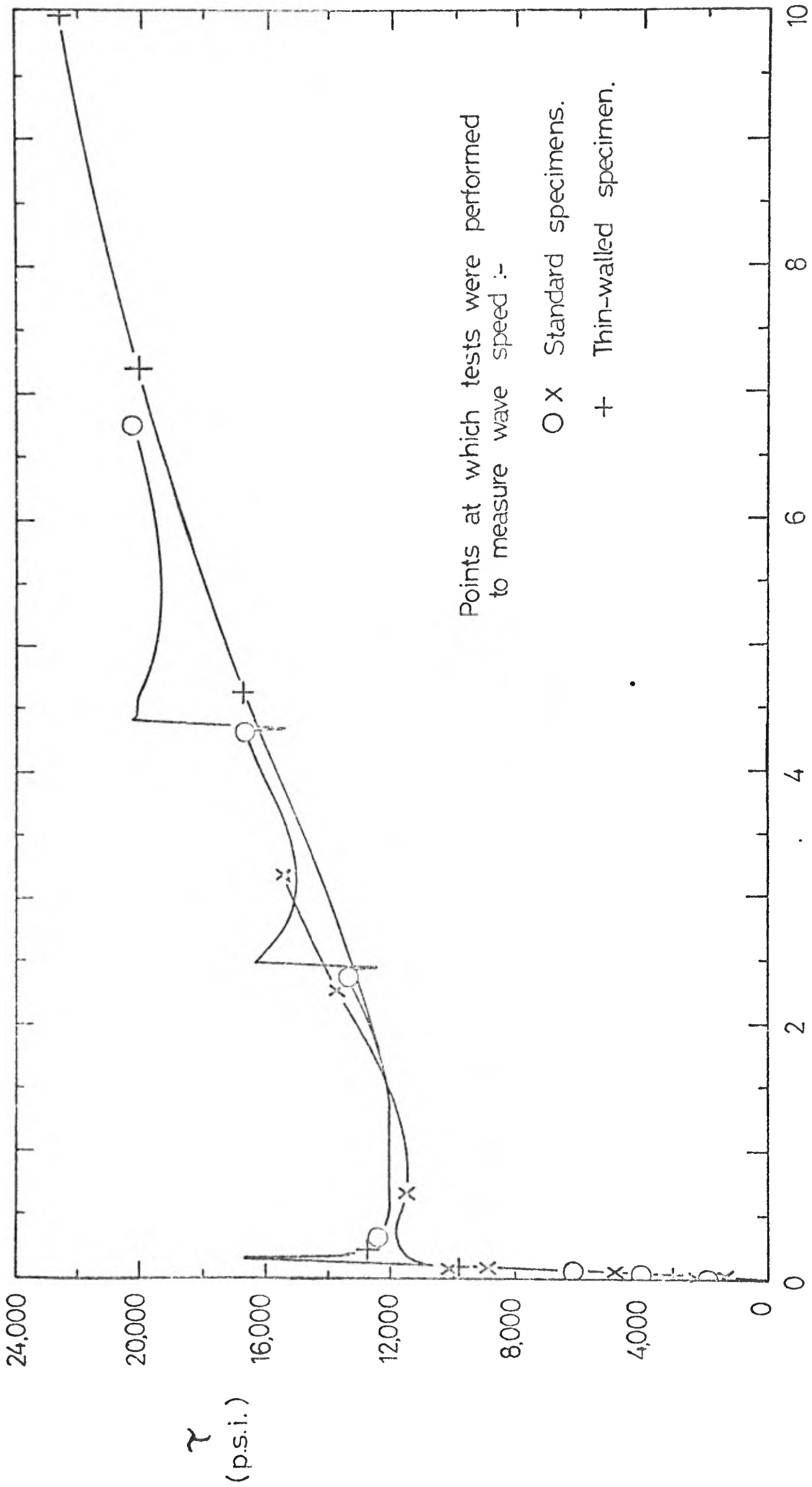


FIG. 6.12 Shear stress - shear strain curves for mild steel.

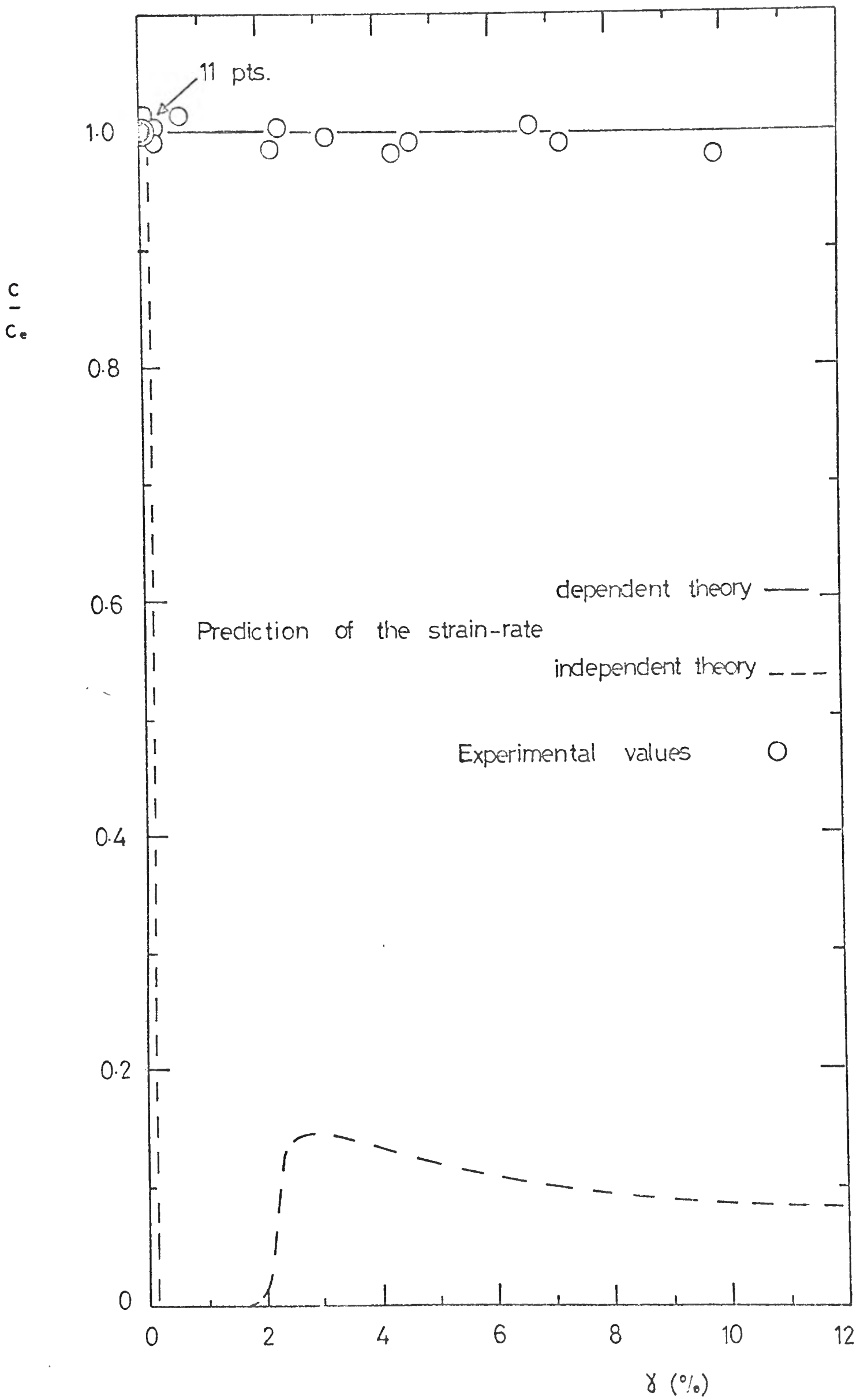


FIG. 6.13 Graph of dimensionless incremental wave speed v. shear prestrain for mild steel.

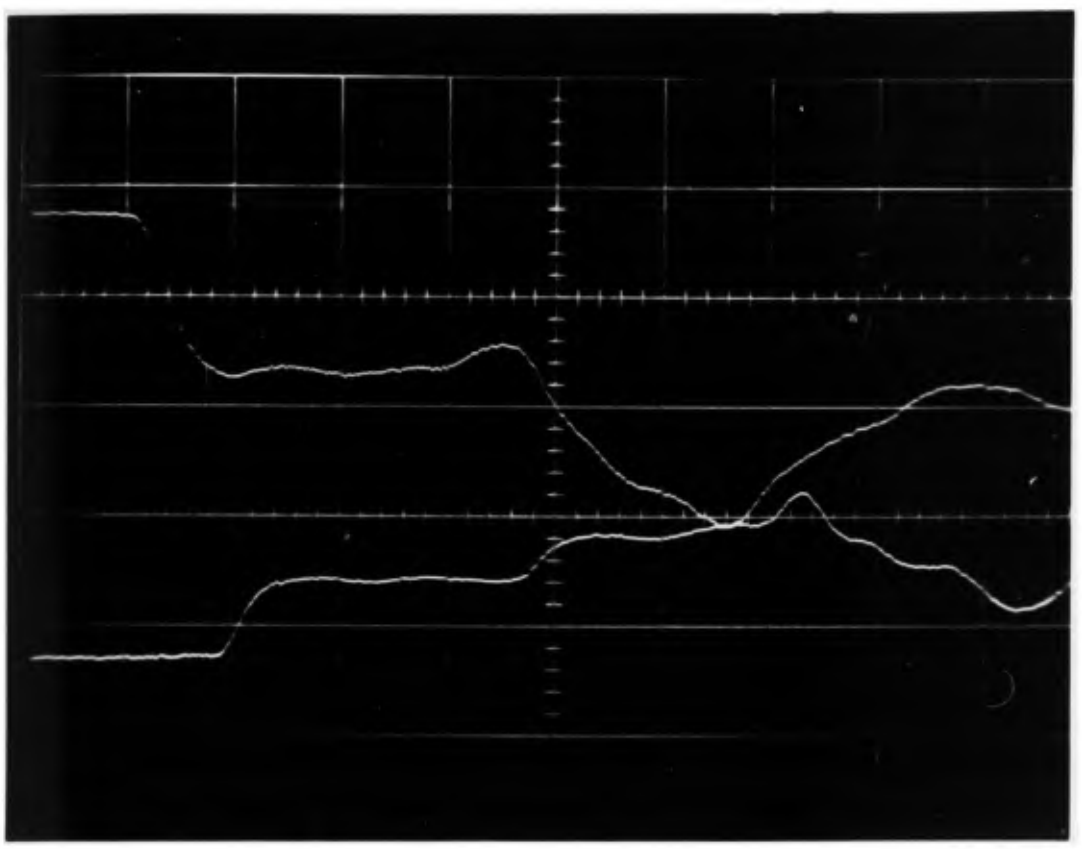
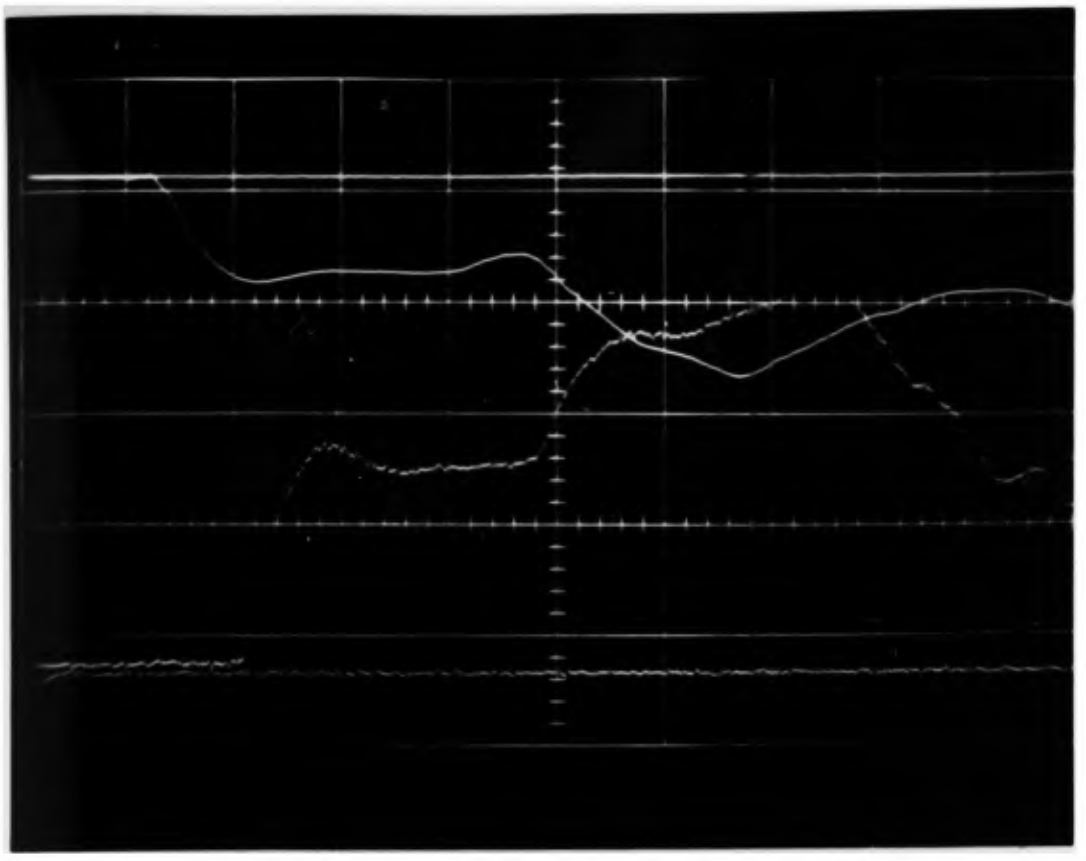
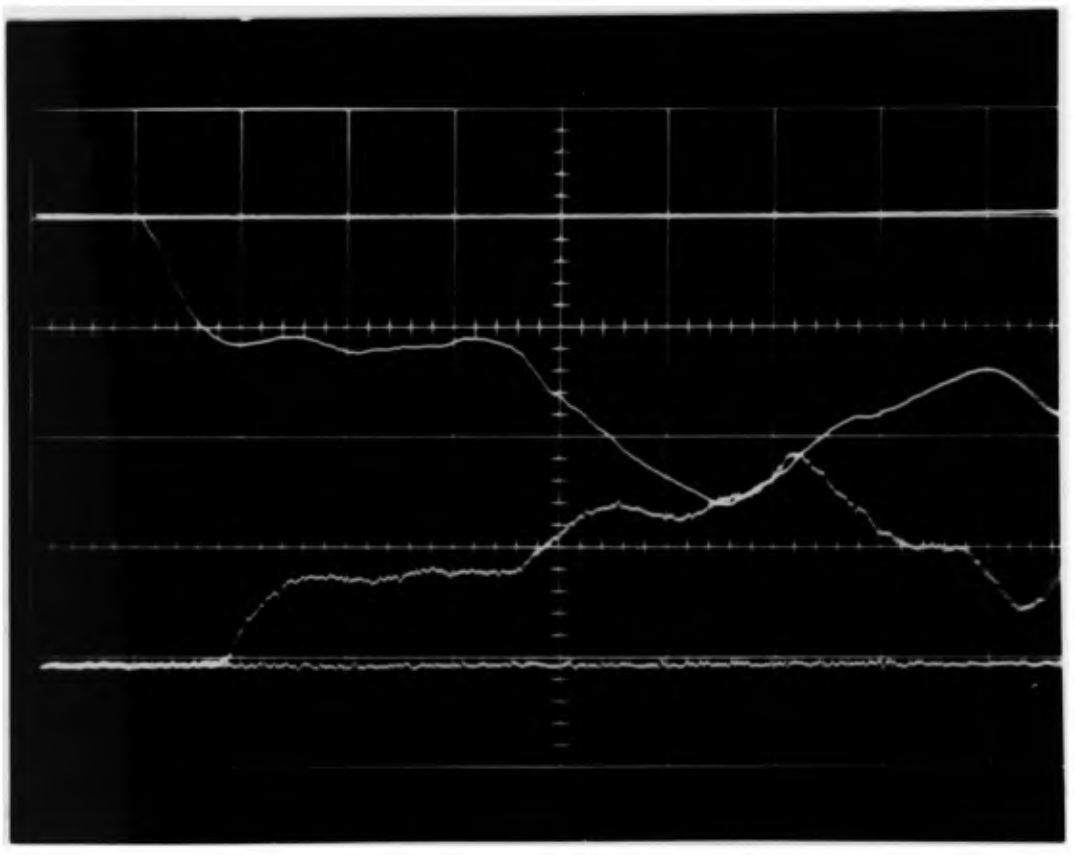


FIG. 6.14 Oscilloscope traces for mild steel (i)

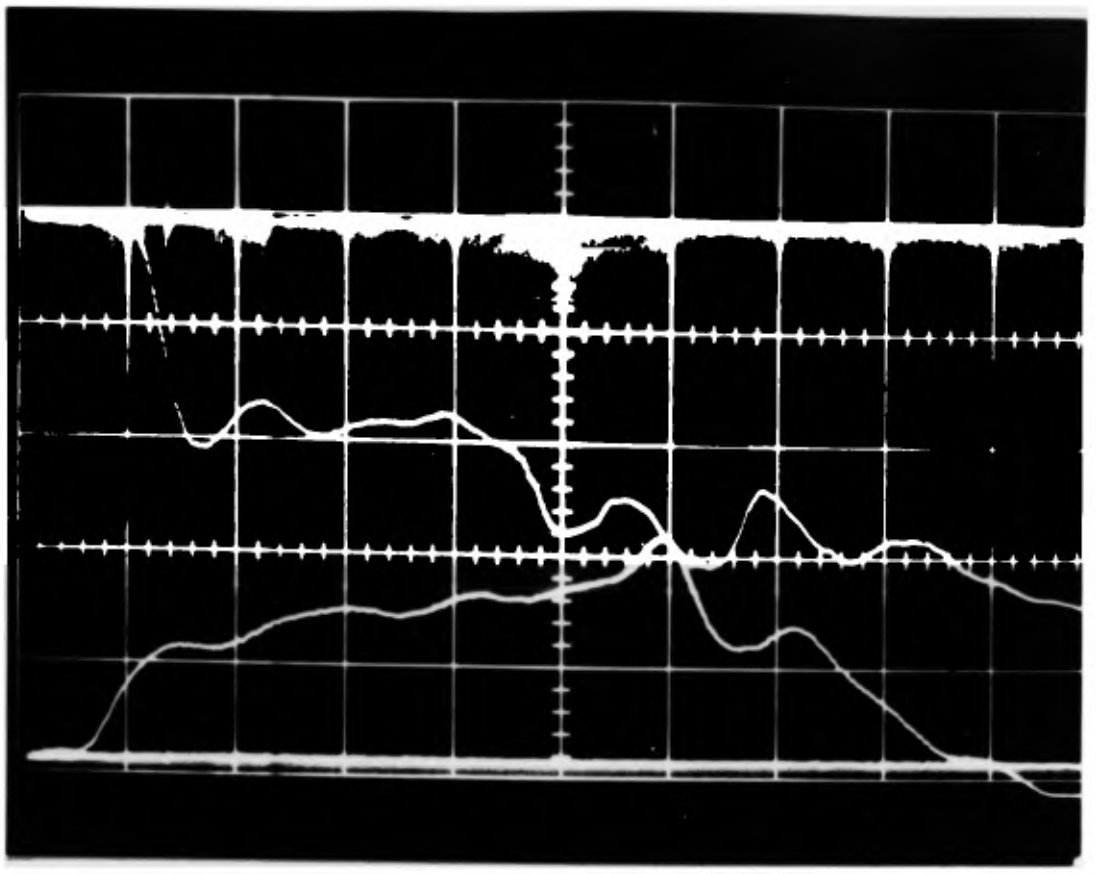


Prestrain 0·25% (lower yield region)

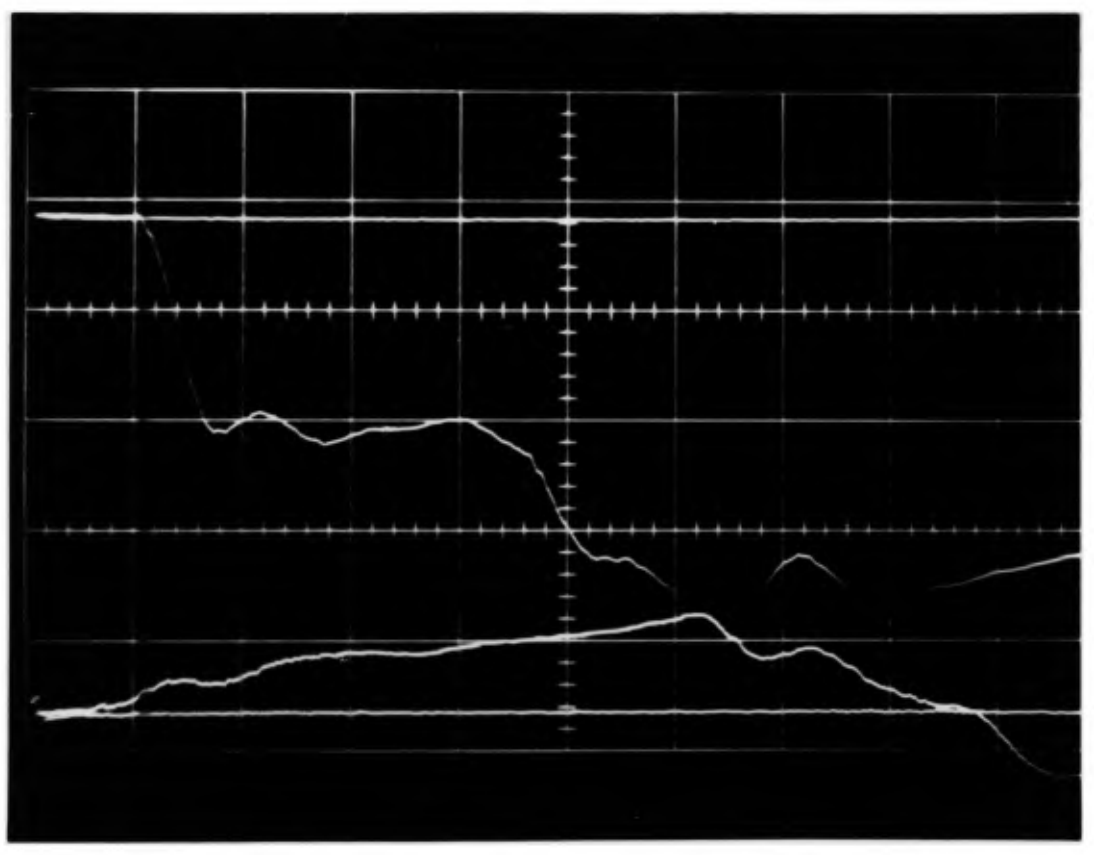


Prestrain 7·2% (work hardening region)

FIG. 6.15 Oscilloscope traces for mild steel (ii).



Aluminium.



Copper.

FIG. 6.16 Oscilloscope traces for very short specimens.

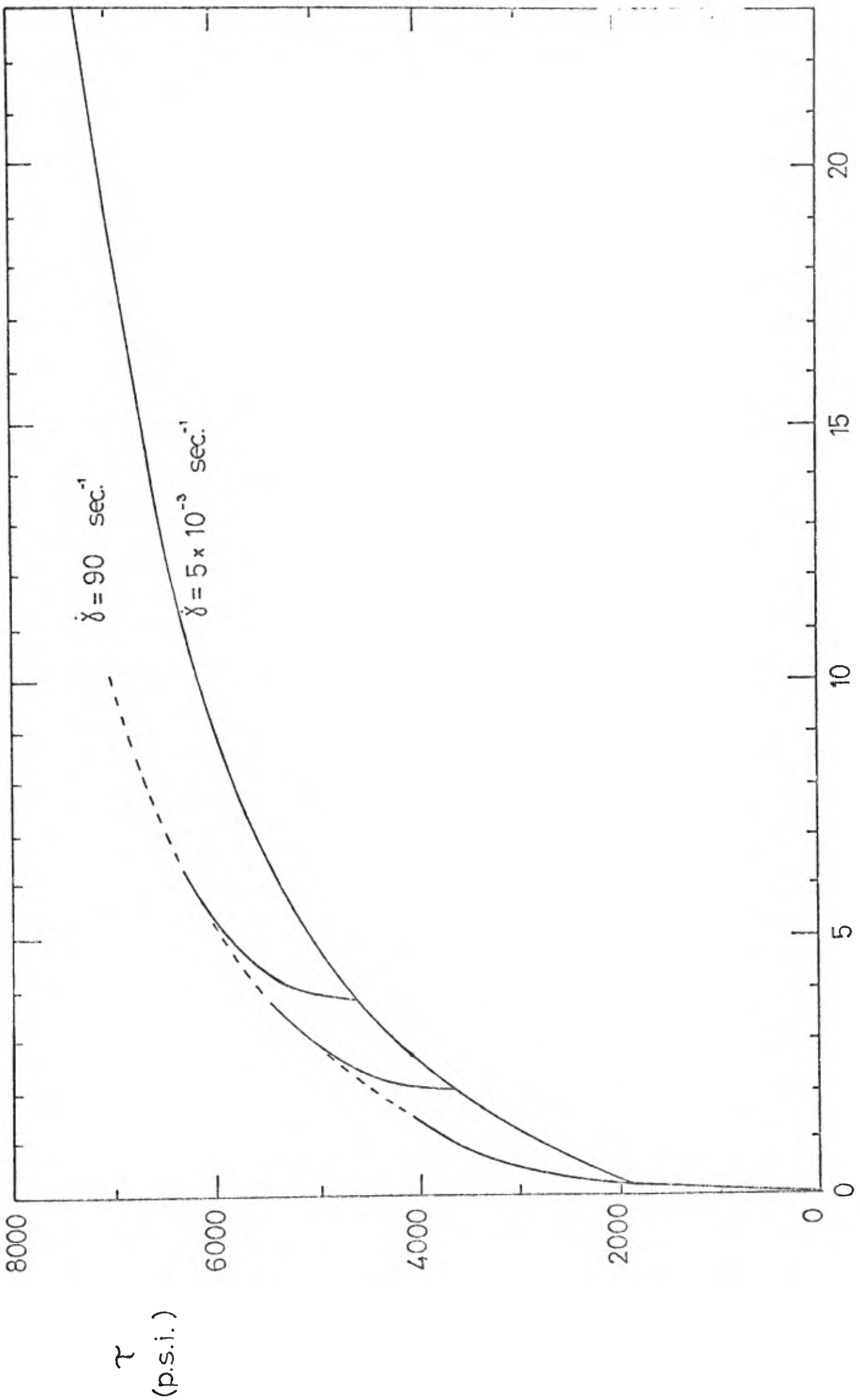


FIG. 6.17 Shear stress- shear strain curves for the short specimens of aluminium.

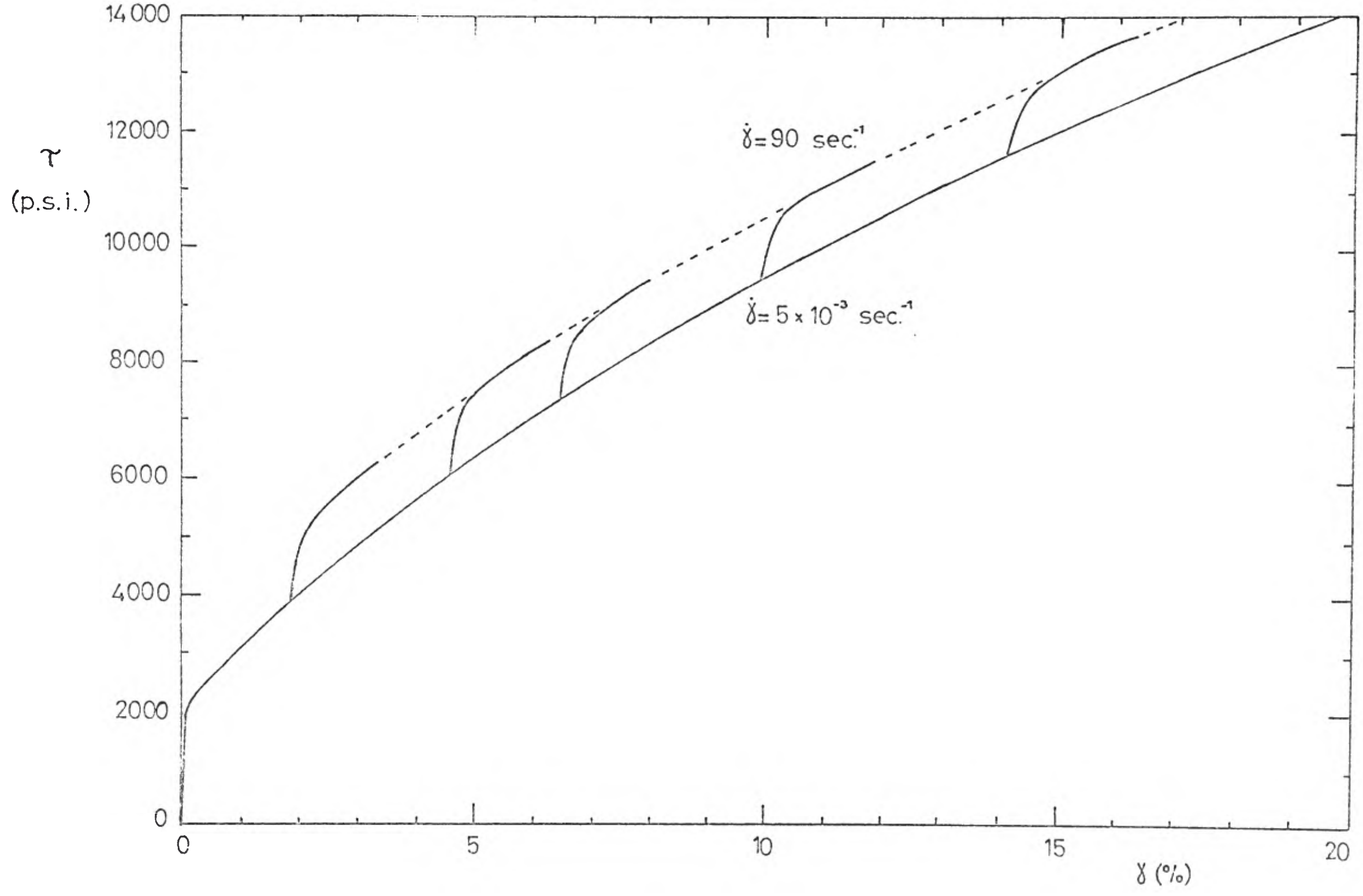


FIG. 6.18 Shear stress - shear strain curves for the short specimens of copper.

P A R T II

CHAPTER 7

AN OUTLINE OF EARLIER WORK ON THE BLANKING OF METALS.

Before considering the work which has been performed on blanking, it is necessary to state what is understood by the term 'blanking'. This is the name given to the process whereby holes of a particular shape are made in sheets of material by means of a punch-die system. In this system the hole of the die and the cross-section of the punch are geometrically similar and only a small clearance exists between the punch and the die. Industrially this process is also known as 'punching' depending on which part is discarded, the punched out piece or the remainder. Since it is irrelevent, scientifically, which piece is required, both terms will be used to denote the process.

Like many other industrial processes, blanking has developed more by trial and error than by scientific research. If one machine worked better than another then it was adopted without considering why it did the better job. Consequently fundamental knowledge of many common metal working practices is rather sparse. This lack of fundamental knowledge is especially noticeable in blanking, and this is difficult to understand since the process seems, outwardly at least, far more simple than say forging or extrusion.

The first research on a process similar to blanking was the study of the effects of bullets passing through metal sheets by Hopkinson (71). In treating this process as blanking,

the punch-die clearance must be taken as infinite. Similarly, the same treatment must be applied to the work by Pell (72), in which the first attempt was made to show a variation of the punching process with velocity of punch. Though he was chiefly concerned with finding metallurgical treatments to show permanent deformation phenomena in steel, a comparison of photographs of the etched metal after the penetration of steel plates by high velocity bullets and by low velocity drifting showed differences in the highly deformed region. The high velocity process showed less extensive yielding though the deformation patterns were similar in the two cases.

The first work on what can truly be called blanking, i.e. with a die as well as a punch, seems to be by Zener and Hollomon (73) in 1944. Their work was concentrated on the size of the plastically deformed region and it was found that the extent of this region was significantly reduced from its value at 'conventional' velocities, when the punch velocity was increased to 120 in./sec. Not only was the extent of gross plastic deformation reduced but the total distortion of the blank was also very much smaller.

Further tests on this aspect of the punching process, with similar results, were carried out by Zener (74) and the findings were verified much later by Novotny. This latter work was reported by Cockroft (75) who said that the punch, in this case projectile, had a velocity as high as 8,500 in./sec. It was reported that the distortion was reduced by about 50%. It was also claimed that 15 - 30% less energy was required for the high-speed process than for the low speed one.

In blanking, there are many variable parameters

of which punch-die clearance, punch diameter to strip thickness ratio, velocity of punch and temperature of the material are just a few examples. In order to observe the effects of any one parameter, the others must be kept constant. The two parameters which are most difficult to vary in a controlled fashion are temperature and punch velocity so that it was, perhaps, not surprising that these were investigated only very recently.

Slow blanking was used for most of the investigations of the 1950's beginning with Chang's (76) work in 1950. Chang investigated the effects of punch-die clearance on the shearing of circular blanks from several materials, finding the clearance for minimum punching energy. He also studied the effects of tool shear and tool curvature and produced a graphical construction relating flat punches to sheared ones. The next parameter to be studied was the die radius. Tilsley and Howard (77) investigated its effects on the dishing and tapering of the blank produced and also on the blanking force. In addition they made metallographic examinations of the shear regions of the deformed material.

Noble and Oxley (78) in 1964 attempted an explanation of the findings of a Production Engineering Research Report (79) in which it was shown that cracks occurred in the highly deformed region but that they could be arrested by radiusing the edges of the die and punch.

The first quantitative account of the relative energies required in low and high speed punching was made by Johnson and Slater (80) as late as 1964. The highest impact speed of the punch was 430 in./sec., using a linear induction

meter, but the punch velocity was almost zero as the blank was separated from the strip. Thus the velocity was by no means constant. A constant punch-die clearance was used with the following materials :- bright mild steel, soft and hard aluminium alloys, soft and hard brass and copper. It was found that, contrary to other investigations, the amount of energy required for a dynamic punch was greater than that required for a quasi-static test, except for one aluminium alloy. The difference between these results was attributed to the fact that this was the first time the energy had been measured directly, previously it had been found from calculations based on the metallographic examination of the blanks. Johnson and Slater also found that the shear fracture was smoother in the high speed punch and that the amount of distortion was reduced.

In further experiments concerned with quasi-static and dynamic blanking, Johnson and Slater (81) varied the radial clearance between punch and die and also added black mild steel and cupro-nickel to their range of materials. It was found that the energy to cause quasi-static blanking had a similar dependence on radial clearance as the dynamic blanking energy. They found a minimum energy requirement at a percentage radial clearance of about 8% for most of the materials. The fact that the energy for quasi-static blanking was less than that for dynamic blanking was attributed to strain-rate and inertia effects. In order to outweigh the observed reduction in the extent of the plastically deformed region, the stresses involved would have to rise by a substantial amount for such an energy increase.

Following this discovery, Johnson and Travis (82)

looked for a continuation of the trend by punching copper at much higher velocities. Punch velocities up to 7,000 in./sec. were used and the upward trend of punching energy was verified. Photomicrographs corroborated previous observations that the size of the shear zone was reduced by increasing the speed of the punch. It was not possible in their experiments to have velocities higher than 7,000 in./sec. due to the punch beginning to break up itself at these impact speeds.

Davies and Thewan (83) compared the quality of blanks formed at high and low velocities. In order to assess the quality they measured the dishing, doming, edge taper and edge condition of the blanks. They found a great improvement in the quality of mild steel due to the higher velocity but not such a marked improvement in the non-ferrous metals tested. They followed Zener and Holloman (73) and Zener (74) in suggesting that high temperatures, formed because of the short time available for conduction, were responsible for the narrower shear zone and reduced deformation. The smaller effect in non-ferrous materials was then attributed to reduced maximum temperatures because of a smaller resistance to shear and higher thermal diffusivity.

The same authors (7) later extended the work to study the maximum load and energy required for blanking at various speeds. The energy measurements showed some marked differences from those of Johnson and Slater (84). It was found that for all the tests on aluminium the energy required for dynamic blanking was greater than that for quasi-static blanking. However for some thicknesses and radial clearances with mild steel and brass the reverse was apparent. Although

they tried to obtain load-penetration curves, the results were highly oscillatory and consequently too much trust could not be placed in them.

In order to resolve the energy question, load penetration curves were required for a wide range of punch velocities, so that the actual energy taken by the specimen could be measured. In all the previous methods of energy measurement it was not possible to separate the energy requirements of the specimen from the energy dissipated in the rest of the system. The present investigation was successful in obtaining load-displacement curves for mild steel for the complete blanking process for velocities ranging from 5×10^{-5} to 900 in./sec., when comparing the strain rate effects of tensile loading with those of punch loading. This work was reported by Dowling and Harding (84). It was found that there was no significant change in the energy absorbed during rupture but that the deformed region was reduced considerably at the highest speeds. The behaviour of the mild steel was ductile and it was found for this material that there was good correlation between the results for tensile and punch loading.

Slater and Johnson (85) studied the effects of temperature on the blanking process using mild steel, copper and aluminium. The results showed that for the dynamic blanking of all three materials the energy required at the elevated temperatures was greater than the quasi-static energy at the same temperature. They also found that the strain-rate sensitivity was much greater above the recrystallisation temperature than below and on these grounds wished to classify the process according to the ambient temperature. If it were above the recrystallisation temperature there would be super-critical

blanking if not, sub-critical.

Another method of classifying the process of blanking was suggested by Maeda and Tamura (86), on the grounds of whether the ratio of die diameter to metal thickness were above or below a specified value. There would then be narrow punching or general blanking. However, such suggestions are unreasonable for, because of the number of variable parameters, the conditions of each blanking test should be specified, and dividing into two or even four classes would mean very little.

It was suggested by Dowling and Harding (84) that the study of brittle behaviour in the punch tests might, as it is in tensile loading, be more interesting. Slater and Johnson (85) used only higher-than-room temperatures in their tests and did not include a brittle-ductile transition. Davies and Dhawan (7) used cast iron as a specimen but unfortunately, paid little attention to the results as being of limited use to industry. What they found seems to be very interesting, however, that as the punch velocity increased the fracture became more ductile, in contrast to the established fact that materials become more brittle with increased strain rate. This last fact seems to have been in the minds of Johnson and Travis (87) when they suggested the results of Davies and Dhawan which showed a decrease of energy in the dynamic tests on mild steel could have been due to a high carbon content and hence increased susceptibility to cracking.

This work of Johnson and Travis (87) explored a new aspect of the punching process, that of the punch penetration required to cause separation. It was found for the material tested, mild steel, that a smaller penetration was required in

the dynamic tests than in the quasi-static.

Recent work by Kulkarni, Ezra and Harding (88) investigated the simultaneous punching of several holes in cylinders of mild steel, tool steel and hard and soft brass. It was found that the amount of explosive required for punching high strength materials could be very accurately predicted but that, due to some of the energy being used for slug formation, the quantity could not be so accurately predicted with low strength ductile materials. In all cases, however, the holes produced were extremely clean and needed no additional finishing or deburring.

C H A P T E R 6.

BLANKING APPARATUS.

A major object in embarking on a programme of blanking was to investigate the possibility of inferring shear stress-shear strain curves from the results. The actual stress system present in this mode of deformation is quite complex even though the process appears to be a very simple one. If it could be shown that such an inference was valid the strain-rate sensitivity in shear of materials could be found without the necessity for highly machined specimens such as those required for torsion testing. In addition, a punch test is performed by squeezing together the top of the punch and the bottom of the die, i.e. the same action as a compression test, so that the actual test is far easier to perform than, say, a torsion test. Some of the difficulties encountered in dynamic torsion machines have already been mentioned in Part I. Apparatus was already available for carrying out compression tests at a wide range of strain rates, so that all that was required to make punch testing possible were suitable punch-die assemblies to fit the relevant machines.

In order to obtain as wide a range of punch velocities as possible, three machines were used :- a standard 10,000 lb. Instron Testing Machine for the lowest speeds, a special hydraulically operated rapid loading machine for intermediate punch speeds and a drop weight impact tester for the highest speeds. It will be convenient to consider the hydraulic machine first.

The Hydraulic Machine and Punch-Die Assembly.

The hydraulic loading machine itself will be described

very briefly, since there is a full description in a paper by Cooper and Campbell (89). A cylinder, into which oil can be pumped at a high pressure, is divided into two regions by a piston. This piston can be moved up or down or kept stationary by suitable control of the pressures on opposite faces of it. In order to provide rapid motion a quick-acting valve releases the pressure on one side of the piston. A rod attached to the piston transmits its motion to the exterior of the cylinder where it can be used for testing purposes.

The dimensions of the punch-die assembly were limited in two ways. Firstly by the dimensions of the hydraulic machine and secondly by the available force which could be applied to the piston and hence to the punch. The latter restriction decided the diameter of the punch, which was 3/8 in., while the former controlled the overall dimensions of the assembly.

Since the primary object of the experiments was to obtain load against displacement curves for the punching process, space had to be made available for measuring these quantities. The instrumentation used on the machine for compression and tension tests was described in the paper by Cooper and Campbell (89), and the same instrumentation was used as far as possible for these experiments. For the measurement of displacement, velocity transducers were attached to the piston rod so that a velocity-time trace could be obtained on an oscilloscope. The displacement was obtained from this by integration. The measurement of load was again performed by means of electrical resistance strain gauges attached to a load cell, but because of the available space a new, shorter cell had to be made.

A diagram of the original punch-die assembly and load

cell is shown in Fig. (8.1a). All parts were machined from En 24 steel which was quenched and tempered to give 150 Kp.s.i. yield stress. Three T.M.L. type P.S.3 strain gauges were equally spaced round the load cell at the position shown, and fixed to it by means of 'Araldite' adhesive. The gauges formed one arm of a Wheatstone bridge whose output signal was fed into the upper channel of a Tektronix type 555 dual beam oscilloscope. The velocity transducers were connected to the second channel.

Two consequences of the rapidity of the tests were that an oscilloscope camera had to be used to photograph the traces and that no dummy gauges were necessary for temperature compensation.

The die-specimen assembly had a screwed connection with the load-cell, with the end face of the load cell acting as a bearing surface. This was to prevent distortion of the threads which might occur if they had to carry large loads. A screw joint was necessary so that assembly and dismantling of the specimen could be carried out where more room was available away from the hydraulic machine. The specimen was clamped to the die by means of six socket screws.

The punch screwed on to the top of the hydraulic machine's piston rod and it can be seen that the parts had to be very carefully machined to ensure good alignment. It has already been stated that the nominal value of the punch outside diameter was 3/8 in.; the accurate value was 0.375 $\pm$ 0.0002 in. The die inside diameter was ground to 0.377 $\pm$ 0.0002 in. so that the radial clearance was 0.001 $\pm$ 0.0002 in.

Using the definition of dimensionless percentage radial clearance given by Johnson and Slater (81), the punch

and die sizes used in conjunction with 1/8 in. thick specimens produced a value of 0.8% for this parameter. According to their work the energy to produce blanking was very high at this value but the small clearance was chosen because it was thought that the smaller the clearance the more uniform would be the deformation and also the higher would be the strain rates. It was believed that much of the energy variation observed by Johnson and Slater was due to frictional and other losses in the machine and that such variation would be overcome by actual specimen measurements as undertaken here.

The Instron Loading Machine.

The punch-die assembly already described was also used for the slow speed punch tests. The assembly was placed between the moving crosshead and compression load cell of the Instron machine with two ball-joints in series to ensure axiality of the forces, Fig. (8.2). Care had to be taken that the guide piece A could rotate freely throughout the test, so that no part of the measured load was transmitted through it. When used on the hydraulic machine the essential centrality of the punch with respect to the die was obtained by careful machining as both the die and punch were fixed to the hydraulic machine. When using the Instron a small elastic band had to be put round the punch to guide it in the hole of the bottom plate of the die assembly to ensure the same alignment.

The Modified Low and Medium Speed Punch Die Assembly.

It was found that after several holes had been punched into mild steel, the edges of the punch and die became slightly rounded. Hence a new punch and die had to be made. Since these two components were the most complicated of the whole

assembly, a new design was sought which would make the replacement of punch and die a much more simple operation.

It had been found that it made no noticeable difference to the punching behaviour whether the clamping screws were done up only finger tight or tightened with a spanner. The specimen material only became very distorted if the screws were left very loose. Thus the first simplification was to do away with these screws, resulting in a much simpler specimen and a final design of the punch-die assembly as shown in Fig. (8.1b).

All parts were again machined from quenched and tempered En 24 steel. The punch was no longer attached to the piston rod of the hydraulic machine and was centralised by means of a clearance hole in the die cage. The slots in the side of the cage made it possible in principle to use strips of specimen material, thus increasing the quickness of testing. In practice, however, it was necessary to dismantle the assembly after each test to free the punch. Spacers of several thicknesses were used to allow for different specimen thicknesses. When the second punch-die pair became rounded it was decided to use maraging steel for the next pair. This was done and all the results except the 1/8 in. mild steel ones were obtained using this punch-die pair. After heat treatment the punch and die were found to have hardnesses of Rockwell C 54.

<u>The Impact Loading Machine and its Punch-Die assembly.</u>

A different punch-die arrangement was necessary for use in the impact loading machine because of the machine's principle of operation. In the lower and medium speed punch tests there was no necessity for taking wave effects into account. This was because the time taken to yield the

specimen material was large enough for many reflections of the loading wave to occur, and hence for there to be homogeneity both in the specimen and the measuring devices. The drop weight tester however, uses a loading wave to deform the specimen and the load and displacement are obtained from analysis of this wave.

To prevent the wave analysis becoming a complicated procedure it was necessary for the stress waves to contain no more than one reflected component at the recording position for the duration of the test. This meant that the punch and die could no longer be as small as in the previous assembly and the impact punch-die system is shown in Fig. (8.3a). Fig. (8.3b) shows the assembly in position, with the remainder of the impact apparatus.

The small radial clearance and close tolerances on the diameter at the specimen end of the punch rod and die tube called for very great care in the construction of these parts and also of the guides by means of which they were aligned. The die hole and punch diameters had to be the same as those in the lower speed assembly. The punch bar was made from a quenched and tempered En 30A alloy steel and the die tube from age hardened Nimar 110 maraging steel. The length of each was 12 in.

Two sets of strain gauges were fixed to the punch bar and one set to the die tube in the positions shown in Fig. (8.3a). Each set of strain gauges was made up of four T.M.L. Type P53 gauges equally spaced round the bar and fixed to the bar using 'Araldite' twin-pack epoxy cement. Essentially all that was necessary to perform a drop-weight test was the punch-die assembly and the drop-weight. The rest of the apparatus was

needed however, for absorbing the large amount of energy of the falling weight. When the weight impacts on the top of the punch bar, an elastic wave is transmitted through the bar. The specimen can only support a load whose magnitude is a function of the yield properties of the material so that when the loading wave reaches the specimen only part is transmitted through and part reflected. The gauges on the die tube record the transmitted stress and the lower gauges on the punch bar record the elastic loading wave minus the reflected wave. In order to obtain a record of the full elastic wave the die tube and specimen were removed and the output from the higher set of punch bar gauges was recorded for a given impact velocity. The differences in velocity and displacement between the ends of the punch bar and die tube were calculated from the specimen test records and the relevant elastic test record.

Returning to Fig. (C.3b), the main guide tube is denoted by the letter A . The screwed collars at its top and bottom ensure good alignment of punch and die away from the specimen. The alignment near the specimen is controlled by the slider B which can be pinned to A . The drop weight is guided as it falls by the tensioned wires C and the apparatus was arranged so that as the weight rested statically on the top of the punch bar, there was about 1/4 in. between its foot and the rubber blocks D . These rubber blocks were mounted on a strong liquid spring and between them they absorbed the great majority of the kinetic energy of the weight. The relative motion of all parts of the apparatus had to be kept to a minimum to avoid breaking the gauge leads and, more important, stripping the gauges off the bars. The punch and die were each restrained

from large displacements relative to the frame by means of pieces of rubber tubing E . These were clamped tightly round the bar or tube by home clips and came into contact with the rigid frame after the bar or tube had travelled about 1/4 in. The punch bar was prevented from travelling a large distance down the main guide tube by means of a ring of solder F which was 'trapped' in a conical hole in the top collar of the guide tube.

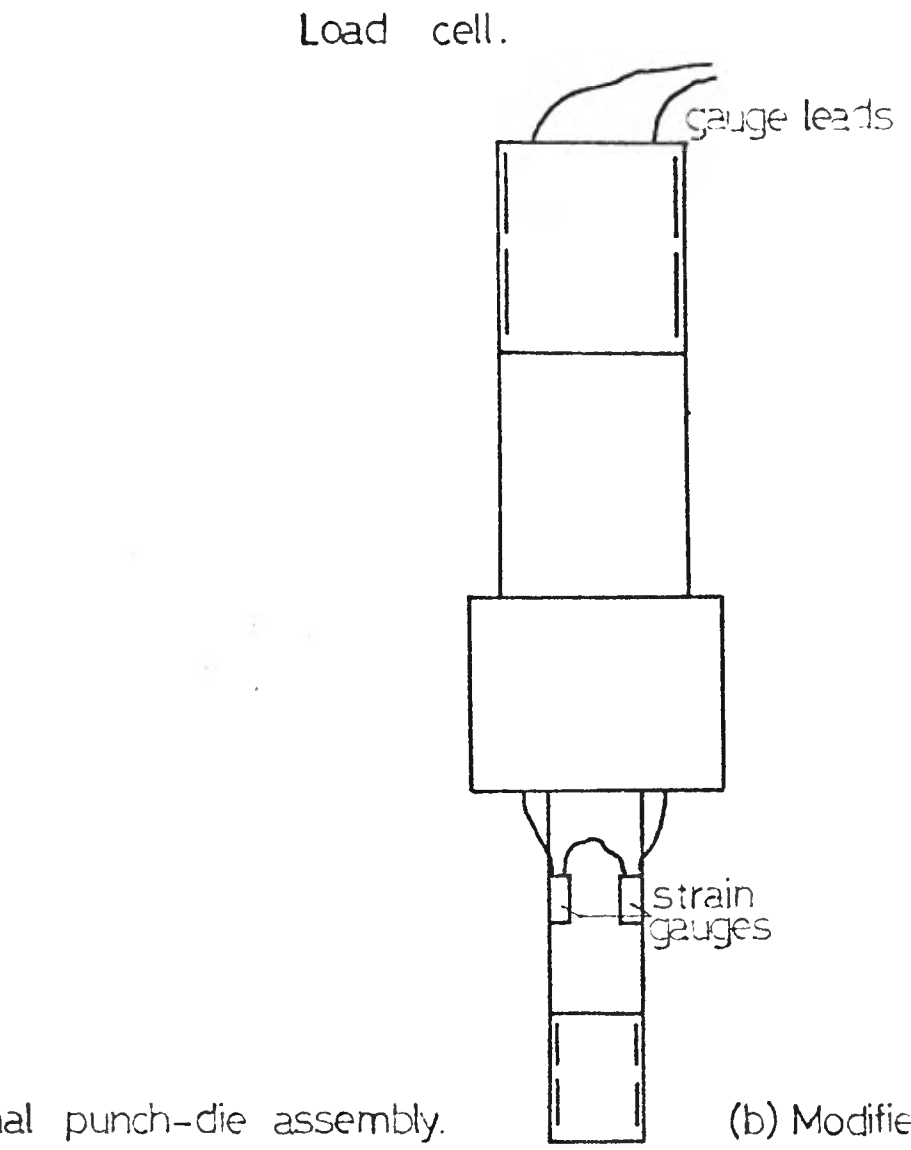
Each set of strain gauges provided one arm of a Wheatstone bridge. As has been previously stated, during a test only two sets of gauges were used, the outputs from the two bridges being fed into the two channels of a Tektronix type 555 Dual beam oscilloscope. A time-mark generator was used to provide an accurate time-base and the vertical scales could be calibrated by shunting a resistance across one arm of each bridge.

The triggering of the oscilloscope was achieved by using a separate trigger circuit. This consisted of a battery, one terminal of which was connected to the guide wires. The other terminal was connected, through a resistance, to the pin G. This pin was screwed into a Tufnol bush in the apparatus frame until it made contact with the guide tube A . The guide tube-punch bar-die tube assembly was isolated electrically from the frame of the apparatus by Tufnol collars H . The trigger circuit was completed by the weight touching the top of the punch bar, thus triggering the oscilloscope. The oscilloscope traces were photographed using a Beattie - Coleman Type K-5 oscillotron camera.

In order to obtain a constant impact velocity for a particular specimen material, the weight was hoisted to the

same height before each test. The height of the weight was indicated by a meter driven by the lifting pulleys. This was zeroed before each test, in case there had been any slipping, and was used for measuring the height of all the drops except the 4 ft. ones. The largest drop used in this experimental programme was 36 ft. For the 4 ft. drops the height of the weight could be measured with a steel rule which was more accurate for these small distances.

Summaries of the experimental procedures for the three types of test are given in the Appendix.



(a) Original punch-die assembly.

(b) Modified punch-die assembly.

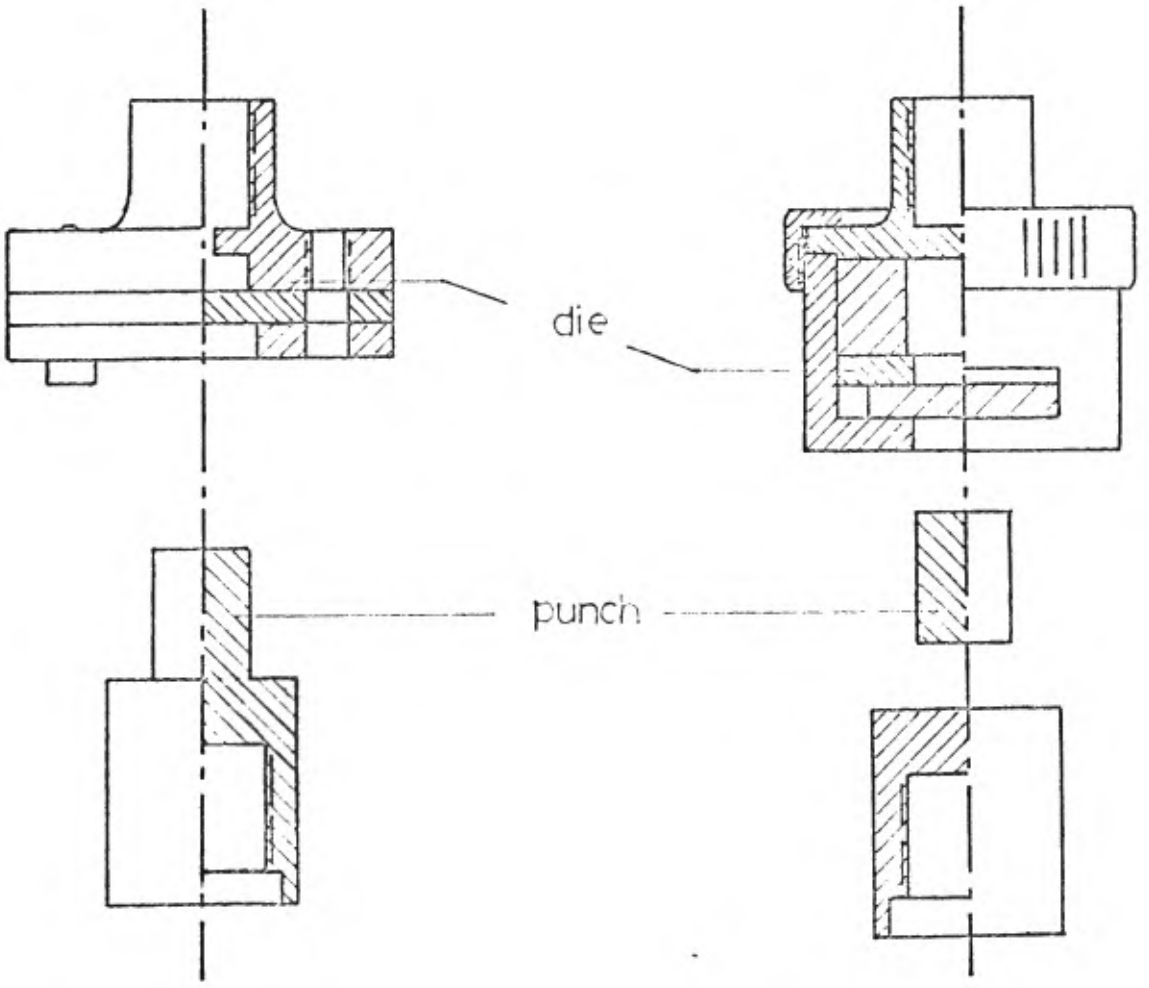


FIG. 8.1 Low and medium speed punch-die assemblies.

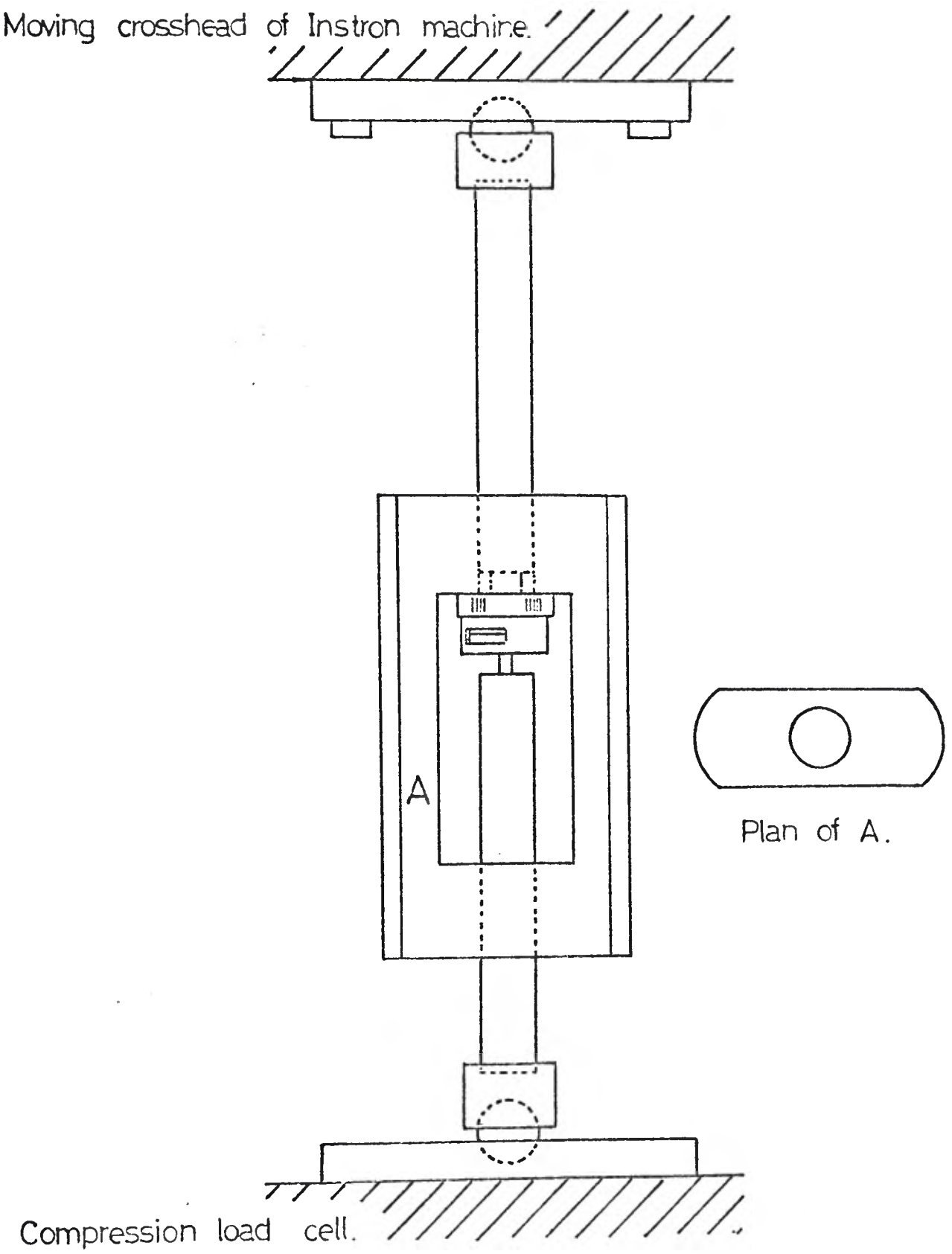
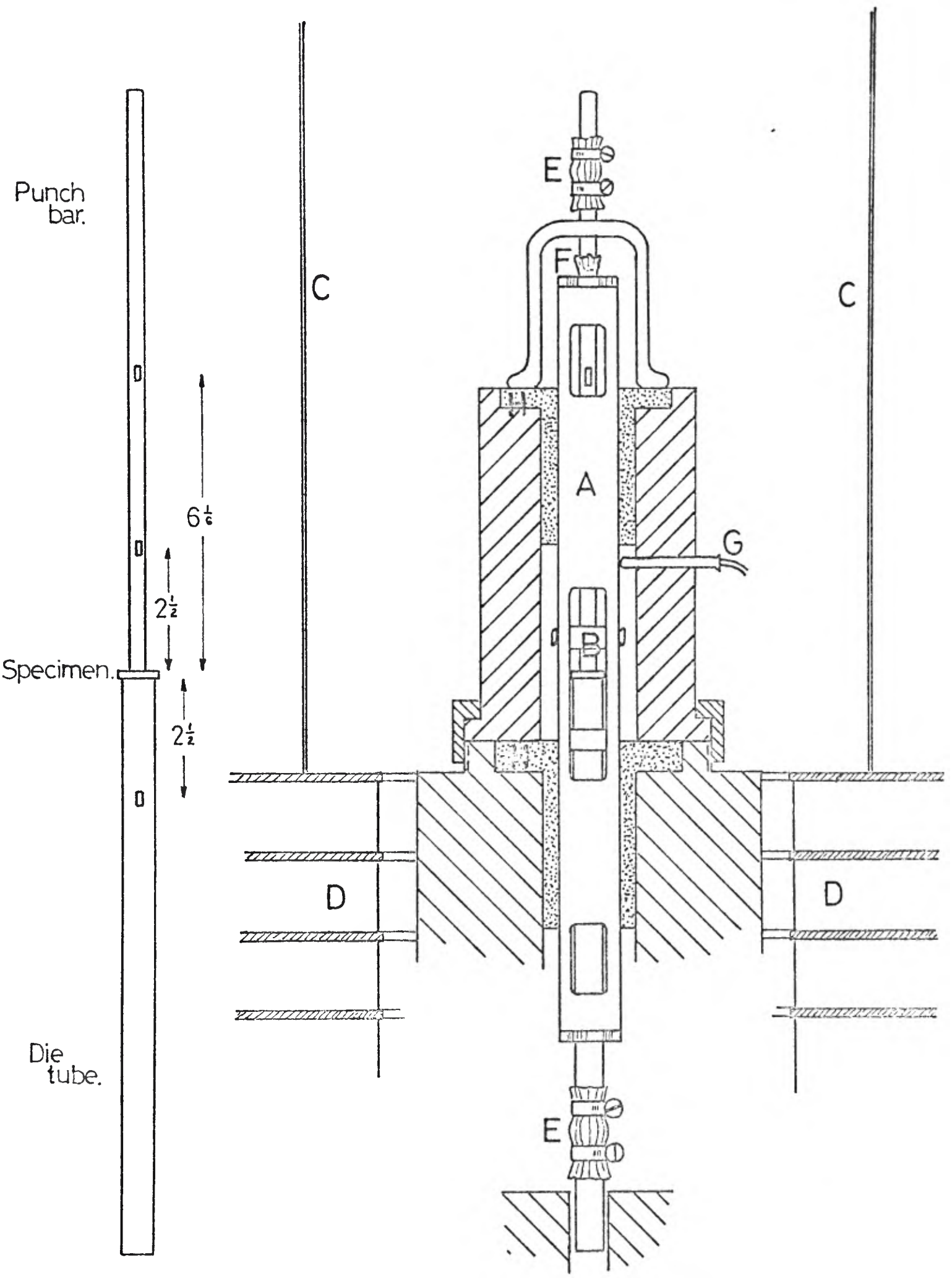


FIG. 8.2 Arrangement for slow speed punch testing.



(a) Gauge positions.

(b) Assembly.

FIG. 8.3 Apparatus for impact punch testing.

BLANKING SPECIMENS AND THEIR TREATMENT.

Dimensions.

The specimens for use in the original low speed punch-die assembly were circular discs of diameter 1.1/2 in. Each had six 5/32 in. holes with their centres equally spaced round a circle of radius 1/2 in. Only six specimens of this design were used and all were machined to a thickness of 1/8 in. The first specimens used in the modified low speed punch-die assembly were also 1/8 in. thick but were in the form of strips 3/4 in. wide and 6 ins. long so that several tests could be performed on each. When it was realised that no experimental time would be saved by using strip specimens, each specimen was made 3/4 in. square. These specimens were easier to machine since they did not have to be flat over as large an area as the strip ones and were more convenient for storing after tests as each tested specimen could be stored and labelled separately. Several thicknesses of specimen were used as will be described later.

3/4 in. square specimens were also made for use in the high speed punch-die system but these had their corners chamfered off to enable them to fit comfortably inside a cylinder of i.d. 1 in.

Materials.

The wave propagation tests were performed on mild steel, copper and aluminium, which were, therefore, the three materials first chosen for this punch work. The materials for the two

studies had to be quite similar in composition for comparisons and inferences to be meaningful. When these tests had been completed the study of the blanking process itself was continued on three other materials, two brasses and a tool steel.

Mild steel.

The mild steel specimens were prepared from an En 2A steel supplied by the British Iron and Steel Research Association in the hot rolled condition. The analysis of this material was (wt. per cent.) :

C	Si	Mn	S	P	Ni	Cr	Mo	Cu
0.043	<0.005	0.45	0.021	0.040	0.11	<0.025	0.019	0.078

Specimens of thicknesses 1/8 in., 1/16 in. and 1/32 in. were ground from this material which was received in the form of flat strips of nominal thickness 1/4 in. All the specimens were annealed by heating in vacuum for 2 hours at 700°C and were then furnace cooled.

Copper.

The analysis of the copper used for the punch specimens was (parts per million except for oxygen which is in wt. per cent.):

O	Ag	Fe	Sn	Zn	Pb	Ni	Bi	Cd	Mg	Si
0.027	100	20	20	20	10	5	1	<1	<1	<1

1/8 in. thickness specimens only were made from the copper which was supplied by J. Smith and Sons, in the form of 1/8 in. nominal thickness plate.

The heat treatment was the same as that given to the

copper tubes for the wave propagation study, i.e. heated in vacuum at 550°C for 20 hours and then furnace cooled.

Aluminium.

The aluminium was obtained in the form of 1/8 in. nominal thickness from J. Smith & Sons. Their designation for the material was PIC and its analysis gave the following result (wt. per cent.) :

Fe	Si	Zn	Mg	Mn	Cr	Pb	Cu	Ni	Ti	V
>0.1	0.05	0.05	0.03	0.01	0.01	0.007	0.004	0.003	0.002	0.001

1/8 in. thick specimens were machined from the plate and were annealed by heating in vacuum for 16 hrs. at 400°C followed by furnace cooling.

Soft Brass.

These specimens, together with those of hard brass and SAE 4130 steel, were obtained from offcuts of material used by Kulkarni, Zara and Harding (88) in their study of the high velocity punching process. In this work holes were explosively punched in tubes of material which had an i.d. of 2 in. and o.d. of 2.1/8 in. and, though the alloy steel was received with a 1/4 in. wall thickness, the brass tubing was received with these diametral dimensions.

In order to obtain flat 3/4 in. square specimens with a thickness of more than 1/32 in. from the as-received brass it was necessary to reduce the curvature of the available material. 1/32 in. was thought to be the smallest thickness of specimen for which the results would be dependable.

The material was CDA alloy 350 which is a low leaded tube brass with nominal composition Cu 66.5%, Zn 33% and Pb 0.5%.

In the as-received, hard-drawn condition it had a hardness of $R_B \triangleq 85$. It was required for testing in the annealed condition with a hardness of $R_F \triangleq 63$. To produce the specimens the material was first of all annealed by heating for half an hour at 550°C in vacuum. It could then be bent by hand and was made approximately flat in this way. The specimens were then rough machined and it was found that specimens as thick as 0.053 in. could be obtained. The roughly machined specimens were then re-annealed under the same conditions and were finally ground to their required size. The thickness of the finished specimens was 0.048 in. and the hardness of sample specimens was found to be $R_F = 63$.

Hard Brass.

The hard brass specimens were made from the same material as the soft brass ones but in the as-received condition with a hardness of $R_B \triangleq 85$. The straightening of pieces for this purpose was more difficult since the material was already at its required hardness and it was uncertain if the extra work done by the straightening operation would increase the hardness. One piece of the material was taken and compressed to 1/32 in. thick and its hardness remeasured. It was found that it did not increase. The required number of pieces was, therefore, straightened very slowly, to prevent brittle fracture which might have occurred with a higher strain rate. Their curvature had to be reversed considerably because of the springiness of the material. On release of the load a small amount of curvature was still present but specimens of thickness 0.040 in. could be ground out of the pieces. When these specimens were tested for hardness it was found that the value was between

R_B=79 and R_B=81, suggesting that the original material had a harder surface than interior. No further heat treatment was given to these specimens.

SAE 4130 Alloy Steel.

This material was received in the annealed condition in tubular form with a wall thickness of 1/4 in. This meant that it was possible to machine 1/16 in. thick specimens direct from the as-supplied material. However, knowing that the steel was to be tested in a quenched and tempered condition, it was realised that the available machines would not be able to punch holes in it unless the thickness of the specimens were 1/32 in. or less. Consequently 1/32 in. specimens were made from this material

The specimens were made 0.040 in. thick and were then heat treated. They were heated in air at 870°C for half an hour and were then quenched in oil. The tempering process was to heat at 345°C for one hour. The final thickness of the specimens, 1/32 in., was obtained by grinding. The hardness of these specimens was measured and found to be $R_c \triangleq 42$.

Post - test Treatment.

Once the load-displacement curves had been obtained, it was necessary to investigate the possibility of converting them into shear stress - shear strain curves. The first step in this investigation was to compare the granular deformation with that obtained from a simple shear process. If the conversion was found to be feasible, then a suitable gauge length had to be evaluated since it was highly improbable that the punch-die clearance would serve as this parameter. For carrying out both these steps, certain of the tested specimens had to be

sectioned, mounted and polished.

The specimens were sectioned using a Buehler specimen cut-off machine. This was used so that the first cut was flat and square to the remainder of the specimen and so that the cutting process would not alter the grain structure of the material. The machine uses a high-speed cutting wheel of abrasive particles bonded in a softer matrix, the cutting area being cooled by a jet of water. The specimen is clamped to the machine in a small vice so that the cut is perpendicular to the specimen.

Since a gauge length was to be measured from the specimen, it was necessary for the section to be across a diameter of the blank or very nearly so, to avoid any angular corrections. Also, to allow for circumferential differences in the deformation, it was advisable that the cuts in the blank and remainder should be co-linear.* By circumferential differences it is understood that at one point the gauge length may be 40% in the blank and 60% in the remainder, whilst at another point 50% in each, or, that the radial clearance at one side of the punch might be 0.0013 in. and only 0.007 in. at the other, reflecting in the gauge length values. Such differences would be reduced by ensuring co-linearity of the cuts, and averaging the values on both sides of the punch.

Obviously if the punch had not passed right through the specimen, the sections of 'blank' and remainder must be co-linear and it was sufficient to ensure that the specimen was sectioned along a diameter. This was done by lightly scribing a guide line on the specimen material. When faced with separate blank and remainder the two had to be lined up

*The use of the word co-linear is a reference to the undeformed specimen where one cut across the middle was effectively required. If this were done and then the test carried out, the resulting sections of the blank and remainder would be exactly what was needed.

before scribing so that the above mentioned conditions would be approximately satisfied. Since the specimens had some possible lateral movement in the punch-die assembly, the line could not be scribed on to the specimen beforehand.

The specimen sections were mounted in bakelite using a Buehler specimen mount press. The 1/8 in. and 1/16in. specimens would stand up straight on their sectioned faces for positioning in the press, but the 1/32in. ones needed the help of a piece of 1/8in. strip of mild steel. The specimen was fixed to this, using 'Araldite' twin-pack epoxy cement, before mounting in the press. The two parts of the specimen then had their correct positions and orientation in the plastic moulding material.

The specimens were polished initially by means of emery paper using, successively, 120, 240, 400 and 600 grades. When a satisfactory finish had been achieved in this way, the final polishing was performed on Cooke, Troughton and Simms polishing machines using diamond paste of particle sizes 6μ, 1μ and lastly 1/4μ. Apart from the use of separate polishing pads for ferrous and non-ferrous materials, the treatment of all the specimens up to this point was identical.

Etchants.

The deformed region of a specimen of each material was studied under the microscope. For this to be possible the specimens were etched with the following etchants.

Mild steel and SAE 4130 steel were both etched in 2% Nital. This is made with 2% by volume of concentrated nitric acid in industrial alcohol, the acid being added carefully to the alcohol. The specimen was immersed in the Nital

for short periods (about 10 sec.) until the optimum contrast was achieved.

Mixed acids reagent was used to etch the soft aluminium, and this had a base of 95 ml. of water. Into this was added 1.5 ml. of concentrated hydrochloric acid, 2.5 ml. of concentrated nitric acid and 0.5 ml. of 48% - hydrofluoric acid in that order. Although Flick's reagent would probably have given an improved contrast the mixed acids etch was adequate for visual examination.

The copper specimens were etched with alcoholic ferric chloride. Industrial alcohol was the main constituent, 96 ml., to which was added . ml. of concentrated hydrochloric acid and 5 gm. of ferric chloride.

60 ml. of water, 20 ml. of concentrated hydrochloric acid and 10 gm. of ferric chloride made up the etching reagent, aqueous ferric chloride, which was used to show the structure of the brass specimens.

In an attempt to show up more clearly the deformed region of the mild steel, some of these specimens were treated with Fry's reagent. This reagent, made from 90 gm. of cupric chloride, 120 ml. of dilute hydrochloric acid and 100 ml. of water, attacks the yielded regions of steel in preference to the undeformed region. Before application of the reagent, the specimens had to be aged by heating at 250°C for half an hour. Theoretically the strained region should show up after 1 to 3 mins. of wiping with a wad of cotton wool soaked in the solution. In practice, however, the yield region was only visible after approximately an hour's immersion in the reagent, this period being punctuated by regular washing.

Microhardness Measurement.

The microhardness of the specimens was measured to improve upon the visual estimate of the gauge length to be used for obtaining shear stress - shear strain curves. A G.K.N. microhardness instrument was used and this enabled measurements to be taken at any point on the polished surface of the specimen. The specimen was mounted on a small table on the apparatus and fixed in position using plasticine. The table had three controlled movements, two linear, perpendicular to each other, and one angular. Using the angular adjustment the linear controls could be lined up so that their directions of motion were parallel to the specimen's edges. A rectangular grid of microhardness measurements could then be completed giving an indication of the field of deformation of the specimen. The width of any particular indentation was of the order of 10^{-3}cm. so that microhardness readings could be taken very close to each other. This small size also produced a disadvantage in that there was considerable difference in the apparent hardness if the indentation was in the centre of a grain or at a boundary. More will be said about this aspect in Chapter 10.

CHAPTER 10.

BLANKING RESULTS.

Apparatus.

All three machines used, the Instron, hydraulic and impact machines, had been well tried and used in compression and tension experiments before this punching work was commenced so that no difficulties were expected, nor in fact experienced with them. The problems which were found with the punch-die assemblies were all minor ones, most of which have been described already in Chapter 8.

The results of tests on the impact loading machine, it has already been stated, were derived from the analysis of the stress waves in the punch bar and die tube. Consequently displacements of the punch and die were calculated actually at the specimen, and the load measured was the load transmitted through the specimen. In contrast, the linear measurement, in this case velocity, on the hydraulic machine was taken at a point on the piston rod and no values were available for the motion of the die and specimen part of the assembly. This meant that the actual velocity observed was not the velocity of the punch relative to the die. To enable a correction to be made for this, a 1/8 in. specimen of tool steel was placed in the die assembly and a test carried out. The machine was not able to punch through or even into the steel so that an elastic test resulted, giving information about the machine stiffness which was used in correcting the displacement values of all the other

tests. The load cell measured the load actually transmitted through the specimen, inertia effects being negligible, so that no correction to this measurement was necessary.

In a similar way, the Instron machine did not measure directly the punch displacement relative to the die, so an elastic correction curve had to be obtained. Here the crosshead was run at constant speed as was the chart which recorded the load. Hence the chart gave a graph of punch load against crosshead displacement, enabling the machine deflection for any particular load to be obtained from the elastic specimen.

Typical records of tests on all three machines are shown in Figs. (10.1) and (10.2). Fig.(10.1) shows a piece of Instron chart (reduced) on which has been superimposed the elastic deflection curve. The lower half of the figure shows a typical hydraulic machine oscilloscope photograph. The lower trace is the velocity, which had to be integrated to obtain a value of displacement, and the upper trace is a measure of the specimen load. A similar record was obtained for an elastic test so that the machine deflection could be calculated. Fig. (10.2) shows the results of an elastic test, without a specimen, on the impact testing machine and a typical test on mild steel.

Mild Steel Result .

Punch tests were performed on three thicknesses of specimen :- 1/8 in., 1/16 in., and 1/32 in. For each size of specimen, tests were performed at two rates in the Instron machine and one rate in the hydraulic machine. Three impact heights were used in the drop-weight tester, 4 ft., 16 ft., and 36 ft., giving impact velocities of approximately 200, 400 and 600 in./sec. The mean velocities of the punch relative to the

die in the lower speed tests were 5×10^{-5} and 5×10^{-3} in./sec. in the Instron machine and 40 in./sec. in the hydraulic machine. The velocity of the punch in the impact loading machine is partly determined by the resistance of the specimen but it was found that complete punching of the specimen was possible for all three heights with a 1/32 in. specimen though only for the two higher drops with a 1/16 in. specimen. Complete punching of the 1/8 in. mild steel specimen was not possible even using a drop height of 36 ft. Typical test records for mild steel are shown in Figs. (10.1) and (10.2).

Load-displacement curves for the three sizes of specimen are shown in Figs. (10.3) (10.4) and (10.5). The punch velocities are shown on the curves. In most of the curves specimen rupture is denoted by a more rapid decrease of the load towards the end of the test. The final load does not fall to zero because of the resistance of the blanked material on the punch and of the blank in the die.

The most noticeable effect in all three sets of curves is the rise in load values with increased punch velocity. With the 1/8 in. specimens there was a 35% increase in the maximum load for a punch velocity change from 5×10^{-5} to 400 in./sec. The magnitude of this change was approximately the same for the other two specimen sizes. There was a marked yield drop in all cases on the impact testing machine, a suggestion of one in the hydraulic machine but only the 1/8 in. specimens at the lowest speed showed such a drop on the Instron loading machine. This is partly due to the machine characteristics but it does show that the yield point is more sensitive to strain rate than the ultimate stress, a trend which has been observed in mild steel

under other loading conditions, e.g. Campbell and Cooper (90).

Other points that can be noted from these sets of curves are that there is a definite trend for the punch displacement at rupture to decrease as the punch velocity increases, and a similar trend in the punch displacement at which the peak load occurs, though this is not as marked.

Each separate curve of these figures was the average of two, three or four tests. In most cases when tests were repeated, the results showed very good reproducibility and for this reason only two tests were generally carried out. If there was more than 5% difference in particular load values then extra tests were performed. In only one case was it necessary to use four tests.

The range of specimen sizes in the series of tests on mild steel was to provide an initial indication of the feasibility of extracting material property information from the punch test. Comparing the parameters, yield load divided by specimen thickness (Y) and ultimate load divided by specimen thickness (U) the following table can be constructed (values of the parameters in lb./in. x 10^4) :-

Punch Velocity (in/s)	5×10^{-5}		5×10^{-3}		40		$\simeq$ 400	
Parameter / Sp. Thickness	Y	U	Y	U	Y	U	Y	U
1/8"	1.9	4.6	2.2	5.0	4.2	5.5	4.8	6.0
1/16"	1.8	4.9	1.9	5.2	4.4	5.7	5.4	6.2
1/32"	2.1	5.0	2.1	5.4	4.2	5.8	5.9	6.4

The agreement between the values of these parameters suggested that there was reason to expect a correlation between

material properties in simple shear and the punch test results. The trend in the above results is to a higher relative strength for the thinnest specimens. If the punch test on a thinner specimen resulted in a smaller deformation zone and hence gauge length, constant punch velocities would produce higher strain rates in them than in the thick specimens. This would then explain the higher relative strengths of the smaller specimens since an increase in load for a higher punch speed and hence strain rate has already been observed.

An estimate of the gauge length to be used in evaluating the shear strain was therefore necessary and several specimens were sectioned to provide this. By examining the region of severe distortion under a microscope it was found that there was indeed a size effect in the deformed region. As expected the deformed region was smaller in the 1/32 in. specimens than in the 1/16 in. and 1/8 in. ones. The width of the deformed region in a 'static' 1/8 in. specimen was estimated as 0.020 in. and about half that value for the 1/32in. specimen. A difference was also noticed in the extent of the deformed zone between the quasi-static and dynamic tests, the width being approximately halved when the punch velocity was increased to 400 in./sec. Fig. (10.6) shows clearly the region of large deformation in a 'half-punched' specimen.

When the deformed specimens were etched with Fry's reagent to show the yielded region, the width of this region was apparently greater than had been earlier estimated. This cast doubt on the accuracy of a visual estimate and it was decided to obtain a more quantitative measurement of the width of the shear zone by means of microhardness traverses.

From the very nature of microhardness measurement on polycrystalline materials, it should be expected that there would be a large variation in the readings. For, the impression of the pyramid covers at most a dozen grains and at its worst just one. So the variation of individual grain hardnesses would be reflected in the values obtained. Such was the case here and to try to overcome this difficulty, the average of three traverses was taken, the traverses being at 1/4, 1/2 and 3/4 of the depth of the specimen. The results of traverses on four specimens are shown in Figs. (10.7) and (10.8). Even after the averaging process, the traverses for the 1/32 in. specimen still showed considerable variation from a smooth curve, though for the 1/8 in. traverses a smooth curve could be drawn through the points.

From these curves it can be seen that the highly deformed region observed visually corresponds very closely to the narrow peak of the microhardness traverse. It can also be seen, however, that there is a considerable region of the specimen where the deformation is not so large, but nevertheless significant. If the specimen had deformed in pure shear, the shape of these traverses would have been square pulses, the gauge length thus being very well defined. In order to obtain a value of the gauge length to be used in the simplified model of the deformation the microhardness traverses acted as useful guides as they gave upper and lower bounds on the value. The lower bound was the narrow central peak which must be narrower than the estimate of gauge length because a large proportion of the work done in deforming the material was used to deform the surrounding region. The upper bound was the total extent of the deformation, at the ends of which the work done per unit volume was approaching zero.

Estimates of the gauge lengths were therefore obtained from these traverses and for mild steel 1/8 in. specimens they were respectively, 0.070 in. and 0.040 in. for the lowest and highest punch velocities. Since no more than an estimate was possible due to the variability in the microhardness readings the gauge length was obtained only for the two extreme velocities. The remainder was interpolated from these since an error of ± 20% in strain rate would make little difference to the apparent rate sensitivity.

Examining the microhardness traverses of the 1/32 in. mild steel specimens, it was seen that the hardness away from the fracture region was much higher in the blanked out material than in the blank. The value of the hardness in the blank was similar to the hardness of the 1/8 in. specimens, suggesting that the 1/32 in. specimens had suffered some deformation in the die assembly. This was probably due to the higher bending stresses in the thinner specimen which were resisted by the die cage. However, whatever the cause it made the estimation of gauge lengths even more difficult but values were assumed to be 0.030 in. for the quasi-static one and 0.020 in. for the high-speed punch specimen.

The 1/16 in. specimens were not sectioned but the gauge length values were taken as 0.050 in. and 0.030 in. for the two velocities. Using these values the peak loads of the lowest punch velocity tests occurred at strains of 51.5, 50 and 45% respectively for the 1/8, 1/16 and 1/32 in. specimens. The peak load of the 400 in./sec. punch velocity curves occurred at strains of 40, 37 and 35% respectively for 1/8, 1/16 and 1/32 in. specimens. This showed that the size of specimen would not

appreciably affect the derivation of shear stress - shear strain curves.

Examination of the sheared edges of the specimens showed that they became smoother as the punch velocity was increased. Comparing the different sizes of specimen it was found in all cases that the thinner the specimen the rougher the surface for equivalent loading rates. Twinning was often found to have occurred near the highly deformed regions of the impacted specimens and in one case the start of a shear crack was observed at the corner of the specimen in contact with the die tube ; Fig. (10.9a). A photograph of some of the mild steel blanks is shown in Fig. (10.10).

Copper Results.

After the experiments using mild steel as a specimen material had shown the results of varying the specimen size, it was decided that 1/8 in. specimens only would be used for the copper tests. This was because it had been shown that the size of specimen made little difference to the derived stress-strain curves, while the measurements and estimates could be carried out much more accurately with the largest size of specimen.

Sample test records from the hydraulic and impact machines appear in Fig. (10.11). The results of various tests on copper are shown in the form of load-displacement curves in Fig. (10.12). It was only possible to punch completely through the copper on the drop-weight testing machine using a drop height of 36 ft. The curves showed the same general trends as the mild steel ones, i.e. that as the punch velocity increased so did the strength of the material, and the higher the velocity the lower the punch penetration to cause fracture. However, the magnitude

of the rise in specimen load was here approximately 25% for a punch speed change from 5×10^{-5} to 400 in./sec., as against 35% for a similar rise in mild steel. Another difference between the two materials was that the yield stress of copper was not very rate sensitive until the punch velocity was increased to more than 100 in./sec.

At the lowest punch speed, a penetration of 0.090 in. was required to cause rupture, but this was decreased to approximately 0.072 in. for a punch velocity of 750 in./sec. This valuewas little more than half the thickness of the specimen. Each constant velocity curve was the average of two or three tests.

One interesting feature of the tests on copper was that the 750 in./sec punch speed test showed a yield drop. Although this behaviour is common with b.c.c. materials, it has not been found to occur in f.c.c. metals in tension, even at very high strain rates, (91, 92, 93). However, yield drops have been found in f.c.c. materials under repeated loading, especially repeated impact loading (94).

The appearance of the specimens after punching showed a much rougher surface with the large punch velocity than from the Instron tests. However, there were no other visible differences, such as doming, tapering or distortion between the specimens.

Microhardness traverses were carried out for the highest and lowest punch speed blanks and the curves obtained are shown in Fig. (10.13). The shapesof this pair of curves were much closer to the 'ideal' shear microhardness traverse. There were definite steps in the values enabling the gauge length to be estimated much more accurately, and the value for 750 in./sec.

punch speed was 0.070 in., the 5×10^{-5} in./sec. gauge length being 0.050 in. The central hardness peaks in the copper specimens were not as large as in the mild steel.

One of the specimens which was sectioned and examined was from a 16 ft. impact test. This was not a complete penetration test but the section showed the start of a shear crack at the corner in contact with the die tube: Fig. (10.9b). A few of the copper blanks were photographed and appear in Fig. (10.14a). The fracture surfaces can be clearly seen on the sides of the blanks.

Aluminium Blanking Results.

Typical records from tests on aluminium in the hydraulic and drop-weight testing machines are shown in Fig. (10.15). Aluminium was the third material used in the wave propagation study so that shear stress-strain curves at different strain rates were required. Hence, 1/8 in. specimens of this material were used to give the best possible accuracy. When the load-displacement curves were calculated it was found that the punch velocity had a very large effect on the load. The maximum load increased by approximately 30% for a punch velocity change from 5×10^{-5} to 500 in./sec. As with copper, however, the yield stress changed only very slightly with increased punch velocity until the latter rose above 100 in./sec.

Both the 36 ft. and 16 ft. tests on the impact loading machine successfully punched through the aluminium although a full analysis could not be carried out for the 16 ft. tests because reflected waves reached the recording positions before the test was complete. Yield drops occurred in both these tests, being more marked in the lower velocity one.

The hydraulic machine curve was the mean of four tests, three tests each were used to obtain the Instron machine results and two specimens each to derive the curves for the highest punch speed.

Although the penetration to cause rupture did decrease with an increase in punch velocity, the magnitude of this effect was much smaller than in either mild steel or copper. With the lowest punch velocity the necessary penetration was approximately 0.102 in. yet it was still as high as 0.092 in. for a punch velocity of 770 in./sec.

The appearance of the blanks at the various punch speeds did not differ very much though the remainder of the specimen was appreciably distorted in the impact tester. The sides of the hole became concave at these high punch speeds. Several of the tested specimens are shown in the photograph Fig. (10.14b).

Microhardness traverses were carried out on sectioned specimens which had been tested at the highest and lowest punch speeds. Again the derived curves Fig. (10.17) are the means of three traverses, which were at the three quarter depths of the material. The resulting curves made the estimation of gauge lengths a much more difficult process than for copper or mild steel. The portions of the two curves representing hardness values in the blanks were very nearly the same in both shape and magnitude but did not show a sudden drop in hardness values like the copper, being similar to the curves derived from the mild steel specimens. However, the curves in the blanked out portions of the specimens both showed a plateau slightly harder than the surrounding material, unlike any traverse previously obtained.

This plateau was larger in the quasi-statically punched specimens resulting in estimated gauge lengths of 0.060 in. for the highest speed test and 0.050 in. for the low speed test.

Soft Brass Results.

Fig. (10.18) shows typical test records from the impact and hydraulic machines, for the soft brass. The rupture point of these specimens can be seen much more easily than with the previous materials since there is only a small decrease in the specimen load before the break occurs. On the hydraulic machine an increase of velocity of the punch can be seen to occur just before rupture but the punch velocity does not appear on the impact machine records so that no comparison can be made.

Load - displacement curves were calculated for the soft brass for six different punch velocities ranging from 4×10^{-5} to 750 in./sec. These are shown in Fig. (10.19). The 4 ft. drops on the soft brass specimens did not cause complete punching though a sufficiently long record was obtained to calculate the majority of the load - displacement curve for this punch speed. Comparing the punch penetration with the value necessary to cause rupture in the adjacent curves, it can be inferred that these tests were very near to completion. Fig.(10.20) shows a micrograph of one of the 4 ft. impact specimens. It can be seen that the punch penetration measured from this section, agrees very well with the derived value on the load-displacement curve. This figure also shows the extent of the heavily sheared region of the soft brass specimens. Only five curves appear on Fig. (10.19) because the two Instron speeds produced almost identical results. They have been drawn as one curve to avoid confusion. The ultimate load of the material showed a moderate

strain rate sensitivity, the load taken by the specimen increasing by 25% for a punch velocity change from 4×10^{-5} to 750 in./sec. The yield stress showed a much more marked dependence on the punch velocity, its value being almost trebled by the same velocity change.

Yield drops were noted for the three impact tests but were not present in the three lower speed tests. The punch penetration to fracture decreased by approximately 0.005 in. from the lowest to the highest testing speed. The greatest punch penetration was 0.026 in. which is just 54% of the specimen thickness.

One specimen each of the lowest and highest speed tests was sectioned to enable microhardness measurements to be carried out. The results of these traverses are shown in Fig. (10.21). As was found in the aluminium and copper specimens and even more decisively in the 1/32 in. mild steel ones, the background hardness level in the blank was lower than in the remainder of the specimen. This was the case in both 'static' and dynamic tests. Considerable scatter was found in the soft brass readings but this was possibly due to the narrowness of the specimen, as similar behaviour was found in the 1/32 in. mild steel microhardness traverses. The height of the hardness peak in the high speed punch test was considerably greater than that of the quasi-static test and though it was difficult to estimate the values, the width of the affected region was noticeably greater in the lowest speed test. Values of the width of the shear zone were estimated as 0.040 in. for the high speed test and 0.055in. for the low speed specimen.

Fig. (10.22a) is a photograph of two mounted specimens

of soft brass, one punched at a velocity of 4×10^{-5} in./sec and the other with a velocity of 750 in./sec. A slight doming of the blank is apparent in the quasi-static blank but this has parallel sides in contrast to the high speed specimen which is tapered. The reduction of doming and increase of tapering were the most noticeable changes in the specimen appearance with an increase of punch velocity. In Fig. (10.22b) can be seen two of the punched soft brass specimens. The distortion of the blanked out material in the impact test can be seen to be quite large.

Hard Brass Results.

The hard brass showed much more brittle behaviour compared with the same material in the annealed condition. This can be seen in the records of hydraulic and impact tests on the material, Fig. (10.23). The yield point is clearly visible in these records.

The load - displacement curves, which were the averages of two or three tests are shown in Fig. (10.24). It can be seen that the yield stress has a much larger strain rate sensitivity than the ultimate load. So much is this so that for the test at a punch speed of 440 in./sec., the yield load was the highest load recorded in the test. The yield stress almost doubled for a punch velocity change from 2.3×10^{-5} to 440 in./sec., while the ultimate load increased by only about 10% in the same interval.

The punch penetration to cause rupture was much smaller at the highest punch speed than at any other and, in fact, at this velocity, the punch had only to travel through 12% of the specimen thickness before fracture occurred.

At the other four velocities at which tests were performed, there was no significant trend in the punch penetration to fracture, in each case the value being approximately 25% of the specimen thickness.

A direct comparison of the behaviour of CDA 330 brass under annealed and as-received conditions by means of Figs. (10.19) and (10.24) is misleading because of the different specimen thicknesses used. For that reason the two sets of curves have been rescaled to a common specimen thickness of 0.044 in. in Fig. (10.25). In obtaining this figure the size effects found in the study of mild steel specimens of varying thickness have been employed. The more brittle behaviour of the hard brass is very noticeable in this comparison.

It was stated in Chapter 9 that extra working of the as-received brass did not raise its hardness value. Consequently it was to be expected that little information regarding the shear zone would be obtained from a microhardness traverse of the specimen. Shear stress - shear strain curves were not required for this material although the nature of any changes in the size of the zone were. Hence it was decided to estimate the zone size from micrographs of the affected area.

Some micrographs for hard brass are shown in Fig. (10.26). Estimates for the width of the heavily sheared region in hard brass are 0.012 in. for the Instron tested specimen and 0.010 in. for the 36 ft. impact test, showing a slight reduction with increase in velocity. The 'cleaner' appearance of the edge of the low speed blank is noticeable in these photographs.

The outward appearance of the blanks from the two velocity extremes Fig. (10.27a) show very little difference.

There was considerably less doming and tapering than in the case of soft brass.

High Tensile Steel Results.

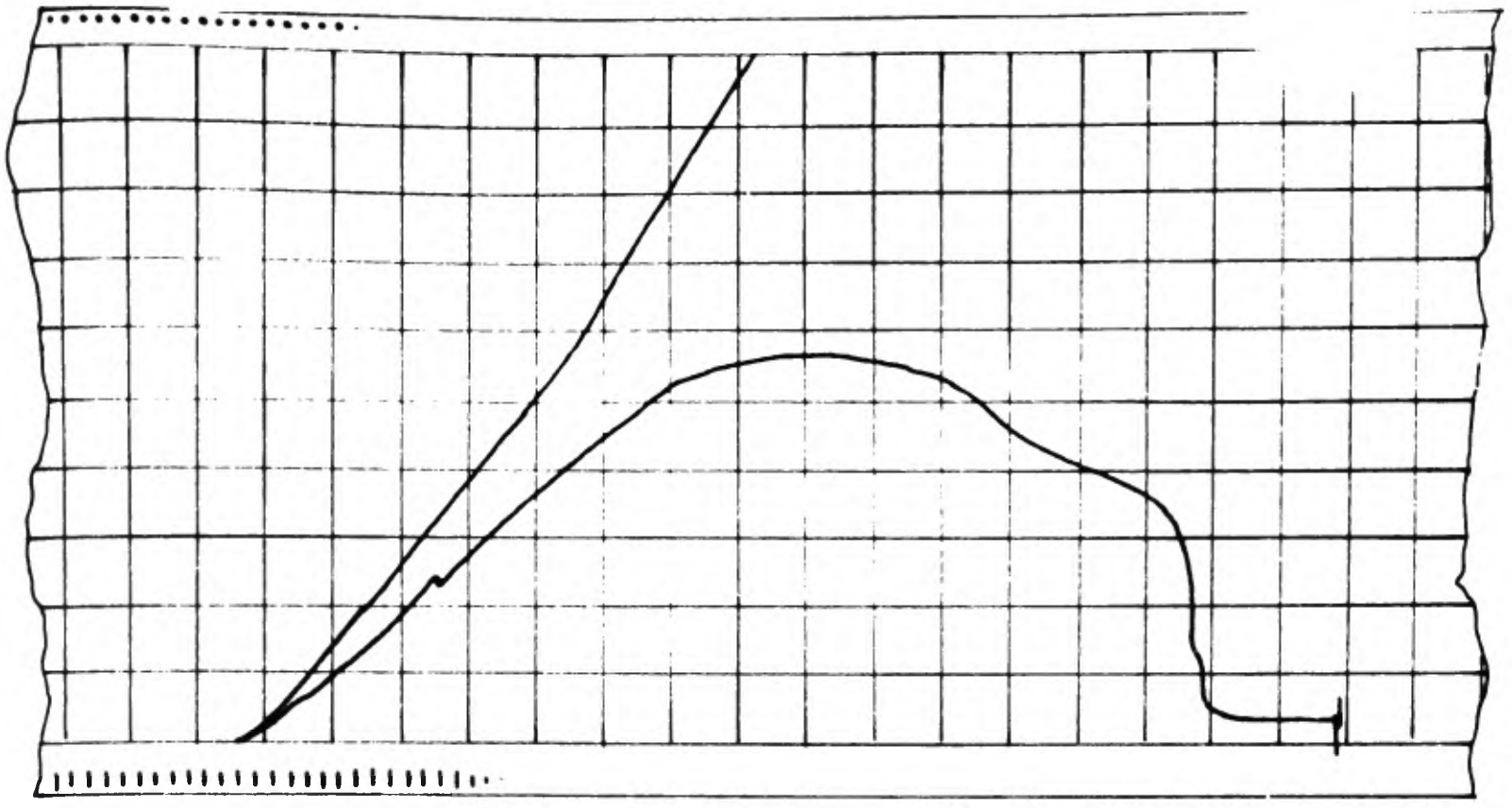
This material was extremely brittle under all applied punch velocities and typical test records, Fig. (10.28), show this. Only four punch velocities were used since, even though the specimens were only 1/32 in. thick, the 4 ft. drop on the impact machine would not pierce them.

The load - displacement curves obtained from the four punch speeds are shown in Fig. (10.29). These curves are drawn on separate axes to avoid confusion. The increase of load with punch velocity was quite small, being approximately 10% for a velocity change from 1.4×10^{-5} to 400 in./sec. However, the punch penetration to rupture decreased remarkably with the same velocity change, reducing from 0.0065 in. to 0.0015 in. This latter value meant that the punch had to penetrate only 4.8% of the specimen thickness before fracture occurred.

The fact that the material was brittle meant that, as with hard brass, the microhardness traverse would show no measureable peak near the fracture surface. Consequently the shear zone had to be estimated from micrographs of the deformed material. Such micrographs are shown in Fig. (10.30) and from these it can be seen that microhardness traverses would indeed have been of little value. For the region of severe distortion was extremely small and even the transition region between this and the undeformed material was small. This is demonstrated very well by the photograph of the Instron specimen which has horizontal lines following the deformation at the specimen edge. Estimates of the shear zone width for the two extreme velocities

were both 0.006 in., a very narrow band which suggested very high strain rates in the highest velocity test.

A photograph of several of the high-tensile steel specimens is shown in Fig. (10.27b) where it can be seen that there is very little to choose between the blanks with regard to appearance. It can be seen that the blanks are the nearest to flat circular discs out of all the different materials tested. Only when the specimens were sectioned was it noticeable that the edge of the high speed blank was smoother than that of the low speed one, Fig. (10.30). The specimen showed no tapering, doming, dishing or any other form of distortion.

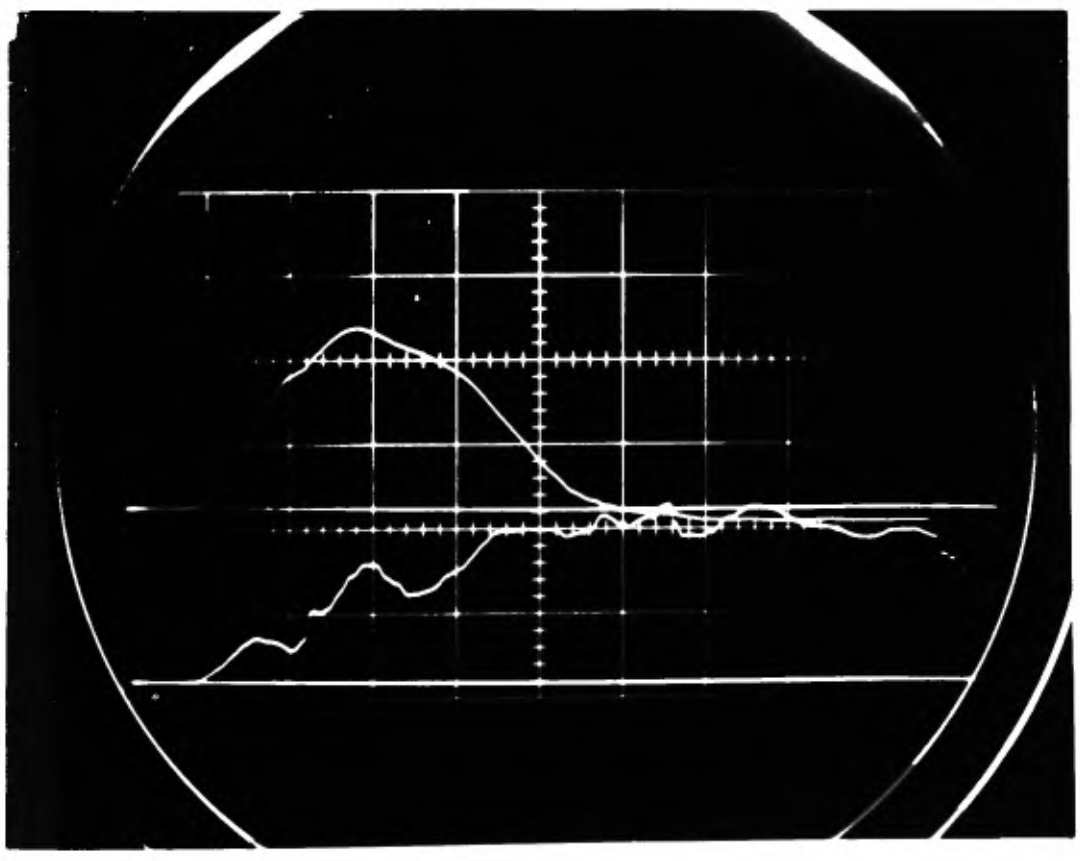


Machine deflection curve and $\frac{1}{8}$" mild steel test.

Vert.: Full scale deflection = 10,000 lb.

Hor. : Each division = 0·010 in.

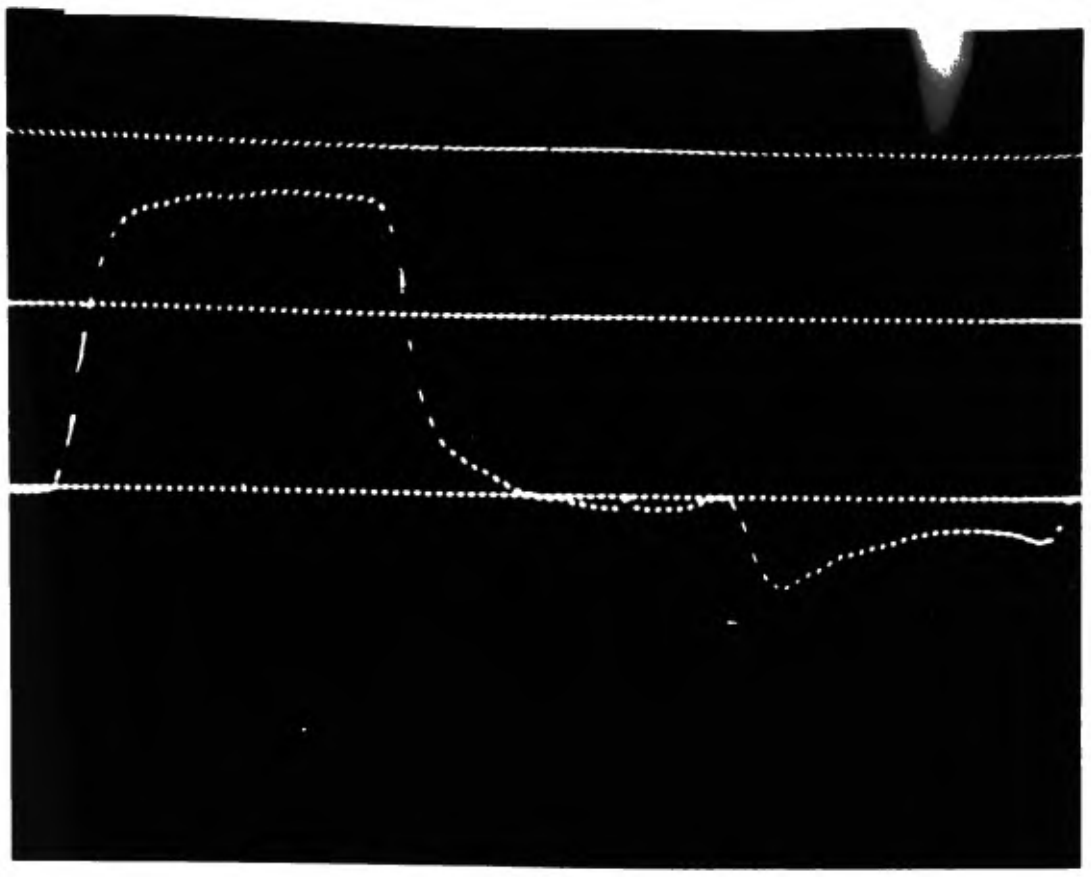
Instron chart (reduced).



Hydraulic ($\frac{1}{8}$" specimen)

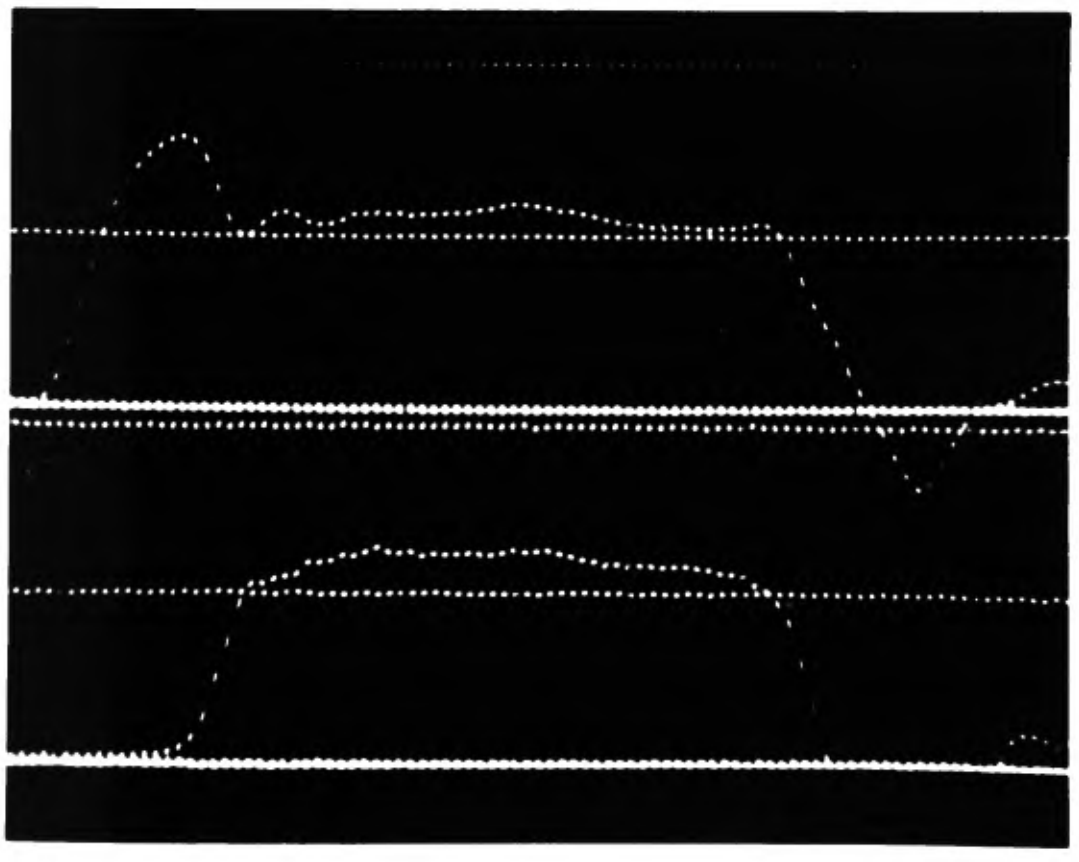
Sweep speed 1ms./cm.

FIG. 10.1 Typical test records for mild steel (i).



Punch bar:
Higher gauge set.

Impact, elastic record (impact velocity 384 in./sec.).
Timing pips at 2μsec. intervals



Upper trace:
Punch bar
(Lower gauge set)

Lower trace:
Die tube

Impact (Punch velocity 210 in./sec., $\frac{1}{52}$" specimen)
Timing pips at 2μsec. intervals.

FIG. 10.2 Typical test records for mild steel (ii).

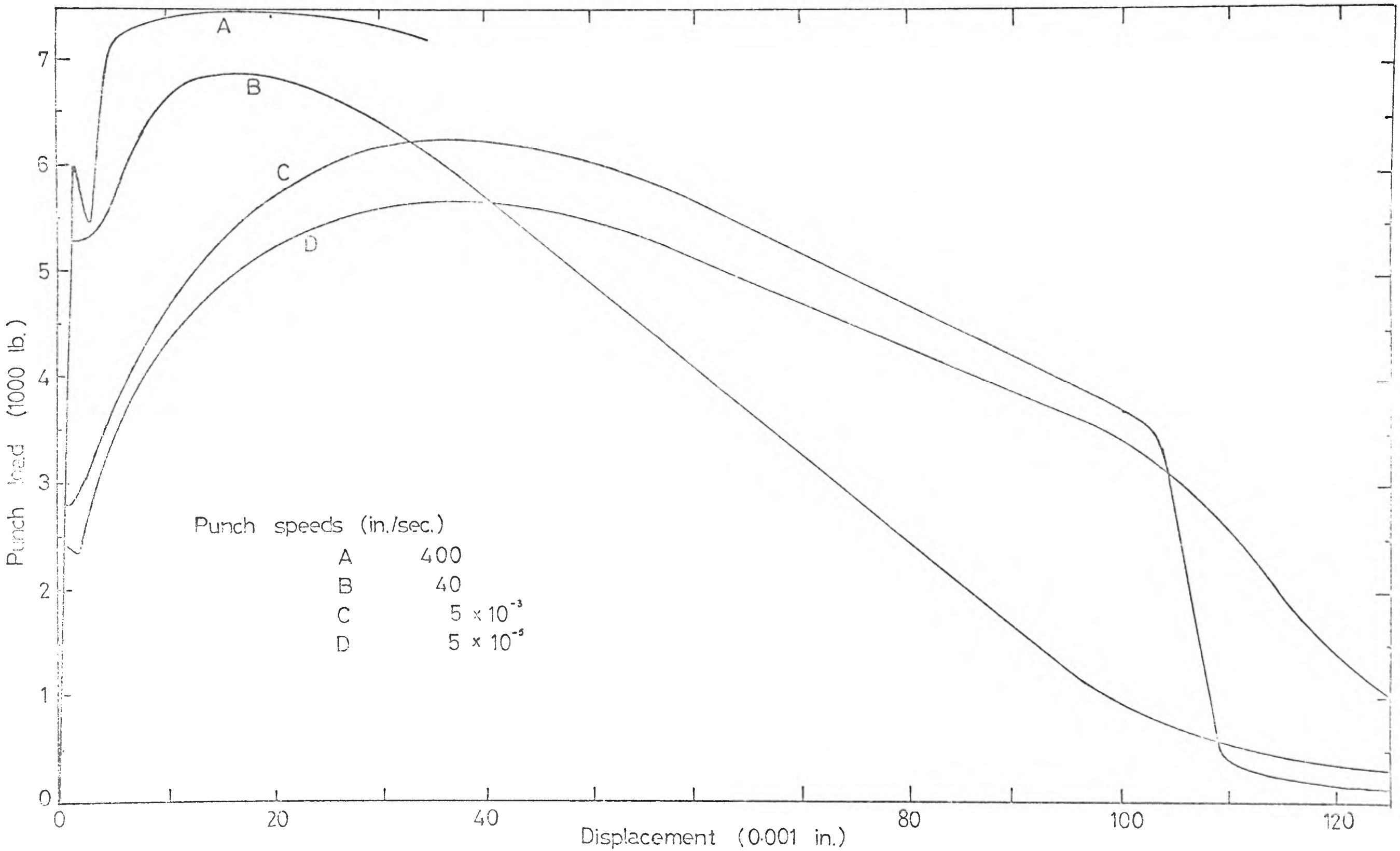


FIG. 10.3 Load-displacement curves for 1 in. mild steel.

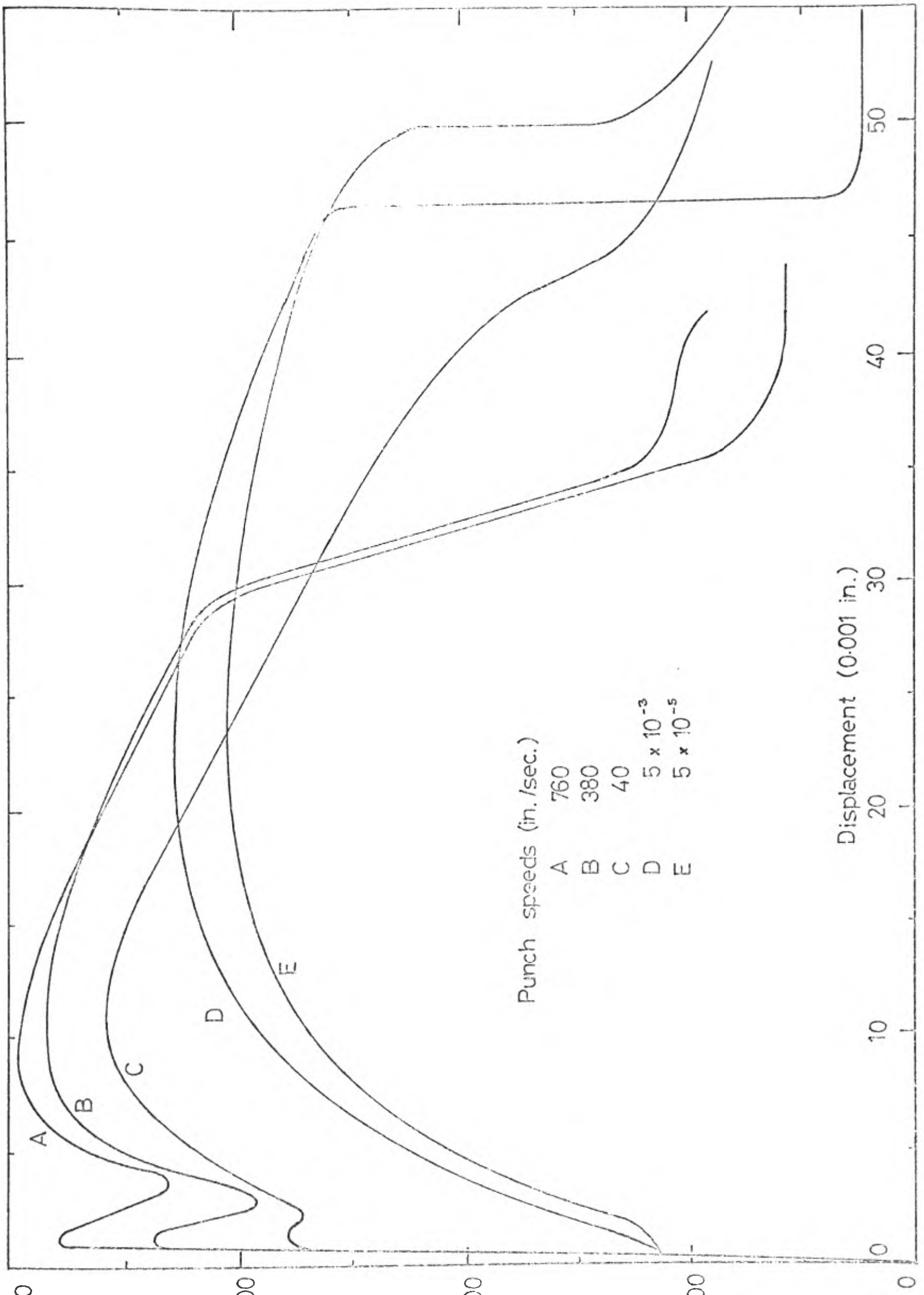


FIG. 10.4 Load - displacement curves for $\frac{1}{16}$ in. mild steel.

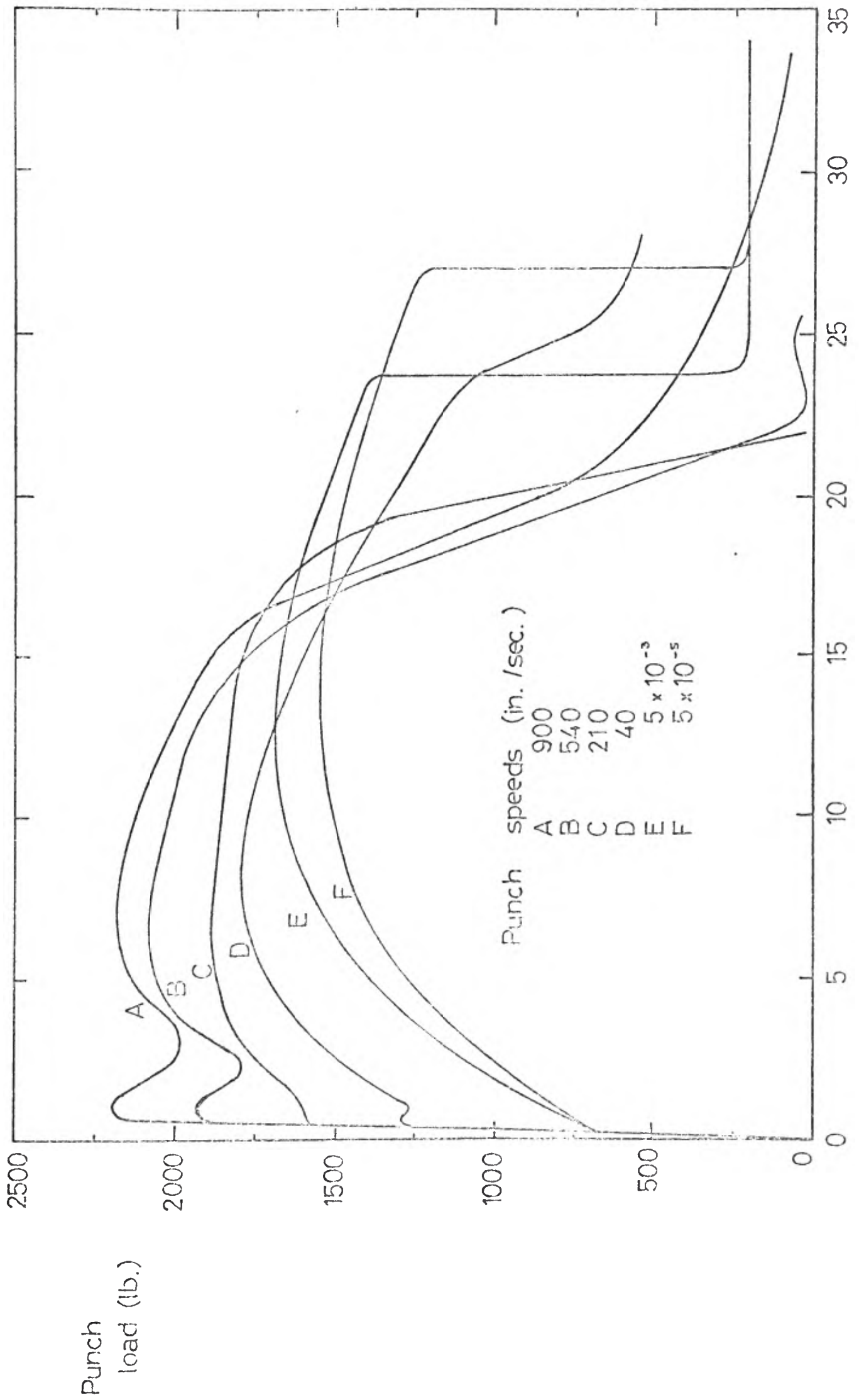
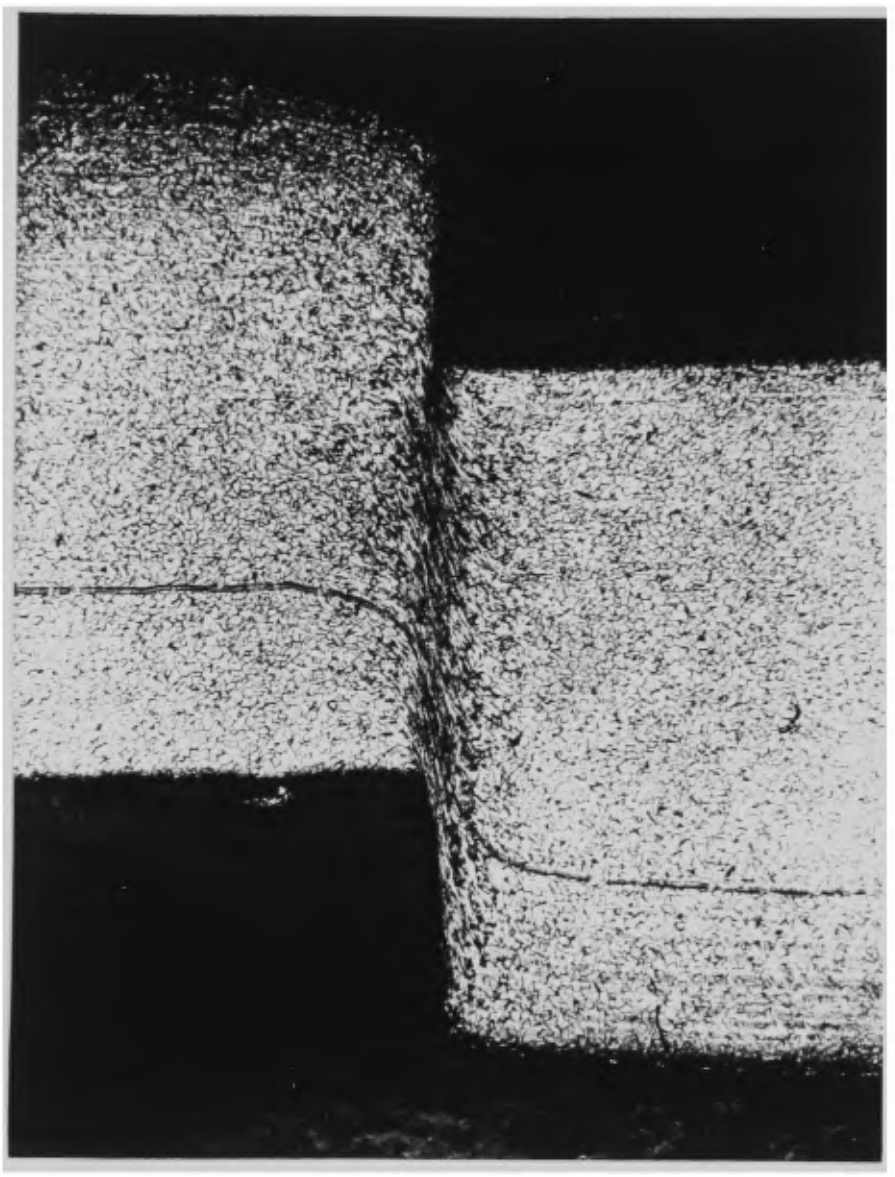


FIG. 10.5 Load-displacement curves for $\frac{1}{32}$ in. mild steel.



$\frac{1}{8}$ in. specimen impacted at 576 in./sec.

FIG. 10.6 The deformed region in mild steel.

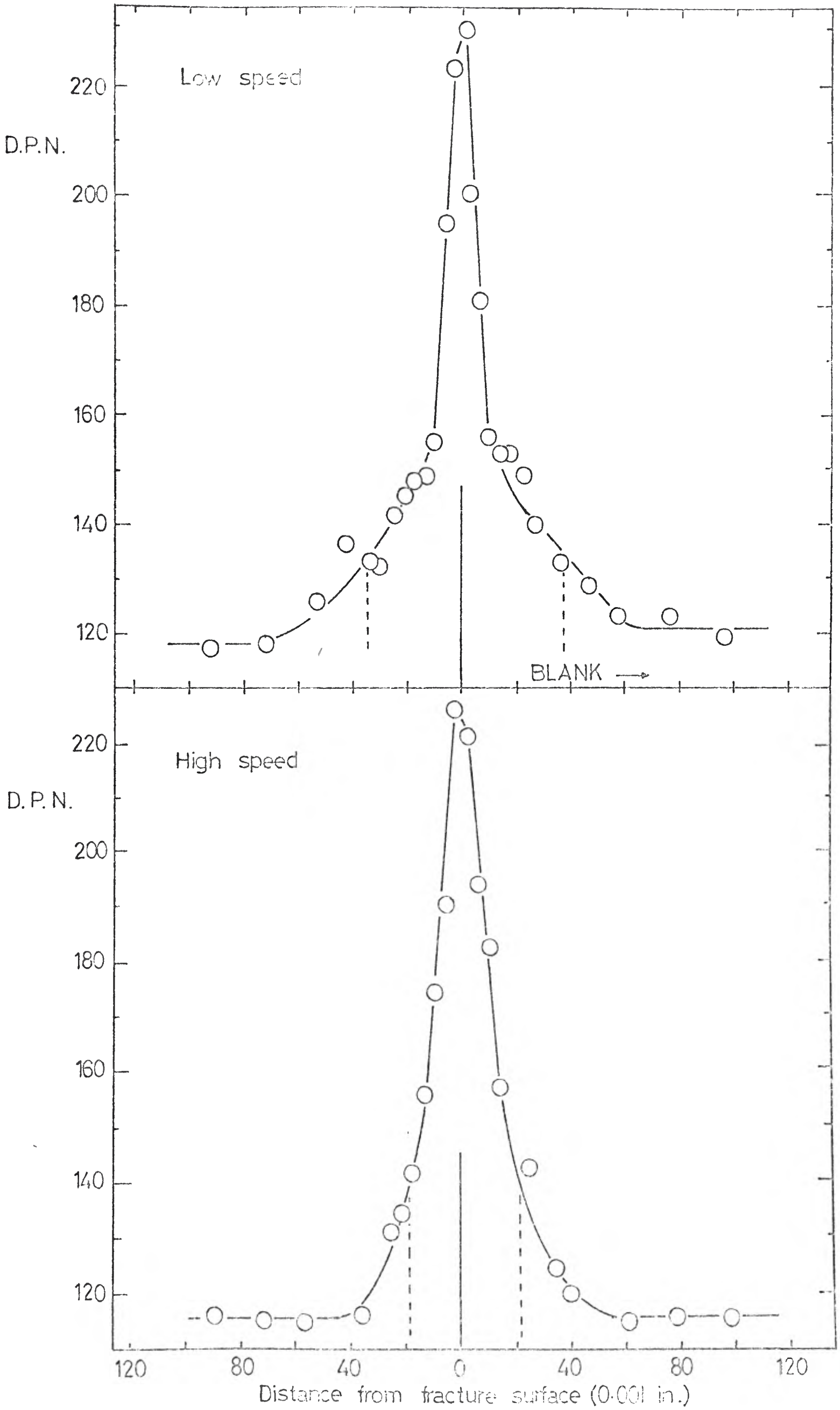


FIG. 10.7 Microhardness traverses for $\frac{1}{8}$ in. mild steel.

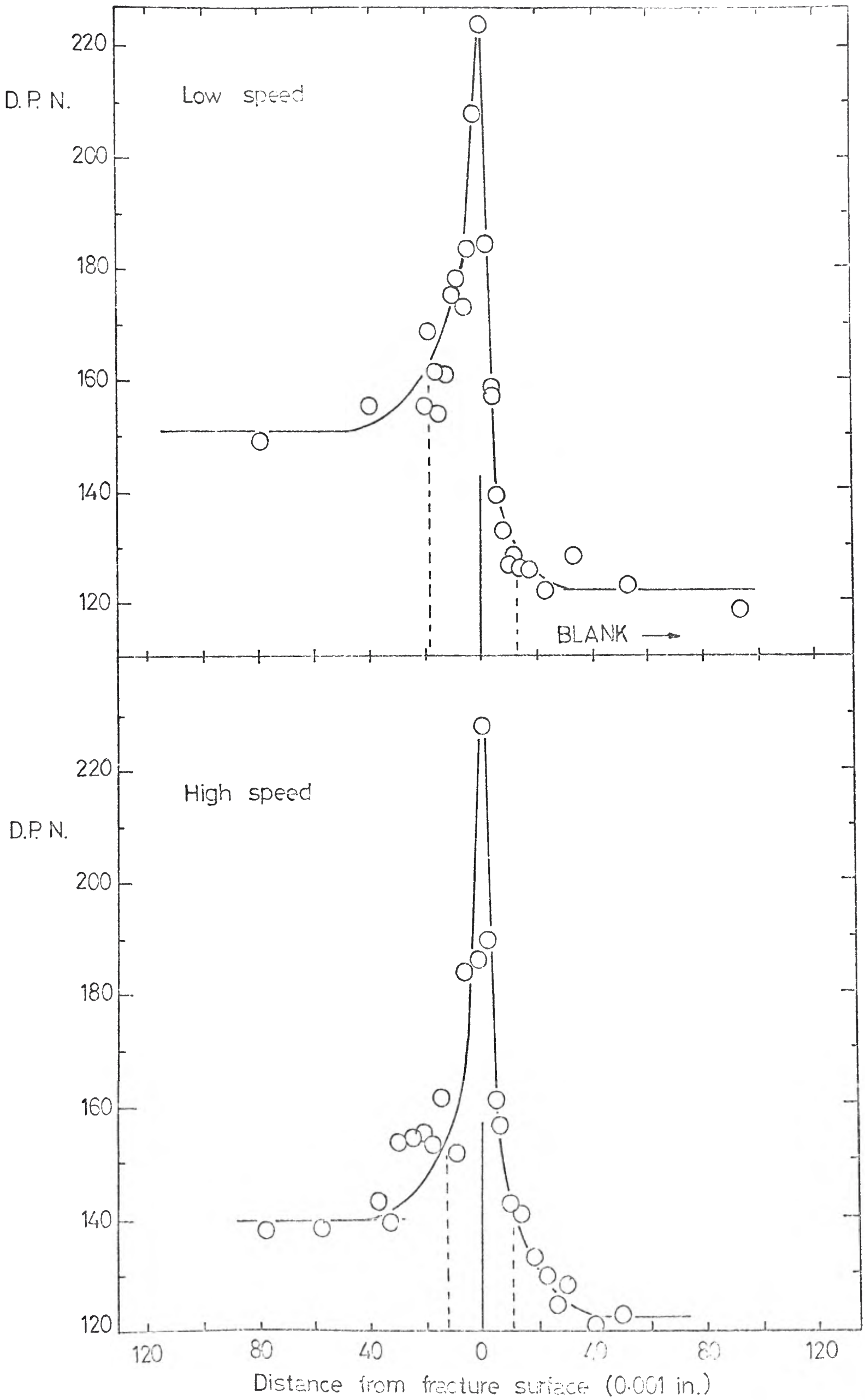
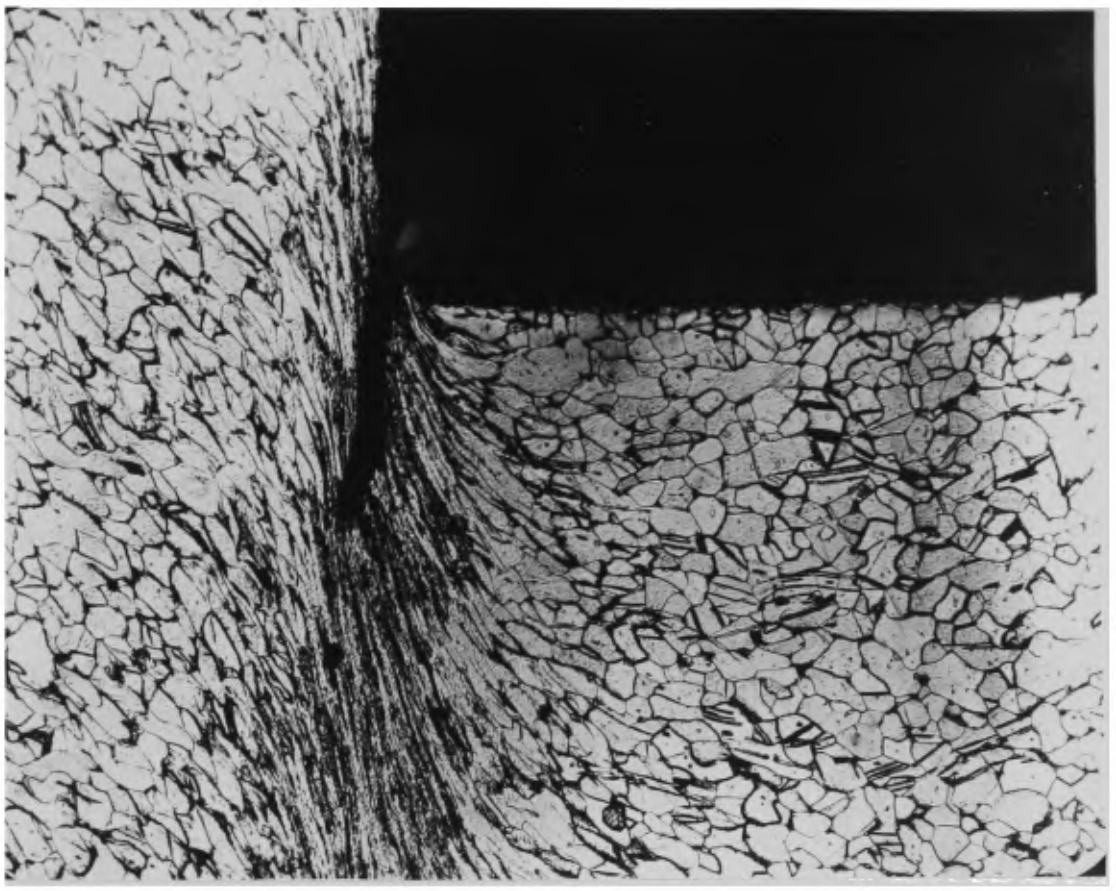


FIG. 10.8 Microhardness traverses for $\frac{1}{32}$ in. mild steel.



Mild steel x 105



Copper x 231

FIG. 10.9 Cracks in part-punched specimens.

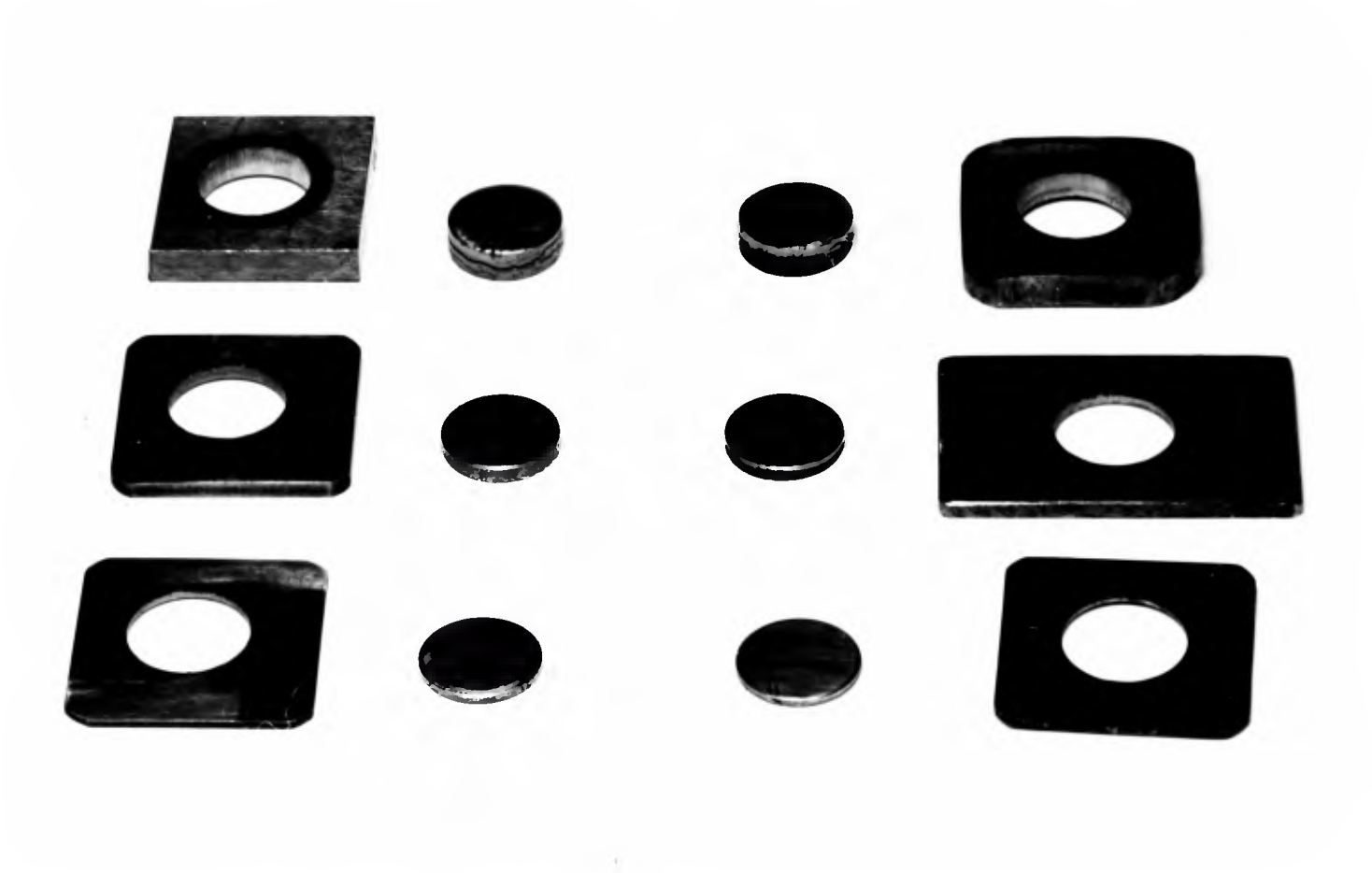
FIG. 10.10 Mild steel blanks.

Specimen thickness

$\frac{1}{8}$ in.

$\frac{1}{16}$ in.

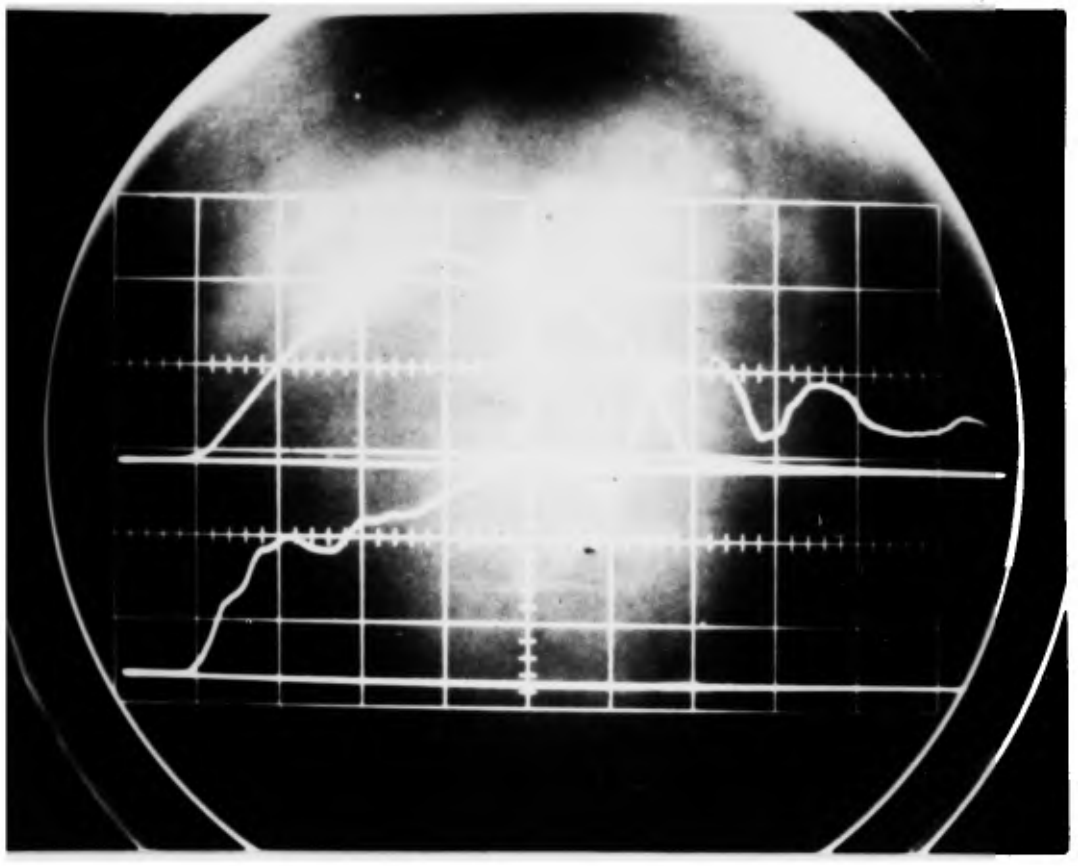
$\frac{1}{32}$ in.



Loading machine

Instron

Impact

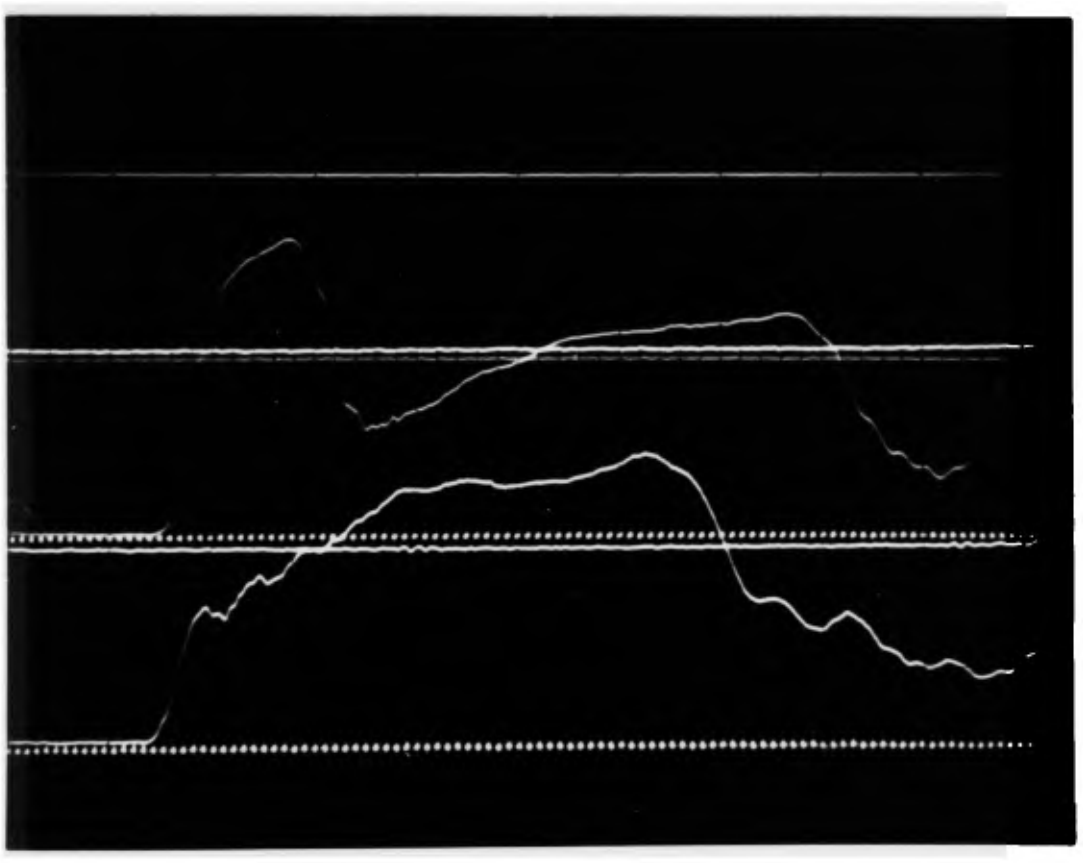


Load:
1500 lb./cm.

Velocity:
86 in.sec.$^{-1}$/cm.

Hydraulic

Sweep speed: 1 ms./cm.



Upper trace:
Punch bar

Lower trace:
Die tube

Impact (Punch velocity 390 in./sec.)

Timing pips at 2μsec. intervals.

FIG. 10.11 Typical test records for copper.

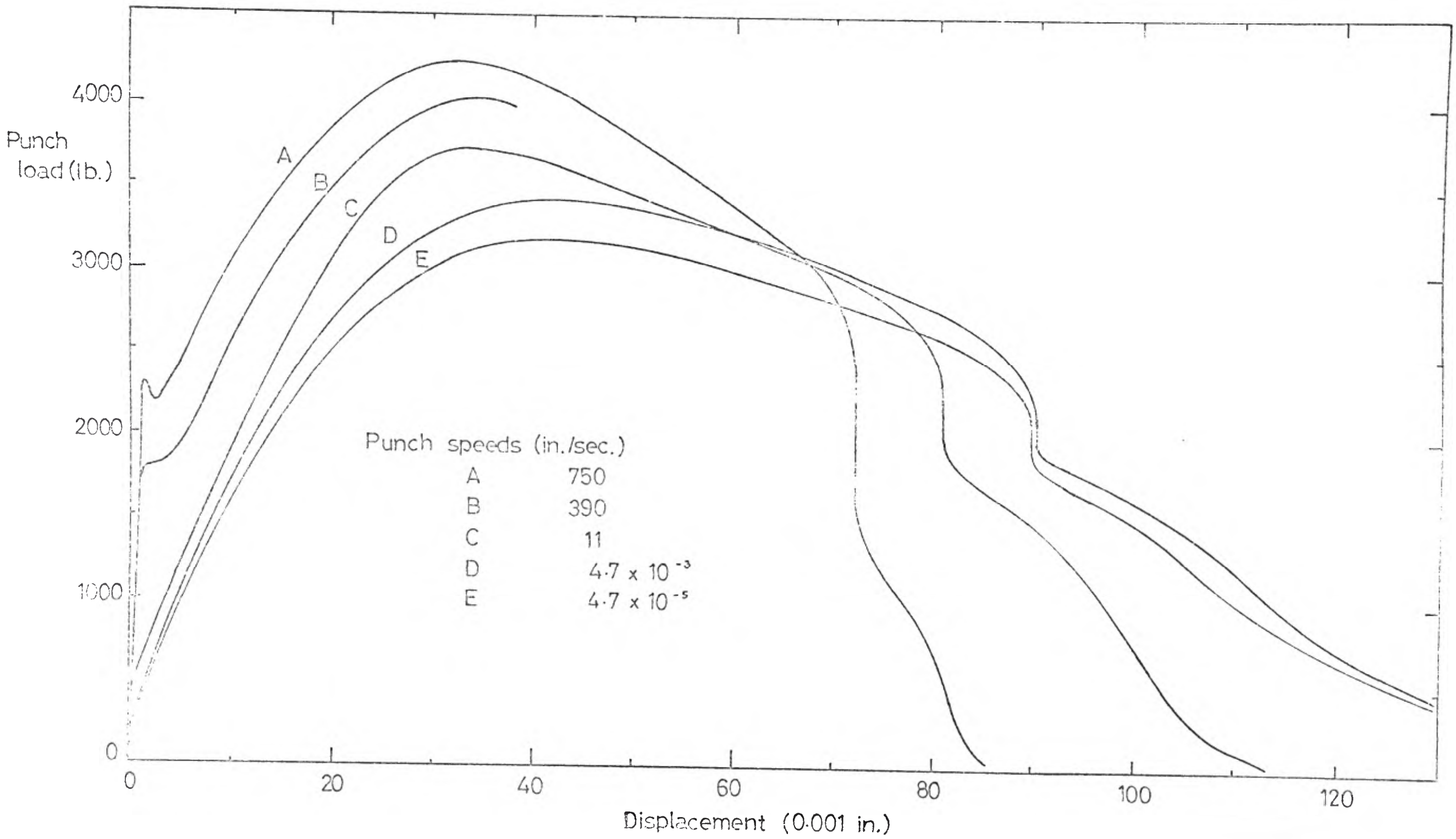


FIG. 1012. Load-displacement curves for copper.

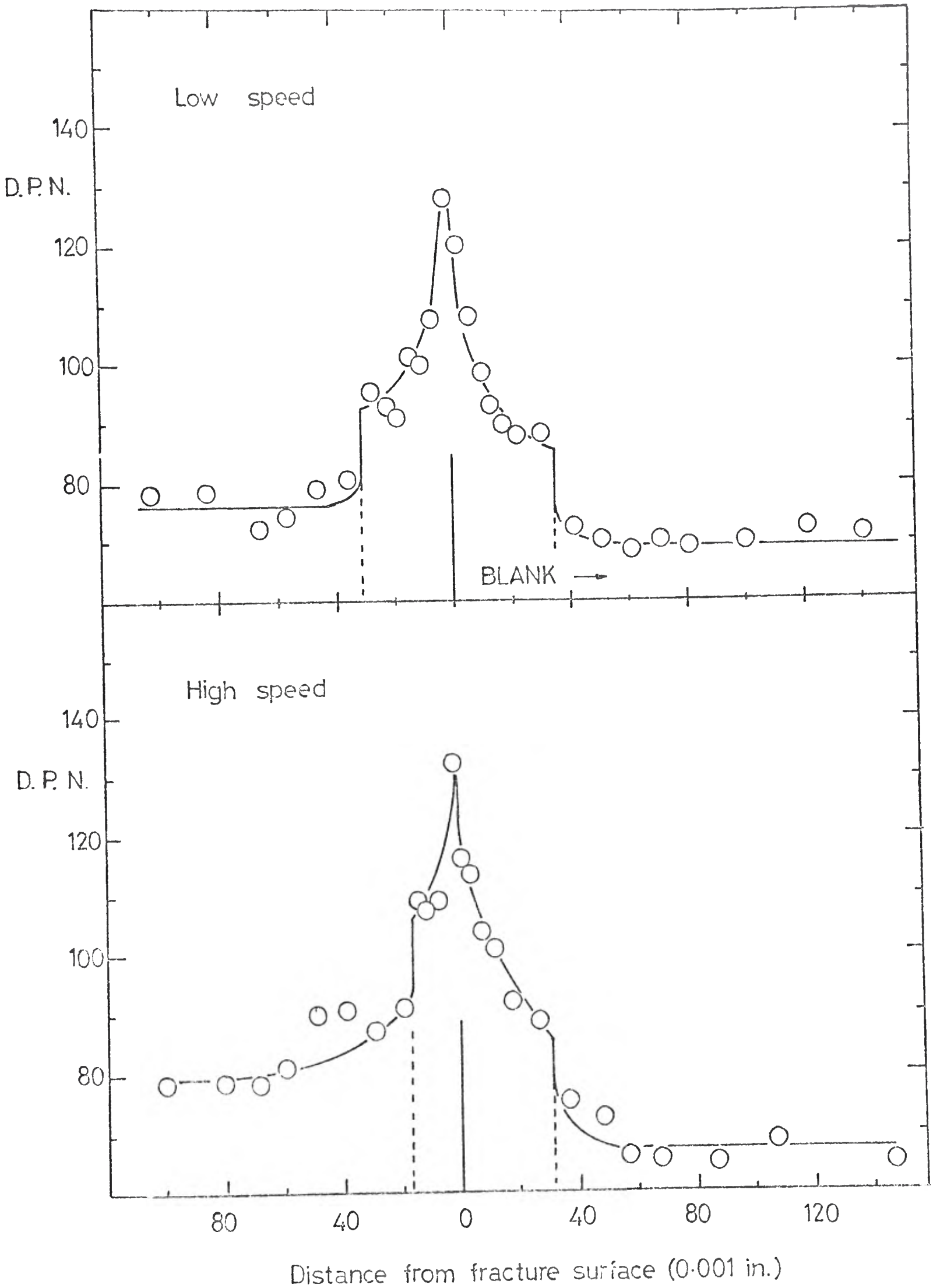
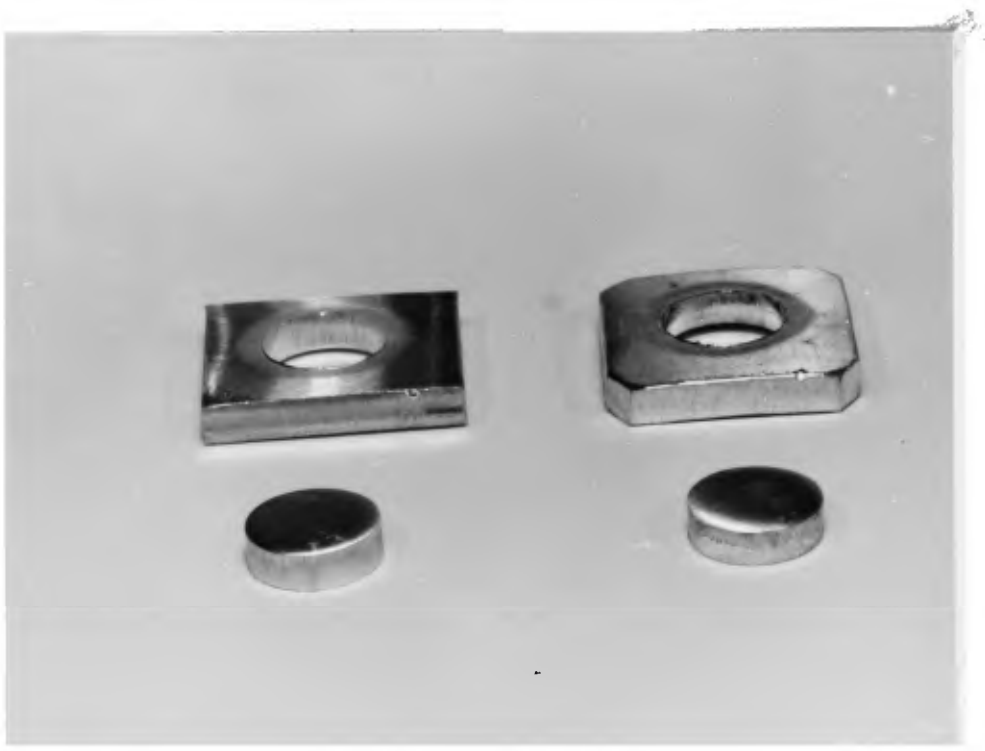


FIG. 10.13 Microhardness traverses for copper.



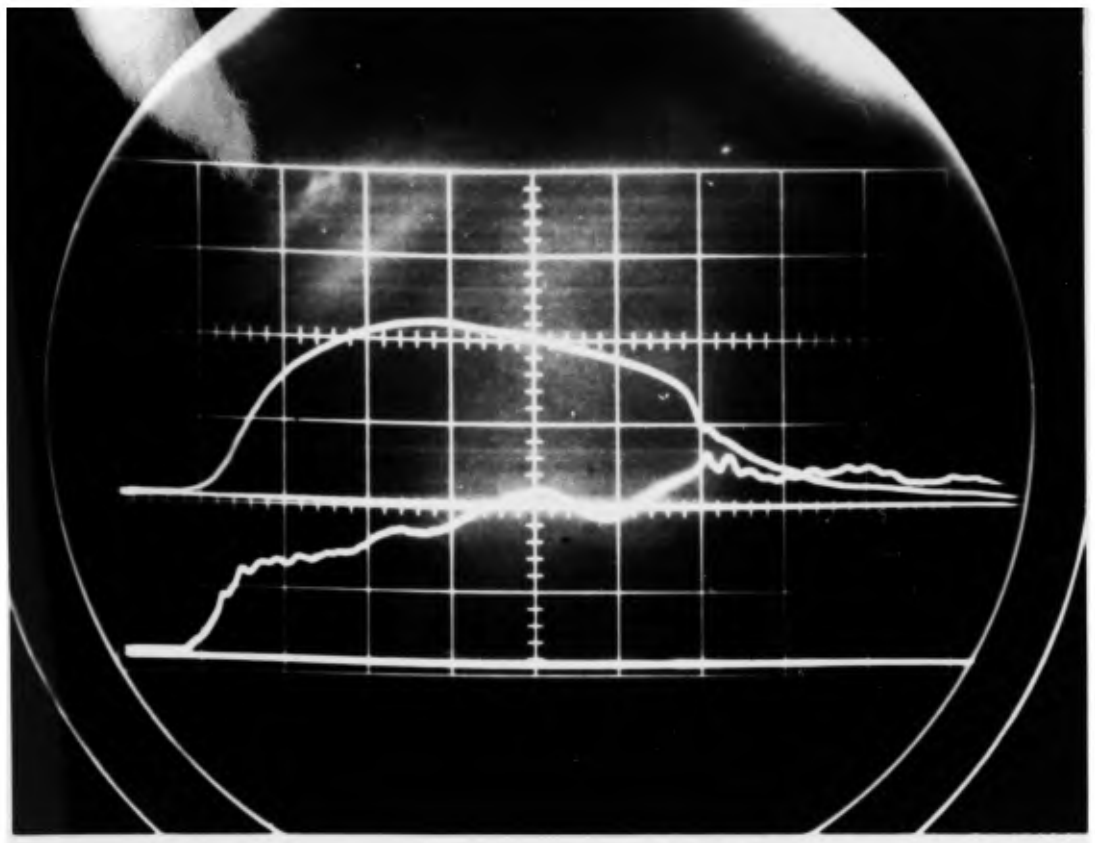
Punch speed: 4.7×10^{-5} in./sec. 750 in/sec.

FIG. 10.14(a) Copper specimens.



Punch speed: 5.8×10^{-5} in./sec. 770 in./sec.

FIG. 10.14(b) Aluminium specimens.

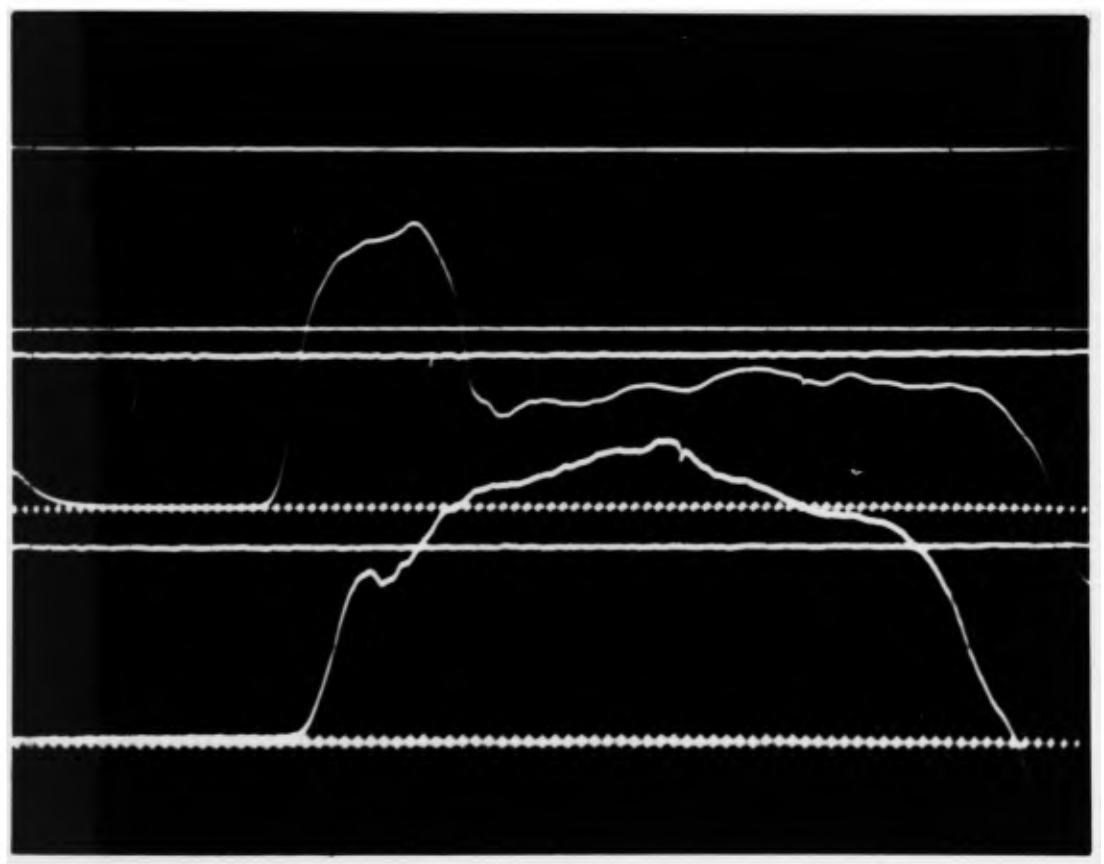


Load:
750 lb./cm.

Velocity:
8·6 in.sec.$^{-1}$/cm.

Hydraulic

Sweep speed: 1ms./cm.



Upper trace:
Punch bar

Lower trace:
Die tube

Impact (Punch velocity 490 in./sec.)

Timing pips at 2μsec intervals.

FIG. 10.15 Typical test records for aluminium.

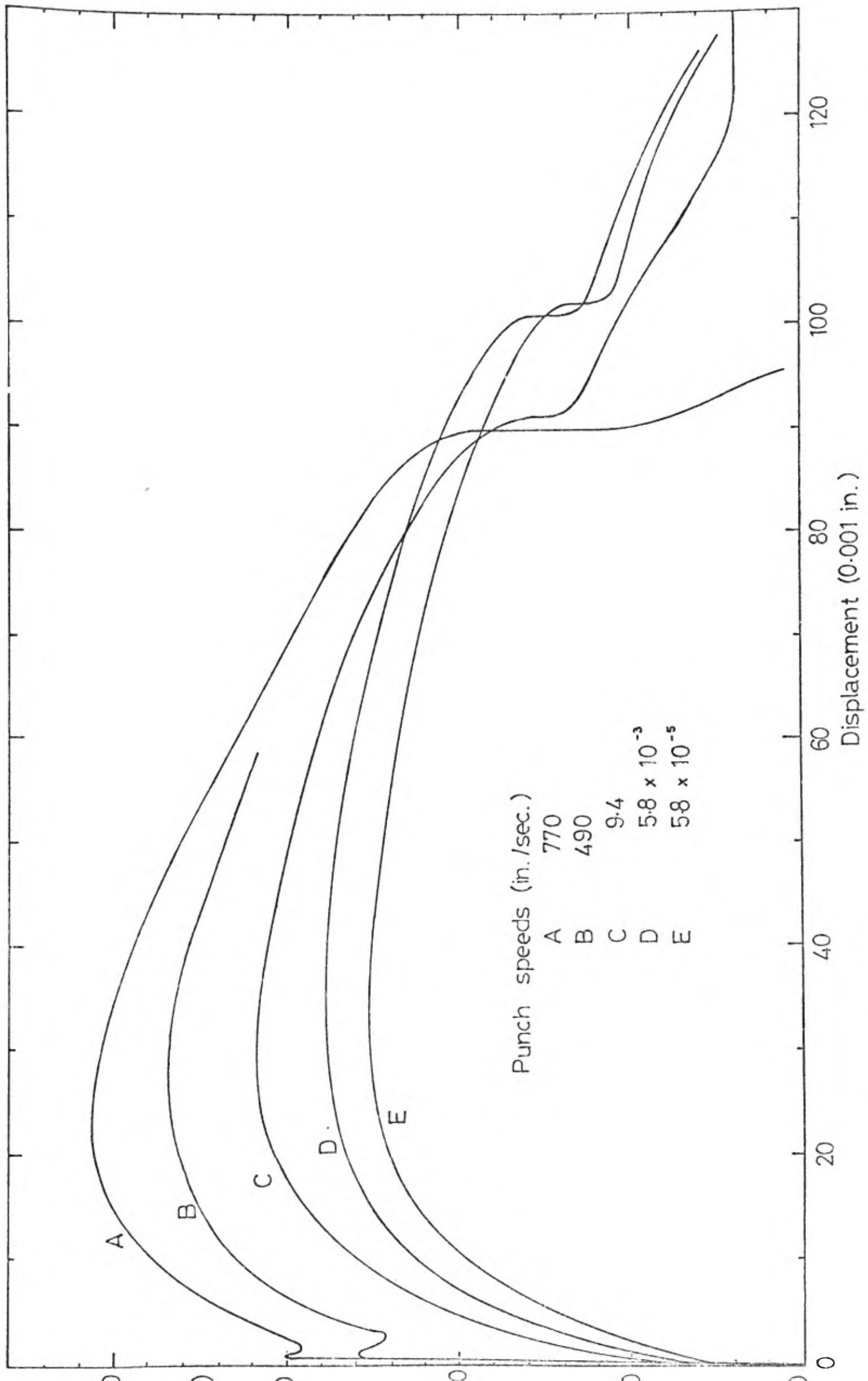


FIG. 10.16 Load-displacement curves for aluminium.

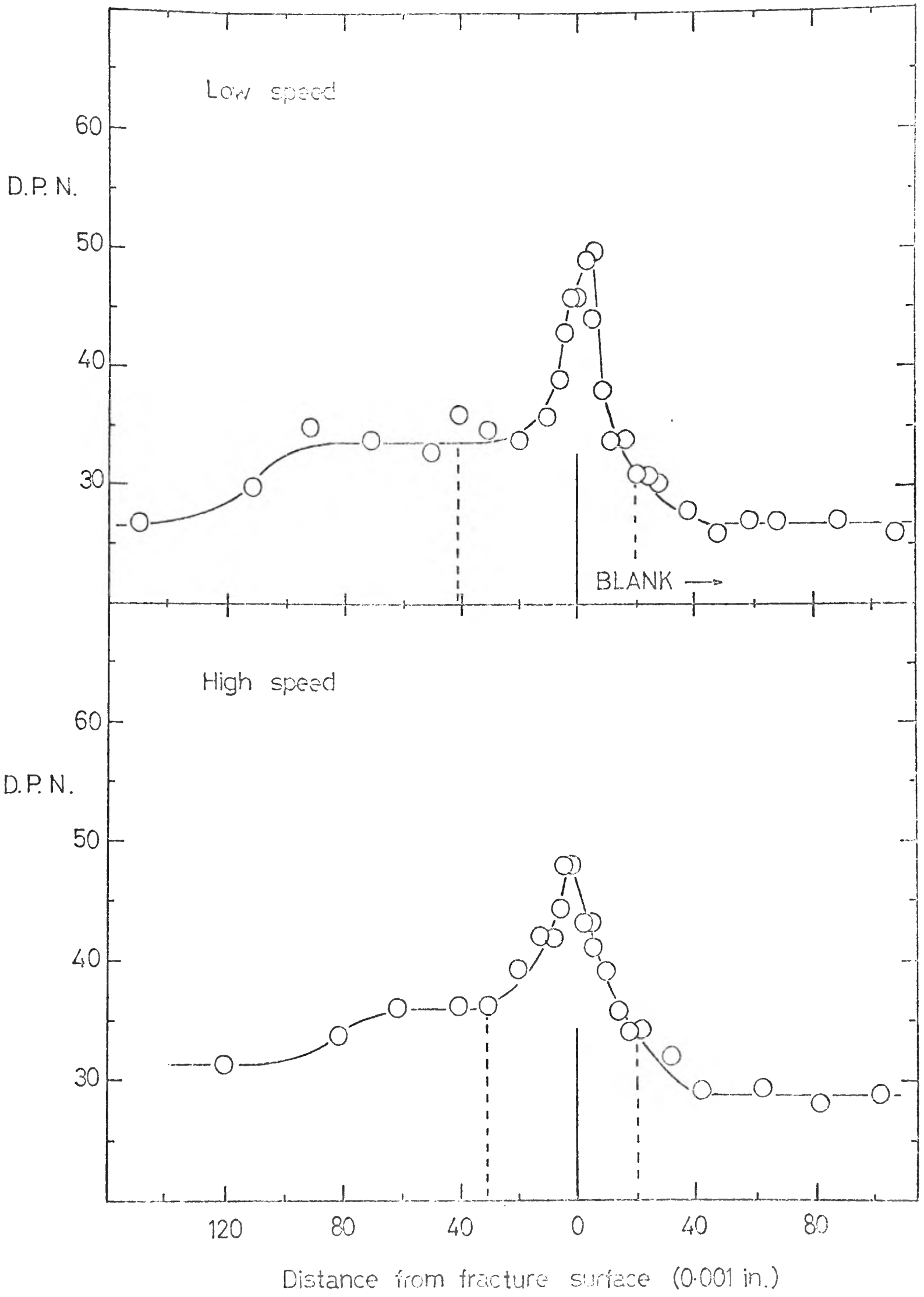
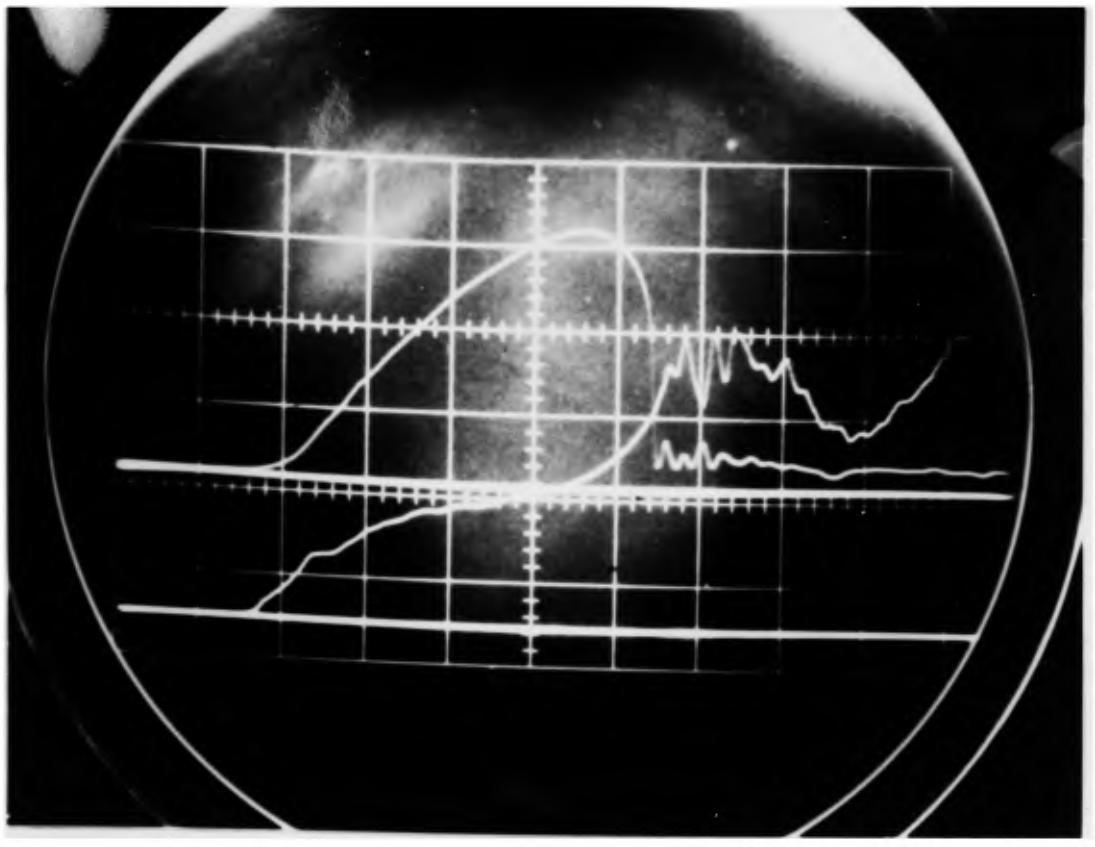


FIG. 10.17 Microhardness traverses for aluminium.

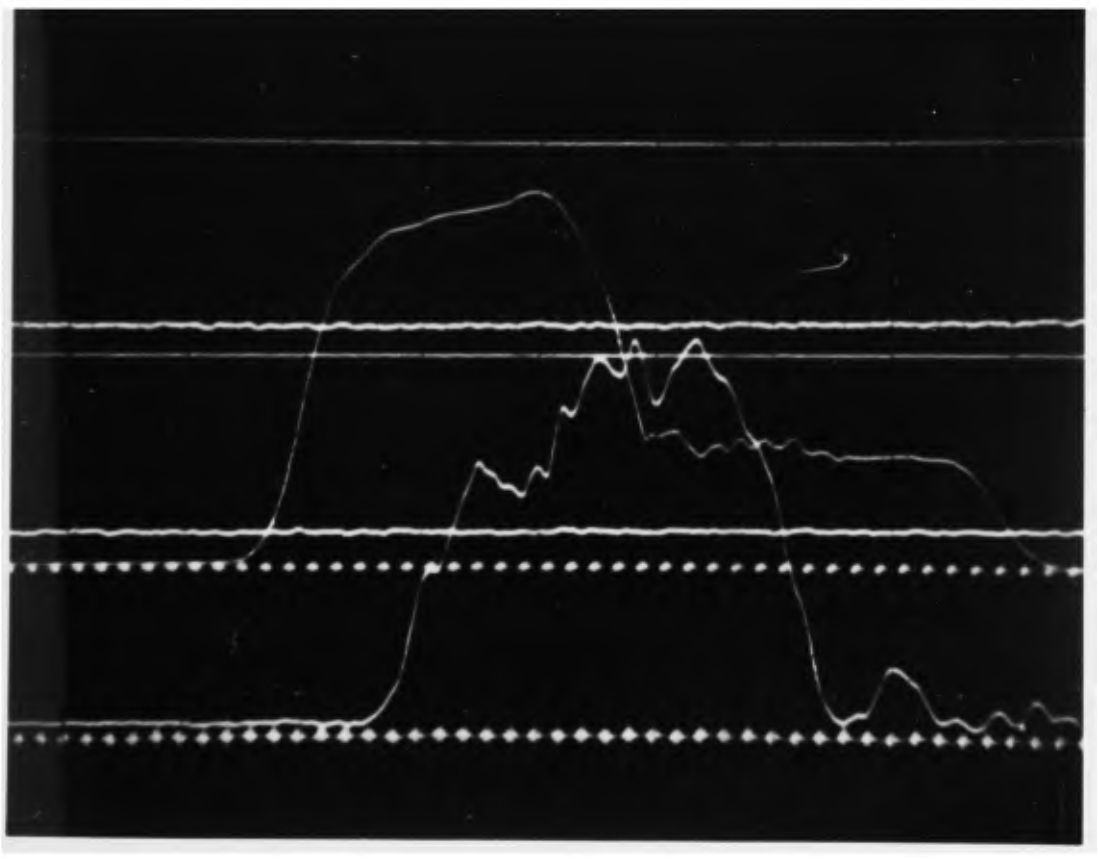


↑ Load:
750 lb./cm.

↑ Velocity:
86 in.sec.$^{-1}$/cm.

Hydraulic

Sweep speed: $\frac{1}{2}$ ms./cm.



Upper trace:
Punch bar

Lower trace:
Die tube

Impact (Punch velocity 740 in./sec.)

Timing pips at 2μsec. intervals.

FIG. 10.18 Typical test records for soft brass.

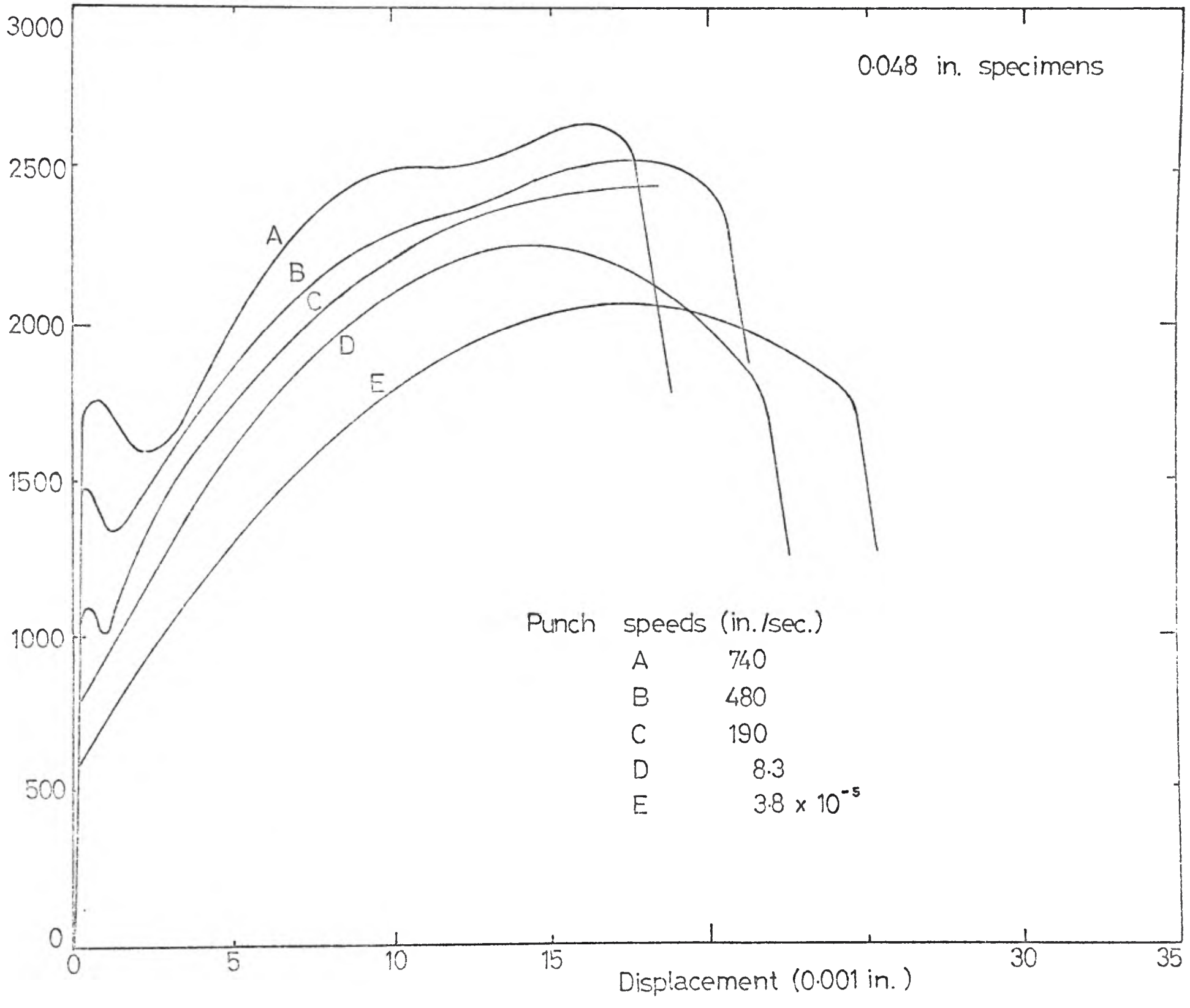
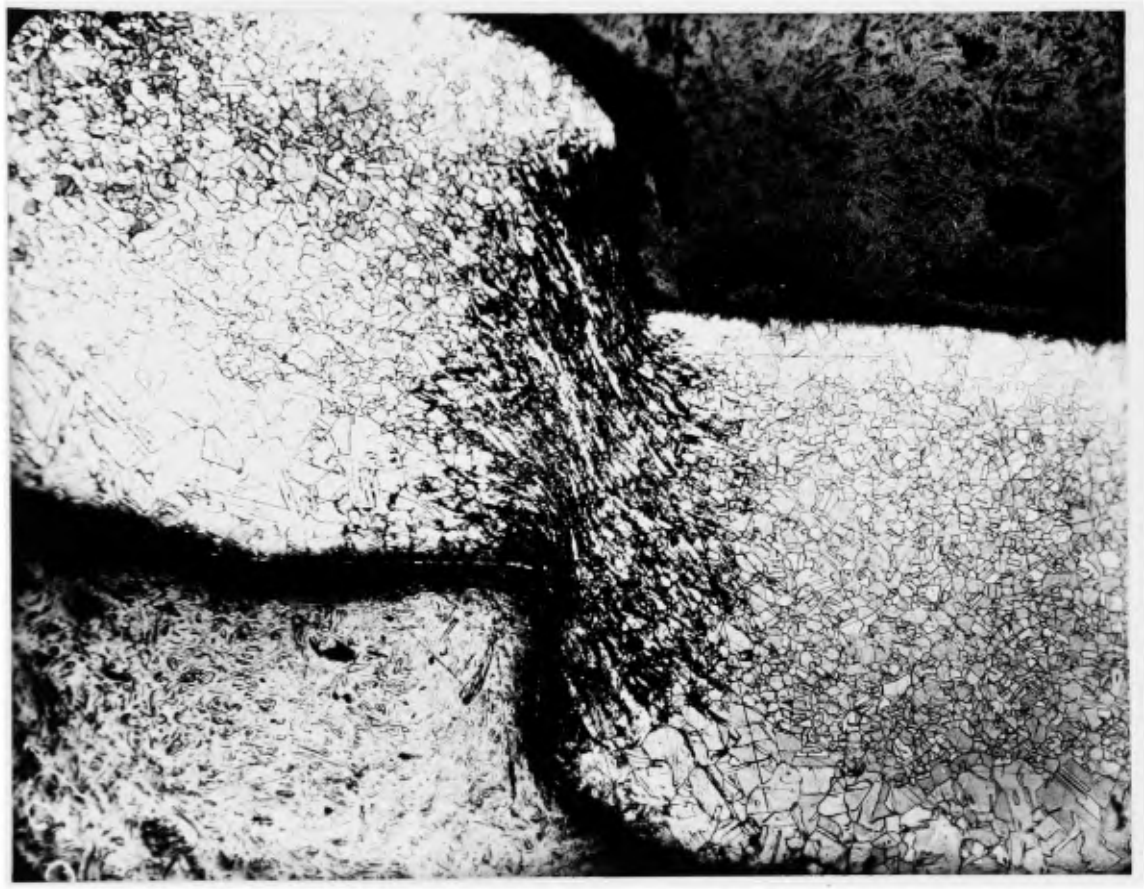


FIG. 10.19 Load-displacement curves for annealed brass.



Impacted at 192 in./sec. x50

FIG. 10.20 The deformed region in soft brass.

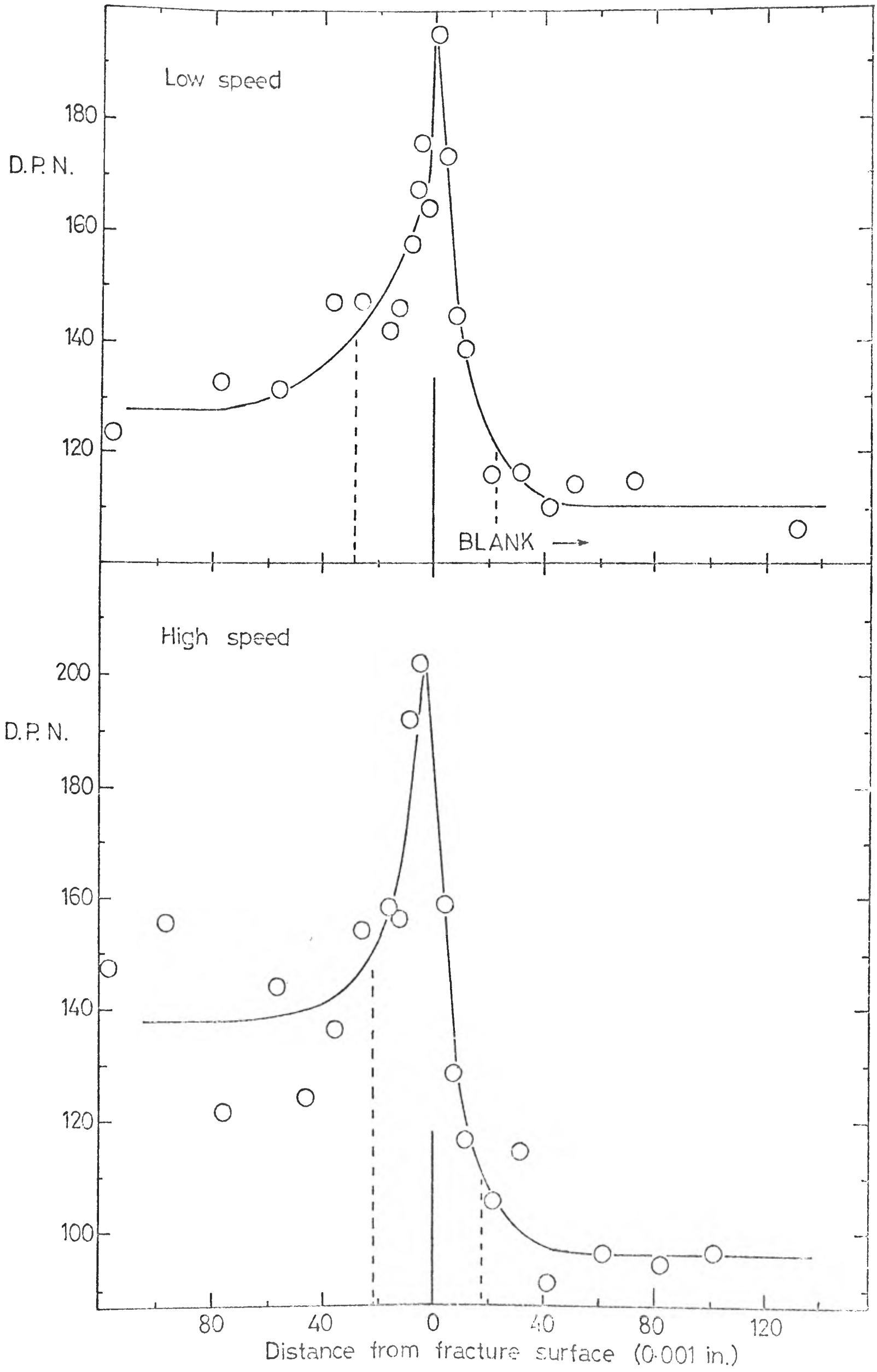
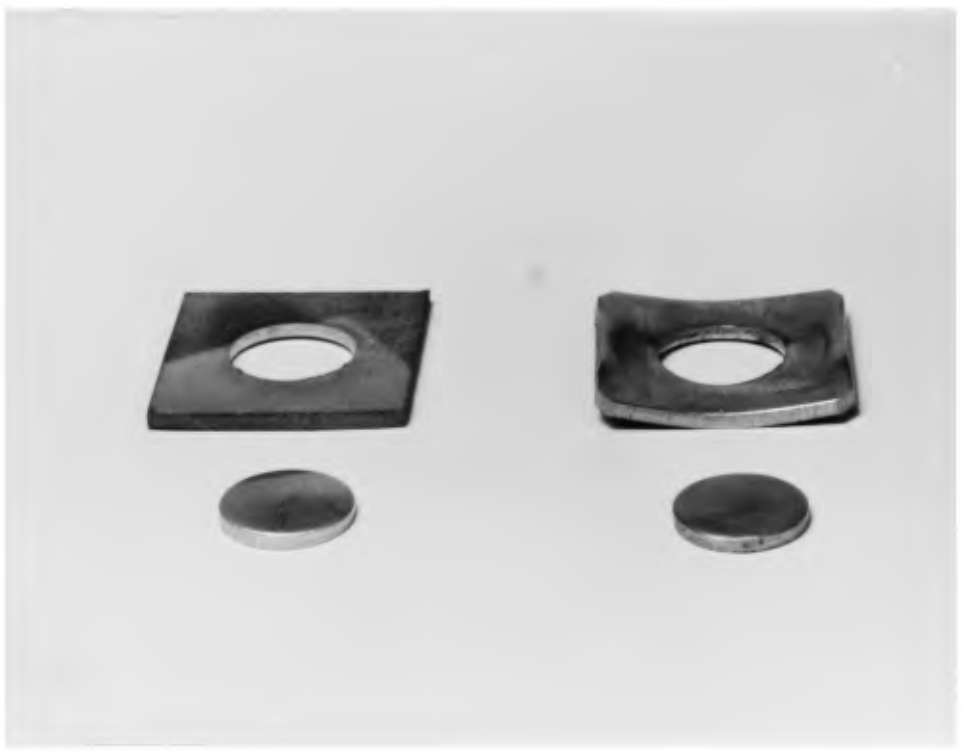


FIG. 10.21 Microhardness traverses for annealed brass.



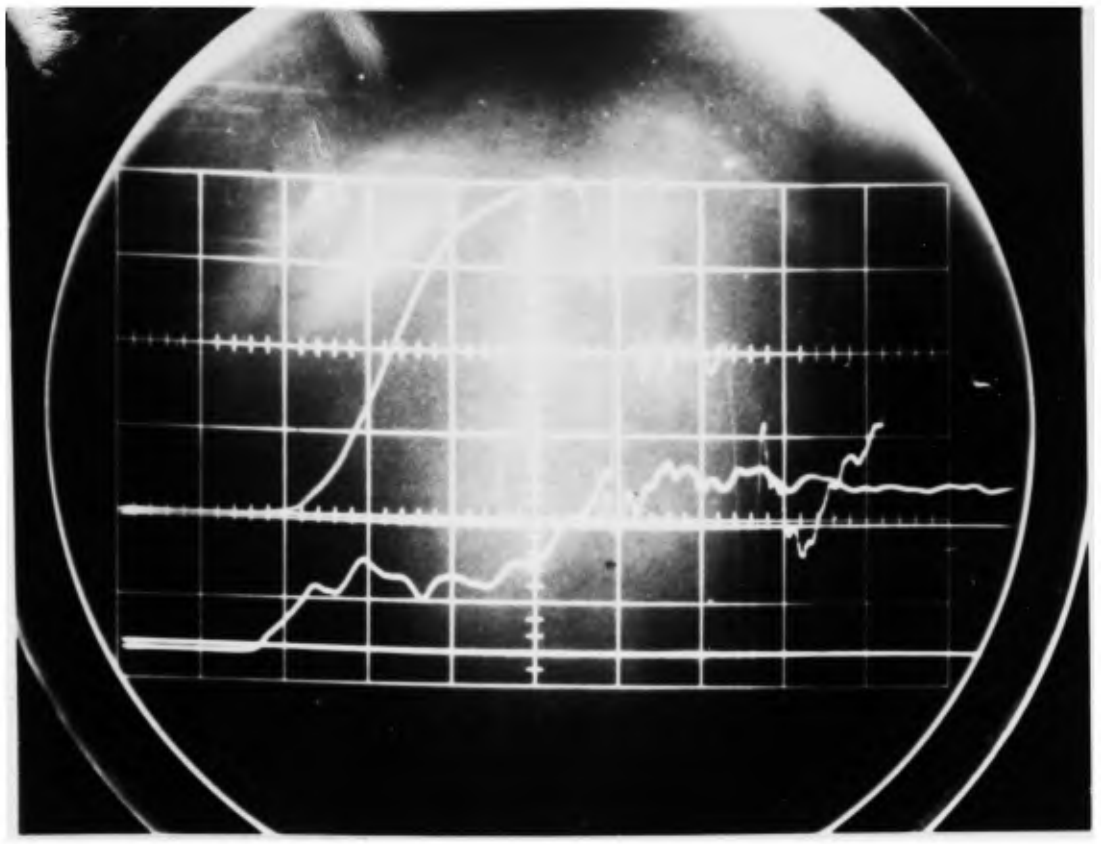
Punch speed: 3.8×10^{-5} in./sec. 740 in./sec.

FIG. 10.22(a) Mounted soft brass sections.



Punch speed: 3.8×10^{-5} in./sec. 740 in./sec.

FIG. 10.22(b) Soft brass specimens.

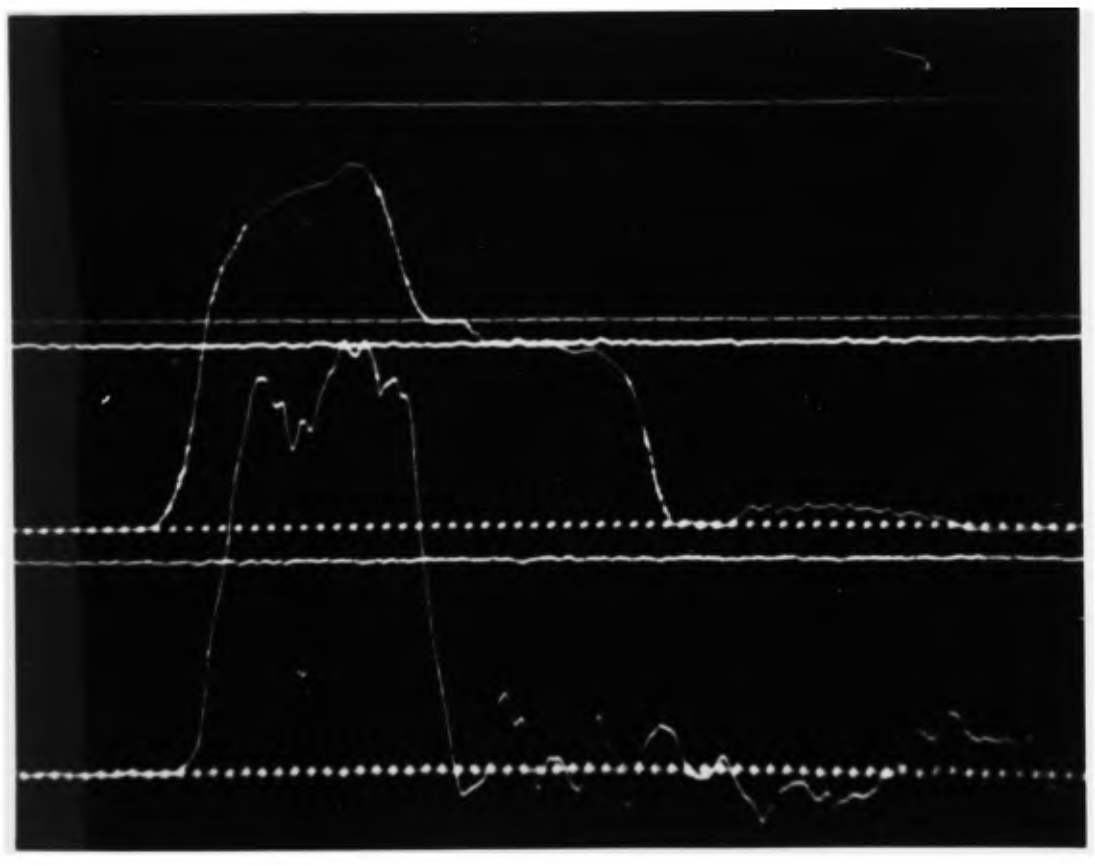


Load:
750 lb./cm.

Velocity:
86 in. $sec.^{-1}$/cm.

Hydraulic

Sweep speed: $\frac{1}{2}$ ms./cm.



Upper trace:
Punch bar

Lower trace:
Die tube

Impact (Punch velocity 360 in./sec.)

Timing pips at 2μsec. intervals.

FIG. 10.23 Typical test records for hard brass.

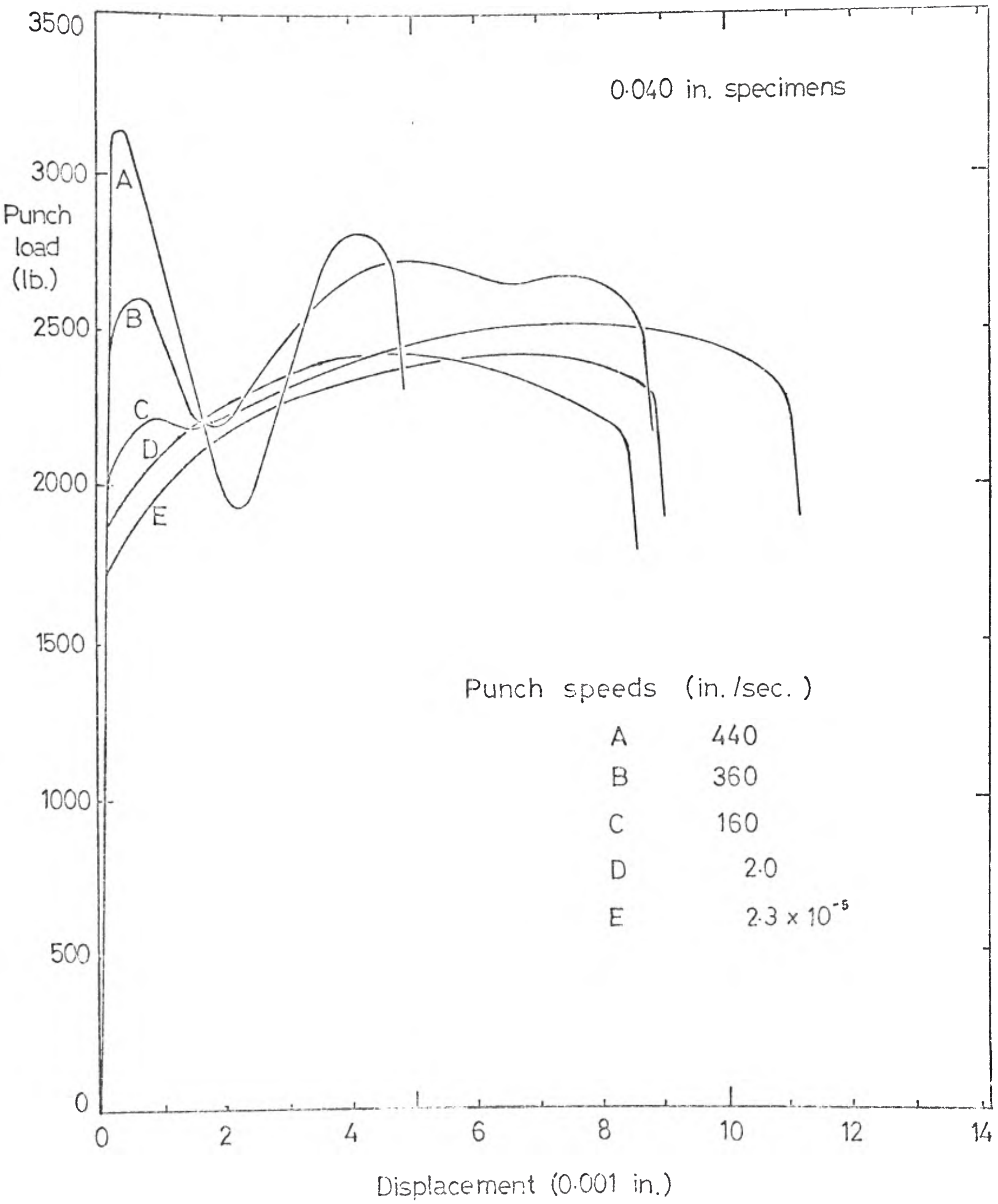


FIG. 10.24 Load-displacement curves for hard brass.

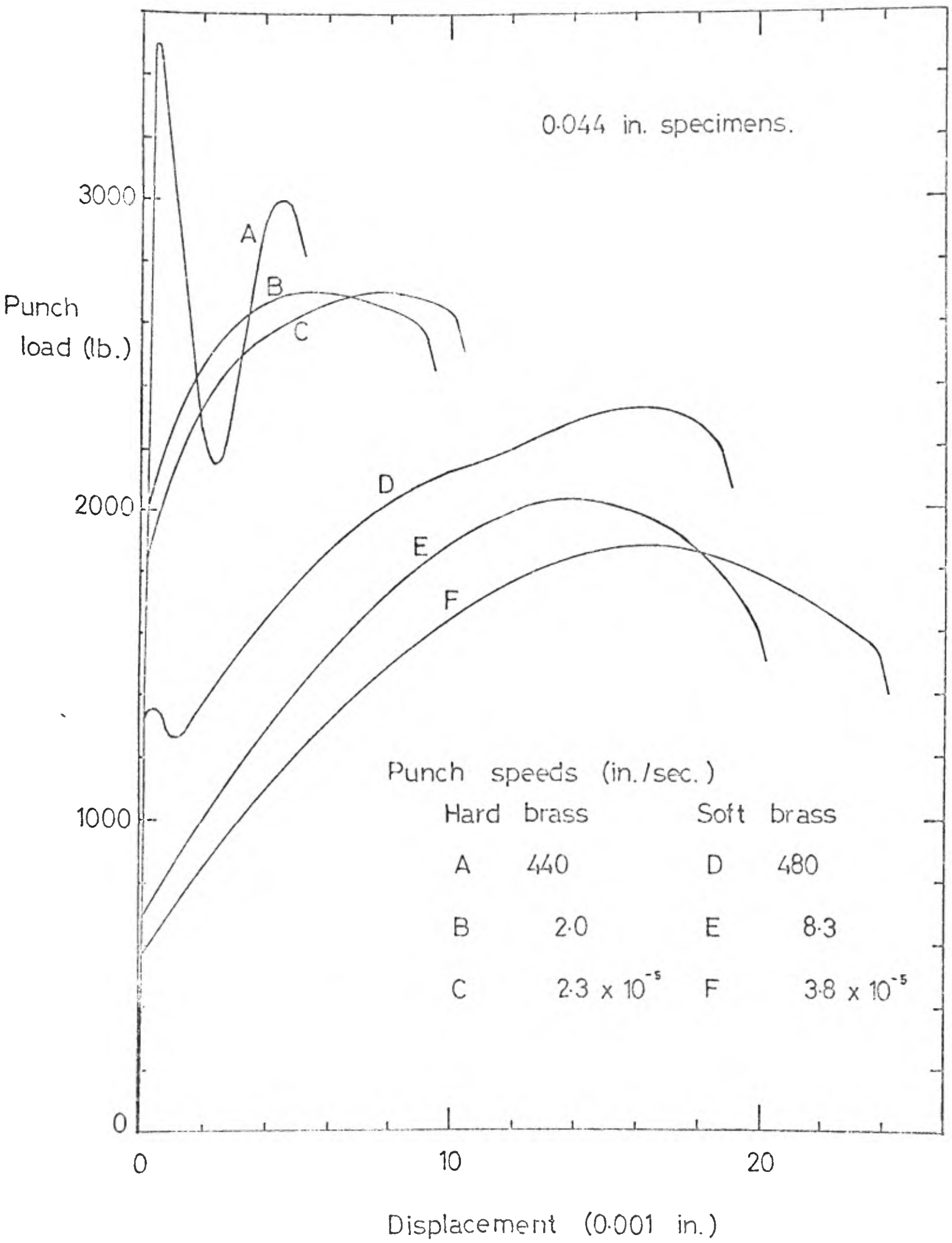
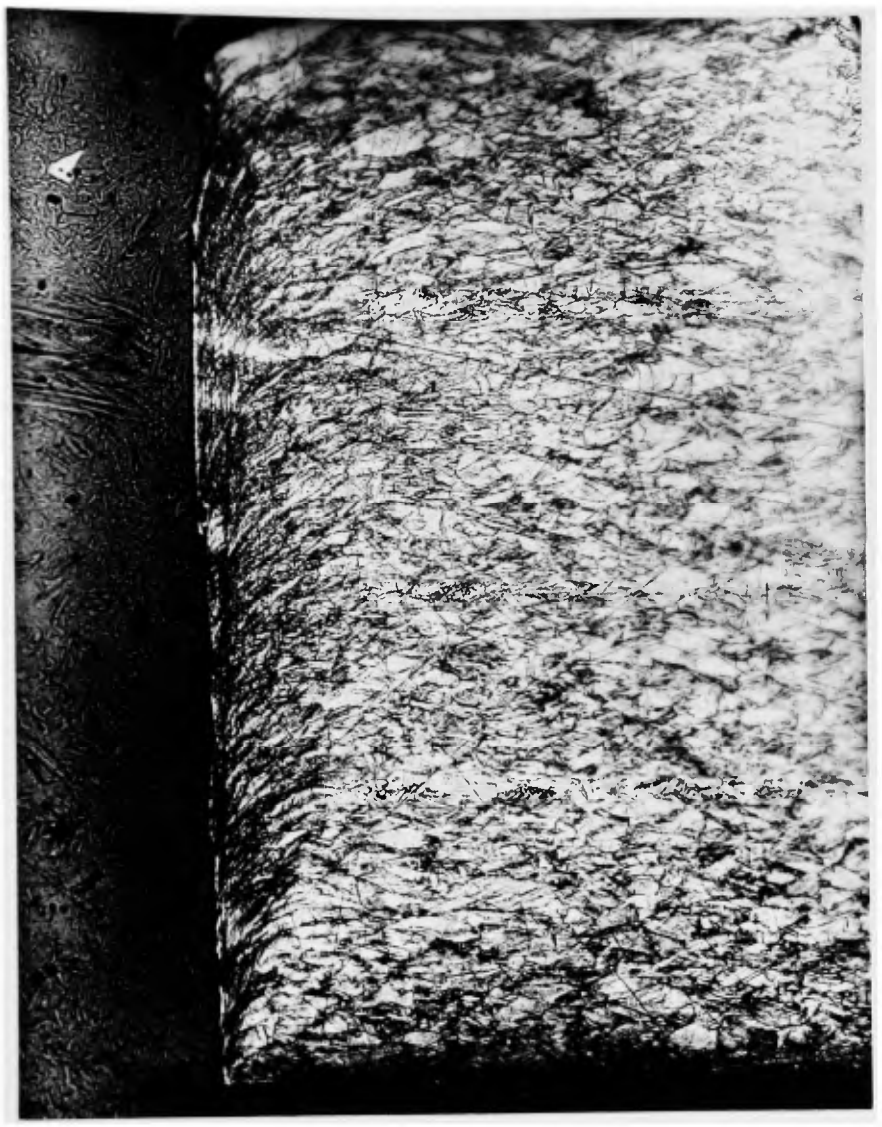


FIG. 10.25 Comparison of the hard and soft brass load-displacement curves.



Mean punch velocity
$2{\cdot}3 \times 10^{-5}$ in./sec.

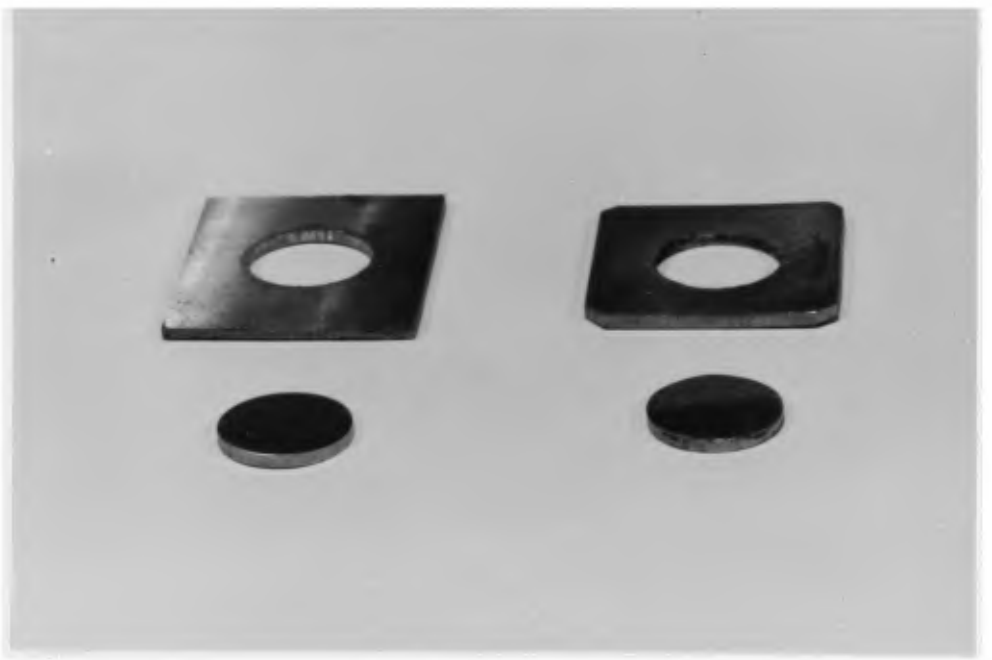
x 105



Mean punch velocity
440 in./sec.

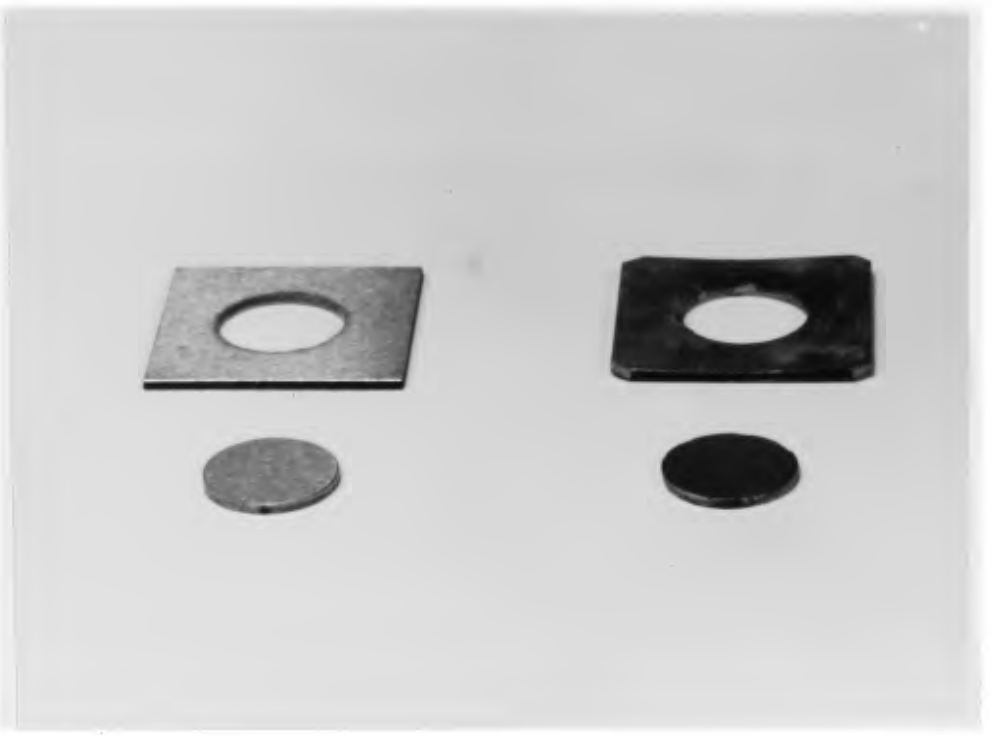
x 105

FIG. 10.26 Micrographs for hard brass.



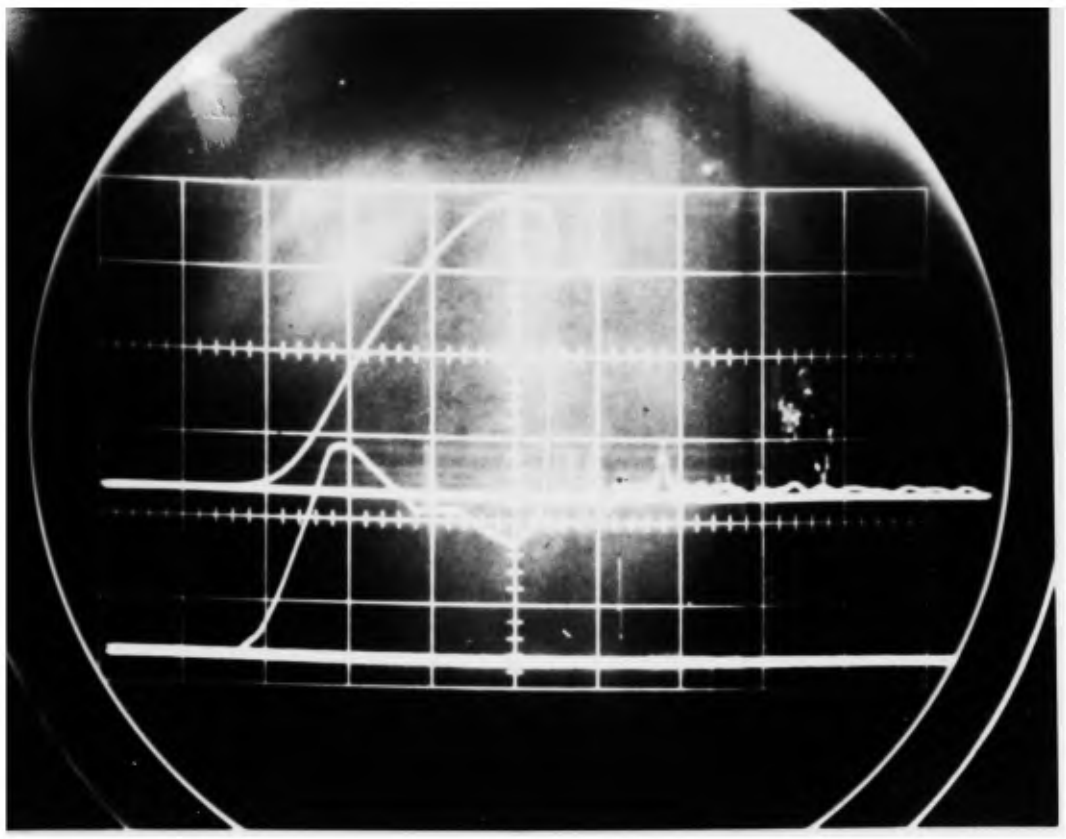
Punch speed: 2.3×10^{-5} in./sec. 440 in./sec.

FIG. 10.27(a) Hard brass specimens.



Punch speed: 1.4×10^{-5} in./sec. 400 in./sec.

FIG. 10.27(b) SAE 4130 steel specimens.

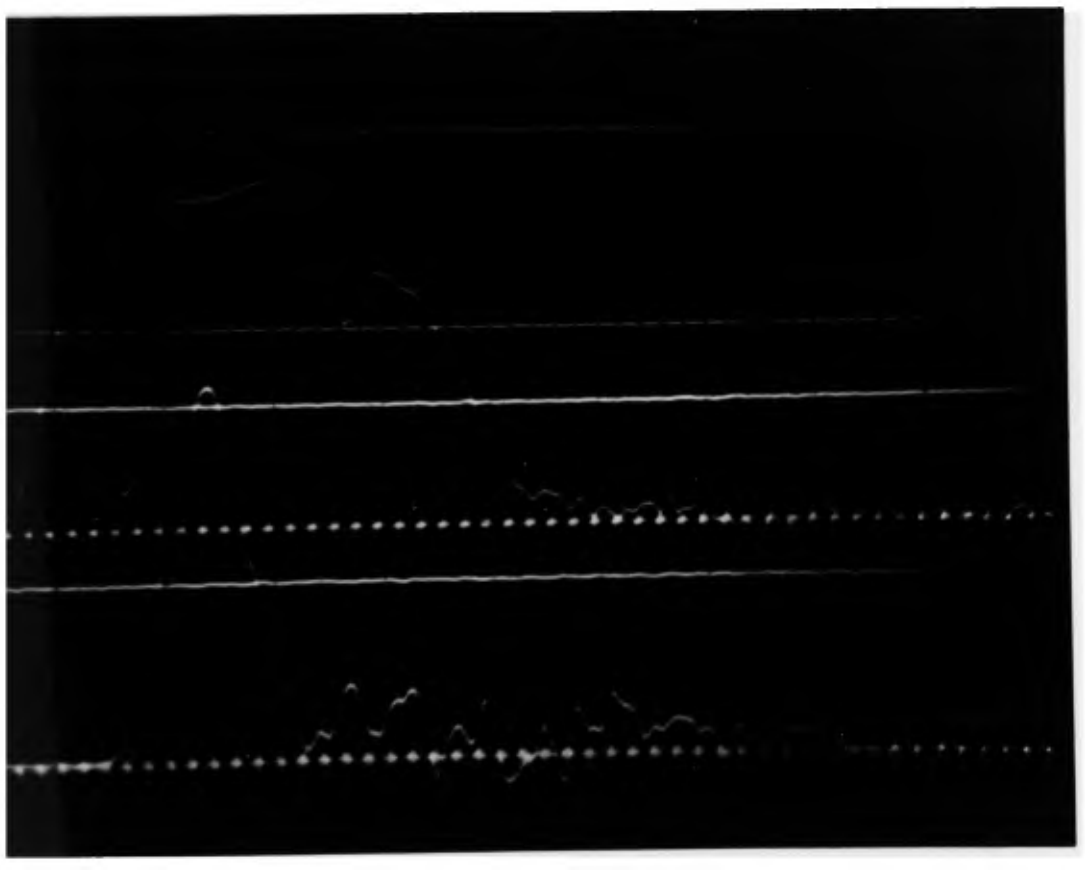


Load:
1500 lb./cm.

Velocity:
4·3 in.sec.$^{-1}$/cm.

Hydraulic

Sweep speed: $\frac{1}{2}$ ms. /cm.



Upper trace:
Punch bar

Lower trace:
Die tube

Impact (Punch velocity 400 in./sec.).

Timing pips at 2μsec. intervals.

FIG. 10.28 Typical test records for SAE 4130 steel.

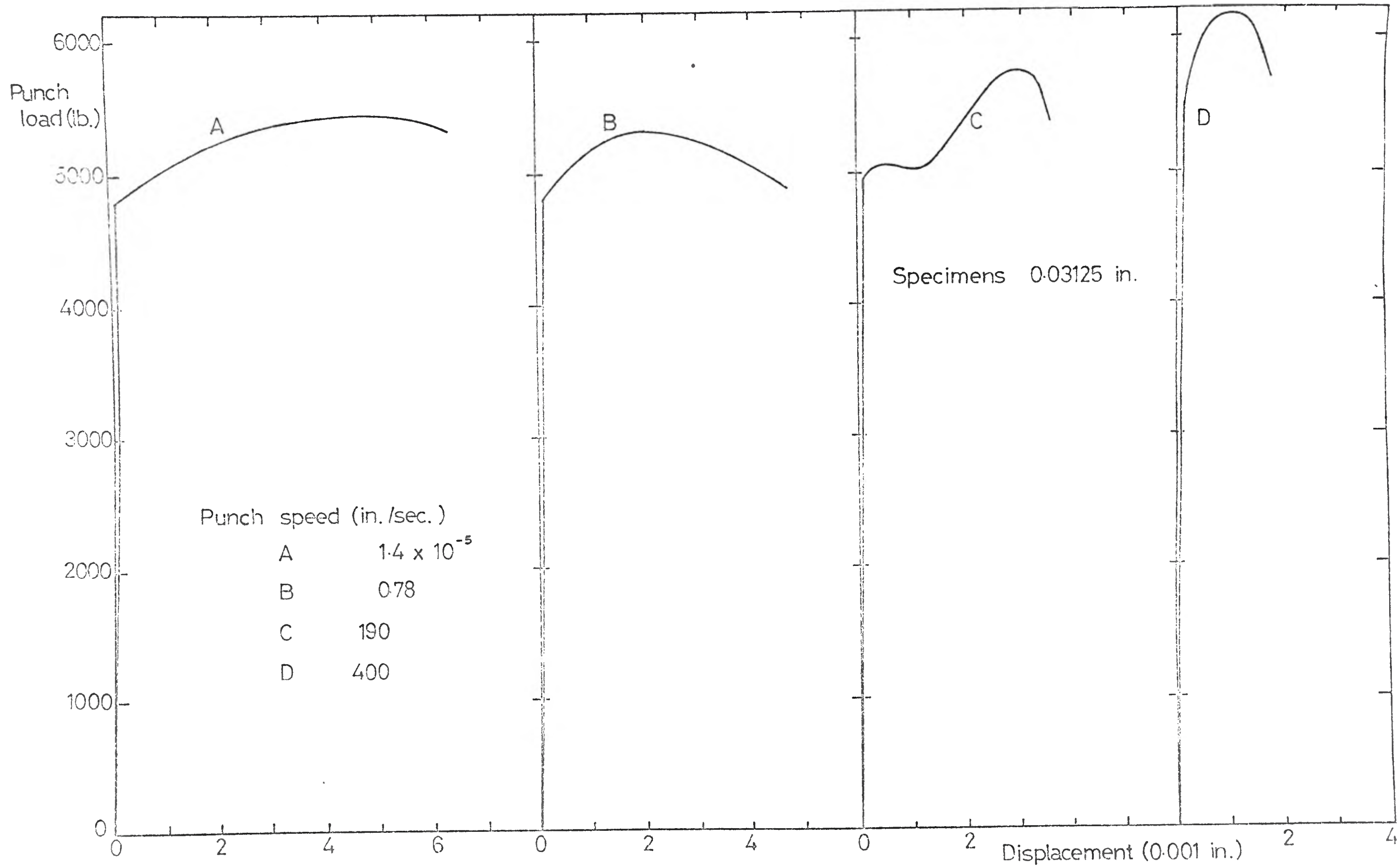
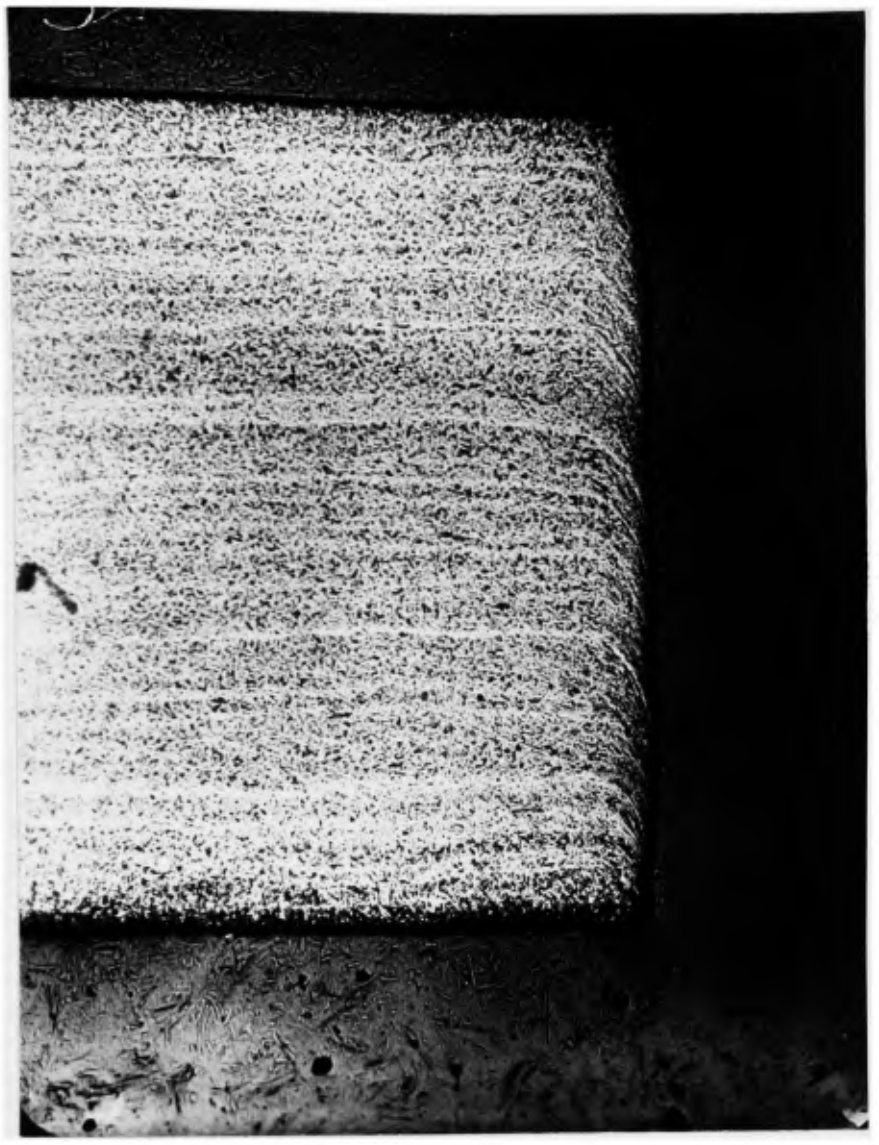


FIG. 10.29 Load-displacement curves for SAE 4130 steel.



Mean punch velocity
1.4×10^{-5} in./sec.

x 105

Mean punch velocity
400 in./sec.

x 231



FIG. 10.30 Micrographs for SAE 4130 steel.

CHAPTER 11.

INTRODUCTION.

This chapter is divided into two parts, the first being concerned with the wave propagation work and that part of the blanking programme relevant to it, the second part being concerned with the blanking process and its effects on various materials.

PART I

The Incremental Torque Propagation Speed.

The results laid out in Figs. (6.3), (6.7) and (6.13) showed quite clearly that the strain-rate-independent theory was extremely inadequate for predicting the propagation speed of an incremental torque in a material which was already plastically strained in torsion. On the other hand the results were very close to the predictions of the strain-rate-dependent theory proposed by Malvern (11). Before deciding whether this work gives conclusive proof of a strain-rate effect, the experiment must be examined in the light of criticisms directed at previous studies of the problem. In addition, the apparatus, in view of its new design, must be examined critically in case there are any inherent assumptions affecting the interpretation of the results.

Craggs (54) pointed out three possible defects in longitudinal incremental experiments. The first of these was that the assumption of uniaxial stress was not adequate for

the propagation of pulses, since the essential condition that the bar radius was negligible compared with the wavelength of the disturbance may no longer be true. As stated in Chapter 3, such an assumption is not necessary when testing in torsion.

Craggs' second point was that, when using a straining machine with only a small incremental load, the specimen material may creep and hence not be at its elastic limit when the increment is applied. In this experiment the specimen was actually being strained when the increment was applied so that it was inconceivable that the material could be in an elastic state.

The third point referred specifically to the experiments of Sternglass and Stuart (14) and concerned the condition of the specimen material which was cold-rolled. It was suggested that this might have suffered differential hardening so that unlike the bulk of the material, the outer layers might be below the elastic limit. The stress waves would then be propagated as elastic waves. The materials used in this investigation were all annealed thus preventing this possibility.

An advantage in using a torsion experiment is that the lateral inertia effect present in longitudinal experiments is eliminated since there are no secondary deformations caused by pure shear, similar to the lateral contraction or dilation caused by tension and compression respectively. This means that the fact that the velocity of the incremental load was higher than the strain-rate-independent theory's prediction could not be attributed to such an effect.

Bell and Stein (33) suggested that the observed elastic velocity of small incremental pulses was due to the

step-like stress strain curves of certain materials, as described in Chapter 2. This problem was avoided in the present study by means of the continual increase in the 'static' pre-strain. Instead of the material always being in a stable state at the foot of a step in the stress strain curve when the increment was added, as would be the case with a stressing machine, constant straining would allow the state of the material to be at any position along the curve. Statistically, therefore, it would be expected that sometimes the increment would be added at the top of a step, sometimes at the foot, sometimes in between. The position at the foot would give rise to an elastic speed for the increment but the situation would be very different when the increment was applied at the beginning of a plateau.

This case will now be considered. The elastic analysis for the torques transmitted through the apparatus is given in the Appendix and from this analysis it can be seen that when the specimen has a modulus of zero the incremental torque transmitted to it is zero. This is the case when the material is in a stress-strain state on a plateau. Incremental loading would only be transmitted when the next rise of the stress-strain curve was reached. For some of the longer plateaux at high strains this would involve delays of several microseconds or more at a strain rate of 9×10^{-3} sec.$^{-1}$ before a pulse was recorded at the strain gauges of the output bar. Considerable variation in recorded times would, therefore, be expected if the unstable form of the specimen's deformation characteristics had anything to do with the observed elastic propagation speeds. Such variation was not observed so that this particular explanation does not apply to the present work.

On examining the apparatus it is seen that both sets of strain gauges were powered by the same source. Consequently the two bridges were not electrically isolated so that the question might arise as to whether the pulse observed in the output gauges might in fact be caused electrically by the pulse in the input bar gauges. However, if this were so, the second pulse would appear at a constant interval after the first and not at a varying time depending on the size or material of the specimen.

Another possibility would be that the specimens were yielding in a non-uniform fashion so that the wave could travel for the majority of its path through unyielded material. This must be discounted because of the high strains obtained in the tests. With some of the specimens it was possible to observe the reorientation of small surface marks on the specimen and it was easy to see that the yielding was uniform. Since the recorded behaviour did not change very much between the low strains after yielding and these high strains, it can be assumed that yielding was sufficiently uniform.

A detailed analysis concerning the siting of the strain gauges showed that, for the static case, the transitional stress distribution caused by the section change between the tube and the bar had negligible effect outside the first inch from the interface. At distances greater than this the stress distribution was uniform such that $\tau = Kr$. In the dynamic case it was found that for a pure step, there would be only a fraction of a microsecond difference between the wave arrival time in the centre of the bar and at the edge, at the plane of the gauges. This would have little effect on the times measured and such a small time would be of even less importance when working with

a wave with a 30 μsec. rise time. It can be concluded, therefore, that all gauges were sufficiently far from an interface.

It is thought that the only other part of the equipment which could have an effect on the pulse propagation speed is the epoxy cement join. This was tested under elastic conditions but if its behaviour did change at the higher stresses, it could not possibly decrease the transit time of a wave between the loading bars, only increase it. Thus it is believed that these experiments do show the existence of a strain rate effect in the metals tested.

There is still one aspect of the wave propagation speeds measured in this research which must be discussed and that is the reduction in the speed with increasing prestrain for copper. The propagation speed stayed constant at the elastic wave speed for aluminium and mild steel so some explanation must be given for the different behaviour in copper. The magnitude of this drop in wave speed was approximately 6% for a strain of 15 , and it appeared to be levelling out to approximately 7.5%. If it is assumed that the wave does in fact always propagate at the elastic wave speed, as for the other two materials, then the elastic wave speed for copper must decrease with strain. It is well known that the elastic wave speed is given by $\sqrt{G/\rho}$ for the tortional case so that either or both of the modulus of rigidity and the density of the material must be functions of strain for this to be possible. Several portions of specimens which had been strained to 20% were used to obtain a measure of the density of the worked material. It was found that the density had increased, but only by approximately 1%.* This was insufficient to cause the observed reduction in velocity. However, earlier work by

* At these strains buckling had begun to occur so that the deformation was no longer pure shear, this probably accounted for the contraction which should not be present in a shear deformation.

Sayre (95) and Smith (96) showed that the Young's Modulus for copper alloys decreased with an increase in stress. The tests used reversed loading on the material and on a phosphor-bronze the magnitude of the effect was a reduction of approximately 5% for a stress of 30 T.s.i. If a reduction of modulus of rigidity with stress occurred in copper in a similar fashion then the reduction of propagation speed could be explained. The work of Sayre showed that the modulus varied linearly with stress and this would explain the levelling off of the velocity curve since the stress-strain curve also decreases in slope at these strains. The magnitude of the effect would need to be slightly larger than was observed in phosphor-bronze, to agree with the propagation speed results, but it is thought that this could explain the shape of the pulse speed against strain curve, Fig. (6.7).

<u>The Strain - Rate Sensitivity of the Specimen Materials.</u>

<u>Copper.</u>

Using the blanking results, shear stress - shear strain curves were obtained for the three materials. They were calculated using the estimated gauge length values of Chapter 10. Fig. (11.1) shows these curves for copper with a maximum strain of 25%. This limit was imposed since none of the wave propagation tests was carried out at a greater prestrain. It will be noticed however, that at this strain only a small portion of the load-displacement curves is used. On the figure the dashed curve is the quasi-static curve obtained from the torsion experiments. Before proceeding further it is necessary to compare the compositions of the copper used in the two studies, which are given in Chapters 5 and 9. In the analyses carried out on the two materials fifty elements were specifically sought of which

38 were not detected in either. A further 5 had less than one part per million in each, the largest differences between the two compositions being that the tube had 0.006% oxygen against 0.027% in the plate and 40 p.p.m. of Nickel against 5 p.p.m. in the plate. However, the plate had a larger quantity of silver and zinc, 100 p.p.m. against 80 p.p.m., and 20 p.p.m. against 0 p.p.m. respectively. In short, the composition can be regarded as being very similar and similar mechanical properties should be expected. The quasi-static curve of the wave propagation experiments was at a strain-rate of ..3 x 10^{-5} sec.$^{-1}$ which is less than the lowest strain-rate derived from the punch test. The strain rate dependency shown in the punch tests suggests that the lower the strain-rate the less load the specimen can support. The torsion curve does not, therefore, fit in to this pattern as for the most part it is above the 6.7 x 10^{-4} sec.$^{-1}$ curve. However, bearing in mind the spread in possible values for the gauge length in the punch tests and also that pure shear is a simplification of this process, the curves from the two types of test agree extremely well.

Having carried out a comparison of the quasi-static curves for the two types of loading it is necessary to compare the apparent strain-rate sensitivity shown by each. In the punch work five different strain-rates were obtained over a large range. Only two strain-rates were obtained from the torsion machine and the data for the stress-strain curve at the higher strain rate was obtained from change-of-strain-rate tests on short specimens. This strain-rate jump was from 5 x 10^{-3} sec.$^{-1}$ to 20 sec.$^{-1}$ and it produced an increase of stress of 1,100 p.s.i. over the whole range of strains of the

tests. A similar strain-rate jump in the punch tests would produce a stress increase of approximately 1,000 p.s.i. at 25% strain increasing from 300 p.s.i. at 5% strain. These results were obtained by interpolation and they show that the two types of test give the same sort of strain-rate sensitivity, at least for this region of the stress-strain - strain-rate surface.

It was stated in Chapter 6 that the consequences of assuming the 5×10^{-3} sec.$^{-1}$ shear stress - shear strain curve to be the same as the 8.8×10^{-5} sec.$^{-1}$ one would be discussed later. Now is the time, for it must be ensured that such an assumption does not invalidate the above comparison. The records of the short specimen tests on the torsion machine provided values, above a datum point, of the stress and strain in the specimen at the higher strain-rate. The stress level at this datum point was calculated from the known torque but the strain was evaluated from the 8.8×10^{-5} sec.$^{-1}$ strain-rate curve. In Fig. (11.2) can be seen the derived stress-strain curve at the highest rate (full line) and also a portion of the stress-strain curve for a strain rate of 8.8×10^{-5} sec.$^{-1}$. To obtain a measure of the strain rate sensitivity, the over-stress caused by a change of strain-rate is the important quantity. That was obtained in this case by subtracting the stress values for the 8.8×10^{-5} sec.$^{-1}$ curve, assumed to be the 5×10^{-3} sec.$^{-1}$ curve, from the values for the 90 sec.$^{-1}$ curve, resulting in the overstress value shown B in Fig. (11.2). For the small excess strains considered the lower strain-rate curve can be considered to be a straight line, whose gradient is the important factor in deriving the overstress value. Assuming only a small strain-rate sensitivity between the two

strain-rates 5×10^{-3} sec.$^{-1}$ and 8.8×10^{-5} sec.$^{-1}$ and also that the curves have little change of curvature in the vicinity of the datum stress level, a portion of the 5×10^{-3} sec.$^{-1}$ curve can be drawn. Since the datum stress level was known, the new datum point for this strain-rate can be fixed and the excess stress - excess strain curve drawn from this (dashed curve). Taking now the overstress as the stress values for the 90 sec.$^{-1}$ curve minus the values for the 5×10^{-3} sec.$^{-1}$ curve a new value of overstress, A, is obtained. However, it can be seen that this is the same as B if the lower strain-rate curves have no curvature, and have the same gradient. Thus the original assumption that the 8.8×10^{-5} sec.$^{-1}$ and 5×10^{-3} sec.$^{-1}$ curves are the same will hold for the purpose of obtaining a measure of strain-rate sensitivity so long as there is little strain rate sensitivity in this region or the stress-strain curves at these strain-rates have very little curvature in the relevant region.

From the results obtained with copper it can be seen that there is little curvature for the most part of the stress strain curves and that there is little strain-rate sensitivity at these strain rates so that the comparison of overstresses from the two types of test is valid.

The strain-rate sensitivity is best represented on a graph of stress against the logarithm of strain-rate for particular strains. This is done in Fig. (11.5) for copper and it can be seen that the sensitivity is very much the same for all strains. Each constant strain curve begins to curve sharply upwards at a strain-rate of approximately 200 sec.$^{-1}$ and the stress increases very sharply with an increase of strain-rate at strain-rates of the order of 10^{4} sec.$^{-1}$.

Also shown on this curve are some results of Baker and Yew (56) for dynamic torsion tests on commercially pure copper. They show remarkably good agreement with the results obtained from the punch tests.

Aluminium.

The shear stress - shear strain curves for aluminium derived from the punch test results are shown in Fig. (11.4), along with the strain-rate values. On this graph is shown the mean shear stress - shear strain curve at a strain-rate of 8.8×10^{-5} sec.$^{-1}$ derived from the torsion experiment. As with the copper results this curve has a greater curvature near the stress axis than those derived from the punch test and also it does not fit in with the trend of higher load for higher strain rates since for the main part the stresses are higher than for the 9.7×10^{-4} sec.$^{-1}$ strain rate curve.

Comparing the compositions of the tube and plate materials used in the tests, as set out in Chapters 5 and 9, it can be seen that they were extremely similar so that similar material properties could be expected. 51 elements were sought in the analyses of which 36 were not detected in either. There were slightly more impurities in the tube material than in the plate, there being 0.004% by weight of Chromium which was not detected in the plate and 0.1% of magnesium against 0.03 % in the plate. This would make the aluminium tube, if anything, stronger than the plate and this is what was found.

Comparing the strain-rate sensitivities indicated by the two types of test the following results are found. In the torsion machine, a strain-rate change from 5 x 10^{-3} sec.$^{-1}$ to 50 sec.$^{-1}$ produced a stress increase of approximately 800 p.s.i.

at strains of up to 15%. Under similar conditions the punch results would have shown a stress increase of approximately 1,900 p.s.i. thus casting doubt on the wisdom of expecting the strain rate sensitivities from two such different tests to be similar. However, work by Klepaczko (97) on strain-rate change tests on aluminium, showed that a change in strain-rate from a lower to a higher value produced a smaller stress change than would be expected from the two stress-strain curves at the particular strain-rates used. The magnitude of this observed effect is shown in Fig. (11.5), the strain-rate jump producing 2/3 the expected stress change. If the tests performed on the torsion machine showed the same effect then the apparent strain-rate sensitivities from the two types of test would be very similar in this region of the material's stress-strain strain-rate state.

The similarity of the compositions of the two samples of aluminium was extremely important for some idea of the dependence of its properties on impurity content is obtained by observing the results of Nachlinger and Yew (98). Using the same machine on which Baker and Yew (56) obtained the dynamic torsion copper results mentioned previously, they found that annealed 1100 aluminium, which was purer than the material used here, was not strain rate sensitive at all.

The strain rate sensitivity of the aluminium used here is shown in Fig. (11.6) in the form of a graph of stress against log. strain rate for constant strains. This shows aluminium to have a higher strain-rate sensitivity than copper at the lower strain rates, between 10^{-3} sec.$^{-1}$ and 10^{2} sec.$^{-1}$, but above this value the same sharp rise in stress values is apparent.

Mild Steel.

Shear stress - shear strain curves derived from the

1/8 in. mild steel specimen load-displacement curves are shown in Fig. (11.7). Although there are only four curves for this thickness of specimen, the values of gauge length are more accurate than for the thinner specimens so that it was felt that the strain-rate sensitivity of mild steel would be best represented by these results.

When plotted as shear stress against log. strain rate for constant strains, Fig. (11.8), the mild steel shows a different type of strain rate sensitivity from that of copper and aluminium. One notable difference is that the curves do not have a sharp rise at a strain rate of 10^2sec.$^{-1}$ though there is a suggestion from the thinner specimens that the strength would rise sharply at strain rates above 10^4sec.$^{-1}$. Instead of this rise at 10^2sec.$^{-1}$, the mild steel constant strain curves have a gradual rise between strain-rates of 10^{-1} and 10^4 which is steeper than the rise at strain-rates lower than 10^{-1}sec.$^{-1}$. The general conclusion is that the mild steel is more strain-rate sensitive than the other two materials used in this study.

Comparing the compositions of the materials used for the punch and wave propagation tests given in Chapters 5 and 9 it can be seen that the two mild steels had different compositions though they had the same major impurities. The tube material had twice as much carbon as the plate and also much more silicon. The manganese and nickel contents were approximately the same while the plate material contained more phosphorus than the tube. However, it would be expected that their mechanical properties in the annealed condition would be similar and that this is so can be seen from Fig. (11.7) where the 8.8 x 10^{-5}sec.$^{-1}$ curve from the torsion experiment fits nicely into the general pattern.

No short specimen tests in mild steel were performed in the torsion work so that no comparisons of the apparent strain-rate sensitivities from the two types of test are possible. However, since such interchanging between tests was shown to be valid for copper and aluminium, it is expected to hold also in the case of mild steel.

The Magnitude of the Initial Peak of the Transmitted Increment.

It was shown earlier in this chapter that the measured wave speeds agreed with the Malvern formulation of a strain-rate-dependent wave propagation theory. This formulation, in addition to predicting the incremental wave speed, described the relaxation of the elastic wave front. It remains now, to find out if the observations made with these three materials agree with this prediction or not.

In Chapter 3, the relaxation of the elastic wave front for the torsional case was shown to be described by the following equation :

$$t = 2\int_{\tau}^{\tau_0} \frac{d\tau'}{g(\tau', \tau'/G)} \qquad (11.1)$$

In this equation t is the time taken for the increment to travel the length of the specimen, τ_0 is the initial magnitude of the increment, τ is the observed final magnitude and the function $g(\tau', \tau'/G)$ is a measure of the strain-rate sensitivity of the material. t, τ_0, τ are known from the wave propagation tests and the strain-rate sensitivity is obtained from the punch tests. Consequently by performing a graphical integration of $1/g$ against τ, the wave front relaxation can be checked.

Fig. (11.9) shows a graph of $1/g$ against overstress for the copper material. The zero of stress is taken at a

strain-rate of 3.8×10^{-3}, the strain-rate used in the wave propagation experiments. The initial stress level of the increment was approximately 450 p.s.i. which is marked on the graph by a full line. The time of transmission of an elastic wave through the copper specimen was 100 μsec. and measuring this area off on the graph, the magnitude of the peak of the transmitted pulse should be arrived at. It can be seen that the theoretical stress drop of 65 p.s.i. was much lower than the observed reduction in pulse height.

Going through the same procedure for aluminium and mild steel, the graphs in Figs. (11.10) and (11.11) are derived. The initial magnitude of the increment is shown on each of these and it can be seen that theoretically the peak in the aluminium should hardly have decayed at all on transmission through the specimen and that in the mild steel should decay by an even smaller amount. The actual behaviour in both the copper and aluminium was therefore at variance with the theorectical behaviour. On the other hand the mild steel behaved as expected from the Malvern theory.

Looking at the results qualitatively rather than quantitavely, now, it will be shown that the trends in the magnitude of the pulse are as predicted by the Malvern formulation. First of all, comparing the three materials, the theory would predict the magnitude of the transmitted pulse to have relaxed most in copper and least in mild steel. This was the order found in the results. In the records for aluminium and copper it was noticed that as the prestrain, at which the increment was added, was increased, the magnitude of the transmitted increment also increased. This was more marked in copper than in

aluminium. Qualitatively this would be expected by the Malvern theory, for the $^{1}/_{g}$ functions of Figs. (11.9), (11.10) and (11.11) were each derived for a strain of 5%. In the copper and aluminium, the strain rate sensitivity increases as the strain increases, moving the curve of Figs. (11.9) and (11.10) to the right. Thus with the same amount of added incremental stress, the peak would be expected to relax less during the transmission time through the specimen. This effect is larger in copper, where the relevant gradient of the τ v. $\log \dot{\gamma}$ curve is doubled for a strain change from ... to 25%. With the same strain change the gradient of the aluminium τ v. $\log \dot{\gamma}$ curve increases by only 30%. Since no tests were done at strains above 10% for mild steel no such conclusions can be drawn.

Turning now to the 'half-length' specimens, the magnitude of the initial peak should theoretically have been larger than for the standard specimens. For copper the stress drop should have been 45 p.s.i. as against 65 p.s.i. for the standard ones. However with the theoretical stress drop for a standard aluminium specimen being negligible, so was the theoretical drop in the short specimen. It was to be expected therefore, that the height of the transmitted pulse in the short aluminium specimens would be identical to that in the standard ones, as indeed it was. However, it was also expected that there would be a measureable difference in the pulse heights for the two sizes of copper specimen. Bearing in mind the difficulty encountered in measuring the pulse height for this material, due to the double peak, and that the difference in the expected levels was only 2% of the pulse height anyway, it is not after all surprising that no difference was detected..

It has been shown therefore that the wave propagation behaviour can be explained qualitatively if not quantitatively by a strain-rate-dependent theory of the Malvern type. To suggest possibilities why the theory is not followed quantitatively it is necessary to make quite clear the circumstances in which the theory can be expected to apply.

It was stated in Chapter 3 when deriving the leading elastic wavefront relaxation equation (11.1) that it applied to a steep wave. By steep was meant a wave with an infinitesimally short rise time. In these tests the rise time of the pulse was of the order of 30 μ sec. which is certainly not infinitesimal at the scale of these experiments. To realise the consequences of this, the third of equation (3.38) will be used :

$$\frac{d\tau}{ds} + \rho c_0 \frac{dv}{ds} + g(\tau,\gamma)\frac{dt}{ds} = 0 \quad \text{on} \quad \frac{dx}{dt} = -c_0 \qquad (11.2)$$

Integrating across the leading wavefront :

$$\tau + \rho c_0 v = -\int g(\tau,\gamma)\, dt \qquad (11.3)$$

This means that the greater the rise time of the wavefront the more the stress is decreased along a C_- characteristic. With a steep wavefront, the amplitude of the peak relaxed only in the direction of a C_+ characteristic, but here it is subjected to relaxations in both directions. Thus the present experiments would be expected to show far greater reductions in magnitude of the pulse height than predicted from equation (11.1).

Another difficulty in trying to apply the Malvern strain-rate dependent theory to the present experiments is that this theory assumes that there is a true 'static' strain-rate

below which the strength of the material does not change. Such a tendency for the τ v. $\log\dot{\gamma}$ curves to flatten out does not in fact occur for the materials tested, so that the overstresses used are all relative to a stress which is already itself an overstress. The full effects of this are not clear though it does appear that the only effect it would have would be to move the whole of the $^{1}/_{6}$ v. overstress curves to the right, including the added incremental stress, thus allowing the previous arguments to stand. However, to be really certain about this it would be necessary to find the 'static' stress-strain curve and do the incremental loading from this state. If a static curve exists, it would probably be obtained at such a low strain-rate however, as to be virtually a creep test and the full plasticity of the specimen would then be in some doubt.

The third possibility concerning the inconsistency between the theoretical and practical increment magnitudes is related to the loading bar-specimen interface. In calculating the stresses present in the specimen and also the magnitude of the transmitted increment, elastic conditions were assumed at the interfaces. This was justified by the fact that the initial wave travelled at the elastic wave speed thus suggesting that the elastic modulus could be used in calculating the magnitude of the transmitted and reflected waves. If it were only the initial portion of the wave which was governed by such conditions, the gradient of the stress-strain path by the time the peak load were reached would be much smaller. This in turn would lead to a smaller transmitted stress pulse in the output bar. In fact work by Fillon (9) did show that there was some reflection of stress waves from an elastic-plastic interface in a single

material so that there would be some error in these tests in assuming elastic behaviour.

Finally, connected with the last suggestion, there is the question of interaction of waves. The first part of the pulse arrives at the change of section about 30 μsecs. before the peak stress. Since part is reflected, the oncoming peak meets the reflected wave before reaching the section change. It is known that any non-elastic stress waves in materials interact with each other so that, it if were wrong to assume elastic conditions until the peak stress had passed, the peak stress may have been subjected to some unloading before reaching the transmitter bar.

To summarize, it has been shown that the Malvern formulation of a strain-rate-dependent wave propagation theory fits the experimental results extremely well for the wave propagation speed and qualitatively for the magnitude of the transmitted increment for mild steel, and commercially pure aluminium and copper. The quantitative discrepancy is though to be due to the rise time of the stress pulse causing two major effects, an additional theoretical relaxation of the pulse and a change from elastic conditions at the specimen joints by the time the peak load arrives. The fact that a 'static' stress-strain curve was not used is not thought to have a very large effect on the results.

PART II

The Blanking Process.

Since, as far as is known, this was the first time that the load had been measured as a function of displacement

at high punch velocity throughout the punching process, it was also the first time it was possible to measure directly the actual energy taken to work the specimen, rather than the total energy supplied by the source. The former is a far more important quantity, since it demonstrates whether, ideally, energy is gained or lost by increasing the speed of the process. Previously, when the energy absorbed by the process was measured, the actual method of punching the material had a great influence on the trend of energy required. However, energy or work is not the only factor which is of industrial importance. Also required is information about the quality of components punched from different materials, and whether extra machining would be necessary when a higher speed of punching was used.

Beginning with the energy question, however, there are two opposing factors to consider in the variation of work done with the punch speed. In all the materials tested the load required to yield the specimen, and the maximum load, increased with punch velocity though by vastly different amounts. Similarly, the punch velocity had an effect on the punch penetration to cause rupture, an increase in velocity reducing the displacement in the majority of cases. These two effects have opposite effects on the energy required to punch through the material and a decision on the net effects can only be made by considering both.

Account is taken of these effects if the energy is measured by integrating the load-displacement curves of the materials. For mild steel it was found that there was a slight reduction in the energy needed to punch the material as the punch speed was increased. The reduction was 20% from

the lowest to the highest punch velocities but due to the ill defined point of rupture in mild steel this can not be said to be significant. This disagrees with the findings of Johnson and Slater (61) who found that dynamic blanking of mild steel required significantly more energy than quasi-static blanking.

On the other hand aluminium with a high sensitivity of the load and a low sensitivity of punch penetration with punch velocity could be seen to have an increasingly large area under the load-displacement curve as the punch speed increased. This was indeed the case and the energy required to punch aluminium with a punch velocity of 770 in./sec was 40% greater than that required at a punch velocity of 5×10^{-5} in./sec. This result supported the findings of Johnson and Slater (61) qualitatively but for equivalent punch speeds showed a much smaller excess energy in the dynamic process over the quasi-static process.

The same workers, and also Johnson and Travis (62), at higher punch speeds, found that copper, too, needed considerably more energy for dynamic blanking than it did for the quasi-static process. On integration of the load-displacement curves obtained in the present work it was found that there was, if anything, a slight increase of energy with increased punch speed though it certainly could not be called considerable. There was a 10% difference in the energies of the highest and lowest speeds, and since the breaking point of the copper was well defined this is thought to be significant.

In the soft brass there was no significant difference in the energy required for different punch speeds, but due to the decrease in ductility of the hard brass with strain rate, the fastest test needed only half as much energy as the other ones.

This trend was in direct contradiction to the findings of Davies and Shaw (7) in the only other known work on the blanking of a brittle material. They found that cast iron specimens, when subjected to a faster punch speed, showed increased ductility.

This result was even more decisive in the 4130 steel since this material hardly increased in strength at the highest speed yet the punch penetration was reduced to less than a third of the quasi-static value. This led to the energy required for punching of the material to be reduced to approximately a third of the quasi-static value.

Thus it would appear in general that only when using brittle materials will an increase in punch speed allow a saving of energy in the punching process, though, contrary to the observations of their observers, such an increase in operation speed results in a considerable wastage of energy only in the case of aluminium.

Still associated with the question of energy, it is interesting to compare the relative punch penetrations to fracture of the six materials used in this study, as functions of strain rate, (Fig. (11.12). From this figure it can be seen that as with the stresses borne by the material, the greatest change in punch penetration occurs at strain rates of above 10^3sec.$^{-1}$ and it seems that at a strain-rate of about 10^5sec.$^{-1}$ the necessary penetration to cause fracture for some materials would be effectively zero.

To give a clearer picture of the strain-rate sensitivity of the brasses and 4130 steel, the variation of yield stress and ultimate stress with approximate strain rate is shown in Fig.(11.13). The strain rate is only approximate due to the

inability of microhardness readings to give bounds on the gauge length. However, since a logarithmic scale is used such approximation leads to very small errors. The strain-rate sensitivities of the three other materials have been discussed earlier in this Chapter. It can be seen that the same type of sensitivity is present in all the materials, a region at strain rates less than 10^{2} sec.$^{-1}$ where there is little effect on the stresses, changing to a region around a strain-rate of 10^{4} sec.$^{-1}$ where the sensitivity is considerably larger.

All these strain-rate sensitivity curves, as well as the punch penetration curves seem to suggest that there is a maximum possible strain-rate which can be applied to metals, a strain-rate between 10^{4} and 10^{5} sec.$^{-1}$. Such a suggestion was made by Hauser, Simmons and Dorn (18) who gave a value of 9.15×10^{5} sec.$^{-1}$ on theoretical grounds and an order of magnitude less from an extrapolation of practical results. These results were for compression strain-rates though here again, a conversion from one to the other would make little difference to the results because of the logarithmic scale of the strain-rate.

Turning now to the reduction of the size of the shear zone with increased punch velocity which was observed in all cases except the tool steel, this trend was in agreement with the findings of Tener and Holloman (73) and Davies and Dhawan (83). If one compares the quasi-static shear stress - shear strain curves of mild steel, copper and aluminium (the only three whose shear zones can be mutually compared, because of the different specimen thicknesses of the other materials) one finds that the copper and mild steel have higher work hardening rates than aluminium. Consequently at quasi-static punch speeds the former

two materials would favour a spreading of the shear zone rather than a continuation of the straining of the already deformed region, aluminium would have less of a tendency and one would expect a smaller shear zone in this material. Such was the case and in the same way the reduction of the zone width with punch speed can be attributed to the lessening of the degree of work hardening with an increase of strain rate. This fall of the degree of work hardening is greater in mild steel than copper but is not apparent in aluminium. One would expect, therefore, that the zone width of steel would have a bigger change than that of copper and that the shear zone of aluminium would not change at all. The degrees of change in the three materials were certainly in the right order though aluminium did show a reduction in the zone width at the highest punch speed. Even though stress-strain curves were not obtained for the other three materials such an explanation of the change in size of the shear zone can be expected to apply to them.

The shapes of the microhardness traverses shown in Chapter 10 can be explained in a similar way. For a material with a bilinear stress-strain curve, the post-yield behaviour being perfectly plastic, a microhardness traverse curve would be the same shape as that of one for pure shear in other materials, i.e. a square pulse. The higher the degree of strain hardening the more rounded and peaky would be the curve for this type of deformation. The copper and mild steel traverses definitely had higher peaks than the aluminium ones, agreeing with this suggestion, but the change from undeformed to deformed material was the most pronounced in the case of copper.

It remains to discuss the quality of the blanks produced. It seems impossible to generalise on this subject

and each material has to be taken on its own merits. Also for this particular aspect it is necessary to consider whether the process is blanking or punching (see Chapter 7) before drawing any conclusions about the effect of speeding up the process. Considering mild steel first of all, it was found that increasing the punch speed gave a smoother surface to both blank and hole. There was no other noticeable outward difference between the specimens tested at the different speeds. The thinner material produced rougher blank surfaces at all loading rates than the equivalent thick material, and this can be accounted for by the increased percentage radial clearance, a trend agreeing with the work of Johnson and Slater (81).

Turning to copper, the reduction in punch penetration to fracture with the higher punch speed meant that a larger proportion of the edge of the blank was a fracture surface, thus giving a rougher appearance. The fact that the punch passed through the specimen material polished the fracture surface of the hole somewhat so that there was little difference in its appearance at the various speeds. However, since there was neither an appreciable decrease in the energy requirement for the higher speed process, nor an improvement in the quality of the blank or remainder with regard to dishing, doming or tapering, it seems that the speed of the process can be chosen quite arbitrarily to suit the remainder of the manufacturing process.

With aluminium it seems that to run a punching or blanking machine at a high speed would be a distinct disadvantage. Not only would more energy be required to deform the material but the quality of a punched hole would suffer, its sides becoming appreciably concave.

The use of the same brass in two different conditions served to illustrate how best the blanking process could be employed. Before venturing further it should be stated that the gross distortion of the blanked material in the impact testing machine could easily be eliminated by holding the specimen against the die as in the lower speed assembly. In the present arrangement such a clamping would have upset the stress waves and hence the interpretation of the results, a problem which would not be of any importance industrially.

The as-received brass showed the sort of blanks that could be produced using the right material; there was hardly any distortion, suggesting that very little extra machining would be necessary. The annealed brass on the other hand showed appreciable tapering and doming and these were respectively increased and reduced by a higher punch speed. Regarding the relative energies needed for the two materials, the energy required to punch the as-received brass was drastically reduced at the highest punch speed yet at all punch speeds the more brittle material used up less energy than the annealed brass.

This demonstration of the advantage of using brittle materials in the punching process was further underlined by the use of high-tensile steel. Here almost perfect blanks were produced at all velocities, polishing of the fracture surface seeming to be the only possible way of improvement. The advantage of the high speed process was the smaller quantity of energy absorbed.

Although the full potential of increasing the speed of the punching process is realised with brittle materials, the shape of the strain-rate sensitivity curves suggests that there

might be an optimum speed of the process. Above this level it is probable that the steeply increasing stresses would more than counteract the decreasing punch penetration and so increase the necessary energy. It may also be wondered whether an increase of speed of the process is desirable in any case since the increase in quality of the product is only marginal and in ductile materials the quality is often reduced. In considering this question the fact must be remembered that though some energy might be saved in the actual deformation of the material, energy might be wasted in the system by increasing the punch speed; for one thing it is difficult to conceive of a way of conserving the kinetic energy of the punch after it has punched the material.

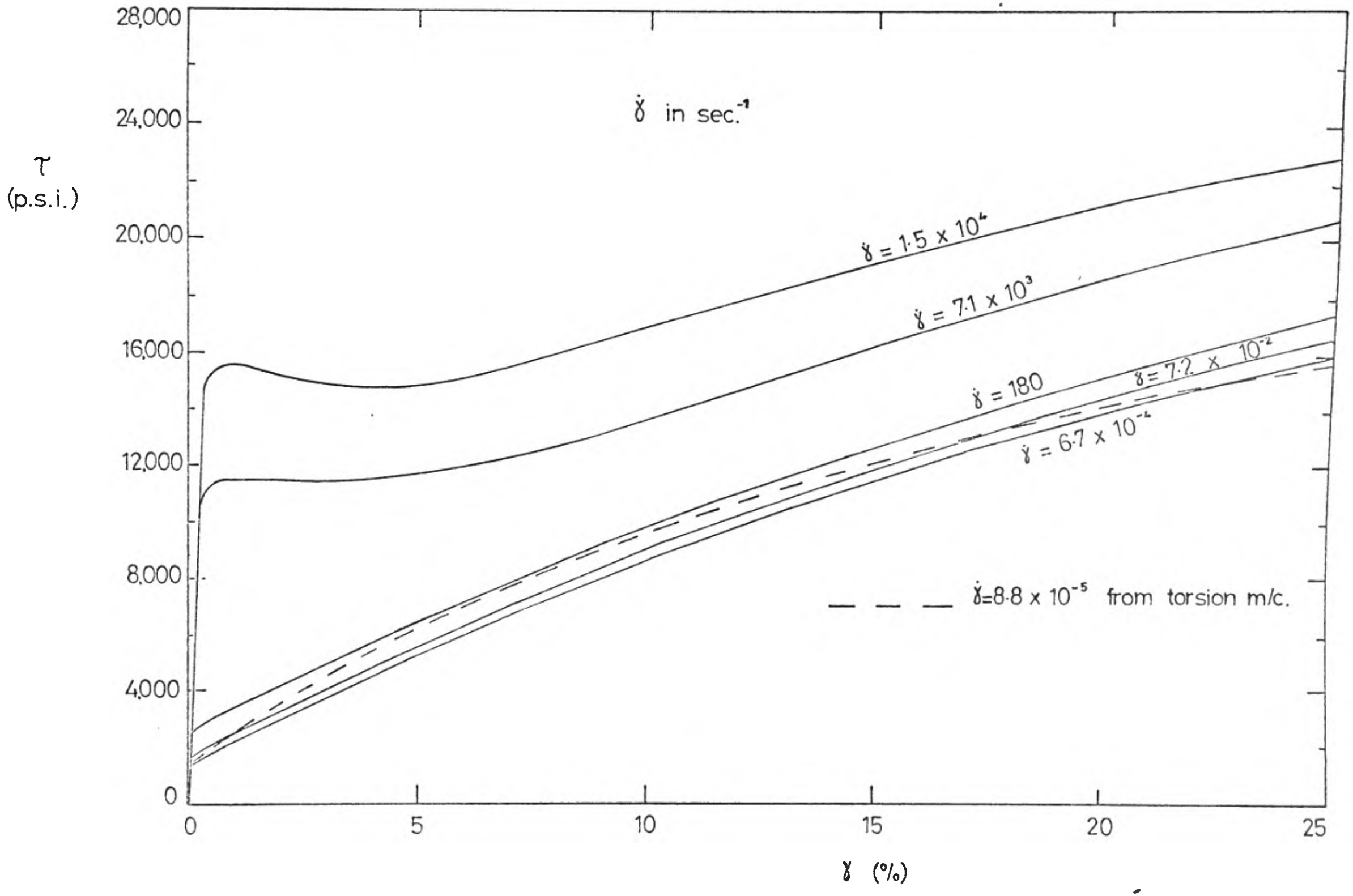


FIG. 11.1 Shear stress - shear strain curves for copper from punch tests.

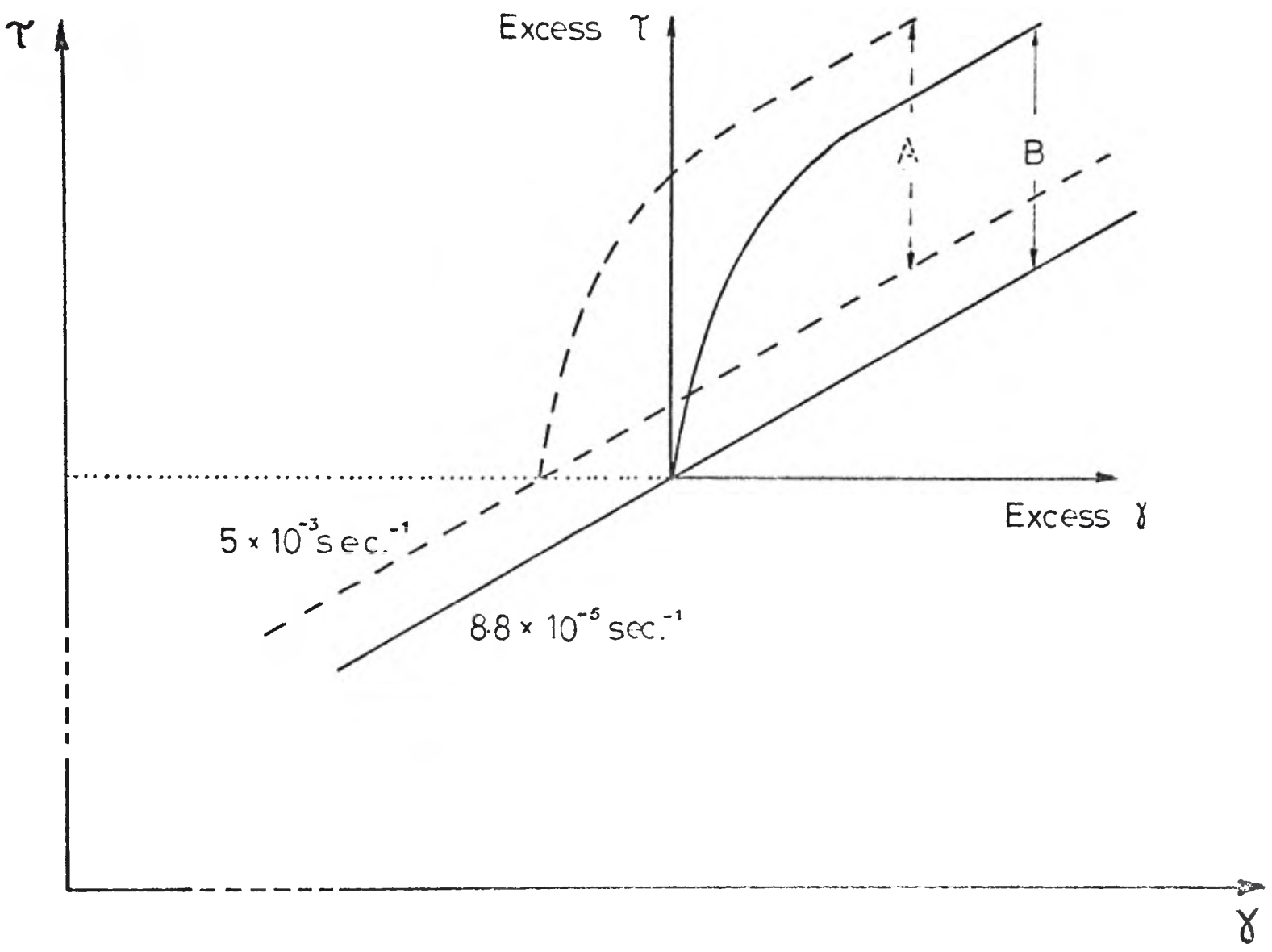


FIG. 11.2 Concerning the lower strain-rate stress-strain curve of the strain-rate change tests.

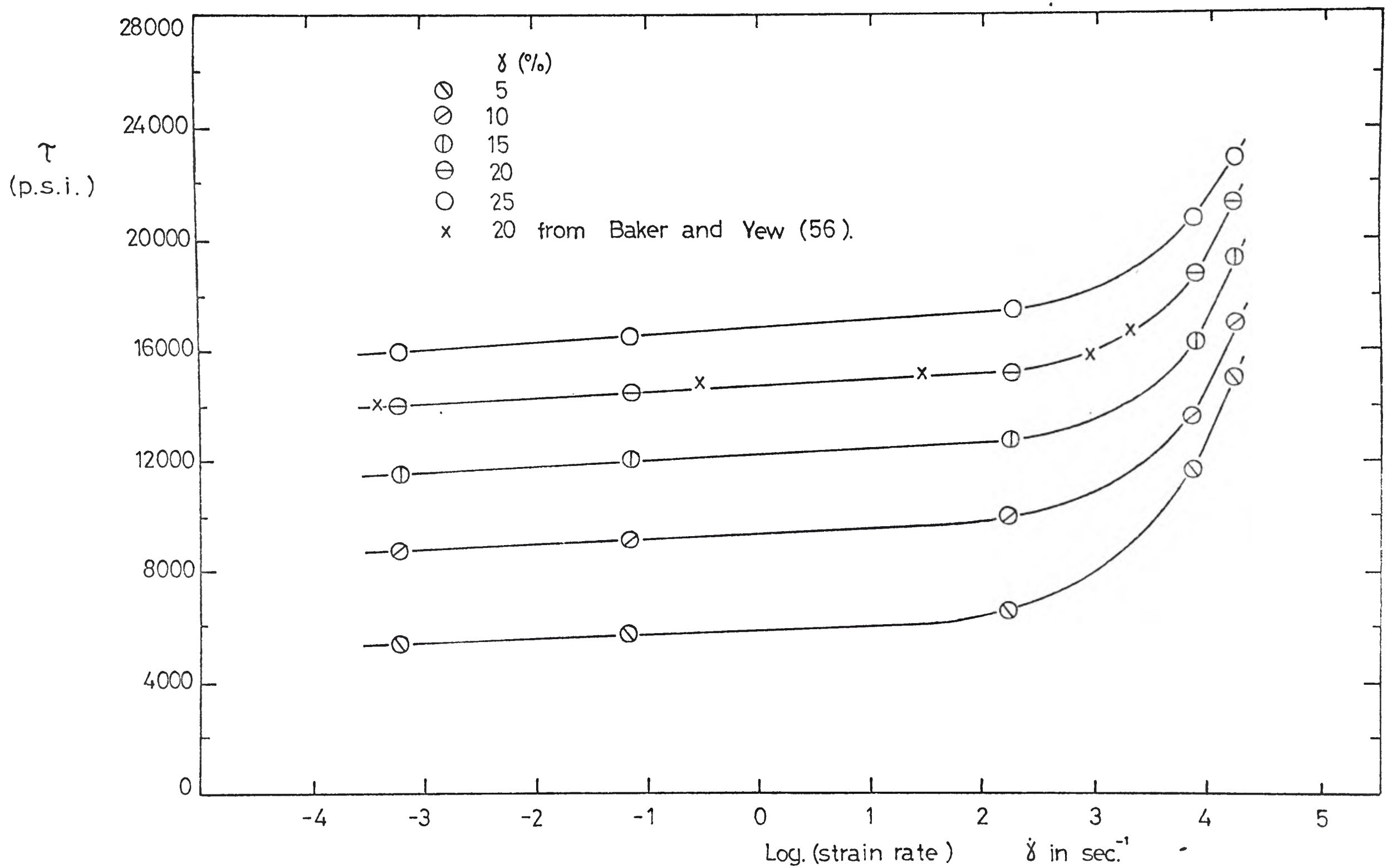


FIG. 11.3 Strain-rate sensitivity of copper.

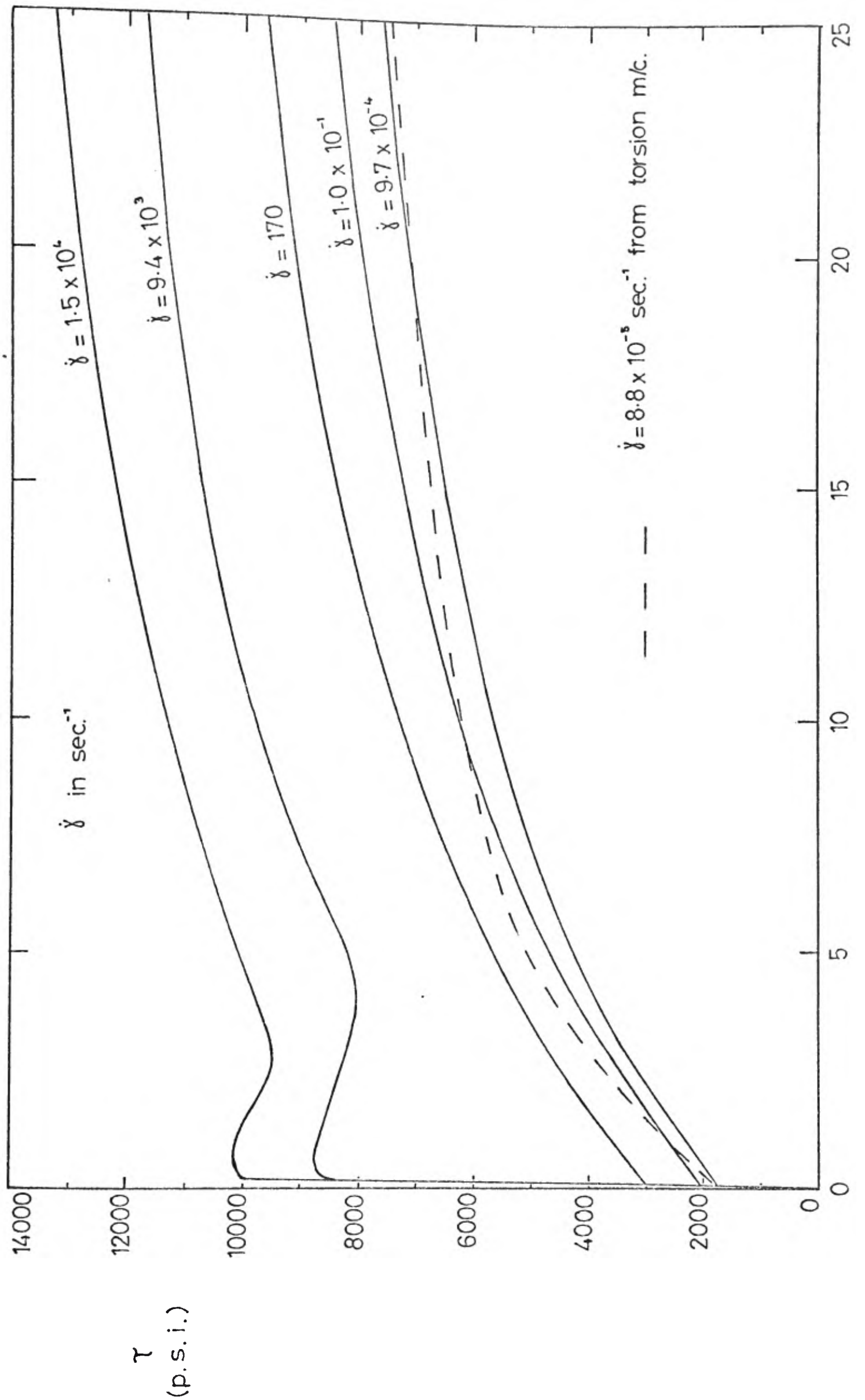
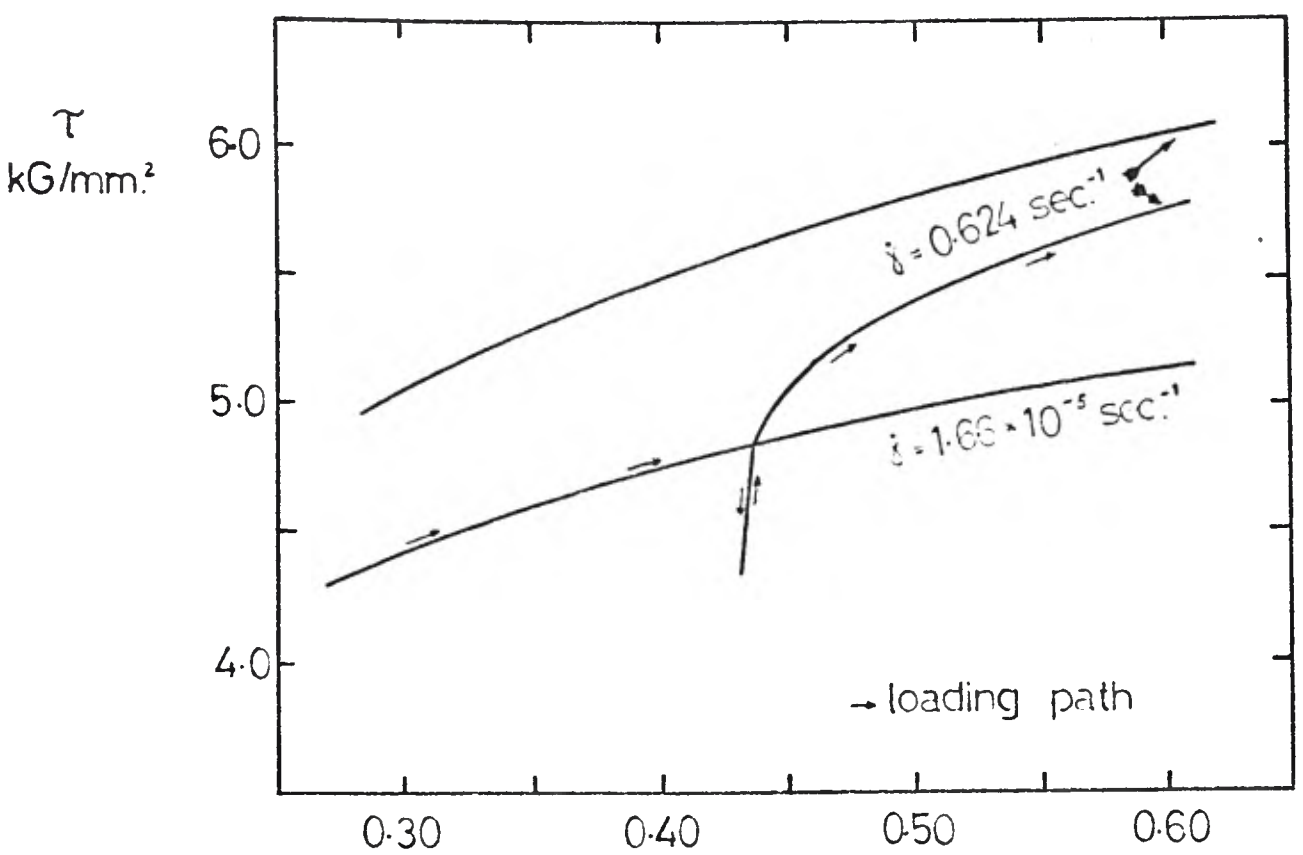


FIG. 11.4 Shear stress - shear strain curves for aluminium from punch tests.



from Klepaczko (97)

FIG. 11.5 The results of a strain-rate change test on aluminium.

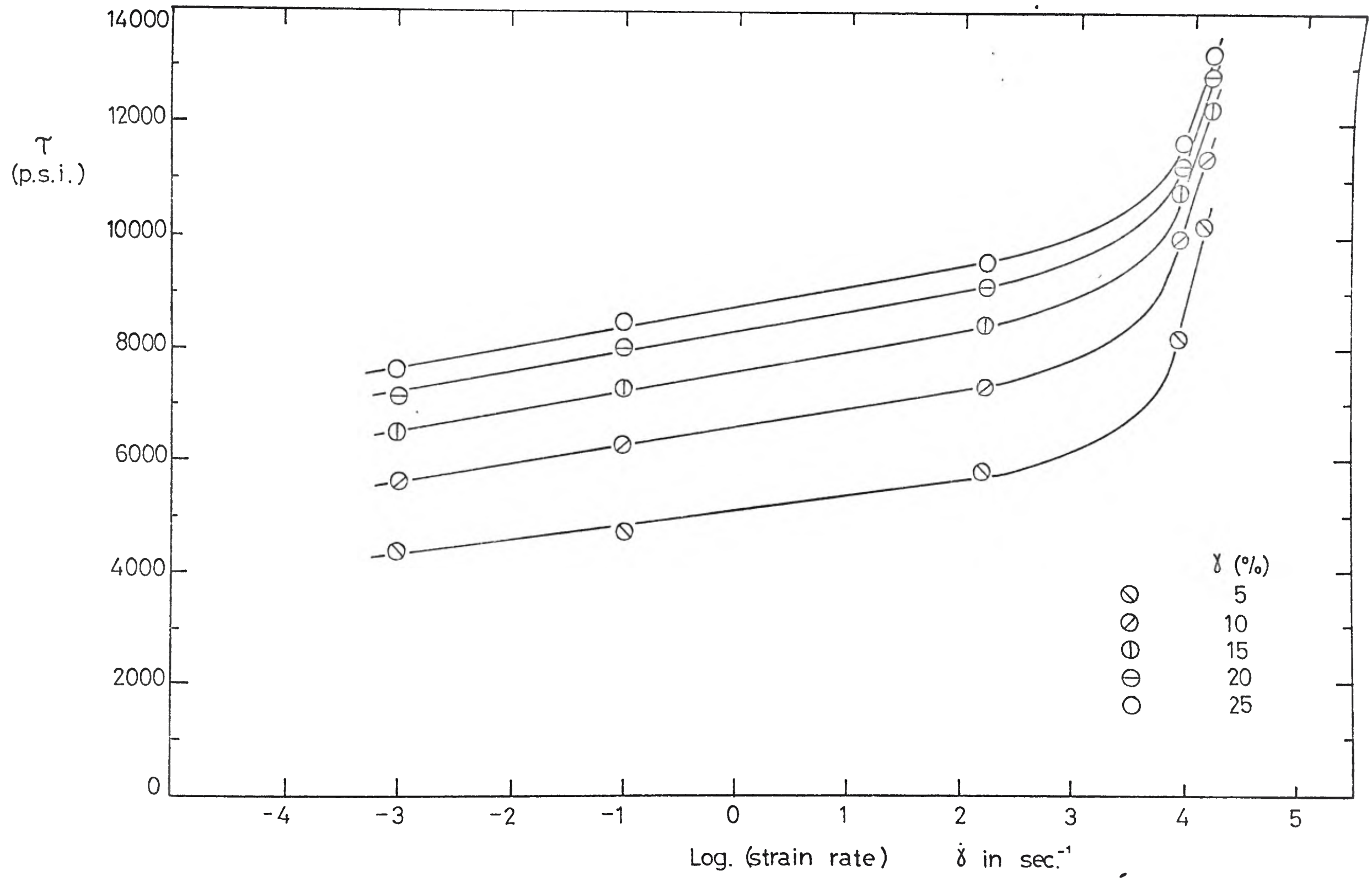


FIG. 11.6 Strain-rate sensitivity of aluminium.

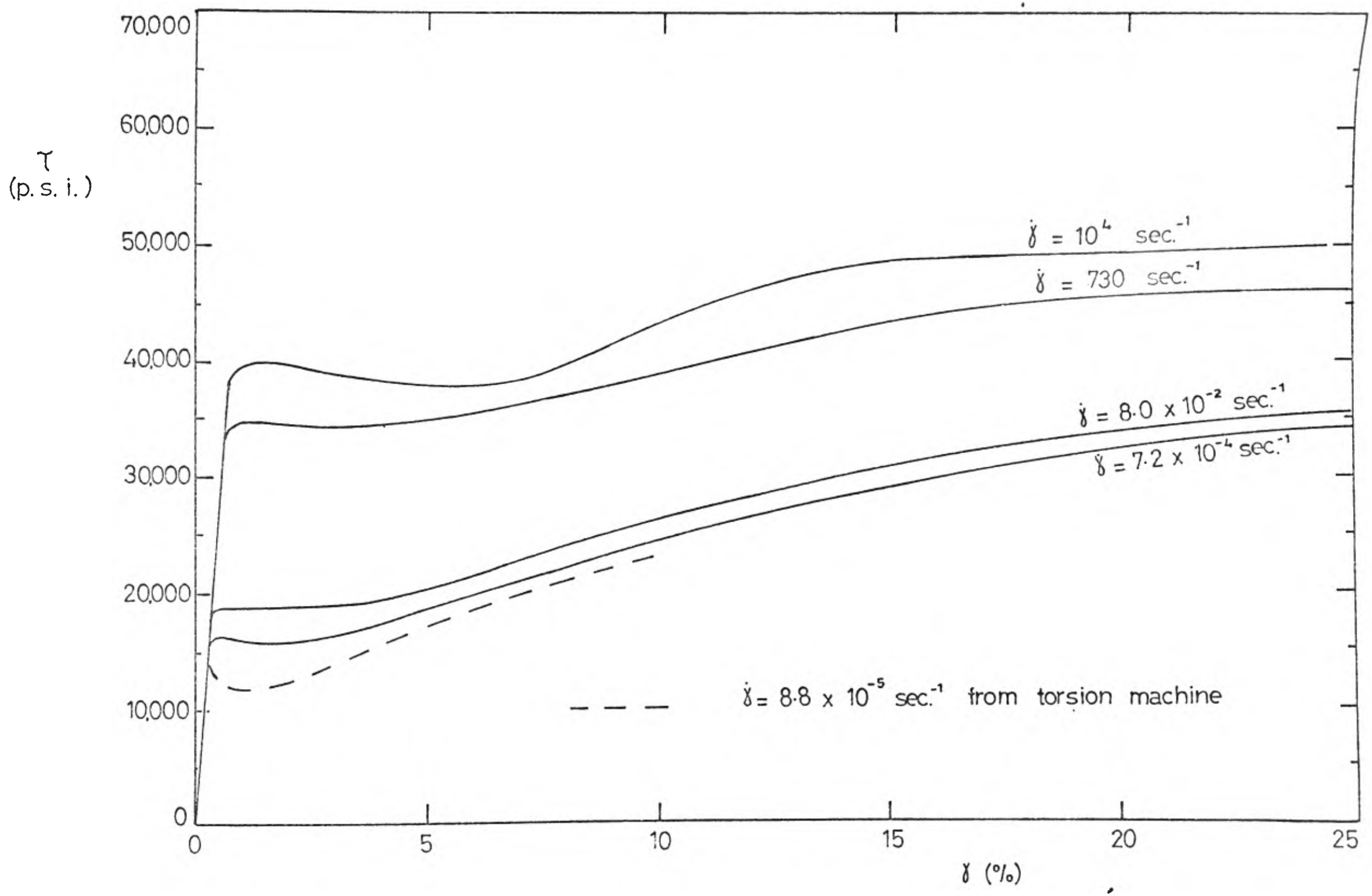


FIG. 11.7 Shear stress - shear strain curves for mild steel from punch tests.

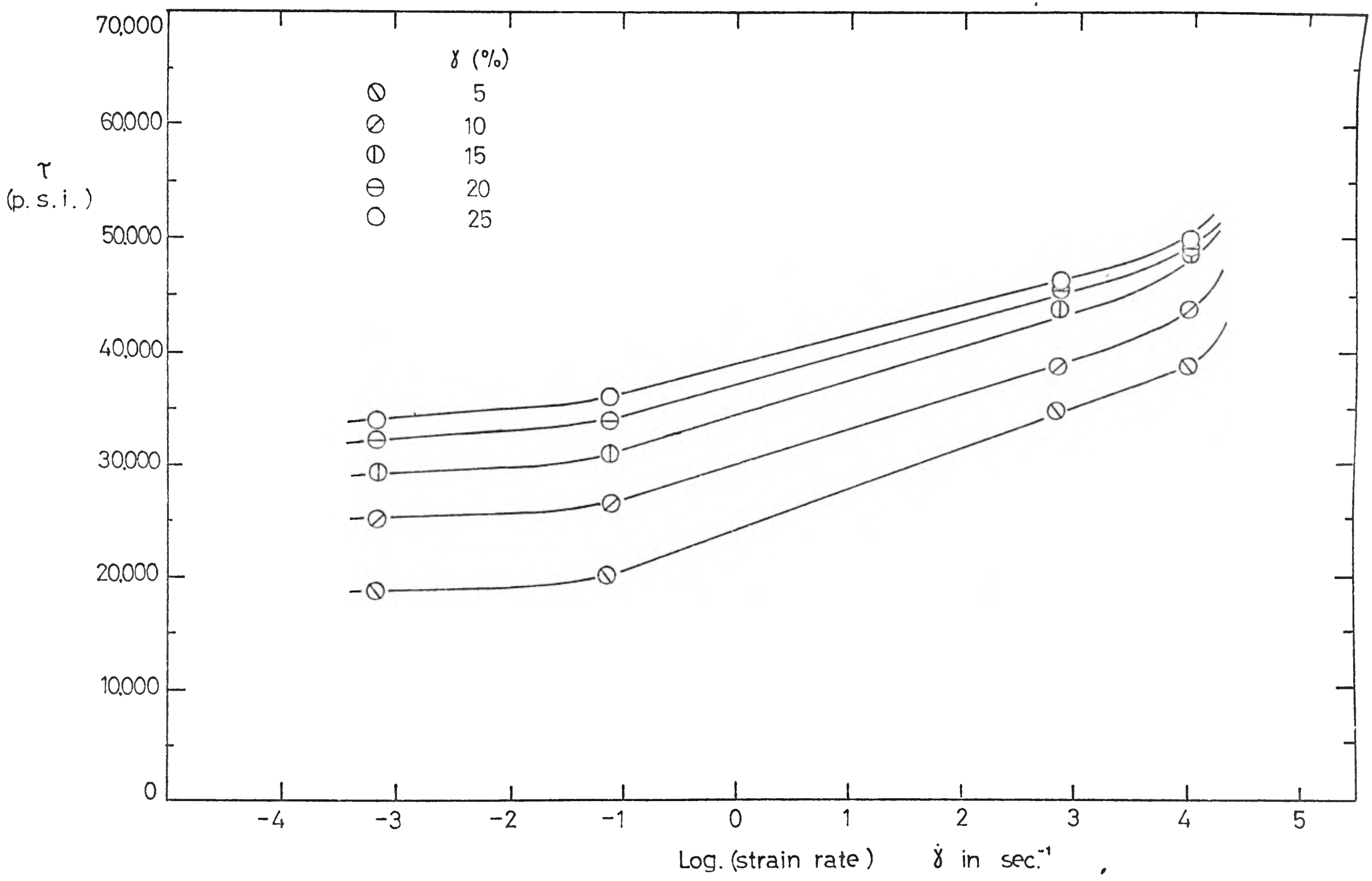


FIG. 11.8 Strain - rate sensitivity of mild steel.

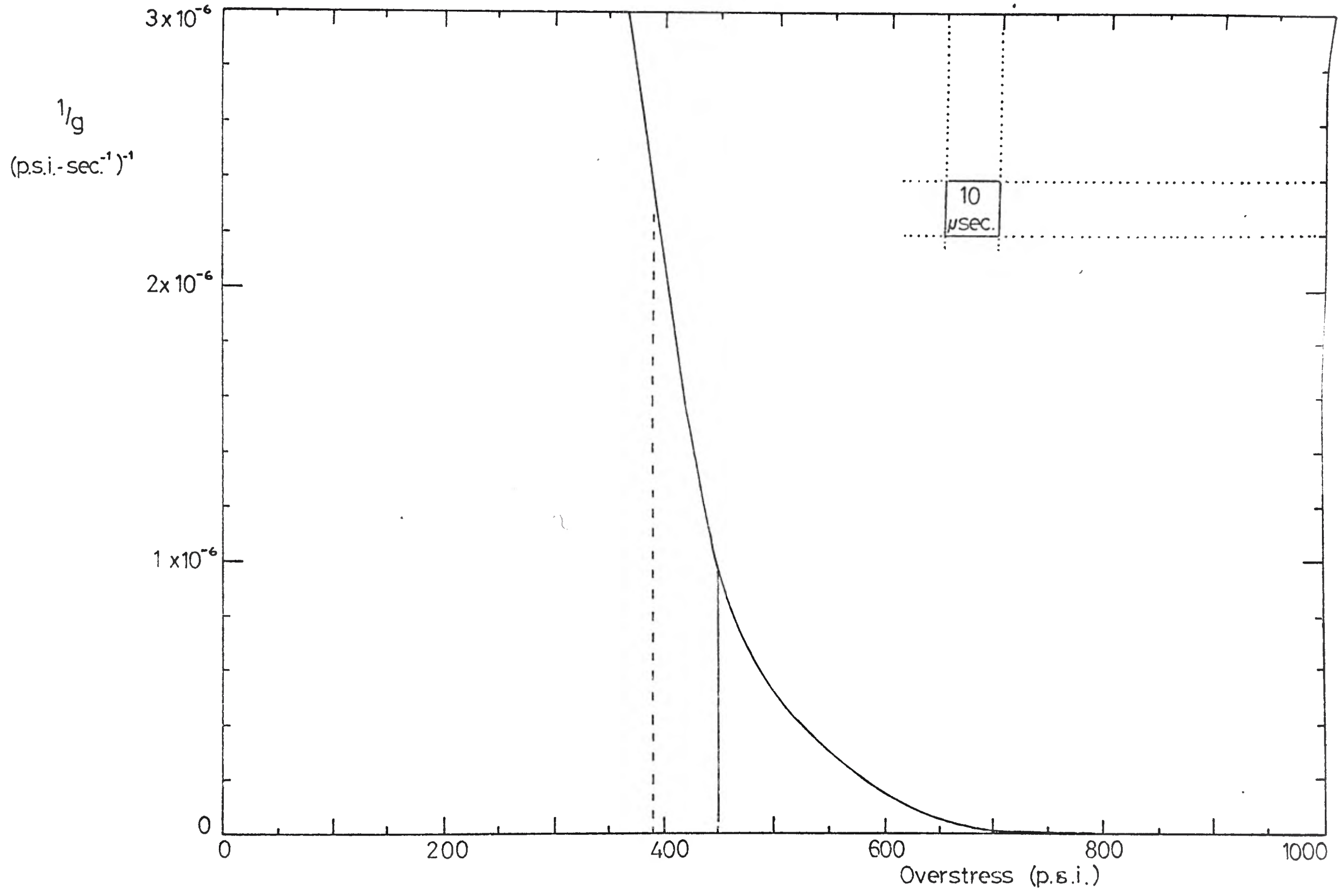


FIG. 11.9 Graph of reciprocal 'g' function against overstress for copper.

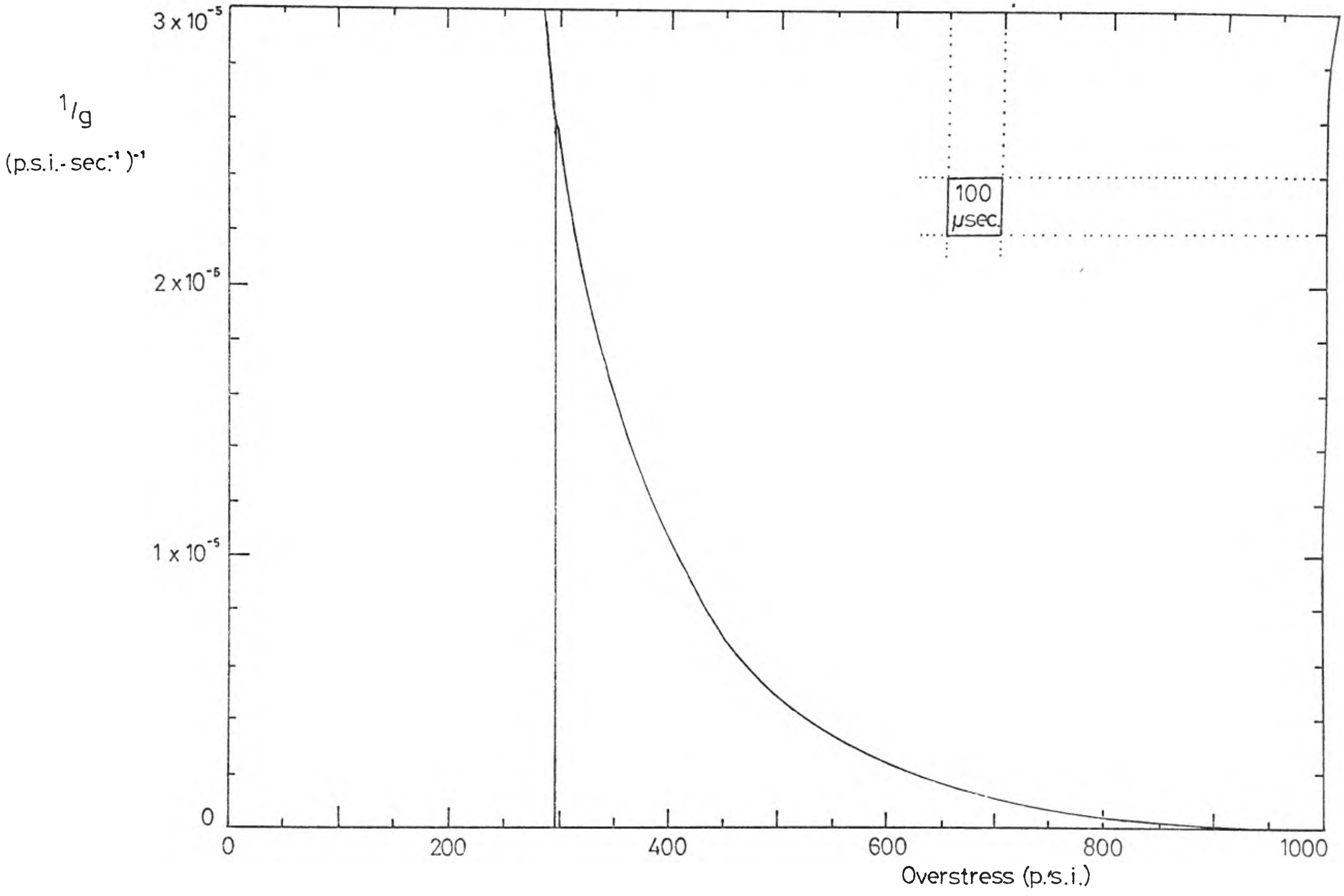


FIG. 11.10 Graph of reciprocal 'g' function against overstress for aluminium.

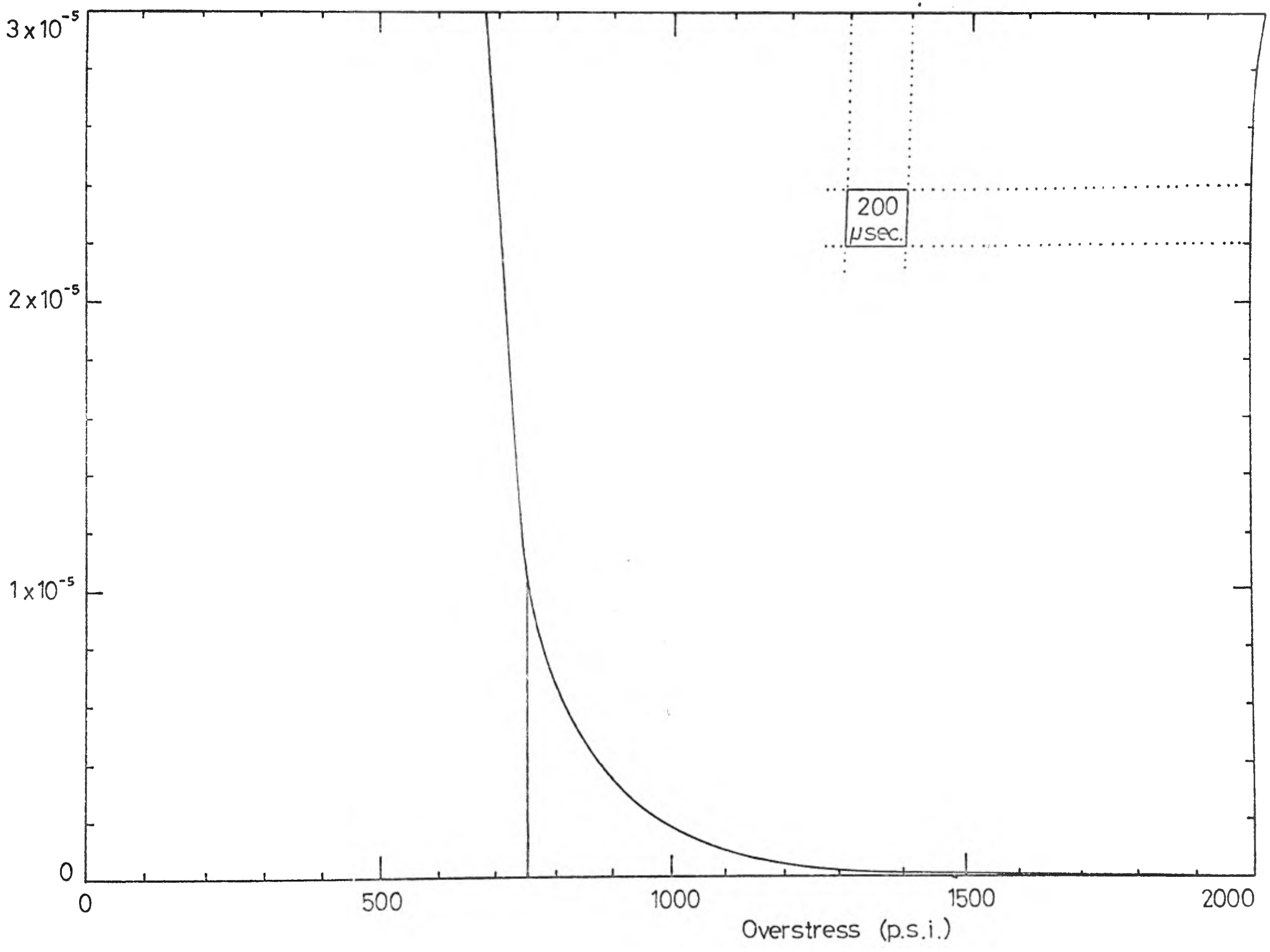


FIG. 11.11 Graph of reciprocal 'g' function against overstress for mild steel.

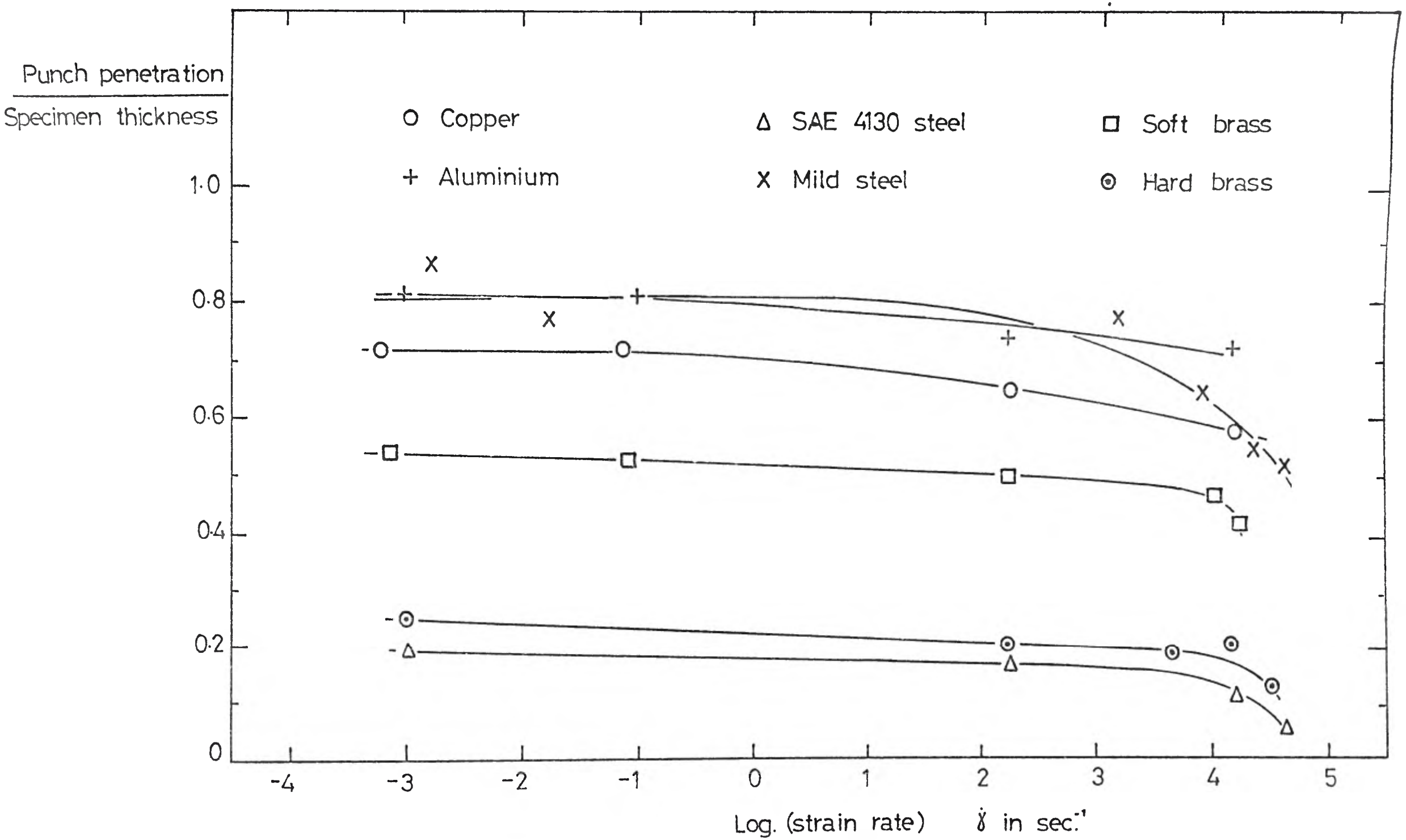


FIG. 11.12 Variation of punch penetration with strain rate.

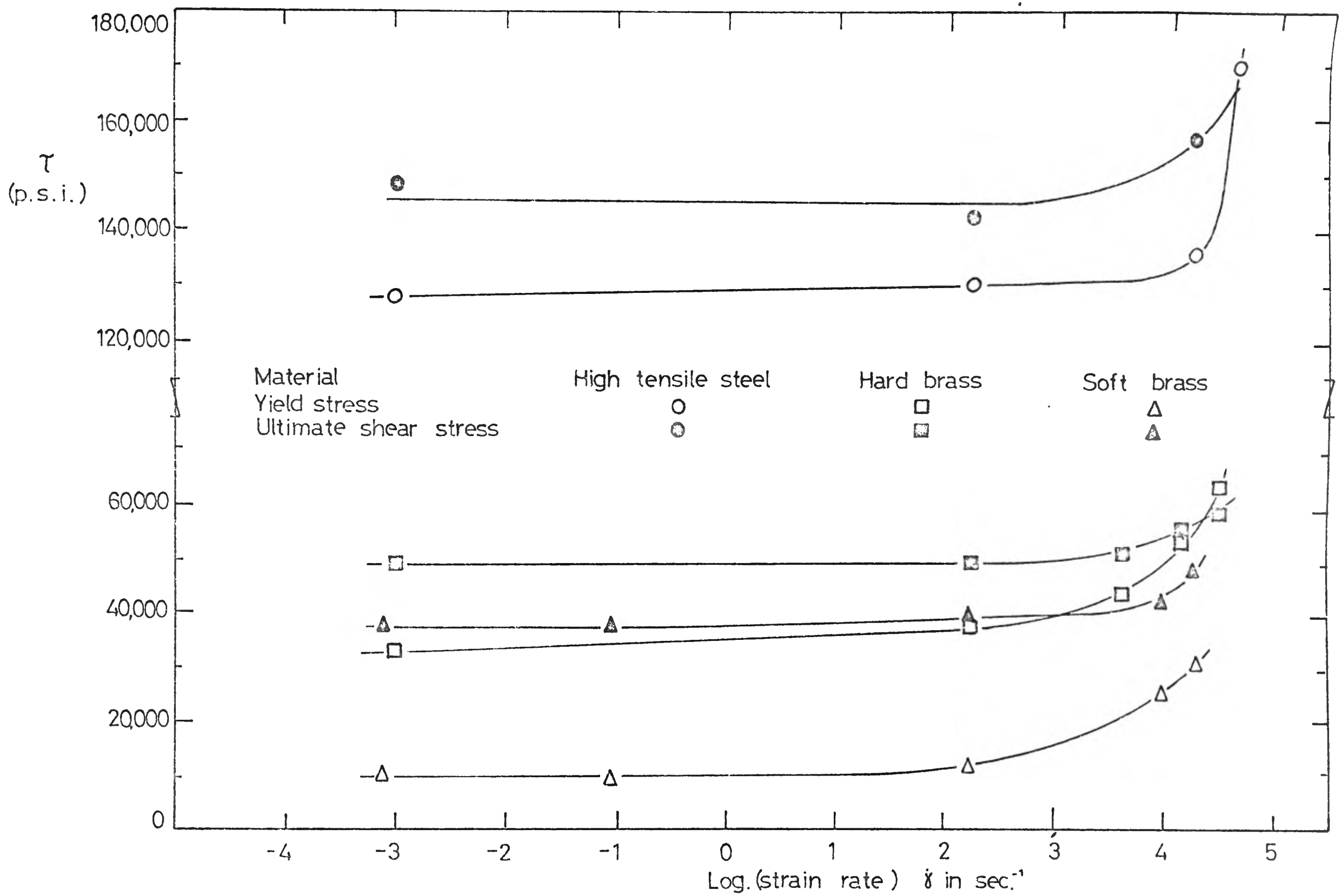


FIG. 11.13 Strain-rate sensitivities of hard and soft brass and high tensile steel.

CHAPTER 12.

CONCLUSIONS.

Using a newly developed apparatus, it has been shown that the speed of propagation of small torsional stress increments in a material already strained plastically in torsion, is equal to the torsional elastic wave speed in the material. This is in accordance with Malvern's formulation of a strain-rate-dependent wave propagation theory and contradicts the predictions of the strain-rate-independent theory. In addition the Malvern theory is qualitatively correct in predicting the sizes of the transmitted increments in the three materials used, the rise time of the increment, small though it was, accounting for the quantitative discrepancies. Since it is successful in connection with the propagation of stress increments, it is concluded that a strain-rate-dependent theory of the Malvern type is necessary for describing thepropagation of large stress waves in mild steel, aluminium and copper.

It is also concluded that the complex stress distribution of the blanking process can be simplified into one of pure shear and that this process then provides a simple method of obtaining the strain-rate-sensitivities of materials in shear. This practice is helped by the fact that for most materials a large change of strain-rate is required to produce a noticeable change in material properties. Thus quite large approximations in the derivation of strain rates make very little difference to

the apparent strain-rate-sensitivities.

In this way stress-strain curves for mild steel, copper and aluminium were obtained at a wide range of strain rates, from 5×10^{-4} sec.$^{-1}$ to 2×10^{4} sec.$^{-1}$. The same general strain-rate sensitivity was found, a small rise of stress with strain-rate at strain-rates below 10^{-2} sec.$^{-1}$ changing to an extremely large dependence of stress on rate of strain at strain rates above 10^{4} sec.$^{-1}$. This change was more abrupt in copper and aluminium than in the mild steel, a marked increase in the strain-rate rate sensitivity in the first two materials not occurring until strain rates of over 100 sec.$^{-1}$, in mild steel the change beginning at a strain-rate of 10^{-2} sec.$^{-1}$.

The strengths of the three materials at 5% strain increased by 100% between strain-rates of 10^{-3} sec.$^{-1}$ and 10^{4} sec.$^{-1}$ though at strain rates below 100 sec.$^{-1}$ the mild steel was definitely the most strain-rate sensitive and copper the least. The work hardening rate of mild steel reduced considerably as the strain-rate increased, that of copper reduced a little while aluminium had the same work hardening rate throughout the range of strain-rates.

General conclusions regarding the blanking process are that an increase of punch velocity increases the loads under which deformation takes place and leads to a reduction in the punch penetration required to cause rupture. These two effects have opposing influences on the energy needed to cause complete punching with the result that a change of punch velocity has little effect on the energy required for the process except in the case of brittle materials.

Using brittle materials a great reduction of energy is

achieved by increasing the speed of the process. With hard brass the energy was halved by increasing the punch speed from 10^{-4} in./sec. to 450 in./sec. whilst using SAE 4130 steel a similar increase of punch speed cut the energy requirement to a third of its original value. Comparative energy changes in the ductile materials were an increase by 40% for aluminium and a 10% reduction in copper, the changes being insignificant in soft brass and mild steel.

It is from the brittle materials, also, that the best quality blanks are produced, suffering little or none of the doming, tapering and other distortions of the more ductile materials.

REFERENCES.

1. Ludwik, P. — Physikalische Zeitschrift, 10 1909

2. Kolsky, H. — Stress Waves in Solids, Clarendon Press, Oxford 1953

3. Taylor, . I. — The Scientific Papers of G. I. Taylor, Vol: 1, Mechanics of Solids. Cambridge University Press, pp.456, 467 1957.

4. von Karman, T. — N.D.R.C. Report, A.29. 1942.

5. Bakhmatulin, K. A. — Prikl. Mat. Mekh. 9, 1945.

6. Malvern, L. E. — J. Appl. Mech. 18 1951.

7. Davies, R. and Bhawan, S. N. — Proc. 7th Int. M.T.D.R. Conf., Birmingham 1966.

8. Donnell, L. H. — Trans. A.S.M.E. 52 1930.

9. Duwez, P. and Clark, D. S. — Proc. A.S.T.M. 47 1947.

10. von Karman, T. and Duwez, P. — J. Appl. Phys. 21 1950.

11. Malvern, L.E. — Quart. Appl. Math. 8 1950.

12. Campbell, J. D. Simmons, J. A. and Dorn, J. E. — J. Appl. Mech. 28 1961.

13. Bell, J. F. — Tech. Report No. 5. Johns Hopkins University, 1951.

14. Sternglass, E. J. and Stuart, D. A. — J. Appl. Mech. 20 1953.

15. Riparbelli, C. — Proc. Soc. Exp't'l. Stress Anal. 14 1956.

16. Alter, . E. E. and Curtis, C. W. — J. Appl. Phys. 27 1956.

17. Lee, E. H. — Deformation and Flow of Solids Colloquim, Madrid, Proceedings 1955.

18. Hauser, F. E. Simmons, J. A. and Dorn, J. E. — Response of Metals to High Velocity Deformation. Conf. of Met. Soc. Estes Park, Colorado, 1960. (Interscience Publications).

19. Karnes, C. F. — Struct. Mech. Research Lab. University of Texas 1963.

20. Bell, J. F. — J. Appl. Phys. 31 1960. (i)

21. Kolsky, H. and Douch, L. S. — J. Mech. and Phys. Solids 10 1962.

22. Clark, D. S. and Wood, D. S. — Proc. A.S.T.M. 49 1949.

23. Campbell, J. D. and Duby, J. — Proc. Roy. Soc. A236 1956.

24. Hoppmann, II., W. H. — Proc. A.S.T.M. 47 1947.

25. Bell, J. F. — J. Appl. Phys. 27 1956.

26. Bell, J. F. — Proc. 3rd. U.S. Nat. Congr. Appl. Mech. 1958.

27. Bell, J. F. — Proc. Soc. Exp't'l. Stress Anal. 17 1959.

28. Bell, J. F. — Experimental Mechanics, 2 1962.

29. Bell, J. F. and Werner, W. H. — J. Appl. Phys. 33 1962.

30. Sperrazza, J. — Proc. 4th U.S. Nat. Congr. Appl. Mech. 1962.

31. Campbell, W. E. — Proc. Soc. Exp't'l. Stress Anal. 10 1952.

32. White, M. L. and Griffis, Le Van — Trans. A.S.M.E. 70 1948.

33. Bell, J. F. and Stein, A. — Journal de Mécanique 1 1962.

34. Dillon, Jr., O. W. — J. Mech. and Phys. Solids 11 1963.

35. Hannon, W. and Wheeler, M. J. — J. Inst. Met. 45 1931.

36. Bell, J. F. — J. Appl. Phys. 31 1960 (ii)

37. Malvern, L. E. — Behaviour of Materials Under Dynamic Loading. A.S.M.E. 1965.

38. de Vault, J. P. — J. Mech. and Phys. Solids 13 1965.

39. Mindlin, R. D. and Herrman, G. — Proc. 1st U.S. Nat. Congr. Appl. Mech. 1951.

40. Pihlowitz, J. — J. Appl. Mech. 24 1957.

41. Grimm, C. — Thesis, Lehigh University, 1964.

42. Plass, Jr., H. J. and Ripperger, E. A. — Plasticity. Edited by Lee, E. H. and Symonds, P. S. Pergamon Press, Oxford. 1960.

43. Ripperger, E. A. and Karnes, C. H. — Symp. on Dyn. Behaviour of Materials. A.S.T.M. Tech. Pub. 1963.

44. Bianchi, G. — Proc. Int. Symp. on Stress Waves in Anel. Solids. Brown Univ. Providence, R. I. 1963.

45. Lubliner, J. — J. Mech.and Phys. Solids 12 1964.

46. Cristescu, N. — Proc. Int. Symp. on Stress Waves in Anel. Solids. Brown Univ. Providence, R. I. 1963.

47. Efron, L. — Ph.D. thesis. Michigan State Univerait, 1964.

48. Bell, J. F. — Discussion on Ref.(42). Plasticity. Edited by Lee, E. H. and Symonds, P. S. Pergamon Press, Oxford. 1960.

49. Mercalo, E. J. — Thesis, Rensselaer Polytechnic Institute, 1963.

50. Wood, E. R. and Philips, A. — J. Mech. and Phys. Solids 15 1967.

51. Bodner, S. R. and Clifton, R. J. — J. Appl. Mech. 34 1967

52. Ripperger, E. A. and Watson, Jr., H. — Symp. Mech. Behaviour of Mat. under Dyn. Loads. San Antonio, Texas. 1967.

53. Craggs, J. W. — J. Mech. and Phys. Solids. 5 1957.

54. Craggs, J. W. — Progress in Solid Mechanics 2 1961.

55. Convery, E. and Pugh, H. Ll. D. — J. Mech. Eng. Sci. 10 1968.

56. Baker, W.E. and Yew, C. H. — J. Appl. Mech. 33 1967.

57. Yew, C. H. and Richardson, Jr., H. A. — University of Texas Report. 1967.

58. Habib, I. T. — J. Appl. Mech. 15 1948.

59. Hopkins, H. G. — Engineering Plasticity. Edited by Heyman, J. and Leckie, F. A. Cambridge University Press 1968.

60. Hunter, S. C. and Johnson, I. A. — Proc. Int. Symp. on Stress Waves in Anel. Solids. Brown Univ. Providence, R.I. 1963.

61. Cristescu, N. — Arch. Mech. Stos. 17 1965.

62. Lubliner, J. — Journal de Mécanique 4 1965.

63. Itihara, F. — Tech. Reports of the Tohuku Imp. Univ. 2, 11, 12. 1933-35.

64. Greene, C. J. and Stout, R. D. — Trans. A. S. M. 28 1940.

65. Work, C. E. and Dolan, T. J. — Univ. of Illinois Exp't'l Station Bull. 1950.

66. Calvert, H. L. — Proc. Inst. Mech. Eng. 169 1955.

67. Chang, S. S. — Thesis. Manchester Coll. of Sci. and Technology. 1960.

68. Rodierne, F. A. — J. Inst. Met. 21 1962.

69. Taylor, D. B. C. and Tudros, A. Z. — Proc. Inst. Mech. Eng. 170 1956.

70. Pepe, J. F. Vreeland, Jr., T and Wood, W. S. — Rev. Sci. Instruments 35 1964.

71. Hopkinson, B. — 'The Pressure of a Blow.' The Scientific Papers of Bertram Hopkinson. Cambridge University Press. 1921.

72. Fell, F. W. — Carnegie Schol. Memoirs. 16 1927.

73. Zener, C. and Hollomon, J. H. — J. Appl. Phys. 15 1944.

74. Zener, C. — Fracturing of Metals. A.S.M. New York. 1948.

75. Cockcroft, M. G. — N.P.L. Report No. 6 1961.

76. Chang, T. L. — J. Inst. Met. 78 1950.

77. Tilsley, L. and Howard, F. — Conf. on Technology of Eng. Manuf. Inst. Mech. Eng. London. 1950.

78. Noble, C.F. and Oxley, P. L. B. — Int. J. Prod. Res. 1964.

79. — Blanking and Piercing. A metallographic study of the mechanisms of constrained shear. P.E.R.A. Report 93 1961.

80. Johnson, W. and Slater, R. A. C. — Proc. Inst. Mech. Eng. 179 1964-5.

81. Johnson, W. and Slater, R. A. C. — Proc. Inst. Mech. Eng. 180 1966.

82. Johnson, W. and Travis, F. W. — Proc. Inst. Mech. Eng. 180 1966.

83. Davies, R. and Dhawan, S. M. — Proc. Inst. Mech. Eng. 180 1966.

84. Dowling, A. R. and Harding, J. — 1st Int. Conf. of the Center for High Energy Forming. Estes Park, Colorado. 1967.

85. Slater, R. A. C. and Johnson, W. — Int. J. Mech. Sci. 9 1967.

86. Maeda, T. and Tamura, K. — Bull. J. S. M. E. 3 1960.

87. Johnson, W. and Travis, F. W. — Engineering Plasticity. Edited by Heyman, J. and Leckie, F. A. Cambridge University Press 1968.

88. Kulkarni, S. B., Ezra, A. A. and Harding, J. — Denver Research Institute Report. 1968.

89. Cooper, R. H. and Campbell, J. D. — J. Mech. Eng. Sci. 9 1967.

90. Campbell, J. D. and Cooper, R. H. — Conf. on Phys. Basis of Yield and Fracture. Inst. of Phys. and Phys. Soc. Oxford. 1966.

91. Harding, J. Wood, E. C. and Campbell, J. D. — J. Mech. Eng. Sci. 2 1960.

92. Lindholm, U. S. and Yeakley, L. M. — Experimental Mechanics 8 1968.

93. Ripperger, E. A. — Behaviour of Materials Under Dynamic Loading. A.S.M.E. 1965.

94. Harding, J. — Private communication.

95. Sayre, M. F. — Trans. A.S.M.E. 52 1930, 53 1931.

96. Smith, C. S. — Proc. A.S.T.M. 40 1940.

97. Klepaczko, J. — Arch. Mech. Stos. 19 1967.

98. Nachlinger, R. R. and Yew, C. H. — University of Texas Report 1967.

99. Dillon, Jr., O. W. — J. Mech. and Phys. Solids 15 1967.

100. Sokolovsky, V. V. — Prikl. Mat. Mekh. 12 1948.

A P P E N D I X I.

(a) Experimental Procedure for the Wave Propagation Experiments.

A. NEW SPECIMEN.

1. Place specimen-bar assembly in machine.
2. Adjust supports.
3. Connect and balance 'static' gauge bridge.
4. Connect input and output bar 'increment' gauges.
5. Test increment gauges by switching on Stabilised Voltage Supply at 10v.
6. If O.K. increase to 24v., if not, repair.
7. Go to B.

B. ALL TESTS.

1. Adjust stand and clamp.
2. Thread correct thickness piano wire, ensuring Tufnol disc round wire, and clamp both ends.
3. Tighten wire till slack taken out.
4. Clamp Tufnol disc to wire.
5. Solder 46 S.W.G. copper wire to piano wire.
6. Solder 46 S.W.G. copper wire to tag in Tufnol disc.
7. Test trigger.
8. Load up wire to maximum value.
9. Test trigger.
10. Balance scope if necessary, and calibrate traces.
11. Select correct Torsion Machine Speed.
12. Photograph graticule.
13. Start torsion machine and Sanborn recorder simultaneously.

14. Trigger ready, shutter open, nick piano wire, shutter shut.

15. Stop torsion machine and Sanborn recorder simultaneously.

16. Obtain photograph, dismantle and restart.

(b) Experimental procedure for the Blanking Tests.

(i) Low speed Instron Tests.

1. Balance and calibrate Instron machine.

2. Select the chart speed compatible with the crosshead speed to be used.

3. Assemble die-specimen assembly and place in machine.

4. Take up the slack at a low crosshead speed.

5. Link the chart and crosshead controls.

6. Begin the test.

7. Stop the machine and replace the specimen when the punch has passed through completely.

(ii) Medium speed Hydraulic Machine Tests.

1. Assemble die-specimen assembly and attach to the load cell.

2. Using a very low oil pressure, raise the punch platform slowly so that the punch is positioned with its top inside the die-assembly guide hole.

3. Close all the valves so that the punch is stationary.

4. Rebalance and calibrate the oscilloscope (by switching a shunt resistance across one arm of the bridge).

5. Photograph oscilloscope graticule and base lines.

6. Using a dial gauge to observe the motion of the punch platform, raise the punch slowly with a small oil pressure until it reaches the lower face of the specimen.

7. Set the dial gauge to zero at this position.

8. Lower the piston a little way, and increase the pressure in the system to the required value, keeping the punch approximately stationary by controlling the valves carefully.

9. Bring the punch carefully back into contact with the specimen.

10. Reset the oscilloscope and camera, (single sweep facility), remove the dial gauge, and release the pressure on the upper side of the piston, by pressing the release button.

11. Test completed, obtain photograph and dismantle the assembly.

(iii) <u>High Speed Impact Machine Tests.</u>

1. Solder a ring round the punch bar at the correct place.

2. Tighten the rubber hose pieces at their correct positions.

3. Place the punch-die and guides in the frame.

4. Solder the gauge leads and switch on the current.

5. Place the specimen in the assembly.

6. Check the gauge resistances.

7. Calibrate the oscilloscope and photograph the base and calibration lines.

8. Check the trigger circuit.

9. Raise the weight off its safety stand.

10. Fold away the safety stand.

11. Place the weight at its correct height.

12. Remove the safety catch on the weight.

13. Open the camera shutter.

14. Reduce the solenoid current, allowing the weight to fall.

15. Test completed, obtain photograph, dismantle the apparatus, having placed the weight on its safety stand and replaced the safety catch.

APPENDIX 2.

The Magnitude of a Torsional Increment under Elastic Conditions.

With reference to Figure Ap.1., the 'static' torque has been subtracted from the values of each given torque so that the increment only is regarded.

Let To = released torque.

It is known that $\tau = \rho c v$

$$\therefore \quad T = \int \rho c v 2\pi r^2 \, dr = \int \rho c \omega 2\pi r^3 \, dr$$

$$= \rho c \omega J$$

Let $\alpha = \frac{1}{2}(\rho c J \omega + T)$, $\beta = \frac{1}{2}(\rho c J \omega - T)$

so $T = \alpha - \beta$, $\rho c J \omega = \alpha + \beta$

At discontinuity $T_1 = T_2$

$$\therefore \quad \alpha_1 - \beta_1 = \alpha_2 - \beta_2$$

and $$\omega_1 = \omega_2$$

$$\therefore \quad \alpha_1 + \beta_1 = n(\alpha_2 + \beta_2) \quad \text{where} \quad n = \frac{(\rho c J)_1}{(\rho c J)_2}$$

whence $$2\alpha_1 = \alpha_2(n+1) + \beta_2(n-1)$$

$$\therefore \quad \alpha_2 = \left(\frac{2}{n+1}\right)\alpha_1 - \left(\frac{n-1}{n+1}\right)\beta_2$$

and $$\beta_1 = \alpha_1 - \left(\frac{2}{n+1}\right)\alpha_1 + \left(\frac{n-1}{n+1}\right)\beta_2 + \beta_2$$

$$\therefore \quad \beta_1 = \left(\frac{n-1}{n+1}\right)\alpha_1 + \left(\frac{2n}{n+1}\right)\beta_2$$

Along AB, $\alpha_1 = \frac{1}{2}T_o$, $\beta_2 = 0$

$$\therefore \alpha_2 = \frac{T_o}{n+1} \quad \text{and} \quad \beta_1 = \frac{n-1}{2(n+1)} \cdot T_o$$

$$\therefore T_1 = \alpha_1 - \beta_1 = \frac{1}{2}T_o - \frac{n-1}{2(n+1)} T_o$$

$$= \frac{T_o}{n+1}$$

$$\text{and } T_2 = \alpha_2 - \beta_2 = \frac{T_o}{n+1}$$

Assuming $\frac{(\rho eJ)_2}{(\rho eJ)_3} = \frac{1}{n}$

$$\alpha_3 = \frac{2}{\frac{1}{n}+1} \cdot \alpha_2 - \frac{\frac{1}{n}-1}{\frac{1}{n}+1} \cdot \beta_3 = \frac{2n}{n+1} \cdot \alpha_2 - \frac{1-n}{1+n} \cdot \beta_3$$

$$\text{and } \beta_2 = \frac{\frac{1}{n}-1}{\frac{1}{n}+1} \cdot \alpha_2 + \frac{2}{\frac{1}{n}+1} \cdot \beta_3 = \frac{1-n}{1+n} \cdot \alpha_2 + \frac{2}{1+n} \cdot \beta_3$$

Along BC, $\alpha_2 = \frac{T_o}{n+1}$ $\beta_3 = 0$

$$\therefore \alpha_3 = \frac{2n}{(n+1)^2} \cdot T_o$$

$$\beta_2 = \frac{1-n}{(1+n)^2} \cdot T_o$$

$$\therefore T_2 = \alpha_2 - \beta_2 = \frac{2n}{(1+n)^2} \cdot T_o ,$$

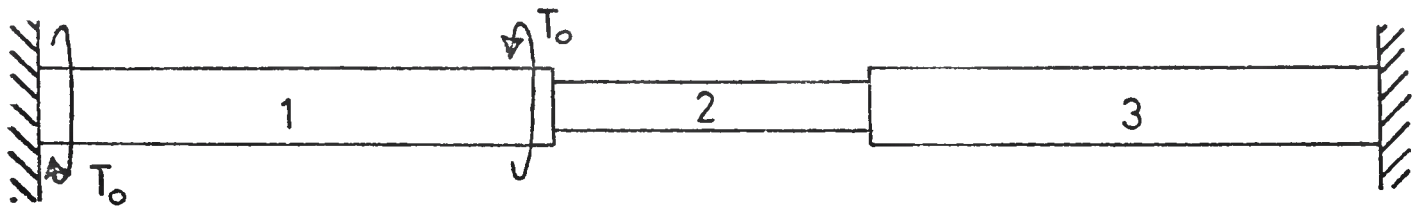
$$\text{and } T_3 = \alpha_3 - \beta_3 = \frac{2n}{(1+n)^2} \cdot T_o.$$

Thus from the strain gauges on bars 1 and 3 it is possible to obtain a measure of the torque in the specimen, assuming elastic conditions, without knowing the values of J or ρe for the materials :-

$$\text{Output (i)} = \frac{To}{n+1} - To = -\frac{n}{n+1} \cdot To$$

$$\text{Output (ii)} = \frac{2n}{(1+n)^2} \cdot To$$

The ratio of the outputs is $/n+1$, hence n and hence the value of torque in the specimen.



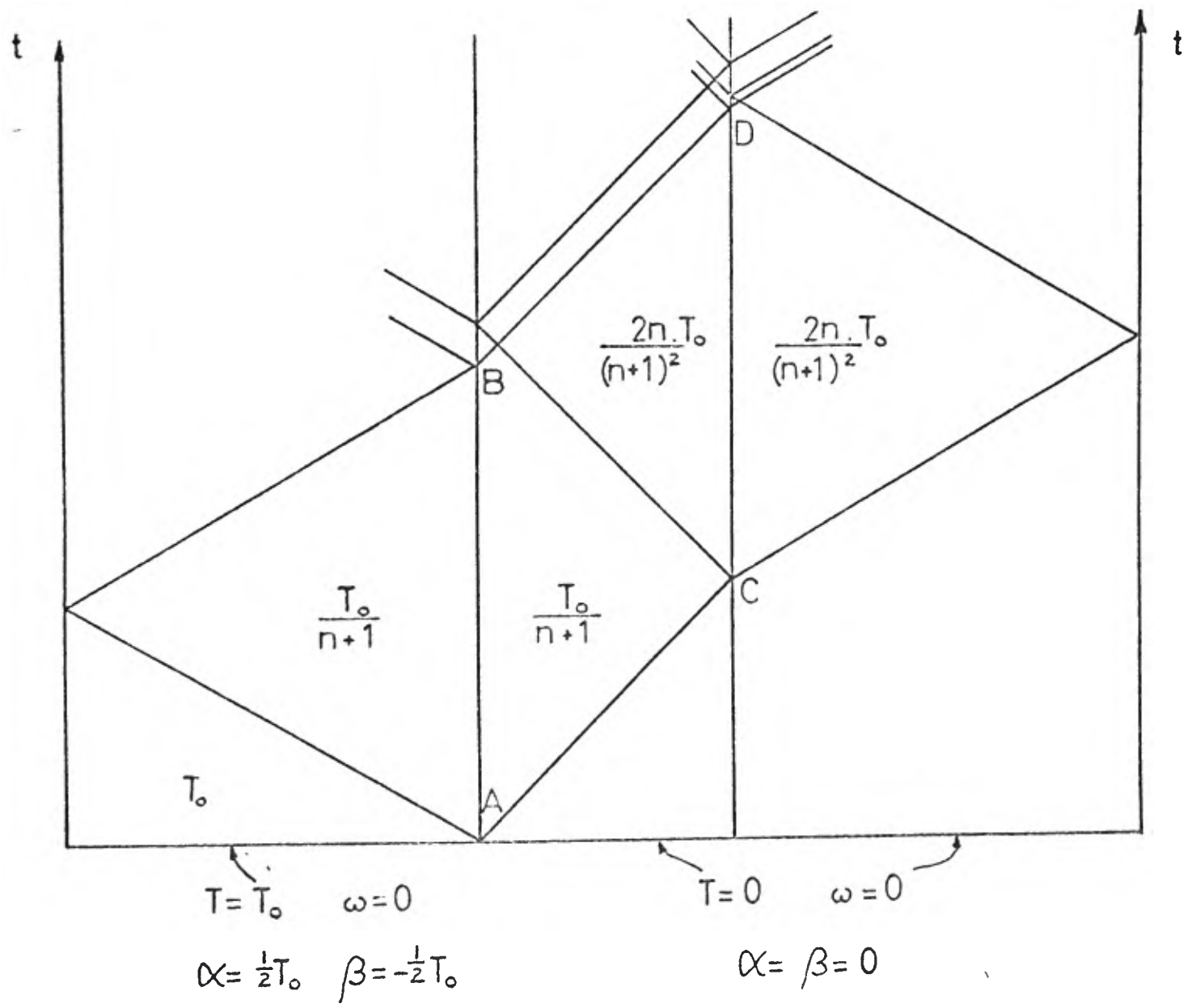


FIG. Ap.1 Elastic incremental torque values.